

Investigation of bacteriophages as potential sources of oral antimicrobials

By:

**Mohammed I. Abud Al-Shaheed
Al-Zubidi**

A thesis submitted for the degree of Doctor of Philosophy
December 2017



The University of Sheffield
Faculty of Medicine, Dentistry and Health
School of Clinical Dentistry

Abstract

Bacteriophages are natural viruses that attack bacteria and are abundant in all environments, including air, water, and soil- following and co-existing with their hosts. Unlike antibiotics, bacteriophages are specific to their bacterial hosts without affecting other microflora. The use of bacteriophages and phage endolysin based therapies to kill pathogens without harming the majority of harmless bacteria has received growing attention during the past decade, especially in the era where bacterial resistance to antibiotic treatment is increasing.

The aims of this study were to characterise a putative prophage (phiFNP1) residing in the genome of the periodontal pathogens *Fusobacterium nucleatum polymorphum* ATCC 10953, investigating the possibility of prophage induction, examining its presence in clinical plaque samples taken from patients with chronic periodontitis cases, and purify its putative lysis module genes to examine their potential antimicrobial activity. In addition, attempts will be made to catalogue phages that are presents in samples from the oral cavity of patients with chronic periodontitis and in wastewater, followed by isolation of lytic phages targeting endodontic and oral associated pathogens, characterisation of the isolated phages, evaluation of the efficiency of phage towards biofilm elimination, and established an animal model to study phage-bacterial interaction in order to develop them for treatments.

The results revealed that phiFNP1 prophage are common in subgingival plaque of patients suffering from chronic periodontal disease but attempts to induce phiFNP1 using Mitomycin C were inconclusive, indicating that it might be defective. Bioinformatics revealed that the genome of phiFNP1 contained potential lysin genes, with one being cloned and purified successfully in soluble form, though its activity as antibacterial was not confirmed, and needs to be further explored as phage lytic enzymes against *Fusobacterium* have not been identified yet.

Various phage like particles with different morphology were visualised by direct electron microscopy from oral and wastewater samples, which reflect the richness and diversity of bacteriophage within those samples. Several phages were isolated namely phiSHEF 2,3,4,5,6,7 which belong to the Siphoviridae family which are specific to *Enterococcus faecalis* and the full chromosome sequence comparisons for three of the isolated phages (phiSHEF 2,4 and 5) revealed that they are lytic in nature reflected by

absence of genes associated with lysogenic cycle, therefore place them as suitable candidate for therapy. They exhibit genomic variations corresponded to their difference in phage-host range especially in the tail region. In addition, phiSHEF 2 was capable of complete biofilm eradication on abiotic surfaces and significantly reduced biofilms formed on the surfaces of tooth root slices. Most importantly phiSHEF 2 recovered a Zebrafish larvae from the deadly infection caused by an oral clinical isolate of *E. faecalis*, indicating the establishment of a successful animal model for testing the efficiency of phage therapy towards *E. faecalis* infection. Finally, Exopolysaccharide mutants of *E. faecalis* were not infected by three of our phiSHEF phages tested, indicating that *E. faecalis* exopolysaccharide capsule and proper bacterial membrane integrity play an important role during the initial stages of phage infection.

In conclusion, bacteriophages exhibit an apparent superiority to fight hard to eradicate pathogens such as those associated with recalcitrant endodontic infections thus “bacteriophage based therapy” could represent an innovative alternative to control and eliminate oral infections caused by biofilm forming and antibiotic resistant pathogens.

Acknowledgments

Firstly, my sincerest gratitude and appreciation goes to my supervisors Dr. Graham Stafford, Prof. Andrew Rawlinson and Prof. Ian Douglas for their attention to details, endless motivation and never ending scientific knowledge. Their kindness, unlimited support, guidance and encouragement throughout this study have been invaluable. I have been blessed to learn from the supportive staff of the Oral and Maxillofacial Department and my PhD colleagues at Graham Stafford research group. My gratefulness also goes to my colleague Sahang Gul who has always supported me in clinical samples collection part of this study, and I will never forget his friendly fellowship and lovely moments that we spent together in the department. I would like especially to thank my colleague Magdalena Widziolek who assists me in establishment of the animal model of my study. I would like to thank Alison Barber and Claire Vallance-Owen in the Charles Clifford Dental Hospital. They have been there to support me when we recruited patients and helped collect data for this study. My PhD journey would have been much more difficult without the amazing technical staff who are second to none. Particularly, technical expertise from Mrs. Sue Newton and the supportive role of Mr. Jason Heath and Mrs. Brenka McCabe has been indispensable regarding methodological problem solving and pleasant discussions. I would also like to express my appreciation for all the advice, encouragement and funny moments I received throughout my PhD time from all the lovely friends I got to know throughout my study.

My gratitude and love goes to my family especially my mother for supporting me spiritually throughout my life and giving me all the advice and encouragement I needed throughout my study. Ultimately, my life would be impossible including this PhD study without the support of my lovely wife, Shaimaa. Her patience, endless support, and continuous encouragement have been invaluable and greatly appreciated. For this, I like to dedicate this work to her and my gorgeous daughters, Rawan and Rama. Last but not the least, I would like to express my gratitude for the Ministry of Higher Education and Scientific Research in Iraq for granting me this fantastic opportunity to finish my PhD study and excel academically, and I recognise that this research would not have been possible without it.

Abbreviations

®	Trade mark
α	Alpha
β	Beta
γ	Gamma
μ	Micro
Ap	Ampicillin
ATCC	American Type Culture Centre
bp	Base pairs
BHI	Brain heart infusion
BSA	Bovine serum albumin
°C	Centigrade
CO ₂	Carbon dioxide
DNA	Deoxyribonucleic acid
dsDNA	Double stranded deoxyribonucleotide
DTT	Dithiothreitol
EDTA	Ethylenediamine tetra-acetic acid
FA	Fastidious anaerobe agar
G	Gram
g	Gravity
GST	Glutathione S-transferase
His-tag	Histidine-tag
h	hour
IL	Interleukin
IPTG	Isopropyl β -D-1-thiogalactopyranoside
kbp	kilo base pairs
kDa	kilo Daltons
L	litre
LB	Luria-Bertani
LPS	Lipopolysaccharide
ng	nanogram
μ g	Microgram
μ l	Microlitre
ml	Millilitre
min	minute
mM	Mmillimolar
MOI	Multiplicity of Infection
M	Molar
MW	Molecular weight
N ₂	Nitrogen
Ni-NTA	Nickel-nitriloacetic acid
nm	Nanometre
OD	Optical density
PBS	Phosphate buffered saline
PCR	Polymerase chain reaction
%	Percentage
PFU	Plaque forming units
phi	Phage
ppm	part per million
psi	Pounds per square inch (pressure)

qPCR	Quantitative polymerase chain reaction
RNA	Ribonucleic acid
rpm	Revolutions per minute
s	seconds
SD	Standard deviation
SDS	Sodium dodecyl sulphate
SDS-PAGE	SDS-polyacrylamide gel electrophoresis
ssRNA	Single stranded ribonucleotide
ssDNA	Single stranded deoxyribonucleotide
TAE	Tris-acetate-EDTA
TEM	Transmission electron microscope
TEMED	Tetramethylethylenediamine
tRNA	Transfer RNA
TNF	Tumour necrosis factor
TSB	Triptone soya broth
UV	Ultraviolet light
V	Volt

Contents

Abstract	iii
Acknowledgments.....	v
Abbreviations	vi
List of Figures	xii
List of Tables	xvi
Chapter 1: Literature Review	1
1.1 Introduction.....	2
1.2 Role of oral microbiome in health	6
1.3 Bacteriophage.....	6
1.3.1 Definition of bacteriophage	6
1.3.2 History of bacteriophage discovery	8
1.3.3 Classification of bacteriophage	9
1.3.4 Lytic phages towards orally derived bacteria	14
1.3.4.1 <i>E. faecalis</i> lytic phages.....	15
1.3.5 Bacterial resistance to bacteriophage	15
1.3.6 Phage mediated bacterial virulence.....	17
1.3.7 Medical importance of bacteriophages	19
1.4 Dental caries.....	26
1.5 Endodontic and periapical infection	28
1.5.1 Persistent and secondary infection.....	28
1.5.2 Endodontic infection treatment.....	30
1.5.3 Pathways of infection.....	30
1.5.4 Pathogens associated with intraradicular and extraradicular infections	31
1.5.5 Bacteria persisting throughout endodontic treatment	34
1.6 <i>E. faecalis</i> and endodontic infection	35
1.6.1 Enterococcal Cell Walls.....	36
1.6.2 Virulence factors of <i>E. faecalis</i> and its relation to endodontic disease.....	37
1.6.3 <i>Enterococcus</i> and antibiotic resistance	45
1.7 Dental plaque and antimicrobial resistance	46
1.8 Timeline of antibiotic resistance	47
1.9 Periodontal disease.....	50
1.9.1 Pathogenesis of periodontal disease.....	50
1.9.2 Bacteriology of periodontal disease.....	52
1.9.3 <i>Fusobacterium nucleatum</i> , periodontal and other oral and non-oral diseases.....	56
1.9.4 Treatment of periodontal disease	61
1.10 Hypothesis and aims	62
1.10.1 Hypothesis.....	62
1.10.2 Aims and objectives	62
Chapter 2: Materials and Methods	64
2.1 Bacterial strains, plasmid vector and primers	65
2.1.1 Anaerobic clinical bacterial source and growth conditions	67
2.1.2 <i>E. coli</i> strains.....	68
2.1.3 <i>Enterococcus</i> , <i>A. actinomycetemcomitans</i> strains and growth conditions.....	68
2.1.4 Isolation of clinical <i>A. actinomycetemcomitans</i> strains	69

2.2 Sample collection and processing	70
2.2.1 Clinical plaque and salivary sample collection from patients with chronic periodontitis	70
2.2.2 Full mouth clinical plaque and salivary sample collection from patients with chronic periodontitis from Sheffield and Baghdad (IRAQ).....	70
2.2.3 Dental chair drain samples collection	71
2.2.4 Wastewater sample collection.....	71
2.2.5 Sample processing.....	72
2.3 Molecular biology techniques	72
2.3.1 Plasmid extraction from <i>E. coli</i>	72
2.3.2 DNA extraction	72
2.3.3 Polymerase chain reaction (PCR)	73
2.3.4 Agarose gel electrophoresis	73
2.3.5 Cloning of putative lysins	73
2.3.6 <i>E. coli</i> transformation.....	74
2.3.7 Extraction of DNA fragments from agarose gels.....	75
2.3.8 Restriction of DNA	75
2.3.9 Ligation of DNA	75
2.3.10 Preparation of electrocompetent <i>E. coli</i> cells.....	75
2.3.11 Sodium dodecyl sulphate polyacrylamide gel electrophoresis (SDS-PAGE)	76
2.3.12 Protein expression and solubility test.....	77
2.3.13 BCA Assays	78
2.3.14 Staining of polyacrylamide gels.....	78
2.3.15 Zymogram	79
2.4 Phage techniques	79
2.4.1 Prophage induction from <i>Fusobacterium nucleatum polymorphum</i> ATCC 10953.....	79
2.4.2 Bacteriophage isolation from wastewater	80
2.4.3 Double layer plaque assay and spot pipetting	80
2.4.4 Enrichment of bacteriophage	81
2.4.5 Phage stock preparations.....	81
2.4.6 Bacteriophage concentration by precipitation with Polyethylene Glycol (PEG 8000)	82
2.4.7 Electron microscopy for the isolated phage	82
2.4.8 Infection cycle, adsorption rate and one step growth.....	82
2.4.9 Analysis of phage proteins	84
2.4.10 Mass spectrometry	84
2.4.11 Phage DNA extraction	85
2.4.12 Restriction fragment length polymorphism (RFLP) and analysis of phage genome size.....	85
2.4.13 DNA sequencing for phiSHEF 2, phiSHEF 4, and phiSHEF 5	86
2.4.14 Molecular determination of phage adhesion	86
2.4.15 Biofilm assay on polystyrene plates	87
2.4.16 Biofilm assay on teeth root surface (<i>in vitro</i>).....	87
2.4.17 Zebrafish as <i>in vivo</i> model for phage treatment.....	88
Chapter 3: Characterisation of a putative <i>Fusobacterium nucleatum polymorphum</i> ATCC 10953 prophage	89
3.1 Introduction	90

3.2 Bioinformatic exploration of <i>Fusobacterium nucleatum polymorphum</i> (ATCC 10953) prophage	91
3.3 Testing for the presence of phiFNP1 in <i>Fusobacterium nucleatum polymorphum</i> ATCC 10953	96
3.4 Induction of phiFNP1 prophage with Mitomycin C	97
3.5 The occurrence of <i>Fusobacterium nucleatum polymorphum</i> and its prophage in clinical plaque samples	102
3.6 Investigation of the phiFNP1 lysis module as a therapeutic	105
3.6.1 Cloning of phiFNP1 lysis module genes.....	109
3.6.2 Overexpression of FNP lysis module genes	120
3.7 Discussion	135
3.7.1 Bioinformatic exploration of <i>Fusobacterium nucleatum polymorphum</i> ATCC 10953 (FNP) prophage.....	135
3.7.2 Induction of FNP prophage with Mitomycin C	136
3.7.3 Testing for the occurrence of <i>Fusobacterium nucleatum polymorphum</i> and its prophage in clinical plaque samples.	139
3.7.4 Investigation of the phiFNP1 lysis module as a source of therapeutic antimicrobial proteins	141
3.8 Conclusions.....	144
Chapter 4: Isolation of lytic Bacteriophage targeting endodontic and oral associated pathogens from oral and wider environments.....	146
4.1 Introduction.....	147
4.2 Isolation of clinical strains of <i>Aggregatibacter actinomycetemcomitans</i>	148
4.3 Investigation of morphological diversity of bacteriophage within oral samples by direct electron microscopy	153
4.4 Phages observed in Sheffield wastewater	157
4.5 Isolation of virulent bacteriophage	163
4.5.1 Isolation of bacteriophage targeted towards periodontal associated pathogens	163
4.5.2 Isolation of bacteriophage targeted towards endodontic associated pathogens	163
4.6 Discussion	208
4.6.1 Isolation of new clinical strains of periodontal pathogen A. <i>Actinomycetemcomitans</i>	208
4.6.2 Cataloguing of phages from the oral cavity of patients attending periodontal department in UK and IRAQ	209
4.6.3 Cataloguing of phages from Sheffield wastewater	210
4.6.4 Isolation of phage against isolated strains, a range of endodontic <i>E. faecalis</i> strains and other periodontal associated clinical strains	212
4.6.5 Biofilm models.....	219
4.6.6 Infection in an animal model- Zebrafish.....	220
4.7 Conclusions.....	221
Chapter 5: Summary, Final Discussion and Future Prospects	222
5.1 Summary of major findings	223
5.1.1 Chapter 3: Characterisation of a putative <i>Fusobacterium nucleatum polymorphum</i> ATCC 10953 prophage.....	223

5.1.2 Chapter 4: Isolation of lytic bacteriophages targeting endodontic and oral associated pathogens from oral and wastewater	224
5.2 General discussion: oral infections control: a target approach	227
5.3 Future prospects	229
References	232
Appendices	238

List of Figures

Figure 1.1 Schematic presentation of tooth in health and disease state.....	4
Figure 1.2 Polymicrobial communities under certain conditions could induce inflammation.....	5
Figure 1.3 Generalised structure of a tailed phage.....	7
Figure 1.4 The three-tailed phage families Myoviridae, Siphoviridae and Podoviridae.....	10
Figure 1.5 The seven families of polyhedral, filamentous and pleomorphic phages.	10
Figure 1.6 The steps of the bacteriophage lytic and lysogenic life cycles.....	14
Figure 1.7 Schematic representation of the modular structure.....	25
Figure 1.8 Schematic representation of carious cavity and bacterial species associated with dental caries.	27
Figure 1.9 Diagram showing various possible pathways by which microorganisms could reach the tooth pulp.....	31
Figure 1.10 Model of the enterococcal cell wall.....	37
Figure 1.11 Schematic model of endodontic disease related to virulence factors of <i>E. faecalis</i>	44
Figure 1.12 Developing antibiotic resistance: A Timeline of Key Events. Adapted from (Ventola, 2015).	49
Figure 1.13 Cross-sectional representation of a posterior tooth in health and disease.	52
Figure 1.14 The “ecological plaque hypothesis” in relation to periodontal disease.	54
Figure 1.15 The association among subgingival species.	55
Figure 2.1 Dental chair sucker drain collector.....	71
Figure 2.2 Double layer plaque assay and spot pipetting.....	81
Figure 3.1 Snapshot from PFAST online program showing an intact prophage phiFNP1 (red box) within the genome of <i>Fusobacterium nucleatum polymorphum</i> (ATCC 10953).....	92
Figure 3.2 Genomic structure of putative prophage of <i>Fusobacterium nucleatum polymorphum</i> ATCC 10953 (phiFNP1).	93
Figure 3.3 FNP_t0043 and FNP_t0044 sequences that share direct repeat sequences (red colour letters).....	94

Figure 3.4 PCR screen for the phiFNP1 phage genome.	97
Figure 3.5 PCR screen of phiFNP1 induction from FNP ATCC 10953 cells with Mitomycin C (1µg/ml).....	98
Figure 3.6 Transmission electron microscope (TEM) imaging of enriched suspension induced from FNP ATCC 10953 by Mitomycin C.....	100
Figure 3.7 Infection of <i>Fusobacterium</i> cells (FNP) with Mitomycin C induced supernatants.	101
Figure 3.8 Diagram showing the flow chart for phiFNP1 and FNP ATCC 10953 screening from patient.	102
Figure 3.9 Collection of plaque sample from diseased site of the patient.	102
Figure 3.10 A) Positive bands PCR screening for healthy (H) and diseased (D) sites from three visits of the same patient.	103
Figure 3.11 PhiFNP1 lysis module investigation.	106
Figure 3.12 Amino acids blast search for the lysis module of PhiFNP1.	107
Figure 3.13 Endolysins cleavage activity towards bacterial PG sites.....	108
Figure 3.14 Codon optimisation of FNP_1699 and FNP_1700.	113
Figure 3.15 Snapshot for the final optimized nucleotide sequence of FNP_1699 and FNP_1700.	114
Figure 3.16 Restriction digestion of pJET1.2-FNP1699.	115
Figure 3.17 Restriction digestion of pJET1.2-FNP1700.	116
Figure 3.18 pET15b vector map and cloning details.	117
Figure 3.19 PCR screen of pET5b-FNP1699 and 1700 DNA from differnt colonies.	118
Figure 3.20 pGEX-4T-3 vector map and cloning details.	119
Figure 3.21 PCR screen of pGEX-4T-3-FNP1699 and 1700 DNA.	120
Figure 3.22 amiC GST-tag protein overexpression and solubility test	121
Figure 3.23 FNP1699 GST-tag and His-tag protein overexpression and solubility test.....	123
Figure 3.24 FNP1699 GST-tag and His-tag protein elution test.....	124
Figure 3.25 Testing FNP1699 GST-tag afters dialysis.....	125
Figure 3.26 FNP_1707 and FNP_1699 GST-tag proteins overexpression in <i>E. coli</i> strains C41(λDE3).	126
Figure 3.27 FNP_1707 and FNP_1699 GST-tag proteins solubilisation.	127
Figure 3.28 FNP19700 GST-tag and His-tag protein overexpression and solubility test.....	128

Figure 3.29 FNP1700 His-tag protein elution and dialysis tests.	129
Figure 3.30 Growth curve of FNP ATCC 10953 in broth medium.	130
Figure 3.31 FNP_1700 lysin–bacterial activity assay.....	131
Figure 3.32 Peptidoglycan degradation assays of FNP_1700 lysin.....	133
Figure 3.33 Zymogram analysis of FNP_1700 lysin for both <i>S. aureus</i> and FNP ATCC 10953 PGN.....	134
Figure 4.1 Gram stain and colony morphology of some oral clinical isolates	153
Figure 4.2 Electron micrographs of bacteriophages in plaque samples from Sheffield samples (A and B) and Iraqi plaque samples (C, D, E).	156
Figure 4.3 Electron micrographs of bacteriophage from wastewater that belong to the family Siphoviridae.....	158
Figure 4.4 Electron micrographs of bacteriophage from wastewater that belong to the family Siphoviridae; show elongated and variable head morphology.	159
Figure 4.5 Electron micrographs of bacteriophage from wastewater that mostly belong to the family Myoviridae.	160
Figure 4.6 Electron micrographs of bacteriophage from wastewater that mostly belong to the family Podoviridae (A and B), cubic like phage (C).	161
Figure 4.7 Electron micrographs of bacteriophages from wastewater	162
Figure 4.8 Phage isolation procedure.	164
Figure 4.9 Isolation of <i>E. faecalis</i> bacteriophages and plaque morphology.	166
Figure 4.10 Transmission electron micrographs of SHEF phage particles.	172
Figure 4.11 Restriction fragment length polymorphism (RFLP) of phiSHEF 2... ..	174
Figure 4.12 Restriction fragment length polymorphism (RFLP) of extracted phage chromosomal DNA and protein profile for phiSHEF phages.....	175
Figure 4.13 Snap shot from MASCOT search results of the 36 KDa protein band analysis of phiSHEF 2 phage.	176
Figure 4.14 A) Genome organization of <i>E. faecalis</i> lytic phages phiSHEF 2, phiSHEF 5, and phiSHEF 4 respectively.	179
Figure 4.15 Snap shot from NCBI conserved domains for phiSHEF 2 and phiSHEF 4 endolysins.....	186
Figure 4.16 Multiple sequence alignment of fourth and fifth tail gens of phiSHEF phages produced by Multalin online program.	189
Figure 4.17 Characterisation of phiSHEF 3 phage.....	191
Figure 4.18 Further characterisation of phiSHEF 3.....	193
Figure 4.19 Molecular determination of phiSHEF phages adhesion.	195

Figure 4.20 Transmission electron micrographs of epaB and OG1RF _11720 mutants, round bacterial cells outline could be visualised.	199
Figure 4.21 One step growth, infection cycle and adsorption rate of phiSHEF 2.	201
Figure 4.22 Transmission electron micrographs taken of cells at 30 min post infection with phiSHEF 2.	202
Figure 4.23 Biofilm assay on polystyrene plates and tooth root slices.....	203
Figure 4.24 Stereo microscope and light microscope images of treated and untreated <i>E. faecalis</i> biofilm on root surface slices.	204
Figure 4.25 Animal model of phage-bacterial interaction.....	207

List of Tables

Table 1.1 The ten families of bacterial prokaryotic phages based on morphology and genetic characteristics. Adapted from (Ackermann, 2007) with permission.....	11
Table 1.2 Some human phage therapy studies performed in the former Soviet Union. Adapted from (Abedon <i>et al.</i> , 2011).....	23
Table 2.1 Anaerobic bacterial strains used in this study.....	65
Table 2.2 <i>E. coli</i> strains used in transformation.....	66
Table 2.3 Plasmid vector used in this study.....	66
Table 2.4 Primers used in this study and their details.....	67
Table 2.5 <i>Enterococcus</i> and <i>A. actinomycetemcomitans</i> bacterial strains used in this study and origin.....	69
Table 2.6 PCR thermal cycling conditions.....	73
Table 2.7 Preparation of resolving gel and stacking gel.....	76
Table 3.1 Names and proposed function of phiFNP1 genes blast hits.	94
Table 3.2 Screening results for phiFNP1 and FNP from 45 patients attending the periodontal departments for treatments at the School of Clinical Dentistry.. ..	104
Table 4.1 The head and tail dimensions for the isolated <i>E. faecalis</i> phages.	167
Table 4.2 PhiSHEF 2, 4, and 5 characterisation. The main nucleotide sequence of each phage was analysed by PHAST online program.	177
Table 4.3 Names and proposed function of phiSHEF 2 annotated genes.	180
Table 4.4 Names and proposed function of phiSHEF 4 annotated genes.	182
Table 4.5 Names and proposed function of phiSHEF 5 annotated genes.	184
Table 4.6 Phage-host range of phiSHEF phages. PhiSHEF 2 exhibits the widest host range followed by phiSHEF 6, 7, 5, and 4 respectively.	190
Table 4.7 Sensitivity of phiSHEF phages to <i>E. faecalis</i> OG1RF and mutants.	196
Table 4.8 Molecular determination of Epa mutants of OG1RF.	198

Chapter 1: Literature Review

1.1 Introduction

Tooth decay and periodontal (gum) diseases are caused in part by bacteria that colonise the human mouth with both potentially leading to deeper periapical infections if left untreated (Hardie, 1992) (Figure 1.1). In addition to bacteria, the human mouth provides the colonisation habitat for a diversity of viruses, fungi, protozoa, and archaea. The oral microbiota greatly contributes as a significant risk factor for human health and is implicated both in systemic and oral conditions, such as in tumours (Farrell *et al.*, 2011), diabetes mellitus (Löe, 1993), cardiovascular diseases (Figuro *et al.*, 2011), bacteraemia (Bahrani-Mougeot *et al.*, 2008), Rheumatoid arthritis (Scher and Abramson, 2011), and preterm birth (Aagaard *et al.*, 2014). Investigation of the oral microbiota in health and disease in periodontitis revealed that it is more related to the increased abundance of certain species/genera than caused by new novel species while taxa associated with health were severely reduced (Abusleme *et al.*, 2013). Recent evidence suggests that the whole microbial community under certain conditions and/or specific organisms can shift the balance from homeostasis to destructive inflammation rather than being caused by individual causative bacteria. These conditions might be: broad-spectrum antibiotic treatment, shifts in diet, or immune deficiencies (Hajishengallis and Lamont, 2016). This hypothesis refers to the potential of a native community to cause disease rather than the presence of causative pathogens.

A range of viruses can be found in the mouth, represented mainly by bacteriophage (Pride *et al.*, 2012). Analyses of the salivary viral-metagenome has uncovered diverse bacteriophage populations residing in the mouth and unravelled the complexity of their bacterial host (Pride *et al.*, 2012, Robles-Sikisaka *et al.*, 2013). In addition to bacteriophage, a variety of disease-associated viruses can also be found, for example, Herpes simplex virus, which causes gingivostomatitis or enters a dormant state in the trigeminal ganglion to cause herpes labialis (cold sores) when reactivated later by external factors such as stress and cold weather (Scott *et al.*, 1997). Additionally several salivary gland viruses that cause mumps and rabies, varicella zoster virus (pathogen of herpes zoster), and human papilloma virus (pathogen of papillomas) which is responsible for a number of oral conditions, including papillomas, condylomas and focal epithelial hyperplasia are also commonly present (Roizman, 2001, Kumaraswamy and Vidhya, 2011). In addition, several oral diseases had been related with virus infection such as oral

hairy leukoplakia which associated with Epstein-Barr Virus EBV (Young *et al.*, 1991) and Kaposi sarcoma that been associated with herpesvirus HHV8 (Russo *et al.*, 1996).

Fungi are also common components of the oral microbiota, with pyrosequencing from oral rinses of 20 healthy individuals revealing the presence of approximately 85 fungal genera (Ghannoum *et al.*, 2010). In this study, *Candida* are the most frequently detected oral fungi, represented mainly by the species *C. albicans* and are present in 75% of healthy individuals followed by *Cladosporium* (65%), *Aureobasidium* and *Saccharomycetales* (50% for both), *Aspergillus* (35%), *Fusarium* (30%), and *Cryptococcus* (20%). Candidiasis is the commonest infection caused by *Candida* spp. (Cannon *et al.*, 1995), and *in vitro* studies have established that *S. mutans* could improve the adherence of *C. albicans* and excrete lactate as a carbon source for yeast growth (Metwalli *et al.*, 2013). In addition, *C. albicans* was identified to be greatly associated with the severity of chronic periodontitis (Canabarro *et al.*, 2013) and positively connected with the occurrence of oral candidal carriage in children (Raja *et al.*, 2010, Yang *et al.*, 2012).

Very few studies have examined oral *Protozoa* species. For example, one study from 1958 described that *Entamoeba gingivalis* and the more structured *Trichomonas tenax* as the *Protozoa* species were the most commonly found in the normal oral microbiota. They have been positively correlated with poor oral hygiene (Wantland *et al.*, 1958).

The *Archaea* are non-bacterial prokaryotes, and they are restricted to a small number of species/phylotypes, methanogens and non-methanogens isolated from oral, intestinal and vaginal mucosae in humans (Dridi *et al.*, 2011). The oral *Archaea* reported from the mouth are represented by the genera *Thermoplasmatales*, *Methanobrevibacter*, *Methanobacterium*, *Methanosarcina*, and *Methanosphaera* (Lepp *et al.*, 2004, Dridi *et al.*, 2011, Nguyen-Hieu *et al.*, 2013). They can be detected in healthy subjects but their occurrence and numbers are raised in those with periodontal disease (Lepp *et al.*, 2004, Vianna *et al.*, 2008, Li *et al.*, 2009, Matarazzo *et al.*, 2012) and endodontic infections (Vickerman *et al.*, 2007, Vianna *et al.*, 2009, Jiang *et al.*, 2009). Although their potential role in human infections needs further investigation (Dridi *et al.*, 2011).

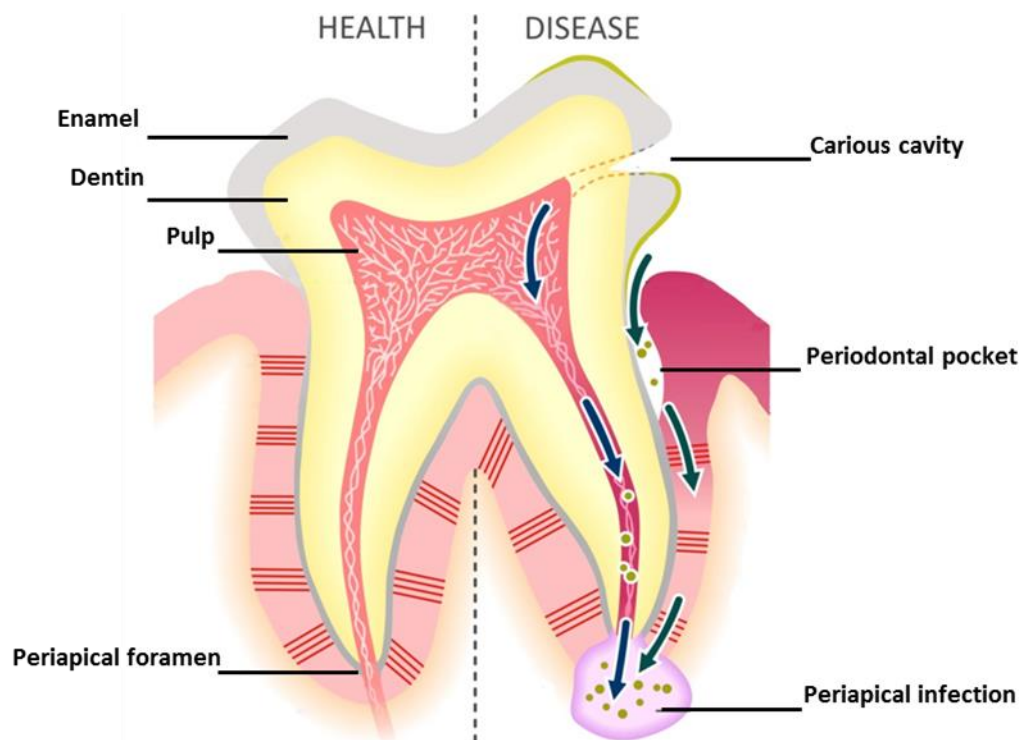


Figure 1.1 Schematic presentation of tooth in health and disease state. Dental caries and periodontal (gum) diseases are caused in part by bacteria that colonise the human mouth. Both can end in periapical infections if left untreated. Adapted from (Douglas *et al.*, 2014) with permission.

In the human mouth, the oral bacterial microbiota contains more than 700 bacterial species that have been identified by culture independent methods, with about 250 having been named and isolated (Wade, 2004, Paster *et al.*, 2006). The major genera with the main representation in healthy oral cavities include the following: *Streptococcus*, *Veillonella*, *Granulicatella*, *Gamella*, *Actinomyces*, *Corynebacterium*, *Rothia*, *Fusobacterium*, *Porphyromonas*, *Prevotella*, *Capnocytophaga*, *Nisseria*, *Haemophilis*, *Treponema*, *Lactobacterium*, *Eikenella*, *Leptotrichia*, *Peptostreptococcus*, *Staphylococcus*, *Eubacteria*, and *Propionibacterium* (Aas *et al.*, 2005, Jenkinson and Lamont, 2005, Zaura *et al.*, 2009, Bik *et al.*, 2010), though nearly half of the bacteria present have yet to be cultured (Wade, 2004). The genome sequence of health associated, uncultivated bacterium *Tannerella* BU063 (oral taxon 286) using a single cell genomics approach (Beall *et al.*, 2014), allowed the identification of virulence factors represented

by KLIKK proteases (possess proteolytic activity in vitro toward collagen, gelatin, elastin, and casein protein substrates) through comparisons to the virulent *Tannerella forsythia* ATCC43037 genome (Ksiazek *et al.*, 2015). This approach will provide a new basis to further understand the genome evolution and various mechanisms of bacterial-host interaction in closely related oral species with different pathogenicity potential (Beall *et al.*, 2014). Indeed, more new species are expected to be recognised as time goes by (Bik *et al.*, 2010, Griffen *et al.*, 2012, Belda-Ferre *et al.*, 2012).

Different types of microorganisms favour distinct niches according to changing surface assemblies and functions (Aas *et al.*, 2005), and there are three different niches recognised within the mouth that different bacteria colonise: the first group settle at the buccal mucosa, gingivae and hard palate, the second group are distinguished mainly from the saliva, tongue, tonsils and throat, while the third group were found in supra- and sub-gingival plaque which had a distinctive community (Segata *et al.*, 2012). Some pathogens can cause both increased biomass (quantitative) and qualitative alterations (changes in microbial composition, metatranscriptome, and metaproteome) to the microbiota (Hajishengallis and Lamont, 2016) (Figure 1.2). These pathogens are termed as “keystone pathogens” because their influence on community is so large compared to their low abundance thus forming a keystone of that community (Power *et al.*, 1996). As a result, they will remodel the normal symbiotic microbiota into a dysbiotic one and accordingly stabilise the dysbiotic state of that community (Hajishengallis *et al.*, 2012).

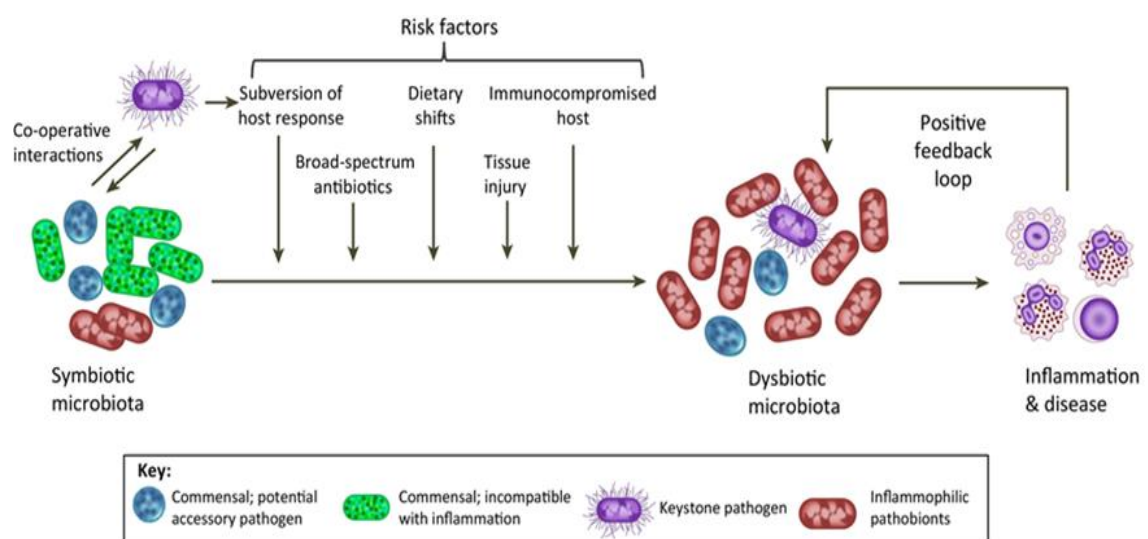


Figure 1.2 Polymicrobial communities under certain conditions could induce inflammation. Keystone pathogens initially subvert host immunity result in dysbiotic microbiota. In this new state, some commensal microorganisms called “pathobionts”

which overactivate the inflammatory response and result in tissue destruction. However, the keystone pathogens initially are aided by accessory pathogens by supporting their colonisation and/or nutrition. Adapted from (Hajishengallis and Lamont, 2016) with permission.

1.2 Role of oral microbiome in health

Commensal interactions among microorganisms permit them to flourish together, and thus conserve biodiversity within the oral cavity. A steady ecological balance is important to maintaining oral health (Ruby and Goldner, 2007, Zaura *et al.*, 2009, Filoche *et al.*, 2010). Hence, any disruption to the commensal microbiota will result in infections by opportunistic pathogens such as infection with *Candida* species and *Staphylococcus aureus* as outcomes of heavy doses of antimicrobials usage (Sullivan *et al.*, 2001). In addition, colonisation by commensal oral microorganisms will prevent disease progression, as all surfaces of the mouth will already be occupied and no more binding sites will be available for adherence of pathogens (Socransky and Haffajee, 1992). Regarding dental caries, some bacteria, such as *Streptococcus salivarius* (alkali producers) utilise arginine and urea to produce ammonia thus aid in maintaining homeostasis, and high expression of urease gene is found to be associated with high acidic conditions (Huang *et al.*, 2014). Furthermore, reduction of nitrate to nitrite from the ingested food by oral bacteria has an anti-hypertensive effect that has been shown to be potentially perturbed by the continual use of antimicrobial chlorhexidine mouthrinses that distinctly reduced plasma nitrite (Govoni *et al.*, 2008, Kapil *et al.*, 2010).

1.3 Bacteriophage

1.3.1 Definition of bacteriophage

Bacteriophage are viruses that infect only bacteria. They are specific for their host cells and completely depend on them for their reproduction, which is why, like all viruses, they are considered obligate intracellular parasites (O'Flaherty *et al.*, 2009). They are abundant all over the world and occur in large numbers in areas occupied by their host, including sewage water, effluent and soil (Hendrix *et al.*, 1999, Wommack and Colwell, 2000). Owing to their ability for rapid reproduction in the presence of ideal host bacteria and their capacity to retain high levels of specificity even when resident in the long term, they are considered the main regulatory factor in maintaining the balance of many

microbial ecosystems (Guttman *et al.*, 2005). For example, phage improves upper-ocean respiration through the release of dissolved organic matter from the lysed bacterial cells that will be utilised by other bacteria (Fuhrman, 1999). Each phage particle consists of a nucleic acid molecule (single or double-stranded RNA or DNA) enveloped in a protein shell, the capsid (Figure 1.3). In spite of carrying the necessary genetic information, they use the host bacterial machinery to generate energy and ribosomes to make their proteins and produce their progeny (Carlton, 1999). Furthermore, bacteriophage are not only found in high concentrations but also exhibit a level of diversity that correlates with the difference in bacterial composition (Suttle, 2005). At the same time, on an individual level they are often specific to certain species, subspecies or even strain but in other examples can infect more than one species of bacteria- such as phage EFDG1 which unusually is specific to *E. faecalis* and *E. faecium* (Khalifa *et al.*, 2015a). Nevertheless, different phage isolates can infect the same strain of bacteria but with varying penetration and infection abilities (Heringa *et al.*, 2010).

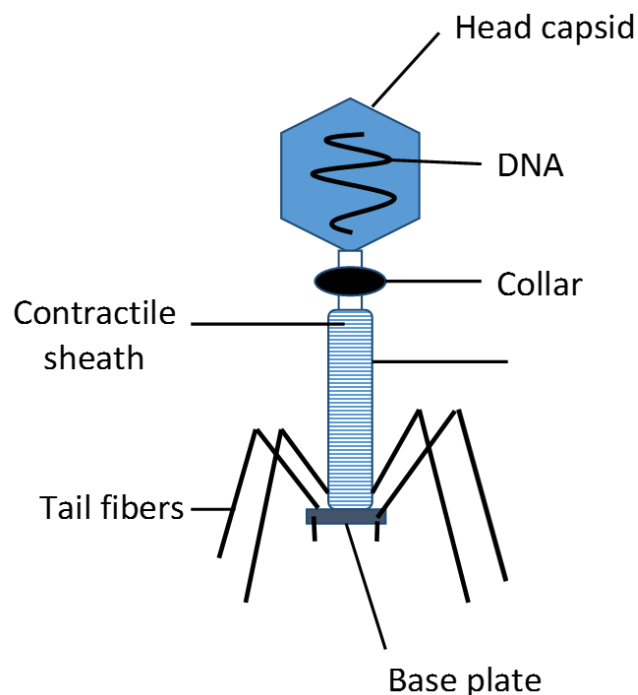


Figure 1.3 Generalised structure of a tailed phage. Adapted from (Elbreki *et al.*, 2014).

1.3.2 History of bacteriophage discovery

Initial observations of bacteriophage, dating back to the late nineteenth-century, were made by two independent scientists, a British bacteriologist named Ernest Hankin and the Russian bacteriologist Nikolay Gamaleya. In 1896, Hankin observed a substance in the Indian river waters of the Ganges and Jumna, which had a bactericidal capability against *Vibrio cholerae* and could pass through fine porcelain filters. Gamaleya reported a similar phenomenon in 1898 while he was working with *Bacillus subtilis* (Duckworth, 1976). Nearly 20 years later, in 1915, while observing similar phenomena, a medically trained British bacteriologist named Fredrick Twort suggested that viruses might cause the bactericidal effect, but his work was interrupted by the onset of World War I and shortage of funding. Almost two years after that, Felix d' Herelle, a French Canadian microbiologist at the Pasteur Institute in Paris, proposed that a virus actually caused this effect by parasitising on bacteria and yielding clear zones of plaques on a lawn of bacterial culture. In addition, he called the virus a bacteriophage or bacteria-eater (from the Greek "phagein" meaning to eat (Sulakvelidze *et al.*, 2001).

In fact, d'Herelle conducted much research concerning this phenomenon during the 1920s, describing the course of bacteriophage growth by means of quantitative plaque assay and quantitative dilution, which attracted scientists worldwide to the new field of bacteriophage research. Furthermore, he realised the importance of eliminating various infectious disease using bacteriophage as therapeutic and prophylactic mediators and called phage "the exogenous agents of immunity" (Sulakvelidze *et al.*, 2001, Summers, 2005).

After the invention of electron microscopy in 1942, phages were clearly identified as viruses (Luria and Anderson, 1942), and since then electron microscopy remains the main test for the morphological identification of bacteriophage (Simon and Anderson, 1967). After ten years, DNA was recognised as the major genetic material in bacteriophage (Hershey and Chase, 1952). In 1969, Nobel Prizes in physiology and medicine were awarded to Max Delbrück, Alfred Hershey and Salvador Luria due to their discoveries of the replication of viruses and their genetic structure.

1.3.3 Classification of bacteriophage

In 1967, Bradley classified bacteriophage according to their morphological characteristics into six basic types including the tailed phages (with contractile tails, long and noncontractile tails, and short tails), small isometric ssDNA viruses, filamentous phages and small ssRNA phages (Bradley, 1967). Four years after that, in 1971, the International Committee on Taxonomy of Viruses (ICTV), classified bacteriophage into six groups: T-even phages, λ , lipid phage PM2, the fXgroup, the "filamentous phage", and the "ribophage group". Groups were listed with type species and properties (Fenner, 1976, Wildy, 1971). Later on, Bradley's morphological classification was implemented by the ICTV and in that era the identified phages numbered about 111 and, for better electron microscopy standardisation, tailed phages were, in 1974, further subdivided into morphotypes (Ackermann and Eisenstark, 1974).

The classification body was formally known as the Provisional Committee on Nomenclature of Viruses (PCNV). It later became the International Committee on Taxonomy of Viruses (ICTV) and is still the only international body concerned with virus taxonomy.

1.3.3.1 Orders and families

Examination of bacteriophage by electron microscopy has been conducted on more than 5500 bacteriophage since the introduction of negative staining in 1959 with phage currently classified in a system of one order and 10 families. Of these 5500, 5360 make up the tailed phages of the order Caudoviridales, which comprises three families characterised by contractile tails, long noncontractile tails, or short tails, and named respectively *Myoviridae* (25%), *Siphoviridae* (60%), and *Podoviridae* (15%) with icosahedral heads. They make up more than 96% of phages and contain dsDNA (Figure 1.4). The remaining 179 characterised phages consist of cubic, filamentous, and pleomorphic viruses represented by seven families of the *Legameniviridales* and several unassigned families of viruses that contain ds or ss DNA or RNA (Ackermann, 2007) (Figure 1.5). These seven families of polyhedral, filamentous and pleomorphic phage are separated by profound differences in nucleic acid and overall virion morphology traits and structure. However, all these families are small, sometimes with just a single representative, and are taxonomically simple. Lipids are contained in the virions of four

groups, while two of them have lipoprotein envelopes (Table 1.1) (Lavigne *et al.*, 2008, Ackermann, 2007).

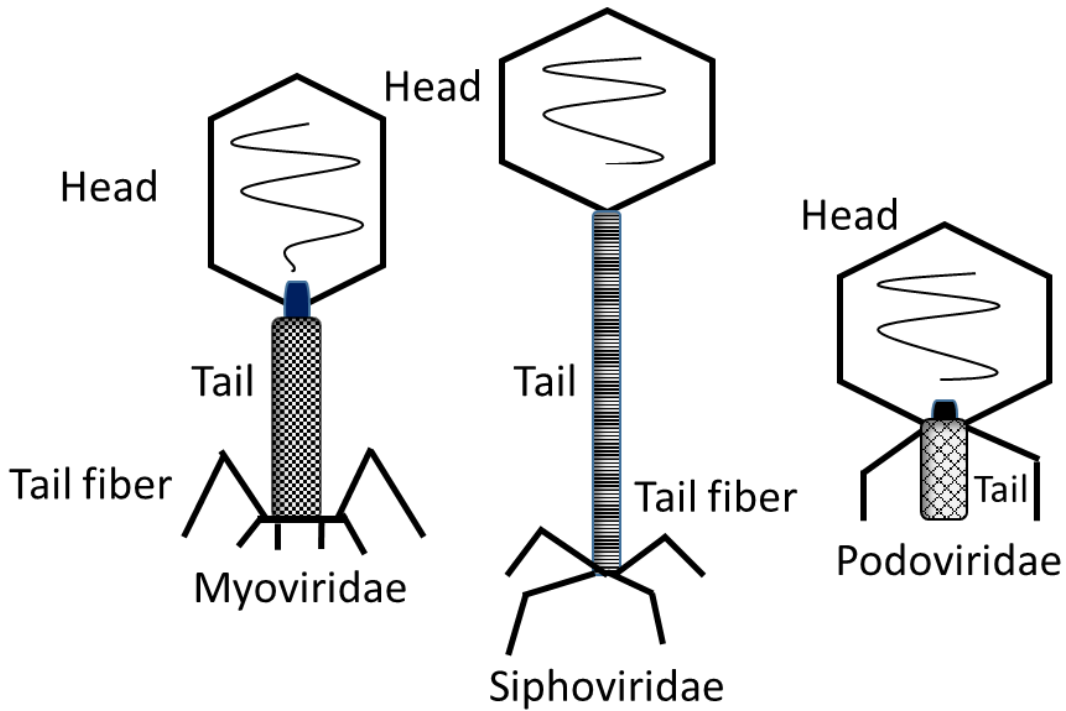


Figure 1.4 The three-tailed phage families Myoviridae, Siphoviridae and Podoviridae. Adapted from (Ackermann, 2007) with permission.

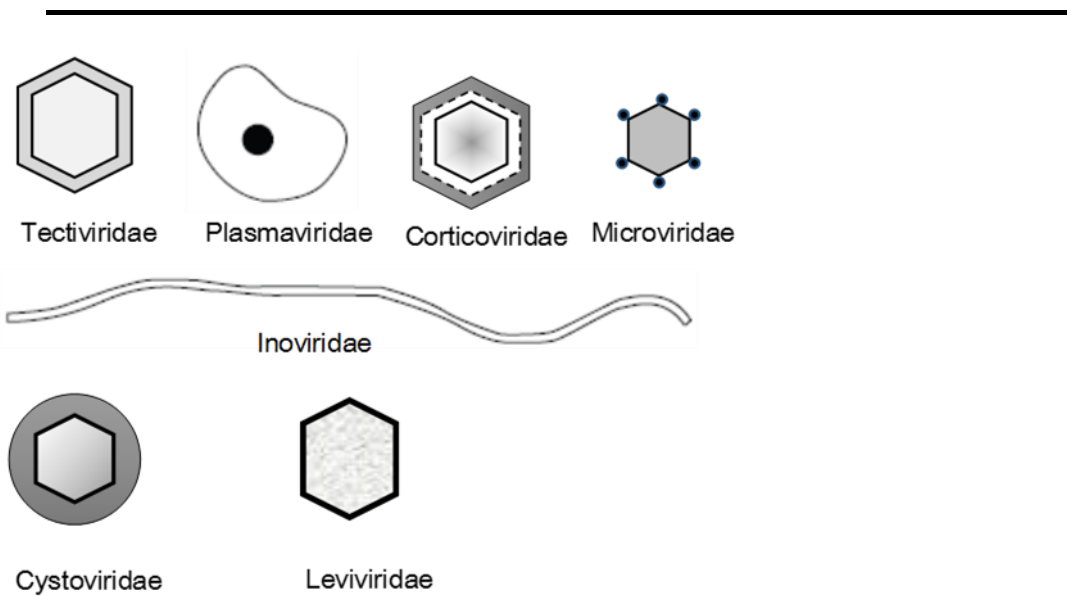


Figure 1.5 The seven families of polyhedral, filamentous and pleomorphic phages. Adapted from (Ackermann, 2007) with permission.

Table 1.1 The ten families of bacterial prokaryotic phages based on morphology and genetic characteristics. Adapted from (Ackermann, 2007) with permission.

Family	Genetic material	Morphology
Myoviridae	dsDNA(L)	contractile long tail, non envelope
Siphoviridae	dsDNA(L)	non-contractile long tail, non envelope
Podoviridae	dsDNA(L)	non-contractile short tail, non envelope
Tectiviridae	dsDNA(L)	double capsid, inner lipid vesicle, pseudo-tail, 60 nm
Plasmaviridae	dsDNA(C)	pleomorphic, lipidic envelope, no capsid, 80 nm
Corticoviridae	dsDNA(C)	complex capsid, lipids, 63 nm
Microviridae	ssDNA(C)	capsid with spike, 27 nm, 12 knoblike capsomers
Inoviridae	ssDNA(C)	filaments or rods, 85–1950 x 7 nm
Cystoviridae	dsRNA(L)	segmented, lipidic envelope, 70–80 nm
Leviviridae	ssRNA(L)	spherical bacteria, 23 nm, like poliovirus
C, circular; L, linear.		

1.3.3.2 Morphology of *Caudovirales*

All *Caudovirales* have heads with icosahedral (20 sides/12 vertices) symmetry or elongated derivatives gathered from multiple copies of specific protein. The phages' head bulk varies in diameter between 45 and 100 nm, depending on the size of phage genome boxed during head assembly (Guttman *et al.*, 2005).

Throughout infection, portal protein, which connects the head and tail structures, undergoes conformational changes that permit the penetration of DNA from the viral core into the bacterial cell. This connector, which is situated at the apex of the phage head, participates in the morphogenesis of new progeny and makes it a vital participant in the phage infection cycle (Valpuesta and Carrascosa, 1994, Agirrezabala *et al.*, 2005).

The tail, base plates, spikes or terminal fibres perform an essential role not only in the attachment of bacteriophage to the host bacteria but also participate in the delivery of phage DNA from the head into the host cell cytoplasm. In the case of phage T2 of the

Myoviridae family the tail sheath contracts, allowing the central tail tube protein to penetrate both the outer cell membrane and cell wall of the host throughout the infection process. On the other hand, the tail of *Siphoviridae* phages remains unchanged during infection, as shown in the phage λ (Leiman *et al.*, 2004). Finally, short-tailed *Podoviridae*, for example T7 phage, form an extensible tail from the ejected internal core proteins, thus providing a passage for the transfer of genome material into the host cell (Molineux, 2001).

1.3.3.3 Bacteriophage life cycles

Phages have two principal life cycles: the lytic and lysogenic cycles. In the lysogenic cycle, phage are able to kill the host or establish a stable long-term sustainable relationship with their host bacteria as temperate phages, during which viral genes that are detrimental to the host are not expressed (Summers, 2001, Strauch *et al.*, 2007). In the lytic cycle, after the initial attachment, the new progeny are released upon cell death, on the timescale of several minutes to hours. The main difference between temperate phage and lytic phage is the presence of integrases in temperate phage that allow their incorporation into their hosts' genome- known as lysogeny (Kaiser and Jacob, 1957). Alternatively, the phage may reside in the host as a stable plasmid (Lehnherr, 2006, Little, 1993, Mardanov and Ravin, 2006, Ravin, 2003), with both forms replicating together with the host's replication and division.

The first contact between the phage and its' host occurs by random collision, when the phage initially binds reversibly and often then irreversibly to a second structure on the bacterial surface (Heller, 1992, Leiman *et al.*, 2000, Makhov *et al.*, 1993). Bacteriophage that infect G-positive bacteria may bind to sugar moieties in the peptidoglycan layer, followed by stronger binding to proteins or other molecules (Monteville *et al.*, 1994, Archibald, 1980), while proteins localised in the outer membrane (e.g. OMPs or flagella) or lipopolysaccharide (LPS) may act as bacteriophage receptors in G-negative bacteria. In most cases, phage require both molecules for adsorption (Prehm *et al.*, 1976). As a rule, injection of DNA follows immediately after the phage is stably and irreversibly adsorbed to the cell surface, with each phage, or phage group having subtly different mechanisms for this process (Anderson, 1948).

In the lytic cycle, the phage undergoes a replication process with the aid of host biosynthetic machinery after it has successfully entered the cell. The new replicates of

phage progeny are then liberated with the help of a holin, a hydrophobic polypeptide that creates pores in the cell inner membrane, and endolysin, which causes lysis to the host cell (Young and Bläsi, 1995, Wang *et al.*, 2000). In the lysogenic cycle, the phage DNA integrates into the bacterial chromosome, becoming what is often known as a temperate phage. Temperate phages often become integrated into bacterial chromosomes by a site-specific recombination mechanism within a short region of perfect homology between host chromosome and phage DNA (Reiter *et al.*, 1989). For example, research on phiC31 showed that DNA deletion near its right end abolishes the phage ability to integrate by site-specific recombination into the *S. lividans* chromosome (Chater *et al.*, 1981, Chater *et al.*, 1982). Integration adjacent to tRNA genes (transfer RNA) flanked by direct repeat sequences and encoding an integrase are also common features of temperate phages. For example, the integrase of phage P4 of *E. coli* and phage P22 that infect *S. typhimurium* catalyse phage insertion into tRNA genes (Pierson and Kahn, 1987). In addition, no phage progeny are produced and the bacterial host cell is not lysed. This is because the integrated phage produce a repressor protein that stops the synthesis of enzymes and proteins needed in the lytic cycle and thus in this incorporated state is often also called a prophage. If the repressor protein stops being produced or is inactivated, an enzyme encoded by the prophage will excise the viral DNA from the bacterial chromosome. The excised DNA will then promote a lytic cycle that end with the lysis of the bacterial cell to release the newly formed progenies (Todar, 2012). Additionally, this mechanism defends the host bacterium from infection by other phages via temperate phage restriction, modification systems and may encode advantageous virulence factors, meaning that between simple lysogeny and carriage of advantageous traits there is an evolutionary selection pressure on lysogeny in many bacterial spp. (Guttman *et al.*, 2005, García *et al.*, 2010) (Figure 1.6).

If the host bacteria that harbour the prophage are subjected to a stressing agent such as UV light, hydrogen peroxide, certain antibiotics like Mitomycin C, or suffer from starvation, prophage can be induced from the host bacterium's genomic material, and its lytic ability is retained (Stevens *et al.*, 2009, Jiang and Paul, 1998, Sandmeier *et al.*, 1995, Lwoff, 1953). These agents usually act by either damaging the DNA or interfering with host replication.

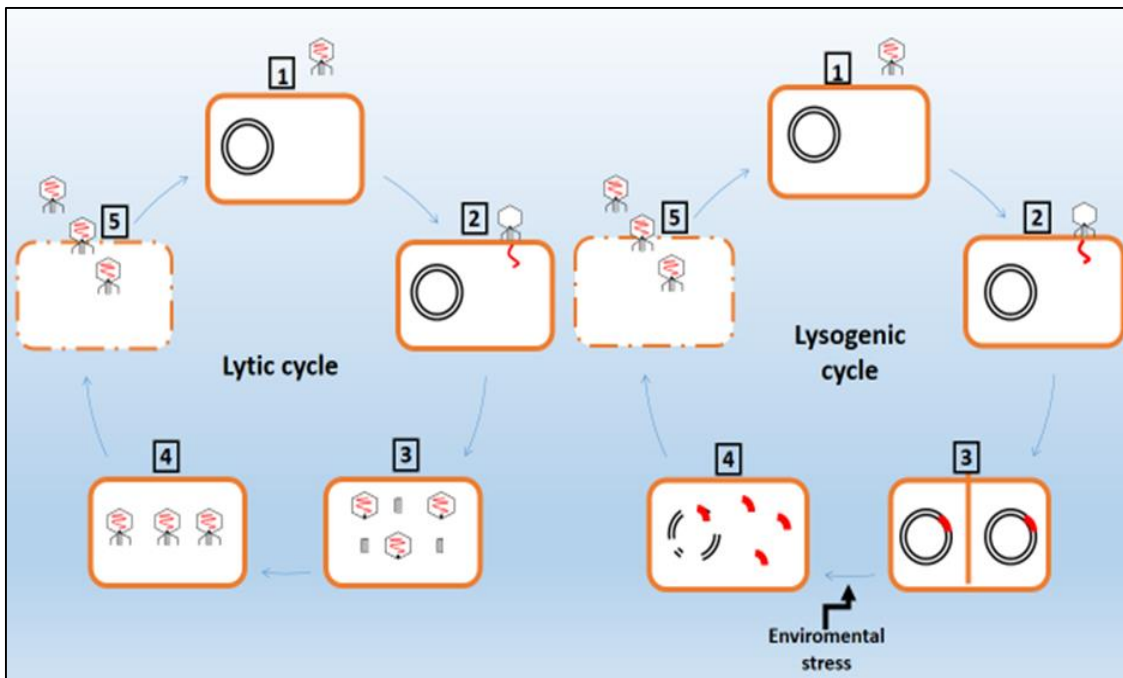


Figure 1.6 The steps of the bacteriophage lytic and lysogenic life cycles. 1.Host recognition, 2.Adsorption and penetration. The Lytic cycle: 3.Replication and synthesis, 4.Phage assembly, 5. New progeny release. The Lysogenic cycle: 3.Viral DNA integrated into host genome, 4.Prophage activation and replication, 5.The host is lysed to release the new progeny. Adapted from (García *et al.*, 2010) with permission to reproduce.

1.3.4 Lytic phages towards orally derived bacteria

In vivo metagenomics studies revealed the presence of a diverse group of phages that inhabited the oral cavity (Edlund *et al.*, 2015). Screening oral samples showed the occurrence of about 10^8 to 10^{10} virus-like particles DNA per millilitre of human salivary samples and per gram of dental plaque respectively (Naidu *et al.*, 2014). Phages belonging to the Siphoviridae family (mostly expected to be temperate phages) dominated this oral viral metagenomic community (Lum *et al.*, 2014, Ly *et al.*, 2014, Pride *et al.*, 2012, Santiago-Rodriguez *et al.*, 2015). However, DNA sequencing of subgingival plaque samples from periodontal disease patients revealed that siphoviruses were replaced by lytic myoviruses (Ly *et al.*, 2014, Santiago-Rodriguez *et al.*, 2015). The predominant prophage hosts belonged to the members of the phyla Actinobacteria, Bacteroidetes, Firmicutes, Fusobacteria, and Proteobacteria (Ly *et al.*, 2014, Naidu *et al.*, 2014, Pride *et al.*, 2012). These studies do not categorise the species targeted by phages because this requires the isolation of phage individually using specific bacterial strain. Therefore, the metagenomic screening needs to be complemented by the isolation of

specific bacterial phage which is proved to be more difficult and challenging (Bachrach *et al.*, 2003, Hitch *et al.*, 2004). Several studies mentioned the isolation of virulent tailed phages that targeted oral bacteria either from oral clinical samples (saliva, dental plaque, and oral washing) or environmental samples (sewage, water) resulting in the isolation of lytic phages towards *Actinomyces* spp. (Yeung and Kozelsky, 1997), *Aggregatibacter actinomycetemcomitans* PAA005 (Castillo-Ruiz *et al.*, 2011), *Streptococcus* spp. (Dalmasso *et al.*, 2015), *Veillonella* spp. (Hiroki *et al.*, 1976), *Neisseria* sp. (Aljarbou and Aljofan, 2014), and *Fusobacterium* spp. (Machuca *et al.*, 2010), with various level of characterisation (Szafranski *et al.*, 2017).

1.3.4.1 *E. faecalis* lytic phages

The vast majority of the well characterised lytic *E. faecalis* phages isolated to date are tailed phages that were isolated using non-orally derived strains of *E. faecalis* and suggested to be used as therapy to eradicate oral *E. faecalis* biofilm associated with endodontic infections (Khalifa *et al.*, 2015a, Khalifa *et al.*, 2016). Sewage were used successfully as a source to isolates phages that targeted non-oral *E. faecalis* phages using samples taken from animal sewage (Son *et al.*, 2010, Fard *et al.*, 2010), hospital sewage (Li *et al.*, 2014), and sewage effluent from treatment facility (Khalifa *et al.*, 2015a, Khalifa *et al.*, 2015b). Thus, phages targeting oral *E. faecalis* bacterial strains could be isolated from wastewater. The isolated tailed phages, either belong to the Myoviridae family e.g. phiEF24C (Uchiyama *et al.*, 2008a), EFDG1 (Khalifa *et al.*, 2015a), and EFLK1 (Khalifa *et al.*, 2015b) or belong to Siphoviridae family e.g. IME-EF1 (Zhang *et al.*, 2013b), IME_EF3 (Li *et al.*, 2014), EFRM31 (Fard *et al.*, 2010a) and EFAP-1 (Son *et al.*, 2010b). Their genomes range from very large size of phiEF24C (142 kbp) to small size genome of FRM31 phage (17 kbp), while the siphovirus *E. faecalis* EfaCPT1 bacteriophage is still uncharacterised. In addition, initial attempts to genetically engineer temperate *E. faecalis* phage phiEf11(vir)^{PnisA} to produce a virulent, highly lytic and wider host range phage were performed successfully (Zhang *et al.*, 2013a, Tinoco *et al.*, 2016).

1.3.5 Bacterial resistance to bacteriophage

Bacteria can develop certain molecular mechanisms to evolve resistance to phages. These resistance mechanisms can occur during any phase of the virus life cycle. It can start in the first step of phage adsorption to the host surface through blocking phage

receptors, producing altered extracellular matrix and production of competitive inhibitors (Hancock and Braun, 1976). This is termed phage adsorption inhibition. One of these mechanisms is the formation or alteration of bacterial capsules, which is known to inhibit the attachment of certain phages (Bernheimer and Tiraby, 1976). Conversely, phages can also evolve and develop counter-measures to degrade capsules (Bayer *et al.*, 1979). For examples, the tailspike proteins (endosialidase) of bacteriophage K1A infecting encapsulated *E. coli* (Jakobsson *et al.*, 2007) and the hyaluronate lyase HylP1 and HylP2 (Hyaluronidases) towards hyaluronate-encapsulated group A streptococci (Smith *et al.*, 2005, Martinez-Fleites *et al.*, 2009). In addition, phage polysaccharide depolymerase action continues within biofilms suggesting them as promising candidates for novel antibiotic supports (Yan *et al.*, 2014).

Injection of the viral genetic materials can be prevented through a process known as injection blocking. The mechanisms of phage-adsorption inhibition and phage-injection blocking are both considered as first lines in bacterial defence against phage infection through preventing the attachment or access of phage genetic materials to the bacterial cell membrane (Coffey and Ross, 2002). Alternatively, bacteria can act to degrade phage DNA post-injection via the action of restriction endonucleases that recognise and destroy foreign DNA, a phenomenon known as restriction-modification. This phenomenon usually starts after successful injection of the Phage genome into the host cell. Bacterial protection of its own genetic material established by methylation at specific points on its DNA sequence will prevent parallel restriction endonuclease cleavage. Restriction results in the cleavage of foreign DNA that does not convey the corresponding methylation configuration (Forde and Fitzgerald, 1999, Coffey *et al.*, 2001). In contrast, phages can evolve certain mechanisms to avoid this resistance, for example, by employing methylase enzymes (Bohannon and Lenski, 2000, Krüger and Bickle, 1983).

Another method of bacterial resistance to phages is termed the abortive infection mechanism, by which the phage progeny repeatedly die before completing the lytic cycle mediated by early bacterial lysis; thus the virus is held back and prevented from multiplying (Klaenhammer and Sanozky, 1985, Hill *et al.*, 1990).

1.3.6 Phage mediated bacterial virulence

Bacteriophages are considered as a tool for mobile genetic element transfer that may play an important role in pathogenicity of certain bacteria in a process called phage conversion. In this route, bacteriophage encoded virulence genes can convert non-pathogenic host bacteria into virulent ones or increase the virulence of certain bacteria by providing mechanisms that might host tissue or avoidance of host immune defences, i.e. provide a selective evolutionary advantage (Figueroa-Bossi *et al.*, 2001, Massignani *et al.*, 2001). In this process, the phage is integrated into the host genome as a stable temperate phage in a process known as lysogenic conversion thus allowing both horizontal and vertical pathogenic gene transfer to the host and therefore clonal expansion. For example the filamentous bacteriophage CTX harbours the *ctxAB* genes which encode the cholera toxin CT and once integrated into the genome results in lysogenic conversion of *V. cholerae* to produce CT toxin (which causes the characteristic ion efflux and effusive watery diarrhoea) and enhance its pandemic spread (Waldor and Mekalanos, 1996). Another example is the bacteriocins of *P. aeruginosa*, which have been derived from two phage-tail gene-clusters (Nakayama *et al.*, 2000). Although it is often the case that the host bacteria benefit- or derive a positive survival advantage due to lysogeny, it is worth mentioning that this is not always true. For example, Chung *et al.* (2014) showed that the expression of a prophage encoded phage Tip protein (D3112 protein gp05) results in loss of surface piliation of the *P. aeruginosa* and, thus decreases its virulence in the model tested. In addition, autolysis caused by lysogeny during stress conditions might provide advantages to the bacterial community by providing nutrients to a starving population, modify the host immune response by the released cell components, and also release free DNA for natural transformation and potential evolution of the entire population (Garcia and Dillard, 2006).

This is further exemplified by phage mediated transduction, in which transformation of genetic traits from donor bacteria to the recipient cell occurs through aberrant DNA packaging into phage particles that infects new cells and via recombination events that new genes are transfer into recipient bacteria. There are two types of transduction: specialised and generalised transduction (Birge, 2000).

In specialized transduction, small segments of bacterial DNA are packaged with the phage DNA materials and transferred to the host bacteria (Ferretti *et al.*, 2001) (Ventura *et al.*, 2002). This usually happens by packaging of bacterial DNA at the

margins of the phage genome, e.g. at *att* sites or adjacent to sites of integration, that are then included by erroneous excision of the phage DNA. Examples of specialised transduction include lysogen associated genes located at the prophage genome ends in several prophages (Johnson *et al.*, 1986). For example, O serotype-converting enzymes of the lysogenic phage SfV, are found near *attL* (temperate phage left end) in *Shigella flexneri* are involved in glycosylation of the type V O-antigen to rhamnose II of the tetrasaccharide repeat through an α 1,3 linkage (Allison *et al.*, 2002). In further examples, many toxin genes are transduced due to their proximity to integration sites of the phage, e.g. staphylokinase and enterotoxin A from serotype F bacteriophages of *S. aureus* (Coleman *et al.*, 1989). Furthermore, the co-packaged genes tend to represent transcription units that are controlled independently from the rest of the prophage (Wagner *et al.*, 2002). In addition, previous studies showed that phage gamma and C1 encode the virulence factors of *Corynebacterium diphtheria* and *Clostridium botulinum*, causing the host to possess a pathogenic phenotype (Freeman, 1951, Barksdale and Arden, 1974). Researchers have found phage-like modules in the bacterial genomic structure, as 3-10% of the bacterial genome comes from prophages (Canchaya *et al.*, 2003, Casjens, 2005). Some of those modules are defective prophages that cannot replicate (Hayashi *et al.*, 2001); others might constitute gene transfer agents that are phage-like particles that assemble bacterial DNA (Humphrey *et al.*, 1997).

In generalised transduction, phage heads usually contain bacterial DNA packaged from any chromosomal location during the synthesis of new phage progeny. These phages are non-infectious, meaning that they can inject their nucleic materials into recipient cells but will not replicate (Sternberg and Maurer, 1991). Their genomic materials can be lost if not combined with the host chromosome, but may be expressed transiently (abortive transduction), but if the DNA that recombines carries an advantageous trait- such as antibiotic resistance then it will be selected for evolutionarily and maintained. Finally, plasmid transduction can also take place when plasmid genetic materials are packaged into transducing phages. The *Vibrio* pathogenicity island (VPI), which contains the gene coding for the receptor of the cholera toxin encoding filamentous phage CTXphi, can be conveyed between *Vibrio cholerae* strains of the O1 serogroup via the generalised transducing phage CT-P1 (O'Shea and Boyd, 2002).

1.3.7 Medical importance of bacteriophages

In the past decades, there has been a dramatic increase in infections caused by multidrug resistant bacteria or superbugs, caused by excessive usage and the failure to follow the full dose regime throughout the time for which the antibiotics should be administered. The problem of bacterial resistance to antibiotics is considered a significant threat to human health (Huys *et al.*, 2013). In parallel, there has been an annual increase in the number of antibiotic prescriptions and public access to non-prescription and over the counter antibiotics (in underdeveloped countries). Furthermore, half of these antibiotics used are usually associated with wrong diagnoses where bacteria are not the major cause, and thus the ailment should not be treated with the prescribed drugs (Kutateladze and Adamia, 2010). In addition, this problem has a great economic impact annually due to extra health care costs and loss of productivity (Roberts *et al.*, 2009). Much damage has already occurred and better education on the proper usage of these drugs is considered a far-off prospect in some countries. Meanwhile, we know that the situation is getting worse and there are now few drugs left with which to treat multidrug-resistant bacterial strains effectively.

Alternatively, the use of bacteriophage as a therapeutic approach against bacterial pathogens without harming the majority of harmless, commensal bacteria has gained interest in the past years, especially now that multidrug resistant and biofilm associated bacterial infection has become a permanent issue.

1.3.7.1 Characteristics of bacteriophages as therapeutic agents

Unlike antibiotics, which change the normal equilibrium of the bacteria balance in the body due to their broad spectrum, Bacteriophages are highly specific to their host. They can attack only one type of bacterial species (monovalent) or they can target two or more bacterial species (polyvalent- although this is rarer) (Kalmanson and Bronfenbrenner, 1942). Since the other species of bacteria in the body are not involved in phage treatment, they will not develop unwanted resistance, unlike in the case of antibiotics (Sulakvelidze *et al.*, 2001). In addition, some bacteriophages possess the ability to enter and degrade extracellular biofilm matrix using specific enzymes and to eliminate the incorporated bacterial cells within the biofilm (Lacroix-Gueu *et al.*, 2005).

Because bacteriophages are the most abundant natural organisms on earth, to which most people are routinely exposed, and their host bacteria form part of normal

gastrointestinal microbiota in humans, it has been deduced that they can be well accepted by humans as therapy against bacterial infection (Sulakvelidze *et al.*, 2001, Häusler, 2006). In order to liberate their new-formed progeny inside the host, Bacteriophages lyse the specific bacterial cell wall and eliminate it, which causes the release of new bacteriophage virions. When the targeted bacteria are sufficiently reduced in numbers and density drops below the detection threshold, the bacteriophages are removed by the reticulo-endothelial system and concentrated in the spleen (Keller and Engley, 1958, Huys *et al.*, 2013) with the phage intervention becoming self-limiting- as removal of the pathogen by phage and our immune systems removes the phage host and so the phage no longer persists. In contrast, the dosage of antibiotics needs to be consistent so that the therapeutic concentrations at the site of infection can work properly (Clark and March, 2006).

In the human body, phages have several proposed functions, through controlling bacterial overgrowth, bacteriophages can return the host–bacteria balance to normal, subsequently restoring physiological functions (Huys *et al.*, 2013). Phages are also suggested to be used as a vehicle for transporting specific molecules (Clark and March, 2004) and to deliver DNA or antimicrobial substances (Russel, 1995, Goodridge *et al.*, 1999). This proposal is based on their demonstrated ability to circulate around the body successfully and to reach a wide range of potential infection sites (Haq *et al.*, 2012, Dabrowska *et al.*, 2005), even across the brain-blood barrier (Tanji *et al.*, 2005).

Since lytic phages do not have the ability to integrate with the genomic materials of the host or to eradicate their host in a short time, there is less likelihood of their conducting virulence factors from one bacterial cell to another, and therefore they offer higher potential in the treatment of pathogenic bacteria (Brüssow, 2005). Furthermore, polyvalent phages, which have lytic potential against more than one type of pathogenic bacteria, can be manipulated to treat various kinds of infections (Verma *et al.*, 2013). In order to improve the safety of phage therapy, bacteriophage should preferably be amplified in non-pathogenic bacterial strains (Bielke *et al.*, 2007).

Based on the above characteristics and recent developments in phage scientific research together with standard superior control measures used in the production process, bacteriophages exhibit strong potential as therapeutic agents, and non-antibiotic therapy could become a reality in the proximate future (Elbreki *et al.*, 2014).

1.3.7.2 Bacteriophages as therapeutic agents

Bacteriophage were suggested as antibacterial agents in infectious diseases in the early twentieth century, when Felix D'Herelle tested them against bacillary dysentery infections (d'Herelle, 1917). These tests were followed by several trials to treat *Staphylococcus* infections (Brunoghe and Maisin, 1921), typhoid fever (Davison, 1922), and cholera (Morison, 1932). After that, the first broad review concerning the use of this therapy was published in 1934 (Eaton and Bayne-Jones, 1934).

During the 1940s, antibiotics were discovered and were subsequently seen as an easier approach to combating infection, given that the success of phage therapy had been limited. The new multipurpose broad- spectrum antibiotics could be used without identification of the pathogenic organisms causing the disease. In addition, antibiotics were easier to formulate and were more stable medicinal preparations, meaning that they were more practical in terms of storage and delivery, rendering antibiotics a more favourable therapy at that time. Whilst phage therapy research soon became less abundant in Western countries, it did continue in Eastern European countries such as Poland and the Ex-Soviet Union (Haq *et al.*, 2012, Bull *et al.*, 2002). Many research papers describing the successful use of phages as therapeutic agents were published in these countries (often not in English). In addition, phage therapy was part of routine healthcare in these places and several phage preparations against the most common human pathogenic bacterial strains were available on the market as late as the 1970s (Clark and March, 2006, Summers, 2001). Indeed, the Bacteriophage Institute in Tbilisi (now the George Eliava Institute of Bacteriophage, Microbiology and Virology) is still researching phage therapy applications and sells phage for the treatment of various bacterial based infections (Summers, 2001, Parisien *et al.*, 2008).

In recent years, the western science community has regained interest in phage research and is considering its clinical usefulness, mainly due to the lack of development of new antibacterial drugs by the pharmaceutical industry. In addition, there has been an increase in the incidence of multi-drug resistance organisms and biofilm associated bacterial infections (Sulakvelidze, 2005), such as *Pseudomonas* spp. (Ahmad, 2002), vancomycin-resistant *Enterococci* (Biswas *et al.*, 2002), multidrug resistant *Klebsiella pneumoniae* (Vinodkumar *et al.*, 2005), multidrug-resistant *Pseudomonas aeruginosa* (Yang *et al.*, 2010, Wright *et al.*, 2009), antibiotic-resistant strains of *Escherichia coli* (Viscardi *et al.*, 2008), and methicillin-resistant *Staphylococcus aureus* (Mann, 2008).

Since in some cases, infections may be caused by more than one type of bacterial strain/species and to overcome the possibility of bacterial resistance (Duckworth, 1976), a phage cocktail has usually been used successfully to overlap and target the pathogen(s) of concern in most clinical trials, meaning that the causative bacteria should be identified first (Clark and March, 2006). Typically, whole-phage preparations may contain a small number of phage strains, each with a broad range of activity or, alternatively, the phage may be applied as a mixture of several phages which have been previously identified for application regarding certain infections. This approach is largely based on the phage preparations used throughout the former Soviet Union.

The first recent clinical studies are from Polish reports, the first report being published in 1984 and dealing with infections caused by suppurative bacterial infections in children caused by *Staphylococci*, *Klebsiella*, *Escherichia*, *Proteus*, and *Pseudomonas* bacteria, with a success rate of 95.6% (Slopek *et al.*, 1984). Following this, another report described clinical observations of 500 patients for five years (1981-1986), but dealing with antibiotic resistant bacteria and various routes of administration (oral, external, on wound and with drops), where 92% of the cases were treated successfully (Slopek *et al.*, 1987). Later on, a combination of antibiotic-phage preparations was used by the same research group to treat antibiotic resistant septicaemia, with 85% of the infections being cured (Weber-Dabrowska *et al.*, 2003).

During the last decade, a more reliable monitoring system parallel with standards of the EU and FDA, under the Declaration of Helsinki and supervised by the centre with responsibility for phage therapy preparations, has been established in Poland. Just under half of the cases were treated successfully but the samples used were all antibiotic resistant clones from chronic infections where all other treatments available had failed previously, meaning that the improvement to quality of life given the complexity of these cases was massive and if used on more routine cases may actually reduce the need for antibiotics (Brüssow, 2012).

Phage therapies performed at the Eliava Institute for Bacteriophage, Microbiology and Virology in Tbilisi, Georgia have been based upon phage cocktails. Each cocktail was directed towards selective pathogenic groups of bacteria (Gill and Hyman, 2010). Two main types of cocktails have been used, the first being directed against pus-causing infections caused by *S. aureus*, *E. coli*, *P. aeruginosa*, 2 *Proteus* species, and several species of *Streptococcus* and called *Pyophage*. The second, which is called *Intestiphage*,

targets infecting strains of *S. aureus* and *P. aeruginosa* of human gut origin and 23 different enteric bacteria that cause diarrhoea and other gastrointestinal upsets (Kutter *et al.*, 2010). These mixtures are not fixed preparations but are subject to continuous updating parallel to infections caused by new pathogen strains (Abedon *et al.*, 2011). A summary of some studies conducted in the former Soviet Union and their results are illustrated in Table 1.2. New products in the form of tablets targeting the pathogens causing dysentery (caused by *Shigella*) and *Salmonella* as well as new specific preparations targeting *Salmonella typhi* (causing typhoid) were added recently in 2008 (Abedon *et al.*, 2011).

Finally, phage therapy has been employed successfully in the treatment of leg ulcers infection caused by *P. aeruginosa* by at a Texas clinic (Clark and March, 2006). Furthermore, a recent private London clinic trial reported a complete post-infection clearance of chronic otitis caused by human *Pseudomonas* ear infection. All the previously mentioned successful clinical trials are indicative of the promise offered by phage therapy (Wright *et al.*, 2009).

Table 1.2 Some human phage therapy studies performed in the former Soviet Union.

Adapted from (Abedon *et al.*, 2011).

Refrence	Target organisms	Disease	Success	Details
Markoishvili <i>et al.</i> (2002)	<i>E. coli</i> <i>Proteus</i> <i>Pseudomonas</i> <i>Staphylococcus</i>	Ulcers and wounds	70%	Healing associated with reduction or elimination of target organisms in 22 patients with ulcers
Perepanova <i>et al.</i> (1995)	<i>E. coli</i> <i>Proteus</i> <i>Staphylococcus</i>	Acute and chronic urogenital inflammation	92%, 84%	92% marked clinical improvement; 84% bacteriological clearance
Miliutina and Vorotyntseva (1993)	<i>Salmonella</i> <i>Shigella</i>	Salmonellosis		Phages versus combined phages and antibiotics was examined with combination effective but not antibiotics alone
Bogovazova <i>et al.</i> (1992)	<i>K. ozaenae</i> <i>K. pneumoniae</i> <i>K. rhinoscleromatis</i>			Adapted phages used; treatment reportedly effective
Sakandelidze (1991)	<i>Enterococcus</i> <i>E. coli</i> <i>P. aeruginosa</i> <i>Proteus</i> <i>Staphylococcus</i> <i>Streptococcus</i>	Infectious allergoses	86%	Phages only, n = 360, 86% success; antibiotics only, n = 404, 48% success; antibiotics plus phages, n = 576, 83% success
Kochetkova <i>et al.</i> (1989)	<i>Pseudomonas</i> <i>Staphylococcus</i>	Post-surgical wounds	82%	Cancer patients; treatment was successful in 61% of antibiotic only treatment
Anpilov and Prokudin (1984)	<i>Shigella</i>	Dysentery (prophylaxis)		Double-blinded; ca. 10-fold lower incidence of dysentery in phage-treated group

1.3.7.3 Phage endolysins as therapeutics

Researchers have started to investigate the potential of using phage peptidoglycan-degrading enzymes, also known as murein hydrolases or endolysins (lysins). Those enzymes are called endolysins due to their effect from the inside to lysis of the host bacterial cells at the end of the lytic cycle (Jado *et al.*, 2003). Endolysins are formed in the late stage of the lytic cycle but for them to gain access to the cell wall an enzyme called holin is needed, which is a lysis factor that provides permeability of the plasma membrane (Fischetti, 2005). In order to release the newly formed virus progeny, both enzymes gather in the cytosol of the host cell at the end of the lytic cycle, with holin protein forming holes in the cell plasma membrane to enable the endolysin to enter and reach its receptors in the peptidoglycan (Young and Bläsi, 1995, Yang *et al.*, 2010) (Figure 1.7). The activation of holin apparently occurs at certain genetically defined times when the newly formed virions reached their threshold numbers. This model based upon secretion of enzymatically active endolysin and the λ lysis system (phage λ that infect *E. coli*) is the best example of this system (Young *et al.*, 2000). However, secretions of enzymatically inactive endolysins into the periplasm or murein layer were also observed in phage that infect both G-positive and G-negative hosts. A study on endolysin Lys44 from phage fOg44 that infects the *Oenococcus oeni* showed that it accumulates in an inactive state in the murein layer until the proper moment for lysis to occurs mediated by holin (São-José *et al.*, 2000). Another example are the endolysins of *E. coli* phages P1 (Lyz^{P1}) and 21 (R²¹) that accumulate at the periplasm of the host cells in inactive forms tethered to the cell membrane until the lysis time, which is imposed by holin (Xu *et al.*, 2005).

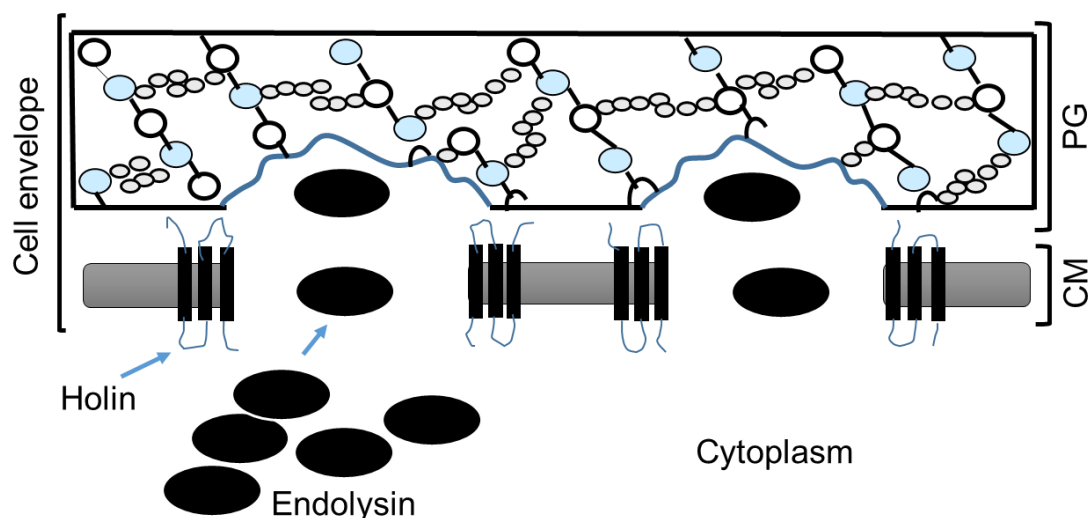


Figure 1.7 Schematic representation of the modular structure. Access of the endolysin to the peptidoglycan (PG) layer is often aided by insertion of the holin into the cytoplasmic membrane (CM). Adapted from (Elbreki *et al.*, 2014).

If purified and applied, lysins are potent peptidoglycan-degrading enzymes against G-positive bacteria, even from the outside, as the outer membrane structure of G-negatives in theory prevents access of exogenous G-negative endolysins (García *et al.*, 2010). Like phages, lysins are specific but their specificity extends to single or a few species rather than single isolates (Yoong *et al.*, 2004). In contrast to phages, resistance to lysins appears unlikely to occur due to their well-maintained and stable fundamental peptidoglycan structure (Fischetti, 2008), and until now no lysin resistant strains have been recognised (Fischetti, 2005). However, their effect is reduced when bacteria reach the stationary phase due to changes to the peptidoglycan layer (Pritchard *et al.*, 2004). Using those enzymes successfully has led scientists to consider phage lysins as "enzymotics" (Nelson *et al.*, 2001).

The pioneer of endolysin antibacterial research is arguably Vincent Fischetti, whose group, 40 years ago, showed that the streptococcal lysin encoded by phage C1 is specific for groups A, C, and E streptococci (Loeffler *et al.*, 2001, Nelson *et al.*, 2001). The Fischetti group also focused on lysins derived from phage γ of *B. anthracis*, which was found to be effective not only against the cells but also against the germinating spores of *B. anthracis* (Celia *et al.*, 2008, Wang *et al.*, 2009). In the genus *Enterococcus*, the lysin PlyV12 was found to have a broad spectrum of activity that involved in addition its hosts, streptococci and staphylococci (Yoong *et al.*, 2004).

Application of lysins to G-negative bacteria has been shown to be possible only after the treatment of the outer membrane with EDTA or by the combination of hydrophobic amino acids with the lysin, as developed by the Lavigne group in Belgium against *P. aeruginosa* (Walmagh *et al.*, 2012, Briers *et al.*, 2011). Both methods allow the transfer of the enzyme across the outer membrane.

Recently the potency of endolysins in eliminating bacterial biofilm has been investigated, suggesting an additional advantage over conventional antibiotics (Son *et al.*, 2010a, Fenton *et al.*, 2013). While biofilm of *S. pyogenes*, or Group A *Streptococcus* showed resistance to antibiotics, the biofilm matrix was readily destroyed by the lytic actions of PlyC endolysin (Shen *et al.*, 2013). Domenech *et al.* (2011) showed that the phage lysozymes Cpl-1 and Cpl-7 encoded by either *S. pneumoniae* phages were very effective in disintegrating *S. pseudopneumoniae* and *S. oralis* biofilms.

1.4 Dental caries

Dental caries is a microbial disease that results from acid dissolution of the mineral structure of teeth (enamel and dentin) produced by oral bacterial metabolism of dietary carbohydrates. Accumulation of acid-producing microbial colonies in mature dental plaque on teeth will lead to loss of the buffering capacity of saliva and change the environment towards acid producing pathogens (Selwitz *et al.*, 2007, Ling *et al.*, 2010). As sustained reductions in pH continue as a result of dietary carbohydrate fermentation (e.g. sucrose), more acid by-products are produced that destroy dental hard tissue. The targets of this acid are primarily the enamel of the crown or cementum of the root, and underlying dentin (Figure 1.8).

Dental caries, or “tooth decay”, has been recognised as the most common chronic disease with 60-90% of children and almost 100% of adults worldwide being affected by dental caries at some point (WHO, 2012). Generally, in order that dental caries develop clinically, three factors should be present over a considerable period of time: tooth structure as substrate, acidogenic bacteria, and fermentable carbohydrates for the bacteria to digest (Touger-Decker and Van Loveren, 2003). However, initial lesions of dental caries can be prevented and reversed with good oral hygiene, proper diet, and fluoride exposure, which enables restoration of the mineral back into the teeth surfaces (Selwitz *et al.*, 2007).

The chief cariogenic initiator of caries on tooth enamel has historically been earmarked as *Streptococcus mutans*, with lactobacilli spp. being associated in advanced lesions of dental caries (Tanzer *et al.*, 2001, Parisotto *et al.*, 2010, Simon-Soro *et al.*, 2013, Simón-Soro and Mira, 2015). These various species reside in biofilm on tooth surfaces. However, other bacteria are now known to be present at higher incidences in rampant caries of primary teeth dental plaque in children than in caries-free children. These include species of *Streptococcus*, *Veillonella*, *Actinomyces*, *Granulicatella*, *Leptotrichia*, *Thiomonas*, *Bifidobacterium*, and *Prevotella* (Becker *et al.*, 2002, Kanasi *et al.*, 2010, Tanner *et al.*, 2011). More considerably, certain gene expression (acid production, DNA uptake, and stress responses) were found to be high in the plaque of caries-active persons (Belda-Ferre *et al.*, 2012). Thus, a new picture has developed in which complex bacterial communities appeared to be related with dental caries (Mira *et al.*, 2017). This is supported by the fact that *S. mutans* accounted for <1% of the bacterial community sampled from dental caries lesions in both DNA-(Gross *et al.*, 2012) and RNA-based studies (Simón-Soro *et al.*, 2014).

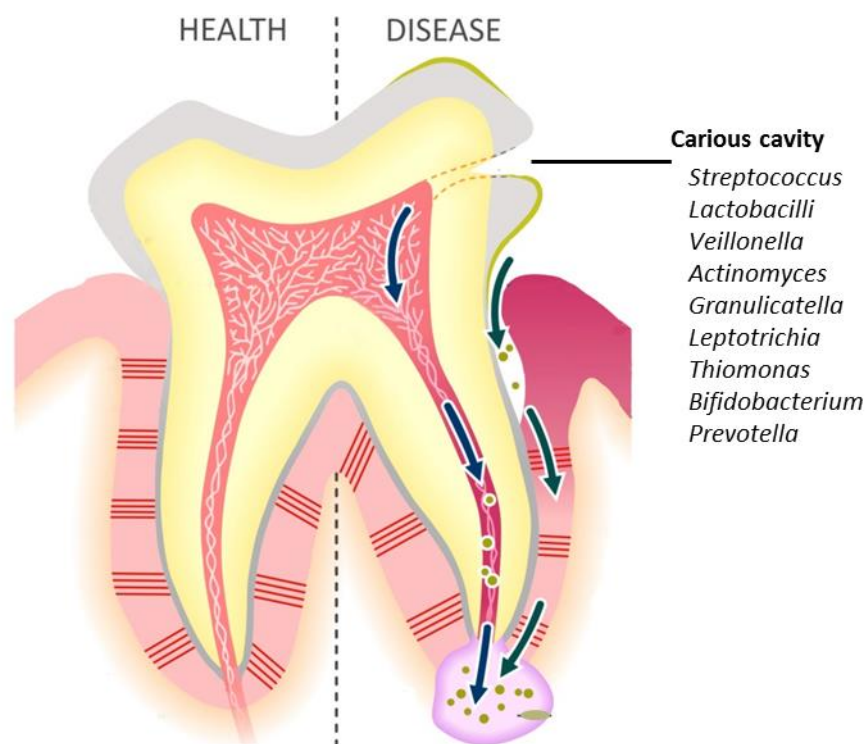


Figure 1.8 Schematic representation of carious cavity and bacterial species associated with dental caries. Dental caries results from acid dissolution of the mineral

structure of teeth (enamel and dentin) produced by oral bacterial metabolism of dietary carbohydrates. Adapted from (Douglas *et al.*, 2014).

1.5 Endodontic and periapical infection

If dental carious lesions are left without treatment, the infection will reach the tooth pulp (which harbours the nerve and vascular supply) as the result of cariogenic bacteria proliferation accompanied by continuous demineralisation (Zero *et al.*, 2011). Eventually, a pulp abscess will be formed as a result of pulpal tissue necrosis followed by dissemination of the infection through the root apical foramen to the area surrounding the root tip to form a periapical infection (Siqueira and Rôças, 2013) (Figure 1.1).

Many microbiological studies have been conducted in order to discover more about endodontic pathology and have shown that the outcome of endodontic treatment is significantly influenced by bacterial persistence in the root canals, especially at the time of filling (Heling and Shapira, 1978, Sjögren *et al.*, 1997, Waltimo *et al.*, 2005, Fabricius *et al.*, 2006). Bacteria detected throughout treatment survived both chemomechanical procedures and intracanal medication (such as calcium hydroxide) or gained access into the root canal via improper temporary restoration (Siqueira and Rôças, 2008). The logic behind endodontic therapy is to eliminate the infection, to prevent microorganisms from infecting or re-infecting the root and/or periradicular tissues (Chavez De Paz *et al.*, 2003). Ideally, chemomechanical procedures and intracanal medication used in treatment procedures should eliminate all living microorganisms present in the entire root canal system. However, due to the complex anatomy of the root canal system, the achievable goal is to reduce bacterial populations to a level below that required to induce disease (Siqueira and Rôças, 2008).

1.5.1 Persistent and secondary infection

Most scientific evidence shows that microorganisms (in addition to many chemical and physical factors) are essential for the progression and spread of diverse forms of apical periodontitis and infection of the dental root canal system (Molander *et al.*, 1998, Pinheiro *et al.*, 2003, Machado de Oliveira *et al.*, 2007, Gomes *et al.*, 2008). The detection of bacteria in the root canal of treated teeth is either due to some bacteria persisting throughout treatment (persistent infection) or as a result of reinfection

(secondary infection). Persistence of endodontic infection is most commonly due to complications associated with or during initial endodontic treatment. Inadequate aseptic control, poor access cavity design, missed canals, inadequate instrumentation, and leaking temporary or permanent restorations are examples of procedural pitfalls that may result in endodontic post-treatment disease (Ørstavik *et al.*, 1998). Pathogens can be established and survive in a particular environment if circumstances are favourable to their growth. In addition, microorganisms have evolved particular strategies that increase their ability to find, compete and survive in these new harsh environments throughout genetic exchange and mutation (Sundqvist and Figdor, 2003). The success rate of endodontic therapy is higher in vital (noninfected) teeth than in teeth with preoperative apical periodontitis lesions, which indicates that persistent infection plays a much more important role as the routine cause of root canal treatment failure (Sjögren *et al.*, 1990, Chugal *et al.*, 2003, Ørstavik *et al.*, 2004, Marquis *et al.*, 2006). However, research has identified secondary infection due to coronal leakage as the cause of after treatment apical periodontitis (Saunders and Saunders, 1994, Ray and Trope, 1995). For bacteria to withstand endodontic treatment, they have to survive not only the chemomechanical procedures and intracanal medication but also they have to adapt to the extremely different environment. To do so, bacteria can form biofilms that adhere to the walls of the tooth root canal that provide antimicrobial resistance (Distel *et al.*, 2002). In order to survive intracanal instrumentation and irrigation procedures, bacteria can be present deep inside dentinal tubules away from the reach of endodontic therapy (Siqueira and de Uzeda, 1996). In addition, anatomical sites and irregularities such as lateral canals, ramifications, and isthmi will provide that protection. Tissue fluids and organic matter could interact with antimicrobial agents and deactivate antibacterial action as a result of dilution of medications concentrations and increasing serum protein (albumin) concentrations (Haapasalo *et al.*, 2007). In addition, dentin collagen found to be a potent inhibitor of chlorhexidine and potassium iodide (Portenier *et al.*, 2002). Furthermore, calcium hydroxide used as intracanal medicament can be resisted by microorganisms such as *E. faecalis* (Byström *et al.*, 1985) and *Candida albicans* (Waltimo *et al.*, 1999b). On the other hand, the persistence of intraradicular pathogens in obturated root canals indicates that they are able to adapt to a new harsh environment with reduced nutrient availability. Microleakage remains one of the major routes by which nutrients can seep through the tight seal of endodontic filling, coming from saliva coronally or apically and laterally from inflammatory exudates (Siqueira, 2001).

1.5.2 Endodontic infection treatment

Chemomechanical instrumentation of the root canal with necrotic pulp tissue removal and disinfection are considered as non-surgical canal treatment. Hence, restoration of the seal barrier between the open oral cavity and periapical tissue is achieved through final sealing of the root canal with bacteria-tight material and proper coronal sealing with primary or permanent restoration (Siren *et al.*, 1997, Siqueira, 2001). The aim of chemomechanical preparation is to remove necrotic pulp tissue and infected dentine in parallel with the application of antimicrobial irrigation in order to eliminate the bulk of the microorganisms from the root canal. Interappointment antimicrobial dressing, commonly calcium hydroxide, might be considered to kill the microorganisms that persist after the initial treatment, followed by obturation if a satisfactory disinfection of the root canal system is achieved (Waltimo *et al.*, 2005). An effective disinfectant, which possesses a wide antimicrobial spectrum even in low concentration, is used as root canal irrigation during endodontic treatment is sodium hypochlorite (Waltimo *et al.*, 1999a, Zehnder *et al.*, 2003). In cases where the treatment is not followed to acceptable standards due to inadequate procedural protocol, failure will occur as a result of intracanal endodontic infection (Sundqvist *et al.*, 1998). If the treatment or retreatment is difficult (fractured instruments, ledges, blockages, filling material impossible to remove, etc.), periradicular surgery will be considered (Gutmann and Harrison, 1985).

1.5.3 Pathways of infection

There are six main pathways by which various microorganisms can reach the tooth pulp (Figure 1.9). The classic way is through progression of the carious lesion reaching close to the pulp. Here the bacteria at the boundary of the carious lesion gain access through dentinal tubules when the dentin distance to the pulp is 0.2 mm (Dahlén and Möller, 1992). Another route is by traumatic exposure of the tooth pulp to the septic oral environment caused by accidental coronal fracture. In periodontitis, deep pocket or gingival sulcus microorganisms may reach the pulp chamber through the periodontal membrane, using a lateral channel or the apical foramen as a passageway (Bammann and Estrela, 2009). The same pathway might conduct pathogens from an infected adjacent tooth to spread through surrounding tissue (Dahlén and Möller, 1992, Bammann and Estrela, 2009). Bacteria from the blood could be attracted to inflamed tooth pulp (called anachoresis) caused by trauma or operative procedure without dental pulp exposure. This might happen during a transient bacteremia that may arise for any reason during a usual

day of a healthy life (Torabinejad *et al.*, 1990). Finally, bacteria in saliva might reach the periapical tissue from the occlusal aspect during intervals between endodontic appointments, even in canals obturated with guttapercha and sealer, mainly caused by a broken temporary seal of faulty restoration or if the tooth structure fractures before final restoration (Torabinejad *et al.*, 1990).

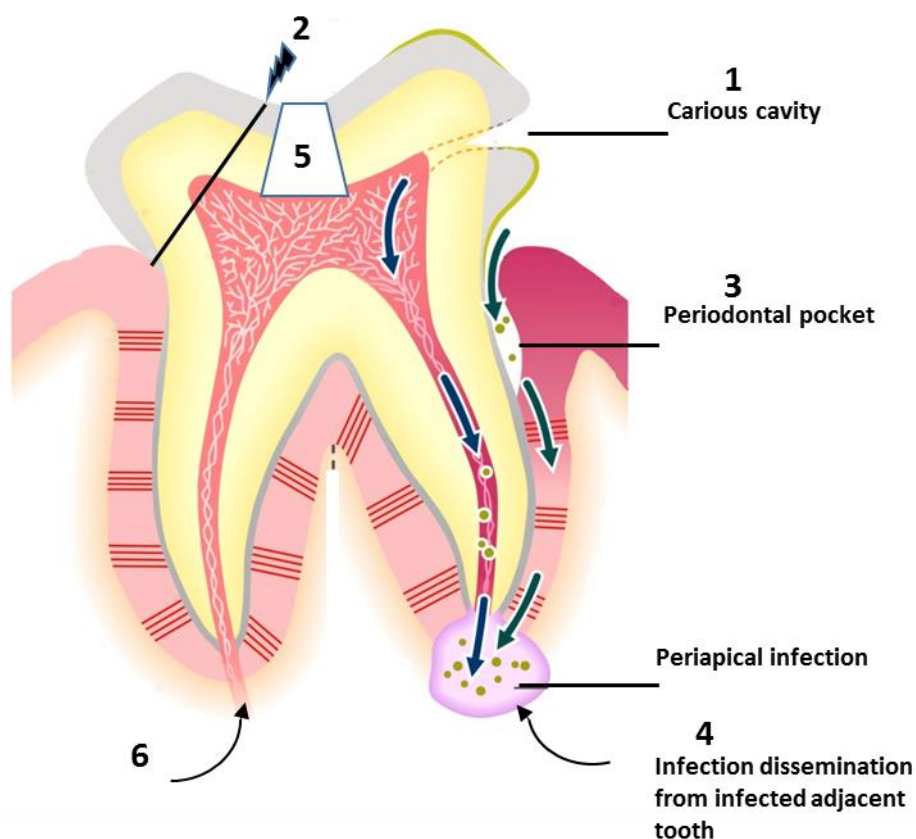


Figure 1.9 Diagram showing various possible pathways by which microorganisms could reach the tooth pulp. 1) Cariou lesion, 2) Traumatic exposure, 3) Deep pocket, 4) Infected adjacent tooth, 5) Broken temporary seal, and 6) Bacteria from the blood. Adapted from (Douglas *et al.*, 2014).

1.5.4 Pathogens associated with intraradicular and extraradicular infections

Many stages have to be passed through before microorganisms can settle at the root canal. After breaching the enamel and spreading through the dentin, they have to leave the nutritionally rich and more hospitable environment of the oral cavity, overcome

the immune response inside the pulp, resolve and compete with other microbes in the remaining necrotic tissue within the root canal (Narayanan and Vaishnavi, 2010). Finally, microbes will induce an inflammation at the root apex resulting in apical periodontitis. Endodontic infections, as with most oral infections have a polymicrobial nature; hence, in primary intraradicular endodontic infection, obligate anaerobic bacteria are clearly the most frequently isolated microorganism (Shah and Collins, 1990). Certain ecological determinants play an important role in the selection of specific root canal microbiota, the first being oxygen and oxygen generating products, as the development of a low reduction–oxidation potential by the primary colonisers favours anaerobic bacteria. This is not surprising because carbon dioxide and hydrogen are produced as bacterial by-products of continual depletion of oxygen levels (Glick *et al.*, 1991, Sunde *et al.*, 2002, Slots, 2005). Second is availability of nutrients; degenerating connective tissue (Slots, 2005), dentinal tubule contents, or a serum-like fluid from periapical tissue in addition to oral cavity derived nutrients select for the growth of anaerobic bacteria expert in fermenting amino acids and peptides, whereas bacteria that obtain energy through carbohydrates fermentation may be restricted by lack of available nutrients (Sunde *et al.*, 2000, Slots, 2005). However, the coronal section of root canals uncovered to the oral cavity in initial infection is dominated by facultatively anaerobic bacteria, while strict anaerobic bacteria take over in the apical section (Dahle *et al.*, 2003, Sakamoto *et al.*, 2006). In later stages of infection, facultative anaerobes will be overcome by the obligate anaerobic population due to a decrease in availability of dietary carbohydrates due to proteolytic activity (the primary energy source) as a result of loss of direct contact with the oral cavity, as well as a decrease in oxygen availability (Sakamoto *et al.*, 2006, Vianna *et al.*, 2006). Seven groups demonstrate the bacterial pathogens that are associated with intraradicular endodontic infections:

1- G-negative black pigmented species of saccharolytic anaerobic rods of *Prevotella* (*intermedia*, *nigrescens*, *tanneriae*, *multissacharivorax*, *baroniae* and *denticola*) and asaccharolytic spp. *Porphyromonas* mainly *P. endodontalis* and *P. gingivalis* (Shah and Collins, 1990).

2- The periodontal pathogen *Tannerella forsythia*, also detected in endodontic infection (Conrads *et al.*, 1997).

3- Obligately anaerobic G-negative coccobacilli of *Dialister pneumosintes* and *Dialister invisus*.

4- *Fusobacterium nucleatum* and *Fusobacterium periodonticum*.

5- The oral spirochetes represented by the genus *Treponema* of species (*denticola*, *sacranskii*, *parvum*, *maltoophilum* and *lecithinolyticum*) (Dahle *et al.*, 2003).

6- G-positive anaerobic rods such as:

- *Pseudoramibacter alactolyticus*
- *Filifactor alocis*
- *Actinomyces* spp.
- *Propionibacterium propionicum*
- *Olsenella* spp.
- *Slackia exigua*
- *Mogibacterium timidum* and
- *Eubacterium* spp.

7- G-positive cocci that are present in endodontic infection:

- *Parvimonas micra*
- *Streptococcus* spp.
- *Enterococcus faecalis*

In addition, low to moderate numbers of other bacterial spp. are also detected:

- *Campylobacter* spp.
- *Catonella morbic*
- *Veillonella parvula*
- *Eikenella corrodens*
- *Granulicatella adiacens*
- *Neisseria mucosa*
- *Centipeda periodontii*
- *Gemella morbillorum*
- *Capnocytophaga gingivalis*
- *Corynebacterium matruchotii*
- *Bifidobacterium dentium*
- anaerobic *lactobacilli*

Acute apical abscesses with purulent inflammation could be formed in periapical tissue as a result of dissemination of infection. However, extraradicular infections are dependent on or independent of an intraradicular endodontic infection. The main bacterial species found are anaerobic bacteria (Tronstad *et al.*, 1987, Gatti *et al.*, 2000, Sunde *et al.*, 2000, Sunde *et al.*, 2002) such as:

- *Actinomyces* spp.
- *Propionibacterium propionicum*
- *Treponema* spp.
- *Porphyromonas endodontalis*
- *Porphyromonas gingivalis*
- *T. forsythia*
- *Prevotella* spp.
- *Fusobacterium nucleatum*.

1.5.5 Bacteria persisting throughout endodontic treatment

G-positive facultative anaerobes or anaerobic bacteria that often resist treatment procedures are frequently isolated (Sjögren *et al.*, 1997, Chu *et al.*, 2006, Siqueira *et al.*, 2007b, Siqueira *et al.*, 2007a). This supports the view that G-positive bacteria can be more resistant to antimicrobial treatment measures and have the ability to adapt to harsh environmental conditions (Siqueira and Rôças, 2008). These include:

- *Streptococcus mitis*, *Streptococcus gordonii*, *Streptococcus anginosus*, *Streptococcus sanguinis*, and *Streptococcus oralis*
- *Parvimonas micra*
- *Actinomyces israelii* and *Actinomyces odontolyticus*
- *Propionibacterium acnes* and *Propionibacterium propionicum*
- *Pseudoramibacter alactolyticus*
- *Lactobacilli paracasei* and *Lactobacilli acidophilus*
- *Enterococcus faecalis*
- *Olsenella uli*

1.6 *E. faecalis* and endodontic infection

The species most often recovered from filled root canals with persistent periapical infection are enterococci, ranging from 29% to 77% of cases treated (Sundqvist *et al.*, 1998, Molander *et al.*, 1998, Peciuliene *et al.*, 2001, Hancock *et al.*, 2001, Siqueira and Rôças, 2004). However, around 5% or less have been recovered from untreated primary root canal infections (Wittgow and Sabiston, 1975, Siqueira *et al.*, 2002). *E. faecalis* are G-positive cocci and facultative anaerobes. They are normal intestinal and environmental organisms and may inhabit the oral cavity and gingival sulcus. The source of these organisms has long been argued because enterococci can be found in human faeces, usually between 10^4 and 10^6 bacteria per gram wet weight (Zubrzycki and Spaulding, 1962, Layton *et al.*, 2010), inhabiting the alimentary canals of both humans and animals (Tendolkar *et al.*, 2003), in water and soil of tropical watershed (Goto and Yan, 2011). In addition, there is evidence that they are capable of multiplying in extra-enteric settings such as beach sands, water containing Kelp, and plankton (Bahirathan *et al.*, 1998, Imamura *et al.*, 2011, Mote *et al.*, 2012). In addition they may originate from our diets, with one study showing that once inside the oral cavity they can persist in the mouth for some time after consumption of cheese (Giraffa, 2002). *E. faecalis* most likely exist in untreated root canals, but in such low numbers that it is not recoverable by culture, thus if the environmental setting improves, it may grow to higher and noticeable proportions as observed in animal experiments (Fabricius *et al.*, 1982, Persoon, 2017). *E. faecalis* has been more frequently isolated from root canals that were imperfectly sealed for an extended period of time during the treatment, or in cases with several sessions (more than 10 or more) (Siren *et al.*, 1997). In addition, *E. faecalis* could find its way in and become established after root filling, as research indicates that poorly restored teeth have a higher rate of post endodontic treatment infection (Ray and Trope, 1995). Furthermore, these organisms are extraordinary survivors because they have certain intrinsic characteristics that enable them to survive high salt concentrations (6.5%) (Gardini *et al.*, 2001, Giard *et al.*, 2001), a wide temperature range (10–60°C) (Boutibonnes *et al.*, 1993), 40% bile (Flahaut *et al.*, 1996), a broad pH range (Flahaut *et al.*, 1997), as well as to persist in the presence of detergents (Hartke *et al.*, 1998, Wada *et al.*, 2012), conditions that would be lethal to other microorganisms. The *E. faecalis* has a cell-wall-associated proton pump by which protons are derived into the cell to acidify the cytoplasm found in highly alkaline environments (Evans *et al.*, 2002). This mechanism is used by *E. faecalis* to resist the high antimicrobial alkalinity of the calcium hydroxide used as an endodontic dressing

during root canal therapy (Sjögren *et al.*, 1991). In fact this microorganism can bear an alkaline pH of 11.5 (Tanriverdi *et al.*, 1997, Evans *et al.*, 2002), which represents a significant clinical task in eradicating persistent infection in an already filled root canal. In addition, the pH level is naturally neutralised by the buffering effect of dentin (Haapasalo *et al.*, 2000, Portenier *et al.*, 2001, Figdor *et al.*, 2003) as pH levels in dentin do not reach higher than 10.8 in cervical and 9.7 in apical dentin (Nerwich *et al.*, 1993). In an *ex vivo* study, Sedgley *et al.* (2005a), showed that *E. faecalis* has the ability to recover in root canal filled teeth under a starvation state; when inoculated into the canals, these microbes sustained viability for up to 12 months without supplementary nutrients. Thus, viable *E. faecalis* present at filled root canal will provide a long term constant source of successful infection. This is supported by a study that conducted a series of long-term starvation assays which demonstrated that *E. faecalis* withstood being in water for more than 120 days with limited levels of nutrient supply, leaving a viable residual small portion of starved cells (Figdor *et al.*, 2003). The same study indicated that the serum-derived fluid from surrounding periapical tissue that seeped into the apical root canal of the treated and filled root canal could provide a clue as to the possible nutrient source at the tooth apex. As indicated by all the above, this organism emerges as the most promising model for testing against various chemomechanical and medication therapies in *ex vivo* tests such as irrigants, medicaments, and antiseptic solutions used in endodontics (Dahlen *et al.*, 2000, Eddy *et al.*, 2005, Portenier *et al.*, 2005).

1.6.1 Enterococcal Cell Walls

The enterococcal cell wall in general is composed of a peptidoglycan layer (PG) that is found above the lipid bilayer membrane (Figure 1.10). As with other related G-positive organisms, the peptidoglycan backbone (PG) and cell membrane displays a variety of polysaccharides and proteins. Polysaccharides, teichoic acids, and surface-anchored proteins are directly chained to the cell wall PG through covalent linkages, while lipoteichoic acid and lipoproteins are anchored to a membrane lipids envelope (Hancock and Gilmore, 2002) (Figure 1.5). The PG consists of disaccharide N - acetylmuramic acid-(β 1-4)-N- acetylglucosamine (MurNAc-GlcNAc) in the form of repeating strands that are cross-linked together by the presence of branch peptides attached to MurNAc (NAM) residues (Navarre and Schneewind, 1999). In addition, the enterococcal polysaccharide antigen (Hancock *et al.*) (suggested to synthesise a rhamnopolysaccharide) together with wall teichoic acid forms the secondary wall polysaccharides (Geiss-Liebisch *et al.*, 2012). Analysis of the purified enterococcal

polysaccharide antigen (Epa) polysaccharide from *E. faecalis* OG1RF revealed that it is composed of rhamnose, glucose, galactose, GalNAc, and N-acetylglucosamine (GlcNAc) (Teng *et al.*, 2009). The peptidoglycan backbone and anionic polymers (teichoic acids and cell wall polysaccharides) account for nearly 90% of the total cell wall weight, with the protein content (wall-associated and wall-anchored proteins) comprising less than 10% of the cell wall weight (Bhavsar and Brown, 2006).

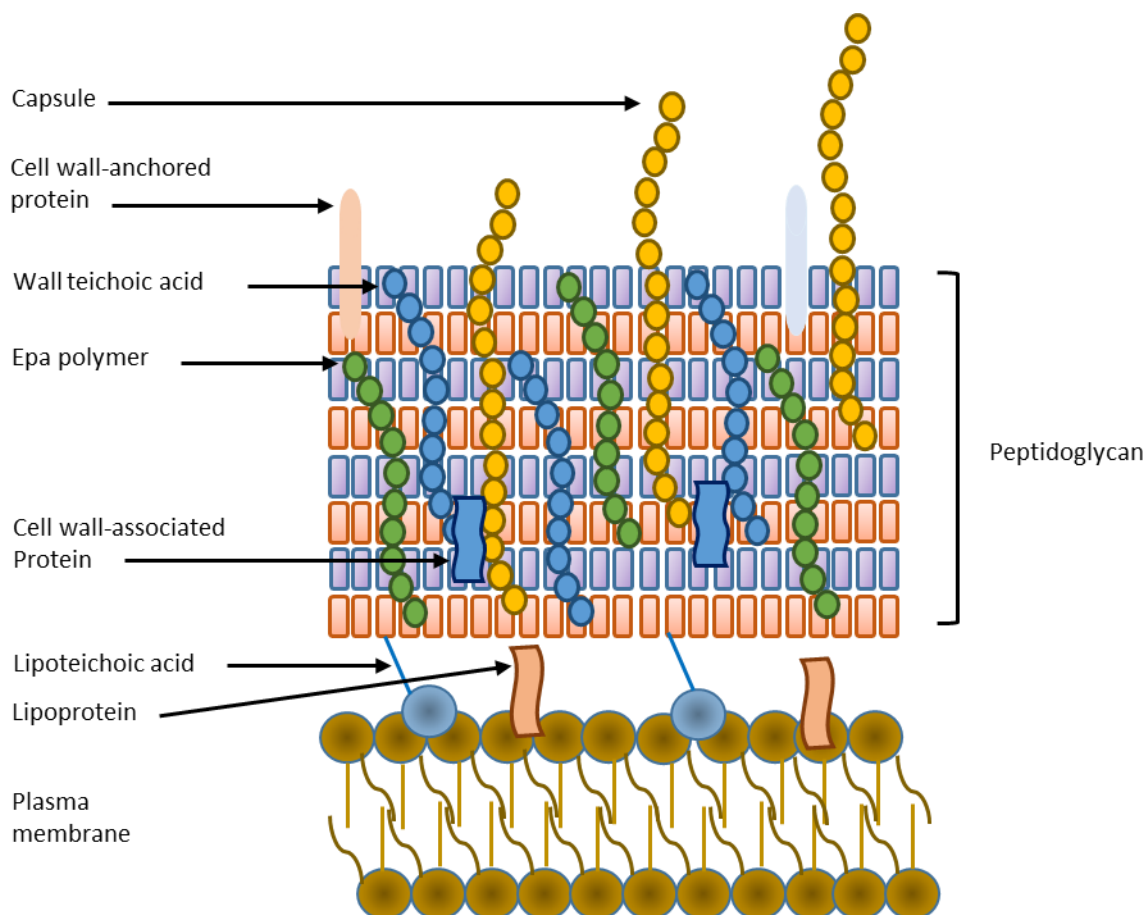


Figure 1.10 Model of the enterococcal cell wall. The peptidoglycan layer can be seen above the lipid bilayer with membrane bound lipoproteins and lipoteichoic acid. Bound to the muramyl residues of the peptidoglycan are wall teichoic acids and the rhamnopolymer, whose synthesis is tied to the *epa* locus, as well as surface-anchored proteins and capsule. Adapted from (Hancock and Gilmore, 2002).

1.6.2 Virulence factors of *E. faecalis* and its relation to endodontic disease

Recent data indicate that up to 75% of enterococcal infections in humans are caused by *Enterococcus faecalis*. This research period spanned from 2001 to 2012 and covered all classes of hospitals in the US (Gilmore *et al.*, 2013). The identified isolates

were collected from samples of bloodstream, urinary tract, and wound infections. *E. faecium* isolates represent around 24%, with similar percentage trends reported for the European Union, while infections with the other enterococcal species have occasionally been found to cause infection in humans (Devriese *et al.*, 1995, Tannock and Cook, 2002). These include such as *E. durans*, *E. avium*, *E. gallinarum*, *E. casseliflavus*, *E. hirae*, *E. mundtii*, *E. dispar*, and *E. raffinosus*. As a result, most studies of enterococci have examined the virulence of *E. faecalis* and its factors (Kayaoglu and Ørstavik, 2004, Gilmore *et al.*, 2013). In terms of *E. faecalis* virulence factors, these mostly relate to surface localised properties and secreted factors (Figure 1.11). They are associated with various phases of an endodontic infection as well as with periapical inflammation. Periradicular tissue damage mainly occurs as an indirect consequence of the host's immune response to bacteria and its products or is directly linked to the bacterial products (Kayaoglu and Ørstavik, 2004).

1.6.2.1 Surface Adhesins

1.6.2.1.1 Enterococcal surface protein (Esp)

Enterococcal surface protein (Esp) was identified initially in a highly virulent, gentamicin resistant *E. faecalis* isolate from both bacteremia and endocarditis isolates (Shankar *et al.*, 1999, Archimbaud *et al.*, 2002). In addition, *esp* gene was found to be enriched in endodontically isolated *E. faecalis* strains as 20 out of 31 were carrying the *esp* gene (Sedgley *et al.*, 2005b). This gene is considered as an important enterococci virulence factor related to biofilm formation (Klare *et al.*, 2005). Toledo-Arana *et al.* (2001), revealed that *esp* plays an important part in primary attachment and biofilm formation of *E. faecalis* on abiotic surfaces (through comparing the biofilm formed by mutants cells to that of wild type), but not to other medically relevant substrates, such as silicone rubber, fluoroethylene-propylene, or polyethylene (Waar *et al.*, 2002). This could allow the bacteria to resist the bactericidal effect of medication used in infected root canals (Distel *et al.*, 2002).

1.6.2.1.2 Adhesin to collagen of *E. faecalis* (Ace)

Attachment of pathogens to extracellular matrix (ECM) is needed at an early stage of the infection course. *In vitro* testing has showed that *E. faecalis* is capable of adherence to collagen, fibrinogen, and fibronectin in the presence of serum compared to growth in BHI only (Nallapareddy *et al.*, 2008). Ace (adhesin to collagen of *E. faecalis*) was found

after searching the complete genome sequence of *E. faecalis* V583. After cloning, the recombinant protein showed ability to bind to the wide tissue distribution fibrillar collagen type I (Rich *et al.*, 1999), with binding to major components of mammalian basement membranes of both collagen type IV and laminin (Nallapareddy *et al.*, 2000), and this has proved to be significant for attachment of *E. faecalis* to dental roots (Hubble *et al.*, 2003). As dentin of the root canal is rich in collagen type I, this suggests that the persistence of *E. faecalis* in endodontic infection is at least in part Ace-mediated (Kowalski *et al.*, 2006).

1.6.2.1.3 *E. faecalis* antigen A (EfaA)

EfaA is a putative substrate-binding lipoprotein component that has been identified from patients with *E. faecalis* endocarditis (Lowe *et al.*, 1995, Low *et al.*, 2003). It is an *E. faecalis* major surface antigen and when disrupted in an experimental peritonitis infected mouse model, it showed a better survival rate of mouse compared to infection with wild type OG1RF (Singh *et al.*, 1998).

1.6.2.1.4 Biofilm-associated pili (Ebp)

E. faecalis endocarditis infected human sera have shown increased antibody titers for the three structural pilus subunits, EbpA, EbpB, and EbpC, which highlights their importance in *E. faecalis* pathogenicity (Sillanpää *et al.*, 2004). Further studies on *E. faecalis* mutant *ebp* locus in a rat endocarditis have revealed that they lost their capability to form biofilm and attachment to plastic surfaces in addition to their better survival rate (Nallapareddy *et al.*, 2006).

1.6.2.1.5 Aggregation substance (AS)

Aggregation substance (AS) proteins Asa1, Asc10, and Asp1 are a group of surface anchored polypeptides encoded by conjugative plasmids with roles in *E. faecalis* plasmid transfer and virulence (Galli *et al.*, 1990, Kao *et al.*, 1991, Galli *et al.*, 1992). The AS proteins have a C-terminal cell wall anchor domain, 2 Arg-Gly-Asp (RGD) motifs, and a number of domains that were found to arbitrate aggregation and lipoteichoic acid binding (Hendrickx *et al.*, 2009). Asa1 was shown to enhance binding to type I collagen and fibronectin, thrombospondin and vitronectin (an ECM element) (Rozdzinski *et al.*, 2001). RGD motifs are thought to help adherence of the bacterium to the host cell via integrins, a family of eukaryotic cell-surface receptors (Galli *et al.*, 1990). *E. faecalis*,

due to having AS, was shown to be resistant to human neutrophils elimination, despite noticeable phagocytosis and neutrophil activation (Rakita *et al.*, 1999).

AS and its cognate ligand BS (binding substance) have together been shown to produce tissue inflammation responses through stimulation of T-lymphocytes, followed by increase release of inflammatory cytokines (Schlievert *et al.*, 1998) and are considered as superantigen molecules. Cytokines released by macrophages, such as tumor necrosis factor beta TNF β and tumor necrosis factor alpha TNF α , participate in bone resorption (Stashenko, 1998). Tumour necrosis factor gamma TNF γ interferon is also released, it is considered as a host defence factor against infection, acting as an inflammatory mediator (Billiau, 1996), and to stimulate the production of the cytotoxic agent nitric oxide (NO) from macrophages and neutrophils. Consequently, periapical tissue damage and bone resorption will be established as a result of host immune response.

1.6.2.2 Secreted Factors

1.6.2.2.1 Cytolysins (CylL)

Cytolysins, the extracellular secreted peptide subunits CylL_L and CylL_S expressed by various *E. faecalis* isolates, exhibit lytic activity towards target cells (Haas and Gilmore, 1999). They are either plasmid-encoded toxins or chromosomally encoded (Ike and Clewell, 1992). CylL_L and CylL_S need further extracellular cleavage by CylA, a serine protease, before becoming fully active, while the secreted bacterium cell will be protected by the *cyII* gene products (Coburn *et al.*, 1999). Cytolysins have been shown to target and lyse erythrocytes (Basinger and Jackson, 1968, Miyazaki *et al.*, 1993), PMNs and macrophages (Miyazaki *et al.*, 1993), and a range of G-positive organisms (Jackson, 1971). The lysis activity of the cytolysin against both prokaryotic and eukaryotic cells leads to the proposal that those cells which exhibit cytolytic activity have access to key nutrients that are not accessible to other strains. For example, haemin obtained from lysis of erythrocytes is needed by *E. faecalis* for the assembling of an electron transport chain and increase in energy yield through aerobic respiration (Pritchard and Wimpenny, 1978). In addition, Day *et al.* (2003) showed that cytolysin production is increased with depletion in oxygen and this might aid *E. faecalis* encounters anaerobic conditions and persist in endodontic infection.

1.6.2.2.2 Gelatinase and serine protease

In *E. faecalis*, the gelatinase (GelE, a matrix metalloprotease) and a serine protease (SprE) are two secreted proteases that have been well studied (Qin *et al.*, 2001). GelE can hydrolyse gelatine, collagen, fibrinogen, casein, hemoglobin, insulin, and many peptides (Mäkinen *et al.*, 1989). *In vitro* studies showed a lower bone resorption rate in tissue culture experiments and periodontal disease models when gelatinase was inhibited (Hill *et al.*, 1994, Ramamurthy *et al.*, 2002). On the other hand, dental pulp and periapical lesions revealed high levels of host gelatinase during inflammation compared to healthy status (Shin *et al.*, 2002), which in turn has been shown to have a significant effect in the degradation of dentin organic matrix (Tjäderhane *et al.*, 1998). The protease-positive strain *E. faecalis* OG1 was capable of dental caries induction in germ-free rats when compared to non-proteolytic strains (Gold *et al.*, 1975). In addition, the importance of proteases in *E. faecalis* biofilm formation through regulating autolysis and release of extracellular DNA has been described (Thomas *et al.*, 2008) and suggested as being regulated by the *Fsr* quorum system of *E. faecalis*.

1.6.2.2.3 Sex pheromones, superoxide and bacteriocins

The secreted sex pheromones from *E. faecalis* have been found to be chemotactic for neutrophils, and to induce superoxide production and lysosomal enzyme secretion (Ember and Hugli, 1989, Sannomiya *et al.*, 1990). Neutrophils that produced superoxide at the site of inflammation were found to possess antimicrobial properties and cause tissue damage (Marton *et al.*, 1993). In addition, secreted extracellular superoxide anion has been reported from strains of *E. faecalis* (Huycke *et al.*, 1996). On the other hand, increased activity of Lysosomal enzyme beta glucuronidase was detected in samples from periapical lesions (Kuo *et al.*, 1998), and Torabinejad *et al.* (1985) found that neutrophil lysosomal enzymes might indirectly cause bone destruction by activating the complement system. Many bacteriocins that are directed mainly towards G-positive bacteria have been reported to be secreted from *E. faecalis*, including Bc-48 (Lopez-Lara *et al.*, 1991), enterocin 4 (Joosten *et al.*, 1996), bacteriocin 21 (Tomita *et al.*, 1997), enterocin 1071A and enterocin 1071B (Balla *et al.*, 2000), and enterocin SE-K4 (Eguchi *et al.*, 2001).

1.6.2.3 Enterococcal capsule, lipoteichoic acid and cell wall polysaccharide

The cell components of *E. faecalis* that play a role in its virulence are those that participate in overcoming various host defence mechanisms. Put in another way, how the

host will recognise and perceive the invading pathogens; these mechanisms include phagocytosis and /or cytokine secretions (Hancock and Gilmore, 2002, Thurlow *et al.*, 2009, Theilacker *et al.*, 2011) As a general rule, there is positive correlation between existence of a capsule and avoidance of host immune response.

1.6.2.3.1 Variable capsular carbohydrate

Neutrophil-mediated opsonisation refers to the mechanism by which the host immune system brings about the clearance of invading enterococci throughout neutrophil-mediated opsonisation. Several studies have demonstrated that an enterococcal capsular polysaccharide (*cps*) might mediate that host defence mechanism (Huebner *et al.*, 1999, Rakita *et al.*, 1999). Hancock and Gilmore (2002) identified a *cps* locus that encodes the creation of various enterococcal carbohydrate capsules. Generation of isogenic mutants in (*cpsI*) part of this locus or blocking of the capsular polysaccharide with specific antibodies facilitate the clearance of *E. faecalis* bacteria by opsonophagocytotic killing in animal models (Hancock and Gilmore, 2002). In addition, the polysaccharide capsule forms a protective shield against C3b complement and protects against opsonophagocytic killing by macrophages (Thurlow *et al.*, 2009).

1.6.2.3.2 Lipoteichoic acid (LTA)

Lipoteichoic acids (LTA) are a group of closely related amphipathic molecules consisting of a polyglycerolphosphate backbone (1-3 phosphodiester-linked chains of 25 to 30 glycerolphosphate residues variously substituted with glycosyl and dalanyl ester groups) joined covalently to a glycolipid moiety (Wicken and Knox, 1975). Many G-positive bacteria possess LTA on their cell surfaces. *E. faecalis* LTA is a cell-wall element that is considered as an important virulence factor in evading host immunity. Research indicates that blocking the LTA with antibodies resulted in opsonic elimination of the invaded pathogen and protected a mouse model from enterococcal infection (Huebner *et al.*, 1999, Theilacker *et al.*, 2011). Similarly, binding of pneumococcal (*S. pneumoniae*) LTAs to erythrocytes rendered them vulnerable to lysis by their own complement systems, suggesting that exposure to bacterial LTA during infection might lead to cellular tissue lysis (Hummell and Winkelstein, 1986). In terms of oral infections, several mediators with tissue-damaging properties released by leukocytes as a result of LTA stimulation have been reported to be present in periapical samples, such as TNF- α ,

IL-1 , IL- 6, PGE2, lysosomal enzyme, superoxide anion, or leukocyte attracting IL-8 (Bhakdi *et al.*, 1991, Saetre *et al.*, 2001).

1.6.2.3.3 Enterococcal polysaccharide antigen (Epa)

Study of the antigenic material in *E. faecalis* cell wall polysaccharide in human infections revealed the presence of an antigenic carbohydrate that is proteinase K-resistant by using serum from infected humans and cloned DNA fragment products from *E. faecalis* strain OG1RF (Xu *et al.*, 1997, Xu *et al.*, 1998). After sequencing the fragments, a genetic locus was identified that bore resemblance to polysaccharide biosynthesis enzymes (Xu *et al.*, 1998). Later on, it was identified as the Epa polysaccharide from enterococcus (Teng *et al.*, 2009). *In vitro* studies could not detect Epa on the surface of the *E. faecalis* membrane so it is assumed to reside deep in the cell wall (Xu *et al.*, 2000, Hancock and Gilmore, 2002). Mutants in the *epa* locus were used in a different study to compare it to wild type, which revealed its pathogenic properties as it showed decreased killing in mouse peritonitis (Xu *et al.*, 2000), tendency to neutrophil-mediated phagocytosis and clearance (Teng *et al.*, 2002), poor biofilm formation on a polystyrene surface (Mohamed *et al.*, 2004), failing in a mouse model of ascending UTI (Singh *et al.*, 2009), and effect on penetration and adhesion to mucosal surfaces (Ocvirk *et al.*, 2015).

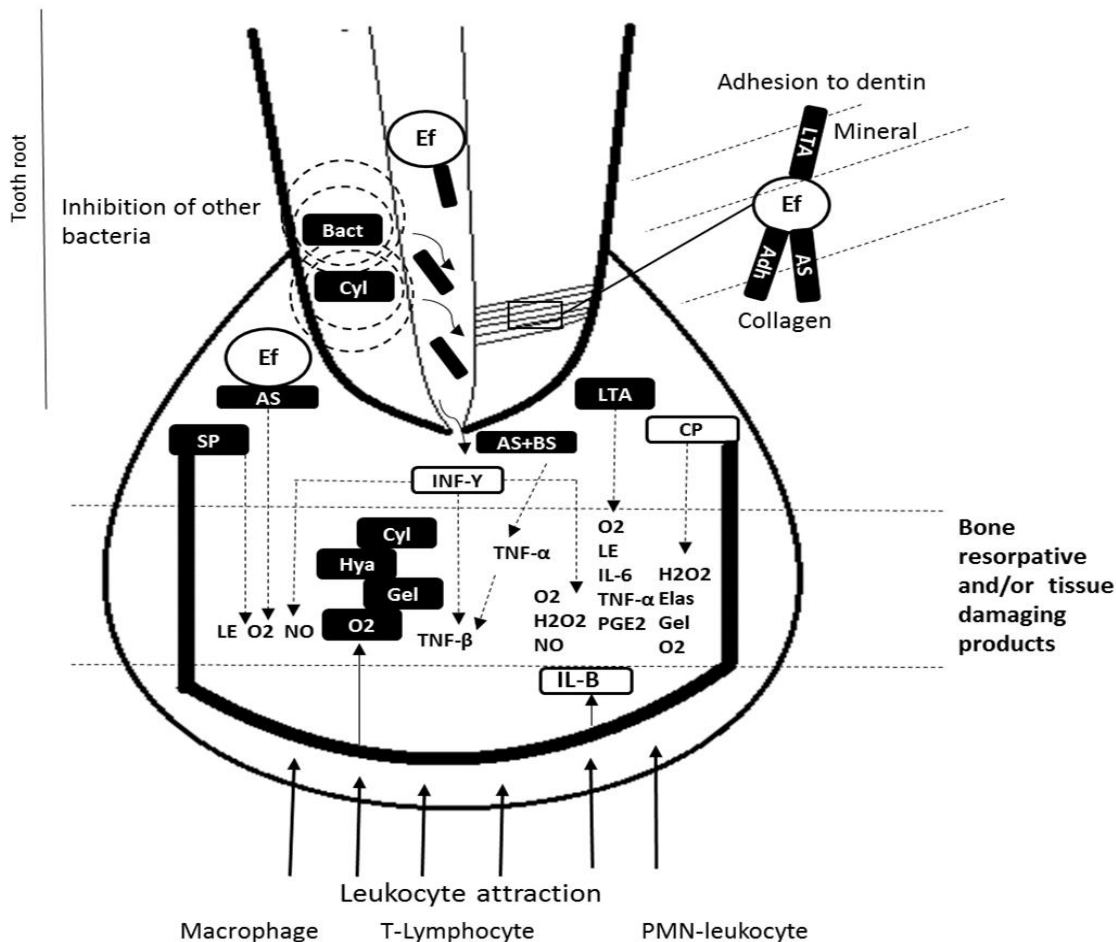


Figure 1.11 Schematic model of endodontic disease related to virulence factors of *E. faecalis*. The *E. faecalis* virulence factors are released inside the dentinal tubules to the root canal periradicular area, where they cause leukocyte attraction or stimulate leukocytes to produce inflammatory mediators or lytic enzymes. Some of the bacteria are localised in the periradicular lesion as well. The harmful virulence factors and leukocyte products are shown in the zone between the interrupted lines. In a magnified window, the adhesion of the bacterium to different dentin elements is shown. Bacterial products that eliminate other bacteria are also included. Note that names in black boxes are the products of the bacterium. Abbreviations: Adh, surface adhesins; AS, aggregation substance; Bact, bacteriocins; BS, binding substance; CP, collagen peptides; Cyl, cytolysin; Ef, *Enterococcus faecalis*; Elas, elastase; Gel, gelatinase; Hya, hyaluronidase; H₂O₂, hydrogen peroxide; IFN, interferon; IL, interleukin; LE, lysosomal enzymes; LTA, lipoteichoic acid; NO, nitric oxide; O₂, superoxide anion; PGE₂, prostaglandin E₂; SP, sex pheromones; and TNF, tumor necrosis factor. Adapted from (Kayaoglu and Ørstavik, 2004).

1.6.3 *Enterococcus* and antibiotic resistance

The antibiotic resistance characteristics of the genus *Enterococcus* can generally be categorised as intrinsic resistance, tolerance, and acquired resistance. They are intrinsically resistant to many generally used antimicrobials (Kristich, 2014). Their resistance ranges between high-level resistance to most cephalosporins and all semi-synthetic penicillins to low-level resistance to penicillin and ampicillin due to expression of low-affinity penicillin-binding proteins. In addition, many *E. faecalis* contain the *lsa* gene that encodes an ATP-binding protein which confers intrinsic resistance to quinupristin/dalforistin (Q/D) (Singh *et al.*, 2002). β -lactam antibiotics and vancomycin, which exhibits bactericidal activity of cell-wall active agents, can be tolerated by enterococci. However, if high concentrated level of these agents are used (which exceed the inhibitory concentration) or used in combination with aminoglycosides (Gentamicin and streptomycin) such as penicillin-streptomycin (Rice and Carias, 1998, Jensen *et al.*, 1999), enterococci could be eliminated. Such a synergistic effect is suggested to be related to the rise in the uptake of the aminoglycoside molecule by the bacterium after the alteration of the cell wall (Arias and Murray, 2008). Interestingly, *E. faecalis* is well known for its ability to become resistant to almost any antimicrobial drug used in clinical practice, including antibiotics of last resort- e.g. Vancomycin. For example, the *Enterococcus* strain V583, was the first of the vancomycin-resistant *E. faecalis* clinical isolates, and has a genome that harbours approximately 25% of acquired DNA (Polidori *et al.*, 2011). The extent of acquired antibiotic resistance appear to be linked to the clustered, regularly interspaced short palindromic repeats with cas genes (CRISPR-cas) which provide immunity against foreign phage infections and plasmid uptake. However, the V583 strain does not have CRISPR-cas systems which in turn makes it accept foreign plasmids that might harbour antibiotic resistance genes (Palmer and Gilmore, 2010). In evidence of this highly chimeric genome, horizontal gene-transfer among enterococci occurs through plasmids transfer, for example, pheromone-responsive plasmids and several broad host range (conjugative) plasmids, pAM β 1, pIP501, and pSM19035 (Panesso *et al.*, 2005). Another example, pCF10 is a plasmid that encodes resistance to tetracycline and minocycline (harbours the *tet(M)* gene conjugative transposon *Tn925*) and has been associated with the transfer of VanB-type vancomycin resistance (Zheng *et al.*, 2009). In the context of horizontal gene transfer, pheromones are peptide fragments (7 or 8 amino acids long) secreted by recipient *E. faecalis* strains that do not have definite

plasmids. In response, the donor cells secrete AS adhesin that leads to clumping of donor and recipient cells that facilitates the conjugative transfer of plasmids (Weaver and Clewell, 1989). However, pheromone-responsive plasmids to date could only be able to replicate with enterococcal species, while broad host-range pAM β 1 and pIP501 could transfer to other species (staphylococci and streptococci), and then transfer back into enterococci *in vitro* (Bruand *et al.*, 1993, Qu *et al.*, 2012).

1.7 Dental plaque and antimicrobial resistance

Periodontal pathogens accumulate in subgingival or periodontal plaque, which is considered as a type of biofilm. Many researchers have shown that the biofilm provides protection to the inhabitant bacteria against antimicrobials (Wright *et al.*, 1997, Shani *et al.*, 2000, Zaura-Arite *et al.*, 2001). This has been shown by comparing the susceptibility to antimicrobials of biofilm and planktonic cells. For example, *P. gingivalis* biofilm is more resistant to amoxicillin, doxycycline, metronidazole than planktonic cells (Larsen, 2002, Noiri *et al.*, 2003).

15-20% by volume of biofilm is composed of microcolonies distributed randomly within the matrix, which represents the remaining 80–85% volume. The matrix is composed predominantly of water and aqueous solutes, extracellular polymeric substances (EPS) such as proteins (<1-2%) including enzymes, DNA (<1%), polysaccharides (1-2%) and RNA (<1%) (Socransky and Haffajee, 2002). The dry weight of matrix is composed mainly of exopolysaccharides produced by bacteria within the biofilm, while the remaining components are proteins, salts and cell material (Sutherland, 2001). The matrix of the biofilm offers several mechanisms to protect its bacteria against antibiotics. It performs a homeostatic function that enables the bacteria in the deepest layers to slow their growth rate, thereby becoming less exposed to antimicrobial activity than the superficial fast growing bacteria (Ashby *et al.*, 1994, Brooun *et al.*, 2000). Furthermore, the matrix contains extracellular enzymes that have specific inactivation potential to certain, but not all, antibiotics such as β -lactamases (Nichols, 1994). In addition, it possesses precise chemical properties that retard the diffusion of antibiotics through the biofilm (Gilbert and Allison, 1999).

Resistance is not simply confined to the penetration of antibiotics, but has also been shown to occur at the cellular level in pathogenic bacteria within the biofilm as represented by changes in phenotype or genotype (Suci *et al.*, 1994). In addition, these

bacteria can acquire pumping capabilities (Pump theory), by which they can extrude unwanted antimicrobial agents from the cell to the outside; thus antibiotics can no longer affect the cell wall synthesis (Brooun *et al.*, 2000). Furthermore, different cells in the biofilm can transfer antibiotic resistant genes within them through bidirectional horizontal gene transfer, such as erythromycin resistance between *E. faecalis* and *S. gordonii* isolated from root canal abscesses (Sedgley *et al.*, 2008).

Finally, besides the above, the overuse of antibiotics (Serrano *et al.*, 2008), provides the pathogenic bacteria with selection pressure that promotes evolution of extra resistance characteristics to routinely used antimicrobials, which highlights the need for new novel methods of treatment as well as improved antibiotic stewardship and compliance.

1.8 Timeline of antibiotic resistance

Antibiotics have not only played a crucial role in increasing the average life span worldwide through elimination of deadly infection but have also provided the basis for new developments in medicine and surgery (Piddock, 2012, Rossolini *et al.*, 2014). In addition, intrapartum antibiotic prophylaxis had reduced infant mortality associated with group B streptococcal disease during the past decades (Schrag *et al.*, 2000). They aid in the prevention and treatment of infections associated with chronic diseases such as diabetes and end-stage renal disease or infections associated with patients subjected to organ transplant and cardiac surgery (Gould and Bal, 2013, Wright, 2014, Rossolini *et al.*, 2014). Unfortunately, there is now resistance to nearly all antibiotics that have been developed (Figure 1.12). Resistance started to be noticed in the 1940s, almost immediately after the discovery of penicillin by Sir Alexander Fleming in 1928 (Piddock, 2012, Sengupta *et al.*, 2013). As a result of this threat, new β -lactam antibiotics were developed to overcome the new serious infections that could not be treated by penicillin (Sengupta *et al.*, 2013, Spellberg *et al.*, 2013). However, during the same decade, methicillin-resistant *Staphylococcus aureus* (MRSA) was recognised in the United Kingdom in 1962 and in the United States in 1968 (Sengupta *et al.*, 2013, Control and Prevention, 2015) (Figure 1.12). In 1972, vancomycin was introduced into clinical practice as the antibiotic of choice for methicillin-resistant *S. aureus* (MRSA) infections (Van Hal and Fowler, 2013). This glycopeptide has been used for more than 30 years, perpetuating the idea of the irresistible antibiotic. Nevertheless, vancomycin-resistant enterococci (Joosten *et al.*) were reported both in the UK and in France in 1988 (Uttley *et al.*, 1988, Leclercq *et al.*,

1988) and eventually emerged worldwide (Bonten *et al.*, 2001). Since 1996, vancomycin-intermediate *S. aureus* (VISA), hetero-resistant VISA (hVISA) and vancomycin-resistant *S. aureus* (VRSA) isolates have emerged, associated with poorer outcomes, elevating the level of concern (Hiramatsu *et al.*, 1997, Control and Prevention, 2002). Since that time, the supply of available antibiotics has begun to dry up due to production of fewer new drugs, and bacterial infections have again become a threat. The rapid emergence of resistant bacteria has been described by health organisations as a “crisis” or “nightmare scenario” that could have “catastrophic consequences” (Spellberg *et al.*, 2013, Viswanathan, 2014), and in 2014 the World Health Organization (WHO) warned of the increasing seriousness of the antibiotic resistance crisis (Michael *et al.*, 2014). The G-positive pathogens that now present as the main threats are *S. aureus* and *Enterococcus* species (Rossolini *et al.*, 2014, Control and Prevention, 2015). This is due to the fact that in the USA infection with MRSA results in more deaths than HIV/AIDS, Parkinson’s disease, emphysema, and homicide combined (Gross, 2013, Golkar *et al.*, 2014), and rising figures of MDR (multi drug resistance) indicate that enterococci isolates have developed resistance not only to vancomycin but also to many common antibiotics (Golkar *et al.*, 2014). In addition, the epidemic resistance of the respiratory bacteria *S. pneumoniae* and *Mycobacterium tuberculosis* is considered as a major concern for the future (Rossolini *et al.*, 2014). In addition, G-negative bacteria have been announced to be a major threat to future human health, with organisms that include MDR bacilli and *Enterobacteriaceae* (mostly *Klebsiella pneumoniae*), *Pseudomonas aeruginosa*, and *Acinetobacter* (Rossolini *et al.*, 2014, Control and Prevention, 2015) that occur in health care settings, and β -lactamase-producing *Escherichia coli* and *Neisseria gonorrhoeae* that are becoming increasingly prevalent in the community (Rossolini *et al.*, 2014). Carbapenem-resistant *Acinetobacter* strains (mostly *Acinetobacter baumannii*) became an important participant in the current antibiotic resistance crisis regarding healthcare-associated infections in Europe, Latin America and the Far East which are challenging due to resistance to almost all anti-*Acinetobacter* agents (Pogue *et al.*, 2013, Zarrilli *et al.*, 2013). In addition, it considered a major multidrug-resistant pathogen associated with extremity injuries infections during combat such as conflicts in Afghanistan and Iraq (Murray *et al.*, 2011, Richards *et al.*, 2015).

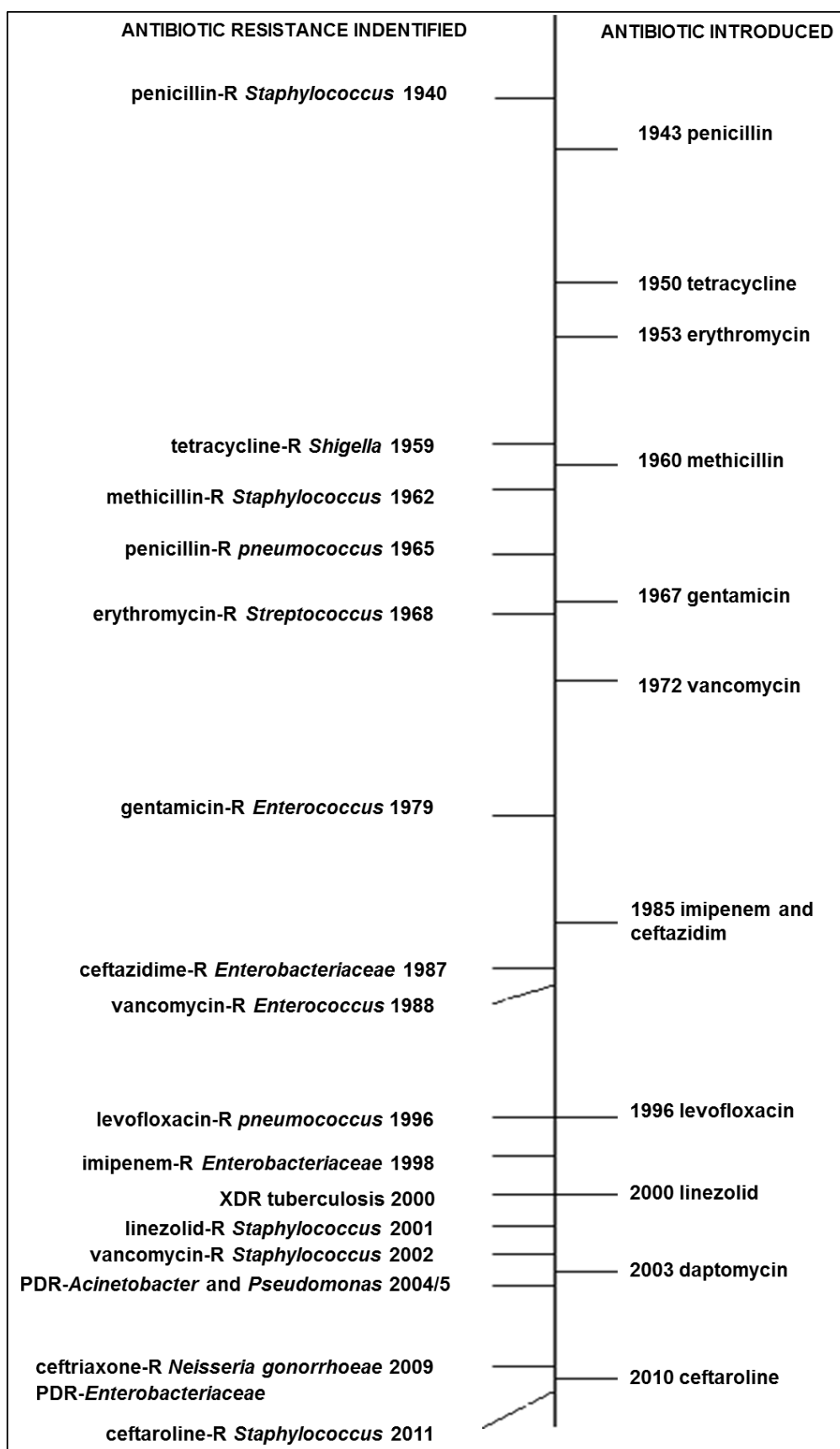


Figure 1.12 Developing antibiotic resistance: A Timeline of Key Events. Adapted from (Ventola, 2015).

1.9 Periodontal disease

1.9.1 Pathogenesis of periodontal disease

Periodontal disease is a general term used to describe inflammatory processes in the periodontium caused by bacterial plaque accumulation, and these are characterised by inflammation of gingival tissues, the formation of periodontal pockets, gingival recession, increased tooth mobility and alveolar bone resorption (Neumann *et al.*, 2004). Usually, there are three statuses concerned in periodontal disease description: health, gingivitis and periodontitis (Armitage, 2004). The plaque induced disease form, in which the bacteria are considered the primary etiological factor, involves gingivitis and periodontitis, which both have positive correlation with poor oral hygiene, although most of the tissue destruction is thought to be due to the host's response (Schenkein, 2006). Smoking and diabetes are considered as risk factors for periodontal disease occurrence (Baharin *et al.*, 2006, Mealey and Oates, 2006). There are eight basic types of periodontitis based on the onset, pattern of infection and the host response (the first two types are the most common forms of periodontal disease): I. Gingival disease, II. Chronic periodontitis, III. Aggressive periodontitis, IV. Periodontitis as a manifestation of systemic diseases, V. Necrotizing periodontal disease, VI. Abscesses of the periodontium, VII. Periodontitis associated with endodontic lesions, and VIII. Development of acquired deformities and conditions (Armitage, 2002).

Gingivitis is a reversible inflammation of the gingiva with no alveolar bone resorption or clinical attachment loss, while chronic periodontitis is usually associated with clinical attachment loss, alveolar bone loss, true pocket formation and inflammation of gingiva clinically (Flemmig, 1999). Gingivitis does not always progress to periodontitis despite continued plaque accumulation, and it appears that the host immune response may control the progression of disease, leading to a more complex pathology (Løe *et al.*, 1986). Consequently, both the bacterial composition and the host reaction response will determine the progression of periodontal disease (Beck *et al.*, 1996). However, it is not clear how much of the damage to periodontal tissue is due to direct effects of the bacteria and how far the immune response evokes that reaction against the bacterial invasion (Løe *et al.*, 1965).

Chronic inflammatory periodontal disease develops in four different steps: the initial, the early, the established and the advanced lesion which is generally viewed as

periodontitis (Page and Schroeder, 1976). In response to bacterial plaque proliferation in the sulcus during the initial and early stages, leukocytes (predominantly neutrophils) migrate into the junctional epithelium and underlying tissue. Neutrophils within the gingival crevices can phagocytose and digest bacteria, which can then lead to degranulation (Offenbacher, 1996, Marsh and Devine, 2011). Bacterial toxin secretion and release of enzymes following neutrophil degranulation causes tissue damage, and if the bacteria penetrate deeper into the sulcus the inflammatory reaction begins to destruct the deeper supporting tissues of the tooth (periodontal ligament, gingival connective tissue and alveolar bone) (Offenbacher, 1996) (Figure 1.13). In the established lesion, a pocket forms around the tooth, signifying a progression to periodontitis as the disease is no longer confined to the gingivae (Listgarten, 1986). Due to the movement of the junctional epithelium caused by the damage that occurred, reversal of the disease to the original healthy state is no longer possible. At this stage, the inflammatory infiltrate is characterised by the predominance of immune cells and by several modifications of the *milieu*: secretion of antibodies, activation of the complement by opsonised antigens, production of several interleukins (notably IL1) and increase of the production of inflammatory prostaglandin. Later in the advanced stage, the pocket that forms becomes inhabited by anaerobic microorganisms in the deeper parts, and some of these produce tissue-destroying enzymes like collagenases and/or toxins (Feng and Weinberg, 2006, Dahan *et al.*, 2001). Collagen destruction and junctional epithelium migration continue. Exacerbation of the inflammatory response leads to bone loss by activation of osteoclast cells. Certain genetic and environmental factors, such as compromised immunity, hormonal factors and smoking, are believed to be risk issues for periodontal diseases (Page and Kornman, 1997). Several studies have demonstrated the relation between smoking and the loss of periodontal attachment and progression of periodontal disease (Martinez-Canut *et al.*, 1995, Bergström *et al.*, 2000). Palmer *et al.* (2005) suggested that smoking causes weakness in the host immune response towards the bacterial biofilm, as a result of the reduction in the transmigration of neutrophils to the periodontal tissue and the drop in its phagocytic ability.

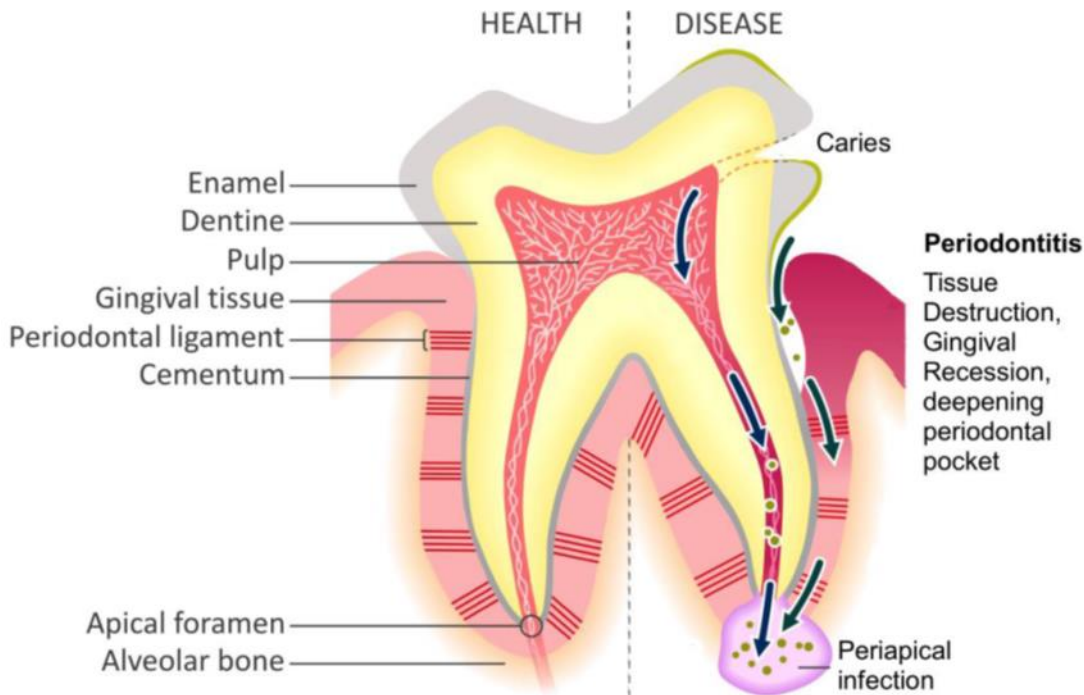


Figure 1.13 Cross-sectional representation of a posterior tooth in health and disease. Periodontitis is associated with the classical gum recession, formation of deep periodontal pockets and a proliferation of subgingival bacteria (green circles) which mainly contributed to prolonged plaque biofilm formation (green material). Adapted from (Douglas *et al.*, 2014) with permission.

1.9.2 Bacteriology of periodontal disease

The oral cavity represents an ecological niche for the large number of bacteria comprising what is called the oral microbiota (Paster *et al.*, 2001). More than 400 bacterial species may be cultivated from subgingival plaque inside the oral cavity and it is estimated that more than half that number again remain uncultivated (Socransky *et al.*, 1998, Aas *et al.*, 2005). Although gingivitis is considered the result of increased plaque mass, it may be considered a natural reaction that permits commensal carriage of bacteria mediated by normal physiological defence mechanisms of the host in its controlled form (Marsh, 2000). Facultative anaerobic G-positive strains are predominant in the supragingival dental plaque of healthy subjects (Socransky *et al.*, 1998). In gingivitis, the proportion of G-negative anaerobic species increases and if plaque is allowed to mature, gingivitis can progress to periodontitis associated with the increased number of certain obligatory anaerobic bacteria within this plaque mass (Socransky *et al.*, 1998, Moore and Moore, 1994). In a more recent study, Kistler *et al.* (2013) used 454-pyrosequencing to

examine the bacterial composition of dental plaque in experimental gingivitis, comparing the oral microbiome of healthy with one and two weeks gingivitis. Aerobic and facultatively anaerobic G-positive cocci and rods, including members of the genera *Actinomyces*, *Rothia* and *Streptococcus*, were predominant in healthy individuals and negatively correlated with bleeding on probing. However, G-negative cocci and rods as well as filaments, spirilla and spirochetes increased in relative abundance as gingivitis developed, and these, represented by the genera *Campylobacter*, *Fusobacterium*, *Lautropia*, *Leptotrichia*, *Porphyromonas*, *Selenomonas*, and *Tannerella*, were positively correlated with bleeding in probing scores.

Gross accumulation of dental biofilm to the point that it overcomes the host defences is considered to be an aetiological factor of periodontal disease. This theory is described as the “non-specific plaque hypothesis” (Theilade, 1986). Consequently, the concept of individual bacterial species within dental biofilm as a causative factor of periodontal disease was put forward and named “specific plaque hypothesis”, which assumed that the increase in numbers of a few bacterial species is the cause behind periodontal disease (Loesche, 1975). The “ecological plaque hypothesis” (Marsh, 1992, Marsh and Bradshaw, 1995) considered that the inflammatory response that occurs in gingivitis has the ability to alter the resident microflora in a direction favourable to periodontal pathogens which, under the correct conditions, go on to cause periodontitis. Furthermore, the inflammatory response produces substrates that are advantageous to the initially low numbers of pathogenic G-negative anaerobes, leading to an increase in their numbers and their metabolic by-products, which in turn favours their proliferation and suppression of the normal host microbiome (Marsh, 2003) (Figure 1.14).

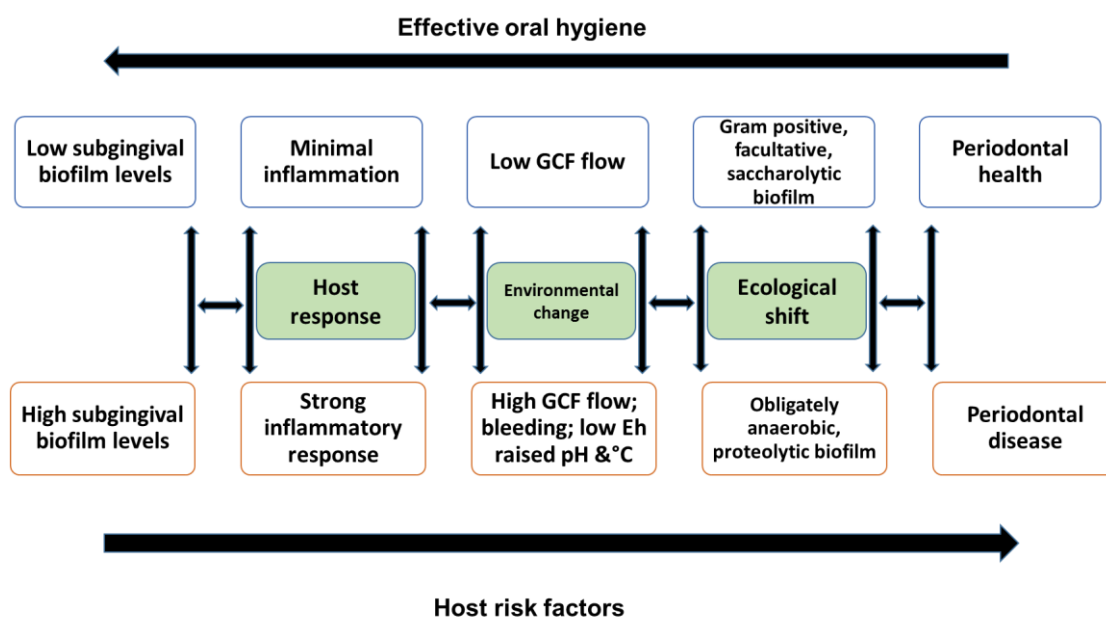


Figure 1.14 The “ecological plaque hypothesis” in relation to periodontal disease.

There is a dynamic relationship between the host environment and the resident subgingival microbiota. An increase in levels of biofilm around the gingival margin leads to a host inflammatory response which, in turn, alters local environmental conditions. These changes will select for a more proteolytic microbial community, which will continue to drive the inflammatory response, providing further selection pressures for a proteolytic and anaerobic microbial consortium that is better adapted to the new environment. Adapted from (Marsh and Devine, 2011) with permission.

Socransky *et al.* (1998) employed cluster analysis of subgingival plaque samples to show that microbial complexes existed within this plaque. They mentioned six closely associated groups of bacterial species (Figure 1.15). Four of these are early colonisers of the tooth surface represented by *Actinomyces*, a yellow complex consisting of members of the genus *Streptococcus*, a green complex consisting of (*Capnocytophaga* species, *Aggregatibacter actinomycetemcomitans* serotype a, *Eikenella corrodens* and *Campylobacter concisus*), and a purple complex consisting of *Veillonella parvula* and *Actinomyces odontolyticus*. The last two groups of complexes are considered late colonisers of the tooth surface and are represented by the red complex containing *P. gingivalis*, *T. forsythia* and *T. denticola*, with the orange complex consisting mainly of (*Fusobacterium nucleatum* subspecies and *Prevotella* subspecies).

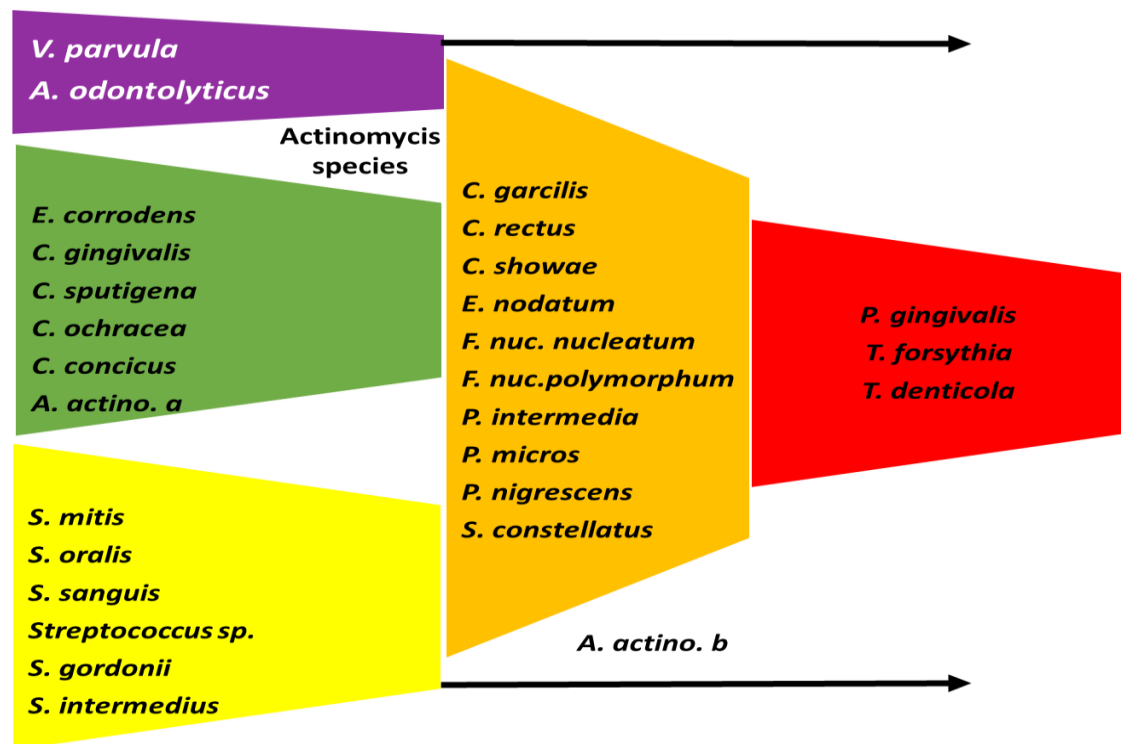


Figure 1.15 The association among subgingival species. The base on the left is comprised of species thought to colonise the tooth surface and proliferate at an early stage. The orange complex becomes numerically more dominant later and is thought to bridge the early colonisers and the red complex species which become numerically more dominant at late stages in plaque development. Adapted from (Socransky *et al.*, 1998) with permission.

The red complex species were rarely detected in the absence of members of other “complexes”, especially the “orange complex”. Both red and orange complexes are recognised to be the cause of periodontal disease, with their constituent bacteria being more dominant in pockets exhibiting periodontitis (Socransky *et al.*, 1998, Socransky and Haffajee, 2002). In addition, they possess the ability to produce virulence factors that are capable of causing direct damage to the extracellular matrix, such as proteinases, epitheliotoxin, cytolethal distending toxin, hemolysin and cytotoxic virulence factors that enable it to evoke an immune response, such as ammonia, and hydrogen sulfide (Haffajee and Socransky, 1994). The notion of periodontal complexes supported the latest theory, named “keystone pathogen hypothesis” (Hajishengallis *et al.*, 2012). At low abundance, keystone pathogens such as *P. gingivalis* manipulate host response to promote remodelling both the composition and levels of community participants transferring the normal symbiotic microbiota into a dysbiotic one (Hajishengallis *et al.*, 2012,

Hajishengallis and Lamont, 2016). In this context keystone pathogens are risk factors rather than causative agents of disease (Hajishengallis and Lamont, 2016). Furthermore, *P. gingivalis* produces trypsin-like proteases, which are considered as virulence factors in periodontitis (Sorsa *et al.*, 1994). Among these, Lys-gingipain plays a vital role in the development of periodontal disease via the direct destruction of periodontal tissue (degraded human type I collagen) and the disturbance of normal host defence mechanisms (immunoglobulins G and A) (Abe *et al.*, 1998). Several virulence factors have been recognised in *T. forsythia*: trypsin-like (Grenier, 1995), cytotoxic methylglyoxal (Maiden *et al.*, 2004), sialic acid utilisation and uptake (Roy *et al.*, 2010), α -D-glucosidase and N-acetyl-b-glucosaminidase by which *T. forsythia* can modify the harmful host proteins effect to protect them and other crevicular bacteria (Hughes *et al.*, 2003) and apoptosis-inducing activity represented by forsythia detaching factor and relating to the disintegration of tissues (Nakajima *et al.*, 2006). In addition, leucine-rich repeat cell-surface-associated and secreted protein BspA may play a role in its adherence to oral tissues or triggering the host immune response (Sharma *et al.*, 1998), while haemoglobin releasing PrtH may participate in increasing the hemin concentration in periodontal sites (Saito *et al.*, 1997), and the sialidases SiaH and NanH play an important role in cell wall synthesis, nutrition and modify the host cell membranes to provide nutrition for their growth (Thompson *et al.*, 2009).

Of the other bacteria that are often associated with periodontal disease, and many other oral bacterial conditions- such as endodontic infections, *Fusobacterium nucleatum* is notable. It was included by Socransky in the Orange complex of organisms, but its high prevalence orally, means it is worthy of special mention and is the subject of the next section.

1.9.3 *Fusobacterium nucleatum*, periodontal and other oral and non-oral diseases

F. nucleatum subspecies are G-negative anaerobes with a characteristic long fusiform shape (Figure 1.16). They are prominent in the oral microbiota and important in biofilm ecology and human infectious diseases (Könönen, 2000, Ximénez-Fyvie *et al.*, 2000). Concerning the oral cavity, *F. nucleatum* species were found to be abundant in both diseased and healthy individuals (Moore and Moore, 1994, Loozen *et al.*, 2014). Griffen *et al.* (2012) performed 454 pyrosequencing of 16S rRNA genes to compare subgingival microbiom from both 29 chronic periodontitis subjects and 29 healthy controls. They concluded that *F. nucleatum* is prevalent in both groups but their numbers

were significantly higher in disease pockets. There is an increase in the prevalence of *F. nucleatum* with the increase in the severity and progression of inflammation in periodontal disease (Moore and Moore, 1994, Yang *et al.*, 2014). In addition, they could be detected in both reversible forms of gingivitis and the advanced forms of periodontitis including chronic periodontitis and generalized aggressive periodontitis (Kistler *et al.*, 2013, Yang *et al.*, 2014, Liu *et al.*, 2014). It can be also associated with endodontic infections such as periapical periodontitis and intraradicular endodontic infections (Didilescu *et al.*, 2012, Fujii *et al.*, 2009, Vianna *et al.*, 2006), and also in head and neck infections such as acute mastoiditis, sinusitis, tonsillitis and chronic otitis (Brook, 1994, Han, 2011b).

There are five subspecies of *F. nucleatum* that inhabit the human oral cavity: *F. nucleatum* subsp. *nucleatum*, *F. nucleatum* subsp. *polymorphum*, *F. nucleatum* subsp. *fusiforme*, *F. nucleatum* subsp. *vincentii*, and *F. nucleatum* subsp. *animalis* (Dzink *et al.*, 1990, Bolstad *et al.*, 1996, Karpathy *et al.*, 2007). The complete genomes of *F. nucleatum* subsp. *nucleatum* ATCC 25586 (FNN) (Kapatral *et al.*, 2002), *F. nucleatum* subsp. *polymorphum* ATCC 10953 (FNP) (Karpathy *et al.*, 2007) are published. In addition, a partially sequenced genome for *F. nucleatum* subsp. *vincentii* ATCC 49256 (FNV) is also available (Kapatral *et al.*, 2003). *F. nucleatum* with *Prevotella intermedia* form the main organisms of the orange complex that have strong correlation with the red complex species (*Porphyromonas gingivalis*, *Tannerella forsythia* and *Treponema denticola*) as the latter were rarely found in the absence of the former (Socransky *et al.*, 1998).

Importantly, *F. nucleatum* is thought to act as a bridging organism that connects early G-positive colonisers and the late anaerobic G-negative species of the red complex, though may also play a major role in pathogenic plaque establishment (Kolenbrander, 2000, Kolenbrander *et al.*, 2006). Mono-species infection with *F. nucleatum* induces periodontal abscess associated with bone loss in mice animal model (Casarin *et al.*, 2013). In addition, *F. nucleatum* has been shown to have a positive synergistic effect on *T. forsythia* (Sharma *et al.*, 2005) and *P. gingivalis* (Bradshaw *et al.*, 1998) in both biofilm growth and cellular invasion experiments as well as acting synergistically with *T. forsythia* to induce alveolar bone loss in a mouse periodontitis model (Settem *et al.*, 2012).

F. nucleatum is also recognised as one of the most ubiquitous species found in extra-oral infections (Han and Wang, 2013). However, they are occasionally associated present as part of a normal flora with their occurrence starting to be detected under diseased conditions (Aagaard *et al.*, 2012, Segata *et al.*, 2012). Recently, more and more they are considered as one of the microorganisms that play a significant roles in human diseases (Han, 2015). Several studies linked between the severity of periodontal disease and detection of *F. nucleatum* in cardiovascular diseases such as the increase in the frequency of detecting *F. nucleatum* in atherosclerotic plaques (Han and Wang, 2013, Elkaim *et al.*, 2008) and the improvement of the rheumatoid arthritis clinical outcomes associated with periodontal treatment (Ortiz *et al.*, 2009). *F. nucleatum* is by far the most prominent oral species that is implicated in adverse pregnancy outcomes that includes preterm labor, preterm premature rupture of membranes, miscarriage, etc (Casarin *et al.*, 2013) and it has been suggested that hematogenous transmission of *F. nucleatum* from the maternal oral cavity is responsible for the bacterial translocation to the intrauterine cavity (Han, 2011a, Han, 2011c).

F. nucleatum possesses several virulence mechanisms that aid this microorganisms to participate successfully in oral and extra-oral infections, those virulence mechanisms can be divided into colonization and dissemination, and host responses induction (Han, 2011b).

Several adhesins had been identified in *F. nucleatum* represented by Fap2, RadD, and aid, which are utilized for interspecies interactions (Kaplan *et al.*, 2014, Kaplan *et al.*, 2009, Kaplan *et al.*, 2010). In addition, it possesses the capability to interact with mammalian cells i.e. endothelial cells, PMNs, and fibroblasts as well as various molecules such as salivary macromolecules, human IgG, and extracellular matrix proteins (Han, 2011b, Bachrach *et al.*, 2005). FadA is the best characterised adhesin that utilized by *F. nucleatum* for host cells binding (Han, 2011b). This virulence factor is encoded by both *F. nucleatum* and *F. periodonticum* and used as potential diagnostic marker for both species detection (Han *et al.*, 2005). FadA is more frequently detected in dental plaque samples from patients with periodontal diseases such as gingivitis and periodontitis (Liu *et al.*, 2014). Rubinstein *et al.* (2013) showed an increased level of *fadA* gene levels from *F. nucleatum* in colon cancer compared to lower gene level in normal individuals (Rubinstein *et al.*, 2013). FadA allows the direct bacterial invasion into the host cells, and causes loosened cell-cell junctions, and thus increasing endothelial permeability as it binds to VE-cadherin on the endothelial cells (it also binds to E-cadherin on epithelial

cells and colorectal cancer cells) (Fardini *et al.*, 2011). *F. nucleatum* also facilitates the penetration of other bacteria into loosened endothelial cells and thus improves the invasion process, such as *Streptococcus cristatus* and *E. coli*, and this is probably the reason behind *F. nucleatum* having an association with other bacterial species in mixed infections (Fardini *et al.*, 2011, Edwards *et al.*, 2006).

F. nucleatum induces a range of host responses (Han, 2011b). Han *et al.* (2000) studied the interactions between human gingival epithelial cells and a group of G-negative periodontal pathogens including *T. forsythus*, *F. nucleatum*, *P. gingivalis*, and *P. intermedia* using an *in vitro* tissue culture model. The study revealed that the adherence and invasion of *F. nucleatum* was associated with high levels of inflammatory cytokine IL-8 secretion from the epithelial cells. In another study, the secretions of TNF- α was detected when *F. nucleatum* incubated with the immune NK cells as a results of direct recognition of natural cytotoxicity receptor NKp46 to the invaded *F. nucleatum* (Chaushu *et al.*, 2012). In addition, it had been demonstrated that *F. nucleatum* induces human lymphocyte cell death (lymphocyte apoptosis) via its outer membrane proteins Fap2 and RadD, which share regions homologous to Jurkat cells autotransporter secretion systems (type Va secretion systems) (Kaplan *et al.*, 2010). FAD-I from *F. nucleatum* induces β -defensin 2 (which regulate adaptive immune functions) upon contact from human oral epithelial cells (Gupta *et al.*, 2010).

The members of the genus *Fusobacterium* to date are genetically intractable due to fact that they are not associated with phage transduction or well known conjugation and natural transformation mechanisms, and thus study their biology were slowed down (Han *et al.*, 2007, McGuire *et al.*, 2014). This is in part due to the variation and differences in restriction-endonuclease systems that *Fusobacterium* species harbored which cleave foreign DNA irrespective of the extent of methylation (Lui *et al.*, 1979). McGuire *et al.* (2014) applied whole-genome sequencing and comparative analysis from a diverse set of *Fusobacterium* species to study their genetic determinants of evolution in host cell invasion. They concluded that active virulent species have larger genomes (e.g. *F. nucleatum* and *F. periodonticum*) than passive invaders (e.g. *F. necrophorum*). In addition, the active invaders species genome harbored twice the number of genes encoding membrane-associated proteins than the passive invader genomes.

F. nucleatum has increasingly brought attention as an emerging pathogen, it is actively participate in diverse infections that affected the oral cavity, head and neck, and

human body. In addition, it is recently recognised as an opportunistic commensal turned pathogen that has been overlooked previously. *F. nucleatum* is an important participants in periodontal disease that been linked to a diverse of human pathologies. However, little is known about the affect of mobile genetic elements on the overall virulence of *F. nucleatum* to date due to its genetic intractability. Thus, it is crucial to close this knowledge gap and further investigates these pathogens that will ultimately enable the development of diagnostic and therapeutic strategies for the detection and treatment of *Fusobacterium* associated infections.

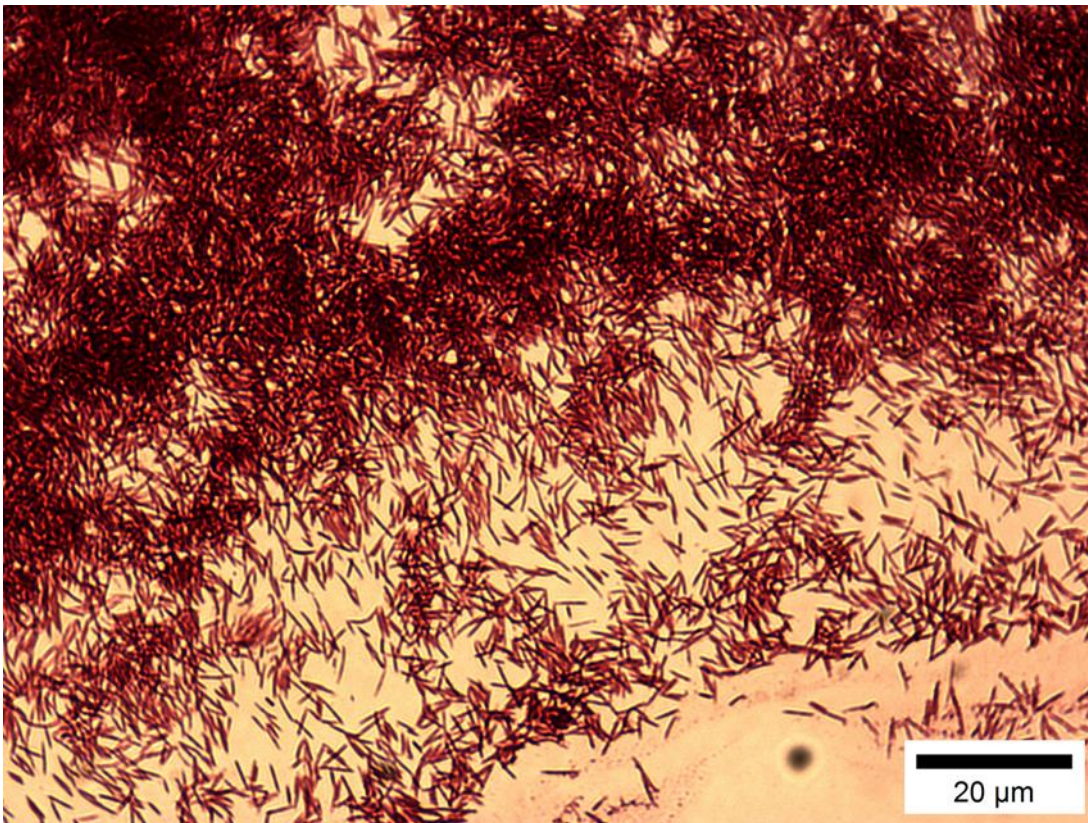


Figure 1.16 Gram stain of *F. nucleatum* clinical strain. This strain was isolated in this study using TSBV selective media see section 4.2.

1.9.4 Treatment of periodontal disease

Currently the treatment for periodontal diseases in dental practice involves two basic procedures, namely mechanical debridement to remove plaque and calculus and the use of adjunctive oral antimicrobial agents. These may be locally or systemically administered. Mechanical removal of plaque and calculus from the tooth crown and root surface will disrupt the biofilm that causes periodontal inflammation (Pihlstrom *et al.*, 2005). This is usually achieved by the use of hand instruments or ultrasonic powered instruments in scaling and root surface debridement procedures, leading to disruption of the pathogenic microbiome present on tooth surfaces to allow the body to overcome the pathogenic status and return to a normal healthy resident microflora plaque. In addition, successful treatment is dependent on the patient cleaning their dentition on a daily basis. Occasionally a mouthwash may be used as an adjunct to treatment in order to reduce tissue inflammation and decrease periodontal pocket depths (Cobb, 1996). In addition, those with systemic disease that affects the host response and the periodontal condition may benefit from the adjunctive use of antimicrobials (Pihlstrom *et al.*, 2005, Slots, 2004).

Several clinical studies have demonstrated that the use of azithromycin as a systemic antimicrobial and anti-inflammatory has the potential to improve chronic periodontitis (Smith *et al.*, 2002, Haffajee *et al.*, 2007). Haas *et al.* (2008) showed that the adjunctive use of azithromycin on a patient suffering from aggressive periodontitis significantly reduces the periodontal probing depth and improves attachment gain. Azithromycin has a wide antimicrobial spectrum with *in vitro* activity against aerobic and anaerobic G-negative microorganisms (Williams *et al.*, 1992) and exhibits an excellent ability to penetrate into both normal and pathological periodontal tissues (Blandizzi *et al.*, 1999). However, combination drug therapies, aimed at enlarging the antimicrobials spectrum and exploiting synergy between antibiotics, are often indicated in cases with complex mixed periodontal infections, for example, the combination of amoxicillin and metronidazole to eradicate *Aggregatibacter actinomycetemcomitans* and suppression of *Porphyromonas gingivalis* in recalcitrant adult periodontitis (van Winkelhoff *et al.*, 1992).

Despite the positive results associated with the use of antibiotics as an adjunct to mechanical treatment, new reports have mentioned a rise in resistance against the usual prescribed antibiotics by pathogenic bacteria, and this is a cause for concern (Ardila *et al.*, 2010, Kulik *et al.*, 2008).

1.10 Hypothesis and aims

1.10.1 Hypothesis

Novel bacteriophages and phage endolysins with therapeutic potential against endodontic and oral associated pathogens can be isolated from human and wider environments and have therapeutic potential.

1.10.2 Aims and objectives

The aims of the research have been divided into two parts:

Aim 1:

Characterisation of *Fusobacterium nucleatum polymorphum* ATCC 10953 prophage and potential prophage lysins:

- Knowing that phage lysis module encodes a hydrolytic protein against bacterial cell wall peptidoglycan, we therefore set out to isolate and purify the protein to examine its potential antimicrobial activity.
- Investigating the possibility of prophage induction from *Fusobacterium nucleatum polymorphum* ATCC 10953.
- Studying the effect of prophage on *Fusobacterium nucleatum polymorphum* ATCC 10953 virulence.
- Examine the presence of *Fusobacterium nucleatum polymorphum* and its prophage in clinical plaque samples taken from chronic periodontitis cases of patients receiving periodontal treatment.

Aim 2:

Isolation of lytic bacteriophages targeted against endodontic and oral infection associated pathogens through:

- Detection of bacteriophages in samples taken from human oral saliva and dental plaque.
- Isolation of a range of bacteriophages using other sources from the wider environment, such as sewage wastewater.
- Morphological, genomic characterisation of the isolated bacteriophages.

- Determining the phage-host range of any isolated bacteriophage against a range of oral laboratory and clinical oral strains.
- Testing the efficiency of isolated phages towards biofilm elimination.
- Establishment of animal model for testing phage towards bacterial infection.

Chapter 2: Materials and Methods

2. Materials and methods

All chemicals in this study were from Sigma-Aldrich Company Ltd, Dorset, UK unless otherwise stated.

2.1 Bacterial strains, plasmid vector and primers

Bacterial strains, plasmid vector and primers used are described in Tables 2.1, 2.2, 2.3, 2.4 and 2.5.

Table 2.1 Anaerobic bacterial strains used in this study.

Strains	Origin
<i>Fusobacterium nucleatum polymorphum</i> ATCC 10953 (FNP)	Purchased from ATCC biological resource centre
<i>Fusobacterium nucleatum nucleatum</i> ATCC 25586 (FNN)	Lab strain Gift from Professor William Wade, Kings college, London
Clinical strains source: dental plaque of patient attending Periodontology Clinic at the Charles Clifford Dental Hospital, Sheffield, UK.	
<i>F. animalis</i> Shef2	Graham Stafford collection, School of Clinical Dentistry, University of Sheffield
<i>F. animalis</i> Shef3	Graham Stafford collection, School of Clinical Dentistry, University of Sheffield
<i>F. nucleatum</i> Shef4	Graham Stafford collection, School of Clinical Dentistry, University of Sheffield
<i>F. polymorphom</i> Shef	Graham Stafford collection, School of Clinical Dentistry, University of Sheffield
<i>Prevotella intermedia</i> Shef6	Graham Stafford collection, School of Clinical Dentistry, University of Sheffield
<i>Prevotella melaninogenica</i> Shef14	Graham Stafford collection, School of Clinical Dentistry, University of Sheffield
<i>Prevotella tanneriae</i> Shef21	Graham Stafford collection, School of Clinical Dentistry, University of Sheffield
<i>Prevotella</i> Shef9	Graham Stafford collection, School of Clinical Dentistry, University of Sheffield
<i>Prevotella salivae</i> Shef12	Graham Stafford collection, School of Clinical Dentistry, University of Sheffield
<i>Prevotella denticola</i> Shef22	Graham Stafford collection, School of Clinical Dentistry, University of Sheffield
<i>Prevotella buccae</i> Shef13	Graham Stafford collection, School of Clinical Dentistry, University of Sheffield
<i>Porphyromonas gingivalis</i> Shef10	Graham Stafford collection, School of Clinical Dentistry, University of Sheffield
<i>Porphyromonas gingivalis</i> Shef15	Graham Stafford collection, School of Clinical Dentistry, University of Sheffield

Table 2.2 *E. coli* strains used in transformation.

Strain	Genotype	Source
DH5 α	<i>F</i> – ϕ 80dlacZAM15 Δ (lacZYA-argF) U169 <i>deoR recA1 endA1 hsdR17(rk–, mk+) phoA</i> <i>supE44 λ– thi-1 gyrA96 relA1</i>	New England Biolabs (NEB)
BL21(DE3)	<i>F</i> – <i>ompT, hsdSβ(rβ–mβ–) dcm gal</i> λ (DE3 [lacI, lacUV5-T7, gene1, ind1, sam7, nin5])	Stratagene
C41(DE3)	<i>F</i> – <i>ompT, hsdSβ(rβ–mβ–) dcm Ion</i>	Graham Stafford collection

Table 2.3 Plasmid vector used in this study.

Plasmid	Description	Phenotype	Reference/ source
pGEX- 4T-3	<i>Ptac</i> (tac promoter) driven glutathione S-transferase fusion expression vector	ampicillin resistant	GE Healthcare Life Science
pET15b	T7 <i>lac</i> , N terminal, His Tag, suitable as a cloning and expression vector	ampicillin resistant	Novagene
pET28a	T7 <i>lac</i> , N terminal, His Tag, suitable as a cloning and expression vector	kanamycin resistance	Novagene
pJET1.2/blunt	T7 promoter, suitable as cloning vector	ampicillin resistant	Thermo Scientific, UK

Table 2.4 Primers used in this study and their details.

Name	Oligonucleotide Sequence
FNP rpoB F	5' TGCTCTGGCATGCATTTTGT 3'
FNP rpoB R	5' ATGGGATTCATGCCTTGGGA 3'
FNP 1688 F	5' CTCCGGGTCAAGTTGAAGCA 3'
FNP 1688 R	5' TGCGTTTGCTGATATTGCTGG 3'
FNP 1707 F	5' AAACATATGAAAAAAGTTGCTTTAATAATAGG 3'
FNP 1707 R	5' TTTGGATCCTTAAACCTCCTTAACTGATC 3'
16s 27F	5' AGAGTTTGATYMTGGCTCA 3'
16s 519R	5' GWATTACCGCGGCKGCTG 3'
T7 primer F	5' TAATACGACTCACTATAGGG 3'
T7 primer R	5' CCGCTGAGCAATAACTAGC 3'
pJET1.2 F	5'CGACTCACTATAGGGAGAGCGGC3'
PJET1.2 R	5'AAGAACATCGATTTTCCATGGCAG3'
pGEX F	5'GGGCTGGCAAGCCACGTTTGGTG3'
pGEX R	5'CCGGGAGCTGCATGTGTTCAGAGG3'
F=forward, R=reverse	

2.1.1 Anaerobic clinical bacterial source and growth conditions

All anaerobic clinical strains were isolated from the dental plaque obtained from deep periodontal pockets of patients with chronic periodontitis by my colleague Sarhang Gul (Table 2.1). Ethical approval was obtained from Yorkshire and Humberside NRES Committee (study number 17158) and undertaken between 2013 and 2015 (Appendix 3).

Anaerobic bacteria were routinely grown either on fastidious anaerobe (FA) agar (LabM Limited, UK) plates containing 7% horse blood (Oxoid, UK) or in liquid culture brain-heart infusion (BHI) (Gould and Bal) broth (Sigma, UK) containing 0.5% yeast extract (YE) (Oxoid, UK), 5.0 µg/ml haemin (Sigma, UK), 1.0 µg/ml cysteine (ICN Biomedicals Ltd, UK) and 2.0 µg/ml menadione sodium bisulphate (vitamin K) (Sigma, UK). They grow at 37°C until colony formation on plates or sufficient liquid culture had taken place in an anaerobic cabinet (Don Whiteley Scientific, UK) with an atmosphere consisting of 10% CO₂, 10% H₂ and 80% N₂ gases (BOC, UK). The bacteria were long term stored at -80°C in a mixture of their respective liquid culture and 20% glycerol (v/v).

2.1.2 *E. coli* strains

E. coli strains were routinely grown aerobically on Luria-Bertani (LB) agar (Sigma, UK) plates supplemented with 50 µg/ml ampicillin (Sigma, UK). It was also grown in liquid LB broth (Sigma, UK) with appropriate antibiotics where applicable (50µg/ml ampicillin) at 37°C aerobically with agitation at 200 rpm. Strains were stored long term at -80°C in LB broth containing 20% glycerol (v/v).

2.1.3 *Enterococcus*, *A. actinomycetemcomitans* strains and growth conditions

All *Enterococcus* and *A. actinomycetemcomitans* strains used in this study and their sources are listed in Table 2.5. G-positive bacteria are represented by nineteen *E. faecalis* strains which were used as indicator strains in this study, eight strains named OS16, EF1, EF2, EF3, ER3/2s, EF54, V583, JH2-2 were kindly donated by ACTA University, Amsterdam, Holland. Four strains named OMGS 3197, 3198, 3885, 3919 were donated by the Department of Oral Microbiology and Immunology, Institute of Odontology, Sahlgrenska Academy, University of Gothenburg, Sweden. The majority of the bacterial strains are in fact oral clinical isolates either directly isolated from endodontic abscess or mouth wash of patients receiving endodontic treatments. OG1RF, OG1RF *epaB* TX5179 mutant and one *Enterococcus faecium* strain named (E1162) were obtained from Molecular Biology and Biotechnology department (MBB), University of Sheffield, UK. In addition, four *A. actinomycetemcomitans* were isolated in this study (Table 2.5). All *Enterococcus* bacteria and *A. actinomycetemcomitans* were cultured aerobically with 5% CO₂ at 37°C in BHI agar culture media (OXOID, UK).

Table 2.5 *Enterococcus* and *A. actinomycetemcomitans* bacterial strains used in this study and origin.

Bacteria source	Strains	Reference
<i>E. faecalis</i>		
Oral rinse-endodontic patient	EF1,EF2,EF3 OS16	Sedgley <i>et al.</i> (2004) Sedgley <i>et al.</i> (2005)
Oral orthograde retreatment	ER3/2s	Johnson <i>et al.</i> (2006)
Oral endodontic strains	OMGS3197, OMGS3198	Dahlen <i>et al.</i> (2012)
Oral mucosal lesions	OMGS3885, OMGS3919	Dahlen <i>et al.</i> (2012)
Non oral human isolate	EF54	Toledo-Arana <i>et al.</i> (2001)
Oral strain	OG1RF	Bourgogne <i>et al.</i> (2008)
Oral strain	OG1RF <i>epaB</i> TX5179; mutant harbouring an insertion in <i>epaB</i> (formerly <i>orfde4</i>)	Xu <i>et al.</i> (2000)
Epa variable region mutants and complements of OG1RF (unpublished)	OG1RF_11720	Donated by Professor Stéphane Mesnage Department of MBB, University of Sheffield
	OG1RF_11715	
	OG1RF_11714	
Non oral human bacteraemia	V583	Paulsen <i>et al.</i> (2003)
Non oral human isolate	U92304	Graham Stafford strain collection
Non oral human strain	JH2-2	Jacob and Hobbs (1974)
<i>E. faecium</i> ; Clinical blood isolate; CC17	E1162	Van den Bogaard <i>et al.</i> (1997)
<i>A. actinomycetemcomitans</i> isolated from dental plaque of patient attending the Periodontology Clinic at the Charles Clifford Dental Hospital, Sheffield, UK.		
Shef30, Shef31, Shef32, Shef33		This study

2.1.4 Isolation of clinical *A. actinomycetemcomitans* strains

An attempt was made to isolate the G-negative *A. actinomycetemcomitans* clinical bacteria strains from deep pockets of chronic periodontitis patients. These clinical strains were used as indicator for bacteriophage screening and isolation. Isolation was performed using the selective media for *A. actinomycetemcomitans* of TSBV (tryptic soy-serum-bacitracin-vancomycin) according to the methodology used by Slots (1982). TSBV agar contained (per liter) 40 g of tryptic soy agar (OXIOD, UK), 1 g of yeast extract (OXIOD, UK), 100 ml of horse serum, 75 mg of bacitracin (Sigma), and 5 mg of vancomycin (Fluka). Dental plaque was collected in 100 µl PBS and immediately transferred to the lab. After vortex, 10 µl was plated on the surface of agar and anaerobically incubated for 72 h at 37°C. The star shaped colonies were carefully picked up into BHI agar and stocks were saved in BHI with glycerol and stored at -80°C after genomic DNA extraction and 16s sequencing (Table 2.5).

2.2 Sample collection and processing

2.2.1 Clinical plaque and salivary sample collection from patients with chronic periodontitis

Clinical plaque and salivary samples were collected by two staff dental hygienists (Nivan Al- Hammouri and Claire Vallance-Owen) with my colleague- Sarhang Gul (PhD student) in attendance. Patients were recruited to the study from amongst those attending the Periodontology Clinic at the Charles Clifford Dental Hospital, Sheffield, UK. Potential participants were screened by the consultant periodontist (Prof. Andrew Rawlinson) against the inclusion criteria of age ≥ 18 years, possession of ≥ 20 teeth, diagnosis of chronic periodontitis with several diseased sites. Clinical plaque samples were collected from the deepest and most diseased site (≥ 6 mm) accessible for sampling and one accessible healthy site (≤ 3 mm). Ethical approval was obtained from Yorkshire and Humberside NRES Committee (study number 17158) and undertaken between 2013 and 2015 (Appendix 3). The samples were collected at baseline, 3 months and 6 months. At each interval, samples of plaque from each representative site and salivary samples are obtained. The clinical plaque samples were collected from patients using a sterile curette and suspended in 1ml PBS, while salivary samples were collected in 50 ml falcon collection tubes, and both samples were stored at -80°C until further processing. Samples of 45 subjects (270 samples in total, 135 from diseased sites and 135 from healthy sites) were analysed in this part of the study. The collected samples were used for the *Fusobacterium nucleatum polymorphum* ATCC 10953 and its prophage screening test.

2.2.2 Full mouth clinical plaque and salivary sample collection from patients with chronic periodontitis from Sheffield and Baghdad (IRAQ)

A new ethical approval was obtained to collect plaque samples from the whole mouth of patients with chronic periodontitis patients attending Charles Clifford Dental hospital (Sheffield) by two staff dental hygienists (Alison Barber and Claire Vallance-Owen) with me in attendance as chief investigator. The ethical permission was approved by NRES Committee Yorkshire and Humberside, study number 19056 (Appendix 1 and 2). As the previous sample collection mentioned in 2.2.1 was from specific sites only due to the nature of the study, and in order to increase the chance for novel lytic bacteriophage isolation from dental plaque, more raw material in the form of full mouth plaque was collected. The collection was performed as explained in 2.2.1 except that supra and sub gingival plaque from the whole mouth were pooled from each patient. In addition,

collection of full mouth plaque samples was performed from Iraqi dental patients attending the Periodontology Clinic, Al-Mustansiriyah University, College of Dentistry, Baghdad, Iraq after obtaining the necessary ethical approval (reference number 3670, Appendix 4). The samples were mixed together in 150 ml PBS and shipped to UK from Iraq by DHL express delivery. 21 and 50 samples were obtained from Sheffield and Baghdad dental patients respectively.

2.2.3 Dental chair drain samples collection

Dental chair drain (sucker drain) samples were collected from the dental chairs, University of Sheffield, School of Clinical Dentistry, Periodontal Department. Hard sewage particles were picked using sterile spatula, while smear samples were collected from the drain walls using sterile cotton swap. Both hard and soft smear samples were collected in 50 ml falcon tube containing 5 ml SM buffer (1 M Tris-HCl Buffer pH 7.4 with 5 M NaCl, 1 M MgSO₄, and 1% Gelatin) and stored at 4°C for further processing (Figure 2.1).



Figure 2.1 Dental chair sucker drain collector.

2.2.4 Wastewater sample collection

Bacteriophage were isolated from wastewater using a plastic container from a treatment plant in Sheffield, UK. The plant treats both industrial and domestic wastewater with the capacity of 185,000 P.E. (population equivalent). The wastewater collected from the inlet of the plant that had been through sieving to remove any large solids but had not been treated chemically or biologically.

2.2.5 Sample processing

Small samples (1 ml) from each category were pooled together (except wastewater, 200 ml), vortexed for 1 min and centrifuged (7,000 xg, 10 min) (Avanti J-26 XP, BECKMAN COULTER) to remove debris. For salivary samples 5 mM of DTT was added in each tube to reduce viscosity. The supernatant was filtered through a 0.45 µm syringe filter (Sartorius, Germany). Samples were then centrifuged 35,000 xg for 90 min to pellet the phage particles. The pellets were then carefully suspended overnight in 4°C with 2 ml of SM buffer and stored at 4°C to be used later either for enrichment or for phage screening through soft agar overlayer or spot pipetting. These samples were used for bacteriophage isolation.

2.3 Molecular biology techniques

2.3.1 Plasmid extraction from *E. coli*

Plasmid harbouring cloned gene of interest was extracted from *E. coli* (DH5 α) using ISOLATE II Plasmid Mini Kit (BIOLINE). Plasmid purification was performed according to manufacturer's instructions, resulting in high quality DNA.

2.3.2 DNA extraction

Bacterial cells from overnight cultures or clinical plaque samples were resuspended in sterile PBS and centrifuged at 10000 xg to pellet the bacterial cells and the volume was adjusted to 300 µl as a starting volume for DNA extraction. All samples were analysed within 2 months of collection, and stored at -80C before extraction. After brief vortexing, 90 µl of lysozyme (10 mg/ml, prepared with Tris-EDTA buffer), 3.6 µl mutanolysin (25,000 U/ml, prepared with Tris-EDTA buffer) and 1.8 µl lysostaphin (4000 U/ml, prepared with free nuclease water) are added and incubated for 1 h at 37°C. After that, 24 µl of proteinase K, 4.8 µl of RNase A (100 mg/ml) and 300 µl buffer AL (kit lysis buffer, QIAmp DNA mini kit column Qiagen) are added and incubated for 10 min at 56°C. Genomic DNA was extracted from the cell suspension using a QIAmp DNA mini kit column (Qiagen) as per the manufacturer's instructions. NanoDrop ND-1000 (Thermo-Fisher Scientific) was used to determine DNA concentrations. These samples were used for *F. nucleatum polymorphum* (ATCC 10953) and its prophage screening.

2.3.3 Polymerase chain reaction (PCR)

For screening applications after plasmid ligations and transformations for recombinant protein production, ThermoScientific DreamTaq Green PCR Master Mix (2x) polymerase was used in conjunction with the manufacturer's instructions in 25 µl reaction volumes. Typically, this consisted of 12.5 µl DreamTaq Green polymerase 2x mastermix, 1 µl of forward primer (5 nM), 1 µl of reverse primer (5 nM), 1 µl DNA and 9.5 µl distilled nuclease free sterile water. Normal reaction conditions were as in Table 2.6 (although annealing temperatures were according to primer used).

Table 2.6 PCR thermal cycling conditions.

Step	Temperature °C	Time	Number of cycles
Initial denaturation	95	3 min	1
Denaturation	95	30 s	30
Annealing	Primer Temp - 2	30 s	
Extension	72	1 min	
Final extension	72	10 min	1

2.3.4 Agarose gel electrophoresis

PCR reactions were analysed via gel electrophoresis. 1% agarose was added to 1x TAE buffer and heated until all the agarose powder had dissolved. Ethidium bromide was added to a concentration of 5 µg/ml to the gel before it was poured into the cast and the comb placed to create the wells. Once set, the gels were run in 1 x TAE buffer in a BIORAD mini-sub-cell for small gels or normal-sub-cell for large gels (BIO-RAD Laboratories, UK). The samples were loaded with 5 µl of Hyperladder I (Bioline, UK) used as a size standard for comparison and run at 100 V until the gel had migrated sufficiently. DNA separation was visualised under a UV light source and photographed using the G:BOX (SynGene) or Ingenius 3 (SYNGENE) and the GeneSnap software system (SynGene).

2.3.5 Cloning of putative lysins

The identified genes FNP-1699 and FNP-1700 were codon optimised *in silico* using the GeneART Gene Synthesis online tool (Thermo Fisher scientific), with suitable restriction sites added at the start and end of each sequence in accordance to the plasmid vector (see results sections). After receiving the constructs, the lyophilised DNA was

resuspended in nuclease free H₂O to obtain 50 ng/μL of DNA in order to be cloned into the cloning vector immediately or stored into -20°C.

Cloning was performed first by ligation into the pJET 1.2 plasmid vector using the CloneJET PCR Cloning Kit (Fisher scientific, UK), according to manufactures instruction's. In brief, 1μL from both the cloned gene (0.15 pmol) and pJET1.2/blunt (0.05 pmol) Cloning Vector were added to 10 μL 2 x Reaction Buffer. Nuclease free H₂O added until 19 μL and 1 μL of T4 DNA Ligase were added finally. The total procedure were set on ice. The ligation mixture was then incubated at room temperature (22°C) for 10 min and transformation into *E.coli* performed immediately.

2.3.6 *E. coli* transformation

2.4.6.1 Heat-shock

Cloning was performed by adding of 0.5 μl of plasmid harbouring the cloned gene of interest into cloning strain DH5α (NEB, 80°C competent cells), placed on ice for 10 min before being heat shocked by floating on 42°C water bath for 1 min. After placing on ice for 5 min, 1 ml of LB broth was added and left in 37°C for 1 h with constant agitation at 200 rpm. After centrifugation at 13.000 xg for 5 min, 950 μl of the supernatants was discarded, the pellets resuspended with the remaining supernatant and, spread onto two LB agar plates supplemented with antibiotic and incubated overnight at 37°C. One colony from overnight plate was subcultured into a new agar plate. Overnight broth was prepared from single colony followed by plasmid extraction as mentioned in 2.3.1.

2.3.6.2 Transformation by electroporation

Transformation was performed by adding 1μl plasmid into 70 μl BL21(DE3) and/or and C41(DE3) electro competent cells in a pre-chilled into a 0.1 cm electroporation cuvette (Bio-RAD laboratories UK) before being subjected to an electroporation pulse of 25 F, 2.5 kV and 200 Ω, giving a time constant of 4-5 milliseconds using the MicroPulser (BIO-RAD Laboratories, UK). Upon a successful electroporation, 1 ml LB broth was added to the electroporation cuvette. Then, the suspension was transferred into an eppendorf tube and incubated at 37° C for 1 h with agitation at 200 rpm for recovery before plating on an LB agar plate supplemented with antibiotic and incubating at 37°C overnight. The presence of antibiotic such as ampicillin allows selection for the cloned plasmid harboured the *E. coli* strain.

2.3.7 Extraction of DNA fragments from agarose gels

DNA fragments of appropriate fragment sizes were separated by agarose gel electrophoresis and were excised from the gel using a scalpel, followed by solubilisation and purification using the PCR and gel purification kit (BIOLINE) according to the manufacturer's instructions.

2.3.8 Restriction of DNA

Restriction endonucleases and their respective buffers were used in the digestion of DNA carried out in accordance to their manufacturer's instructions (New England Biolabs, UK). For double restriction digestion 30 µl volume reaction typically contained 20 µl plasmid DNA or DNA product, 1 µl of each restriction enzyme, 3 µl 10 x compatible buffer and 5 µl distilled nuclease free water. Reactions were incubated at 37°C for approximately 2 h or longer as necessary. The restriction enzymes used in cloning were *Nde*I, *Bam*HI, and *Xho*I.

2.3.8.1 Dephosphorylating the 5' end of the restricted DNA strand

To prevent the unintended re-circularisation of plasmid DNA in a ligation reaction, 1 µl high activity calf intestine alkaline phosphatase (CIAP) (New England Biolabs, UK) was added along with appropriate buffer to dephosphorylate the 5' end of DNA strand and left at 37°C for a further hour. This was followed by DNA purification using the PCR and gel purification kit (BIOLINE, UK) according to the manufacturer's instructions to remove the CIAP prior to ligation.

2.3.9 Ligation of DNA

In order to clone the gene into a suitable plasmid, double digestion of both vector and the gene with corresponding enzymes are performed first, the two could be ligated together as complimentary cut nucleotide sequences were available to attach. A 20 µl ligation mixture was set up as described in section 2.3.5. Transformation of the plasmid that harboured the cloned gene was performed immediately otherwise the ligated mixture was stored in -20°C until further work.

2.3.10 Preparation of electrocompetent *E. coli* cells

A 5 ml LB broth was inoculated from a single colony of *E. coli* BL21(DE3) or C41(DE3) strain. This was cultured aerobically overnight at 37°C with agitation at 200

rpm. Fresh 50 ml LB broths were inoculated with 1 in 100 of this overnight culture and grown under identical conditions until an OD₆₀₀ 0.6–0.7 achieved. The mid-log phase cells were harvested by centrifugation at 3,500 rpm (HERMLE Z400K centrifuge, Germany) for 20 min at 4°C and then washed and pelleted in 10 ml of ice cold 10% glycerol twice. After the final centrifugation, bacteria were re-suspended in 100 µl ice cold 10% glycerol and aliquoted into pre-chilled eppendorfs and used in DNA transformation immediately or stored at -80°C for future use

2.3.11 Sodium dodecyl sulphate polyacrylamide gel electrophoresis (SDS-PAGE)

Protein samples were analysed by SDS-PAGE. A 5% stacking gel was used in conjunction with a 12 or 15% resolving gel to resolve the protein samples (Table 2.7). Pre-casted gel NuPAGE® Novex® 4-12% Bis-Tris Gels, 1.0 mm, was used to run larger sized protein.

The following preparations were sufficient to make two gels:

Table 2.7 Preparation of resolving gel and stacking gel.

Components	Resolving gel 15%	Resolving gel 12%
Distilled water	3.55 ml	4.3 ml
40% (w/v) acrylamide	3.75 ml	3 ml
Upper resolving gel buffer: 18.17 g Tris Base, 0.4 g SDS dissolved in dH ₂ O, adjusted to pH 8.8 with NaOH, total volume 100 ml	2.5 ml	2.5 ml
TEMED (Tetramethylene diamine)	5 µl	5 µl
10% Ammonium persulphate (fresh)	350 µl	350 µl
	Stacking gel (Upper)	Stacking gel (Upper)
Distilled water (dH ₂ O)	4.7 ml	4.7 ml
40% (w/v) acrylamide	0.975 ml	0.975 ml
Lower resolving gel buffer: 6.06 g Tris Base, 0.4 g SDS dissolved in dH ₂ O, adjusted to pH 6.8 with HCl, total volume 100	2.1 ml	2.1 ml
TEMED (Tetramethylene diamine)	17 µl	17 µl
10% Ammonium persulphate (fresh)	100 µl	100 µl

Once the gel was set up, it was mounted in the mini PROTEAN Tetra Cell (BIO RAD Laboratories, UK) and 1 x SDS-PAGE running buffer (248 mM Tris Base, 1.92 M glycine and 1% w/v SDS). The protein samples to be loaded were prepared by adding equal volume of sample with 2 x SDS lysis buffer (125 mM Tris HCl, pH 6.8, 4% SDS, 0.05% bromophenol blue mixed with 1 M DTT) before heating at 100°C for 10 min. The comb was carefully removed from the gel before loading the 10 µl protein along with the

EZ run-protein ladder (Fisher, UK) of known size, and electrophoresed at a constant voltage of 200 V until the tracking dye had migrated to the bottom of the gel.

2.3.12 Protein expression and solubility test

Protein expression trials were used by inoculating a single colony of BL21(DE3) and/or C41(DE3) in 10 ml LB media. These were then grown to mid log phase ($OD_{600} = 0.8$) before induction with 1 mM Isopropyl β -D-1-thiogalactopyranoside (IPTG) and incubated for 5 h at 37°C. 1 ml of sample were taken at 0, 2, 4 and 5 h for a protein expression test. Once recombinant protein overexpression was confirmed, a repeat was done but with a 1 litre volume of LB. For solubility test the cells are harvested by centrifugation (5000 xg, 20 min, 4°C) before resuspending the resulting pellet, containing overexpressed proteins, with 25 ml of appropriate binding phosphate buffer (420 mM NaCl, 0.27 mM KCl, 10 mM Na_2HPO_4 , 1.8 mM KH_2PO_4 , pH 7.3), and then disrupted in a French pressure cell (SLM Aminco Instruments) at 1050 psi repeated 2-3 times. The soluble fraction was isolated from the supernatant after centrifugation (11,000 xg, 30 min, 4°C). Both the supernatant and the pellet were analysed in SDS-PAGE.

2.3.12.1 His-tagged recombinant protein purification

His-tagged recombinant protein purification from a cell lysate under native conditions was performed by gravity metal chelate affinity chromatography using Ni-NTA metal chelate affinity resin (Amintra, expedeon) and was based on purification via resin chelating groups that immobilize transition Ni^{2+} ions (Porath, 1988; Sulkowski, 1989). The 6 x histidine tag engineered at the N or C terminus of the protein amino acid can act as electron donors on the surface of the protein and bind reversibly to the transition Ni^{2+} ion in the resin. This will allow the binding, washing and elution of the protein of interest. The preferred elution method for purifications under native conditions is through using competitive counter-ligand (imidazole). 0.5-1 ml of resin beads was equilibrated with 10 ml phosphate buffer (420 mM NaCl, 0.27 mM KCl, 10 mM Na_2HPO_4 , 1.8 mM KH_2PO_4 , pH 7.3) to remove ethanol from beads and then centrifuged (500 xg, 5 min). The binding buffer (containing 10 mM imidazole) with the soluble protein was added to the beads, mixed for 1 h at room temperature and applied to the column. Washing was performed next by adding 10-20 ml of buffer containing 10-30 mM imidazole (repeated three times) and passed through the column slowly (1 ml/min), this is followed by elution

of the protein with 1 ml of 250-350 mM imidazole buffer- reapplied three times. In total 10 fractions of eluted protein were collected. The collected eluates were evaluated SDS-PAGE protein gel electrophoresis. Protein-containing fractions were pooled and dialysed against phosphate buffer for 10-18 h at 4°C, and stored at 4°C for use in the short term (NaCl concentration ranged from 140-200 mM).

2.3.12.2 GST-tagged recombinant protein purification

Purification of glutathione S-transferase tagged proteins was performed by using Glutathione covalently coupled to a high crosslinked agarose matrix resin (Amintra, expedeon). The principle is the same as His-tag purification except that protein is tagged with a large (26 kDa) GST tag, which binds immobilised reduced glutathione. 1ml of resin beads was equilibrated with 10 ml phosphate binding buffer to remove ethanol from beads and centrifuged (500 xg, 5 min). The binding buffer containing the soluble protein was added next to the beads, mixed for 30 min and applied to the column. Washing was performed by adding 10-20 ml of buffer (repeated three times) and run through the column slowly (1 ml/min), followed by elution of the protein with 1 ml of 20 mM fresh reduced L-glutathione in phosphate buffer. If the expression of the target protein was confirmed by running the eluted fragments on SDS-PAGE protein gel, a second expression attempt with on column cleavage of the GST tag and elution of target protein by adding of 1 ml of phosphate buffer (420 mM NaCl, 0.27 mM KCl, 10 mM Na₂HPO₄, 1.8 mM KH₂PO₄, pH 7.3) containing 1 mg/ml thrombin (Amersham Biocience) to the resin beads, followed by incubation at 4°C overnight. Protein-containing fractions were pooled and dialysed using dialysis phosphate buffer for 10-18 h at 4°C, and stored at 4°C for use in the short term (NaCl concentration is ranged 140-200 mM).

2.3.13 BCA Assays

BCA assays performed in order to calculate protein concentrations. Pierce BCA assay kit (Thermo-Fisher Scientific) used in accordance with the manufacturer's instructions. The bovine serum albumin (BSA) standards and the protein sample were suspended in the same buffer for production of standard curves.

2.3.14 Staining of polyacrylamide gels

The polyacrylamide gels were stained either with Instant Blue (Expedeon, UK) for 15 min then suspended with water, or with Coomassie blue staining solution (1.25 g

Coomassie R-250, 225 ml methanol, 225 ml H₂O and 50ml glacial acetic acid) for 2-3 h. Excess stain was washed with water and the gel destained (300 ml methanol, 100 ml acetic acid and 600 ml H₂O) until the background of gel became clear. The protein gel was documented using either a gel documentation system (Image scanner power look1120 USG, Amersham Bioscience) or using gel documentation system (Ingenius 3, SYNGENE).

2.3.15 Zymogram

In order to investigate the potential activity of FNP1700, cell wall materials were extracted from FNP ATCC10953 as described in Kato *et al.* (1979), in which overnight bacterial cells were harvested and boiled in 4% SDS for 1 h, the boiled cell suspensions were then ultracentrifuged at 110000 xg for 30 min. The sedimented residues were submitted to successive treatments with Pronase-P and trypsin to obtain purified peptidoglycans after being thoroughly washed with distilled water. Finally, bacterial cell wall components were resuspended in PBS after ultracentrifugation. Both PGN from commercial *S. aureus* and prepared cell wall components of FNP ATCC10953 were used in zymography for FNP_1700 lysin activity testing. Zymograms were performed by incorporating 0.1-0.2% PGN as substrate for enzymatic activity in 12% polyacrylamide SDS-PAGE gels (final concentration). The FNP_1700 lysin was loaded in denaturated form and run through the gel till end, renaturation of the enzyme in the gel in suitable denaturation buffer (0.1% Triton X-100 and 10 mM MgCl₂ in 20 mM sodium phosphate buffer pH 7.0) overnight at 37°C. Positive activity should be seen as clear zones in a background of PGN/KOH solution (Bernadsky *et al.*, 1994).

2.4 Phage techniques

2.4.1 Prophage induction from *Fusobacterium nucleatum polymorphum* ATCC 10953

To attempt to induce prophage from the FNP using Mitomycin C. 1 µg/ml Mitomycin C was added to 20 ml exponential phase *Fusobacterium nucleatum polymorphum* ATCC 10953 (FNP) (10⁸ CFU/ml). The CFU of bacterial cells were counted after spot dilution onto FA agar plates using the method of Miles and Misra. This was left for 2-5 h before the bacterial pellet was taken off via centrifugation at 15,000 xg (Avanti J-26 XP, Beckman Coulter) for 10 min and the supernatant passed through a 0.45 µm cellulose acetate membrane filter (Gilson, UK). This was further concentrated using

an ultracentrifuge of 85,000 xg for 60 min (Optima TLX Ultracentrifuge, Beckman Coulter). The pellet was resuspended either overnight in sterile nuclease free H₂O at 4°C to be used in phage screening or resuspended overnight in 4°C with 150 µl of 0.1 M ammonium acetate (pH 7) to be used in TEM Imaging.

2.4.2 Bacteriophage isolation from wastewater

10 µl of the suspended/ concentrated sample was spotted on BHI soft agar (0.7% top agar) (OXOID, UK) overlays containing 200 µl of indicator bacteria (overnight culture), spot assay. The bottom agar was composed of BHI solid agar supplemented with 5% horse serum (OXOID, UK). The formed plaques were picked using a sterile Pasteur pipette into 1 ml SM buffer to allow the phage particles to be released from the agar into the buffer overnight in 4°C. The suspended phage particles were then filtered with a 0.45 µm syringe filter and 100 µl of this then mixed with 200 µl of exponential growth phase indicator bacteria for 10 min to allow the phage particles to adsorb to the surface of host bacteria, then mixed with 2-3 ml of 45°C soft agar overlay, and poured above the bottom solid agar followed by overnight incubation at 37°C for plaque screening (double-layer assay). The phage were purified using three consecutive rounds of single-plaque isolation. The plaque from the third round was then picked into SM buffer containing 1% (vol/vol) of chloroform and stored at 4°C.

2.4.3 Double layer plaque assay and spot pipetting

10-50 µl of processed concentrated samples or enriched samples are mixed with 100-200 µl of mid log phase of the indicated clinical strain of bacteria; left for 10-30 min to allow the phage particles to adsorb into the bacteria. The resulting suspension was mixed with 5-6 ml soft top agar (50°C) and poured onto a previously solid bottom agar, following incubation at suitable conditions to allow the phage present in the samples to diffuse throughout the media and infect growing bacteria and give discrete plaques. This also will result in even distribution of plaques within the top agar layer (Lillehaug, 1997). In spot pipetting the phage-bacterial suspension are not mixed with the soft top agar but 5-10 µl of the suspension are pipetted into a previously set top bacterial-agar layer (Figure 2.2).

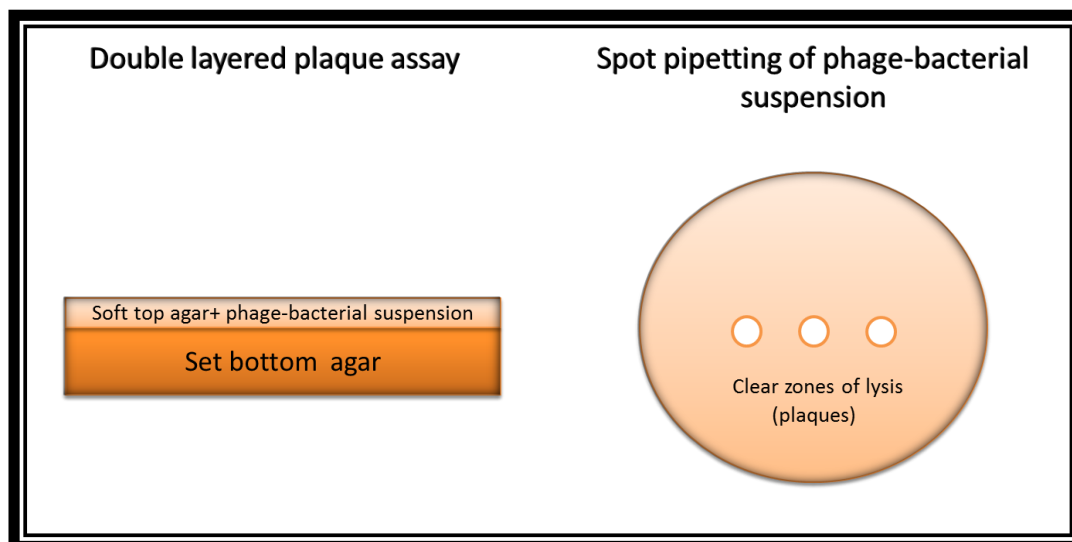


Figure 2.2 Double layer plaque assay and spot pipetting. In spot pipetting 5-10 μl of phage suspension are pipetted into a previously set top bacterial-agar layer. While in double layer plaque assay, phage-bacterial suspension and the soft top agar are mixed together and poured into a bottom set agar.

2.4.4 Enrichment of bacteriophage

Mid-log phase ($\text{OD}_{600} \sim 0.4$ to 0.6) of 20 ml BHI broth of host bacterial indicator pathogens strains were infected with 100 μl concentrated environmental or clinical samples and incubated overnight at 37°C . The enriched media were centrifuged ($5,000 \times g$, 5 min, 4°C), the supernatant was filtered with a $0.45 \mu\text{m}$ filtering and stored at 4°C .

2.4.5 Phage stock preparations

In order to prepare a working phage stock with known PFU (plaque forming unit) used in further phage characterisation, 40 ml exponential growth indicator bacteria were infected with 100 μl of stored phage suspension, followed by incubation for three hours at 37°C to allow phage to multiply and increase in numbers. The broth was then centrifuged at $7,000 \times g$ for 15 min and filtered through a $0.45 \mu\text{m}$ syringe filter to remove debris. Serial dilutions from the resultant broth were used in triplicate for plating in soft-agar overlayer as described in section 2.4.2 to count the PFU/ml for each isolated phage. For TEM preparation of the phage particles, the 40 ml filtered broth is subjected to $50,000 \times g$ centrifugation for 90 min, the resulted phage particles pellets were carefully resuspended overnight in 200 μl SM buffer and stored at 4°C .

2.4.6 Bacteriophage concentration by precipitation with Polyethylene Glycol (PEG 8000)

Further concentration of phage was made in order to yield a suitable working suspension for protein profile, genomic digestion, and DNA extraction. This was performed through precipitation with PEG 8000 according to Yamamoto *et al.* (1970) in short, 200 ml of exponential growth phase indicator bacteria (5×10^8 CFU/ml) were infected with phage suspension stock at MOI of 0.01 (multiplicity of infection) for 3 h, 1 M NaCl added with continuous mixing using magnetic stirrer at 4°C for 1 h. To precipitate phage particles, 10% PEG 8000 w/v was gradually added with continuous mixing and left overnight in 4°C. Centrifuge 11,000 xg for 20 min to sediment the precipitated phage. The resulted pellets then carefully resuspended overnight with 1 ml of SM buffer and stored in 4°C.

2.4.7 Electron microscopy for the isolated phage

Purified phage particles (3 µl) were placed onto carbon-coated copper grids, negatively stained with 2% (wt/vol) uranyl acetate (pH 4) for 1 min before the liquid on the grid withdrawn with the help of filter paper and washed with 3µl sterile distilled water. Particles were visualised by using a FEI Tecnai Transmission Electron Microscope at an accelerating voltage of 80 Kv at the Department of Biomedical Sciences, University of Sheffield. Electron micrographs were recorded using a Gatan Orius 1000 digital camera and Digital Micrograph software. To observe the phage along with bacteria, 1 ml exponentially growing cells were infected with phage at MOI of 1 for 30 min, after centrifugation at 7000 xg for 10 min, the pellet was resuspended with 1 ml 3% glutaraldehyde for 1 h at room temperature and examined under TEM as described above.

2.4.8 Infection cycle, adsorption rate and one step growth

2.4.9.1 Infection cycle

Exponentially growing cultures of the *E. faecalis* OS16 strain (5×10^8 CFU/ml) were inoculated with the phiSHEF 2 phage at MOI of 0.05, 0.1, 0.2, 2, 4, 8, 16, 30 and 120. The mixtures were incubated at 37°C, and the changes in the bacterial culture were monitored over time by measuring OD₆₀₀ every 10 min with 2 seconds circular shaking before each reading in plate reader spectrophotometer (Tecan infinite 200, Austria). The same procedure was done with the *E. faecalis* OS16 alone as negative control of infection.

2.4.9.2 Adsorption rate

The adsorption rate experiments were performed with a procedure described by Yoon *et al.* (2013) with small modifications. Briefly, overnight cultures of the bacterial strains were diluted 1:100 in BHI medium. Phage were added at an MOI of 1 to the diluted culture after counting the cells number (5×10^8 CFU/ml), mixed gently, and incubated at 37°C. An aliquot (100 µl) was removed immediately for determination of the initial phage titre. Incubation was continued for 12 min, and samples (100 µl) were collected every minute and diluted immediately in 900 µl cooled SM buffer. The diluted samples were centrifuged at 10,000 xg for 5 min and filtered using a 0.45 µm filters. Finally, the titres of unabsorbed phages in the supernatant were determined after serial dilution and infection into exponentially growing indicator strain in a double layer assay. The adsorption levels were represented by the percentage of the total number of phages present calculated as follows: [(initial phage titer / free phage titer in supernatant)/initial phage titer] / 100.

2.4.9.3 One-step growth

The test was performed to determine the latent period, eclipse period, and burst size. The procedure described by Carlson and Miller (1994) with some modifications was used. Briefly, 5 ml of exponentially growing cultures of the *E. faecalis* OS16 cells (5×10^8 CFU/ml) were infected with phiSHEF 2 phage at MOI of 0.1. After 5 min of phage adsorption, the cells were diluted 200 times (to reduce further infection), and incubated at 37°C. Two samples were taken every 5 min. The first sample was plated immediately without any treatment, and the second set of sample was plated after treatment with 1% (vol/vol) chloroform to release intracellular phages. The number of viral particles (PFU) was determined by spotting serial dilutions on 0.7% BHI soft agar overlay. Plaques from the treated samples indicated the number of free phage plus all the mature phage inside infected cells while the number of free phage plus infected cells are represented by the plaques from the untreated (no chloroform and therefore no cell lysis) samples. The eclipse period was determined as the time of the initial intersection of the two curves while the latent period was determined as the time when the initial steep curve of the untreated samples increase. The burst size was calculated by dividing the post-cell-lysis plateau value by the initial prelysis plateau value of the untreated samples.

2.4.9 Analysis of phage proteins

To define the major proteins present in the bacteriophage phiSHEF 2, 3, 4, 5, 6, and 7, SDS-polyacrylamide gel electrophoresis (PAGE) was performed. A PEG 8000 concentrated phage stock was mixed with equal volume of chloroform in order to release the phage particles, samples were vortex until an emulsion form, and centrifuged 10,000 xg for 10 min. Following mixing 50 µl from the upper layer (10^{11} - 10^{13} PFU/ml) with 50 µl of SDS-PAGE loading buffer, and heated at 95°C for 7 min. 10 µl volume of lysate was loaded directly onto 4-12% NuPAGE® Bis-Tris precast gels (Thermo fisher scientific, UK), and electrophoresed for 60min. Gels were stained with Instant Blue (Expedeon, UK) and documented using a gel documentation system (Image scanner power look1120 USG, Amersham Bioscience).

2.4.10 Mass spectrometry

For the identification of major phiSHEF 2 phage proteins, 'in gel digestion' with trypsin followed by MS/MS was performed. The gel band from an SDS-PAGE gel containing excised protein was cut into smaller pieces 1-1.5 mm for processing and resuspended in 200 µl destain solution (200 mM NH_4CO_3 in 40% v/v solution of acetonitrile CH_3CN), vortex, incubated at 37°C for 10 min. This process was repeated twice until the solution and gel pieces were clear. The gel pieces were then washed and equilibrated with 500 µl of 50 mM NH_4HCO_3 that will be used as the buffer later, for addition of trypsin. Reduction and alkylation was performed next, the gel pieces were reduced in the presence of fresh 10 mM dithiothreitol (DTT) for 30 min at 50°C. Followed by adding 55 mM iodoacetamide at room temperature in the dark, then resuspension in 50 mM NH_4HCO_3 . Dehydration of the gel pieces was done by adding 500 µl acetonitrile until it became white when removing the solution, followed by an overnight trypsinisation at 37°C by adding 50 µl trypsin (diluted from stock to 10 µg/ml trypsin in 50 mM NH_4CO_3) to gel pieces. Extraction of digested Proteins (Peptides) were followed by adding 20 µl of absolute Acetonitrile (MeCN) for 10 min at 37°C, followed by adding 50 µl of 5% Formic acid and incubated at 37°C for 10 min and centrifuged at 13000 xg (repeated twice). The supernatant was subjected to mass spec in Maxis hybrid ultra high resolution (quadruple time of flight system, Bruker Daltonics, Coventry, UK) which was kindly performed by Dr Caroline Evans, Department of Chemical and Biological Engineering, University of Sheffield, UK. All MS/MS data were searched using Mascot (Matrix Sciences) against the previously uploaded full genome sequence of phiSHEF 2

(fully annotated fasta amino acid file format). The coverage levels of 5% of the total protein length were used as cutoff values when identifying gene products as components of the viral particle (Casey *et al.*, 2014).

2.4.11 Phage DNA extraction

In order to remove contaminated DNA and RNA from the PEG 8000 concentrated phage stock, a 10 µg/ml DNase and RNase added. The mixture was incubated at 37°C for 30 min. A final concentration of 100 µg/ml of proteinase K was added to the mixture to degrade the enzymes and incubated at 50°C for 45 min. Removal of proteins from nucleic acids were achieved by extraction with phenol: chloroform: isoamyl alcohol (25:24:1). A small amount of isoamyl alcohol is added to further ensure the deactivation of any remaining RNase activity. DNA precipitated by adding two volumes of ice cold ethanol and left overnight at -20°C. DNA was Pellet through 16,000 xg for 20 min then the supernatant was carefully removed. 70% ethanol was added and centrifuged 5 min (repeated for two times). The supernatant was removed carefully without disturbing the pellet and left on the bench for 15-30 min to let the remaining ethanol disperse. Finally, DNA was dissolved with sterile water and stored in -20°C. The DNAs were used as templates for nucleotide sequencing and in restriction fragment length polymorphism (RFLP) of phage genome.

2.4.12 Restriction fragment length polymorphism (RFLP) and analysis of phage genome size

RFLP and agarose gel electrophoresis were applied to define the mapping and size of the phage genome. Phage genomic DNA was subjected to *HindIII* restriction enzyme (New England, Biolabs, UK) according to manufacturer's instruction. However, other restriction enzymes were also tried at initial stages such as *AfeI*, *EcoRI*, *DpnI*, *AgeI*, and *NedI*. The digested products were separated by 1% agarose gel electrophoresis (15 x 15 cm) in 1 x TBE buffer running at 90 volts for 4 h to determine the map and genomic size of bacteriophage. Generuler 1 kb DNA ladder (Thermo scientific) was used as the molecular size standards for the estimation of genomic size in a gel documentation system (Ingenius 3, SYNGENE).

2.4.13 DNA sequencing for phiSHEF 2, phiSHEF 4, and phiSHEF 5

Approximately 20 µg phage genomic DNA was extracted and verified by nanodrop (Nanodrop 2000; Thermo Scientific) quantification prior to delivery to the sequencing facility (MicrobesNG, Birmingham, UK). Sequencing was performed on the Illumina MiSeq and HiSeq 2500 platforms with 2 x 250 bp paired-end reads. Identify the closest available reference genome using Kraken (Wood and Salzberg, 2014), and map the reads to this using BWA mem (Li, 2013) to assess the quality of the data. Performing a *de novo* assembly of the reads using SPAdes (Bankevich *et al.*, 2012), the reads were trimmed using Trimmomatic (Bolger *et al.*, 2014) and the reads mapped back to the resultant contigs, again using BWA mem to get more quality metrics. An automated annotation was performed using Prokka (Seemann, 2014). Mauve align software tool (Darling *et al.*, 2004) were used to perform visual multiple comparisons while multiple sequence alignment was performed by Multalin (Corpet, 1988). In addition, PHAST (PHAge Search Tool) (Zhou *et al.*, 2011) and PHASTER (PHAge Search Tool Enhanced Release) (Arndt *et al.*, 2016) web servers were used for further confirmation of the annotated phages genomes and manually annotated using the Basic Local Alignment Search Tool (NCBI) (Altschul *et al.*, 1990). Conserved protein domains (where relevant) were detected using Pfam (Sonnhammer *et al.*, 1997). Complete genomes were visualized using Artemis (Rutherford *et al.*, 2000) and image produced using SnapGene® Viewer 1.1.3 Software.

2.4.14 Molecular determination of phage adhesion

In order to estimate the possible reasons behind the loss of successful infection of phiSHEF 2, 6 and 7 to *epaB* mutant and to point which stage of phage-host infection might effected, adsorption rate was performed as described earlier in phage adsorption rate experiment section 2.4.9.2. Free phage particles of phiSHEF 2 was counted at 0 min, 10 min, and 24 h after infection with *epaB* mutants cells and compared to that the control OG1RF cells. The free phage particles were counted from 24 h suspension after treatment with 1% (vol/vol) chloroform in order to lyse the cells and to release any possible trapped intracellular phage. In addition, 1ml from the 24 h phage-bacterial suspension was pelleted and resuspended with ice cold 1 ml PBS with high NaCl molarity of 0.28 M for 10 min in 4°C, and filtered using a 0.45 µm syringe filters. The titres of free phages in the supernatant was determined directly after serial dilution in order to determine the increased NaCl concentration on phage-bacterial adsorption strength. The phage count

from the 0.28 M NaCl sample was deduced from the free phage count of the control group of PBS (0.150 M NaCl) and to exclude cell lyses caused by increasing the molarity of NaCl, CFU was counted from and compared to control group. This experiment was repeated twice with triplicate each time.

2.4.15 Biofilm assay on polystyrene plates

The ability of the enterococcal strains to form a biofilm on an abiotic surface was quantified based on a previously described method with suitable modifications (O'Toole and Kolter, 1998). Briefly, *E. faecalis* strains were grown overnight in BHI at 37°C. The cultures were diluted 1:40 in fresh BHI medium and 1 ml of this cell suspension was used to inoculate sterile flat-bottomed 48-well polystyrene microtiter plates (Cellstar, greiner bio-one). Six wells per strain were inoculated with BHI alone used as negative controls. After static aerobic incubation at 37°C for 24 h (young biofilm) or 144 h (mature-stationary phase biofilm), a fresh BHI broth was changed every 24 h for mature biofilm to ensure a constant supply of nutrients. Broth was carefully drawn off from wells and, 1 ml fresh broth contain 10⁸ PFU/ml phiSHEF 2 phage or BHI only controls were added to three of the six wells of each group before incubation for another 3 h. Wells were then gently washed three times with 1 ml of phosphate-buffered saline (PBS). The plates were inverted on a paper towel and air dried and stained with 1% crystal violet for 15 min. The wells were washed again 3 times, and the crystal violet was solubilised in 500 µl of ethanol-acetone (80:20, vol/vol). The optical density at OD₅₇₀ was measured using a microplate reader spectrophotometer (Tecan infinite 200, Austria). Each assay was performed in triplicate and repeated three times.

2.4.16 Biofilm assay on teeth root surface (*in vitro*)

The ability of phiSHEF 2 phage to eradicate *E. faecalis* biofilm on extracted natural root surface was quantified based on previous described method of Resazurin dye change in colour and fluorometric assay (Perrot *et al.*, 2003). 1 mm thick root slices were cross sectioned above the root bifurcation area of multi-rooted human teeth (ethical approval number STH18841, Appendix 5) by water cooled 0.1 mm cutting saw (MEDREK 859088) and divided into two groups in 24-well microtitre plates (Cellstar, greiner bio-one) with final equal surface area for each group of root dentin pieces. A 7 day, mature, stationary phase (168 h) *E. faecalis* biofilm was grown as described earlier in the biofilm assay on polystyrene plates- i.e. 24 h media changes for 6 days. After that, the first group

(treated) was treated with 1 ml BHI containing 10^8 PFU/ml phiSHEF 2 phage while BHI only were added to the second group (untreated) before incubation for another 3 h. The root slices were transferred into 48-well microtitre plates and washed three times with 1 ml PBS. After treatment and washing, 0.350 ml of PBS containing resazurin solution at a final concentration of 1 $\mu\text{g/ml}$ was added to both groups in a 48-well plate and incubated at 37°C for 20 min. 0.3 ml from each well of both groups (treated and untreated) was transferred to 96-well microtitre plates and resorufin fluorescence was read using a microplate spectrofluorometer (Tecan infinite 200, Austria at λ_{exc} 570nm, λ_{em} 590 nm). The reading of the non-emitting dye of resazurin (treated) was subtracted from a control group, which contained only the resazurin dye. This assay was repeated 2 times with at least 3 samples in each group.

2.4.17 Zebrafish as *in vivo* model for phage treatment

Zebrafish maintenance and experimental work was performed in accordance with UK Home Office regulations and UK Animals (Scientific Procedures) Act 1986. Ethical approval was given by the University of Sheffield Local Ethical Review Panel. London. Wild-type (LWT) inbred zebrafish larvae were obtained from The Bateson Centre, University of Sheffield. All larvae were maintained in E3 medium at 30°C according to standard protocols and monitored for up to 4 days post-fertilization (dpf). *E. faecalis* OS16 strain were microinjected systemically by PhD student Magdalena Widziolka into the Duct of Cuvier of dechorionated larvae at 30 hours post-fertilization (hpf) while PBS and phiSHEF 2 phage was injected into two separately controls groups. Groups of at least 20 larvae were used for each treatment condition. Briefly, tricaine-anesthetised larvae were injected individually with 2 nl of *E. faecalis* at a final dose of 30,000 CFU (Colony Forming Units) and larvae were incubated for 2 h as described above. The CFU of bacterial cells were counted after spot dilution onto FA agar plates. Half of the *E. faecalis* infected larvae were then injected again with 2 nl of phiSHEF 2 phage at MOI of 20 and fish health status was monitored for up to 72 hour post infection (hpi). Zebrafish mortality assessment was based on the examination of the presence of a heart beat and blood circulation. Images of 10% formalin - fixed zebrafish larvae were captured using the fluorescence zoom microscopy Axio Zoom.V16, Zeiss with Zen Black software.

**Chapter 3: Characterisation of a putative
Fusobacterium nucleatum polymorphum
ATCC 10953 prophage**

3.1 Introduction

Bacteriophages are viruses that can infect and kill only bacteria and unlike antibiotics which kill harmful and harmless microorganisms at the same time, they are specific to their hosts. Due to their precise selection of hosts, small size and predictability of behaviour, they have been studied as a tool to investigate bacterial genetics- with a heyday in the 1970s-80s exemplified by for on Phage Lambda of *E.coli*. In addition, they have historically, and increasingly been considered as potential modes of antibacterial therapy (phage therapy) for human and animal treatment (Kutter and Sulakvelidze, 2004). Recently attention in phage therapy has grown due to increase in the issues of antibiotic resistance and biofilm associated infections in all major divisions of healthcare, including dentistry (Khalifa *et al.*, 2016). In dentistry and the resident oral bacterial flora, *F. nucleatum* is considered an important periodontal pathogen that has been repeatedly associated with the development and progression of periodontal disease, endodontic infection and gingivitis, alongside being noted for an association with colon cancer as well as vaginosis and preterm birth. This, on top of its role in the oral cavity as a bridging organism within dental plaque that may be key to biofilm structure, means it is imperative to improve our understanding of this organism.

In addition, Machuca *et al.* (2010) described the isolation of a bacteriophage called Fnpphi02 that infected *F. nucleatum* while Foglesong and Markovetz (1974) reported phage like particles associated with *F. varium* in 1974 that probably represented induced prophages- all of which sits alongside the published genome of *F. nucleatum polymorphum* 10953 containing an intact predicted prophage. In order to investigate the potential of phage therapy towards fusobacterial infections and the potential to harbour any antimicrobial proteins within the prophage genome, besides understanding the potential role of this prophage in the microbiology of the oral cavity, it was decided to study the putative prophage of FNP ATCC 10953, recently annotated in the released genome sequence (Karpathy *et al.*, 2007).

Specific Aims:

1. **Bioinformatic exploration of *Fusobacterium nucleatum polymorphum* ATCC 10953 (FNP) prophage.**
2. **Attempted induction of FNP prophage with Mitomycin C.**

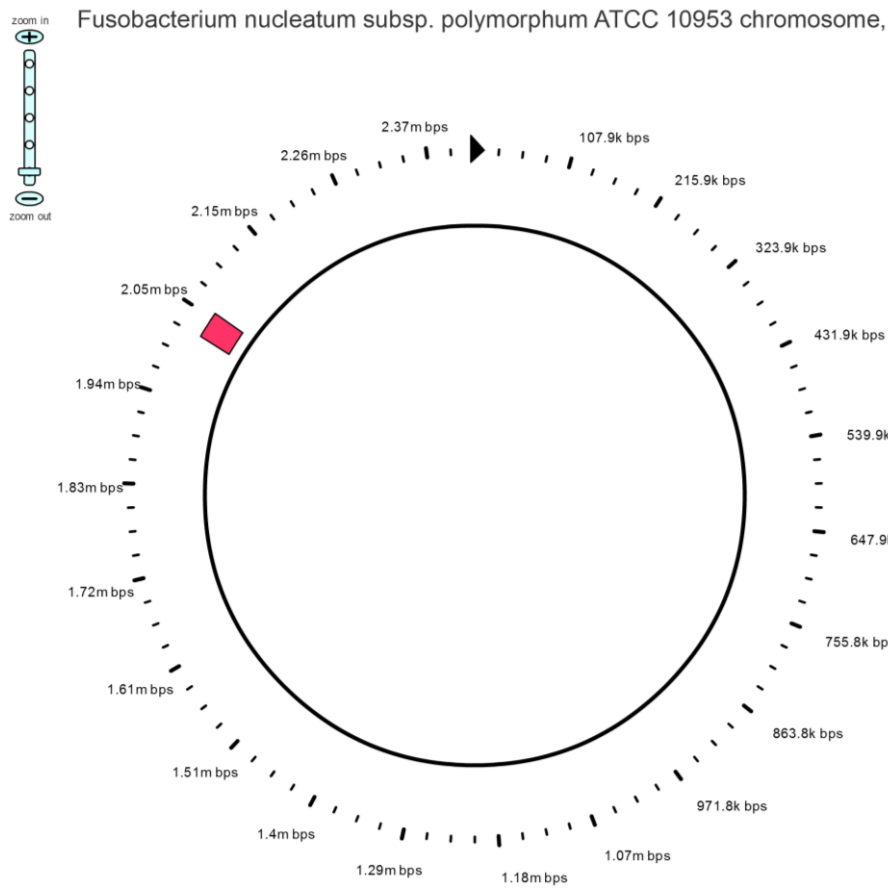
3. **Testing for the occurrence of *Fusobacterium nucleatum polymorphum* and its prophage in clinical plaque samples.**
4. **Investigation of the phiFNP1 lysis module as a source of therapeutic antimicrobial proteins.**

3.2 Bioinformatic exploration of *Fusobacterium nucleatum polymorphum* (ATCC 10953) prophage

The full chromosome sequence of *Fusobacterium nucleatum polymorphum* (ATCC 10953) is available with the GenBank number: CM000440.1 from the National Center for Biotechnology Information NCBI (<https://www.ncbi.nlm.nih.gov>). A prophage like genetic element was identified during the original genomic analysis of *F. nucleatum polymorphum* (ATCC 10953) and is considered to be a unique prophage genome (Karpathy *et al.*, 2007). This prophage will be referred to as phiFNP1 from herein in this thesis.

As a first step of analysis, the genome was reanalysed using the online web server: PFAST, a phage searching tool <http://phast.wishartlab.com>. An intact prophage (phiFNP1) of 34.9 Kb was identified within the circular bacterial genome (Figure 3.1, Fig 3.2 and Table 3.1). The prophage composed of 48 putative open reading frames (ORFs) or Coding DNA Sequences (CDs) (the number of coding sequence) located between 2023949-2058861 that covered FNP_1662 to FNP_1709, with GC% percentage of 26.82%, and located between tRNA- Arg3 and tRNA-Arg4 coding regions that form direct repeats at either end of the prophage boundary (FNP_t0043 and FNP_t0044) as seen in Figure 3.3 and Figure 3.4. Both tRNA coding regions are sharing the same direct repeat sequence of 5' GCTCAATTGGATAGAGCATCTGACT 3' (Figure 3.3 and Table 3.1 CDS position 1 and 50) that gave the assumption of potential site-specific direct repeats that flank phiFNP1, and might be very important for future excision and were important for it's initial integration.

The phiFNP1 sequence has no similarity with homologous phage in the sequence databases, with the nearest phage being Clostr_phiMMP04_NC_019422 with 17.02% similarity at the DNA sequence level as revealed from the PFAST online program analysis.



Accession: N/A

Length: 2,429,698 bps; Phages: 1

Prophage types

intact prophage
 incomplete prophage
 questionable prophage

Figure 3.1 Snapshot from PHAST online program showing an intact prophage phiFNP1 (red box) within the genome of *Fusobacterium nucleatum polymorphum* (ATCC 10953).

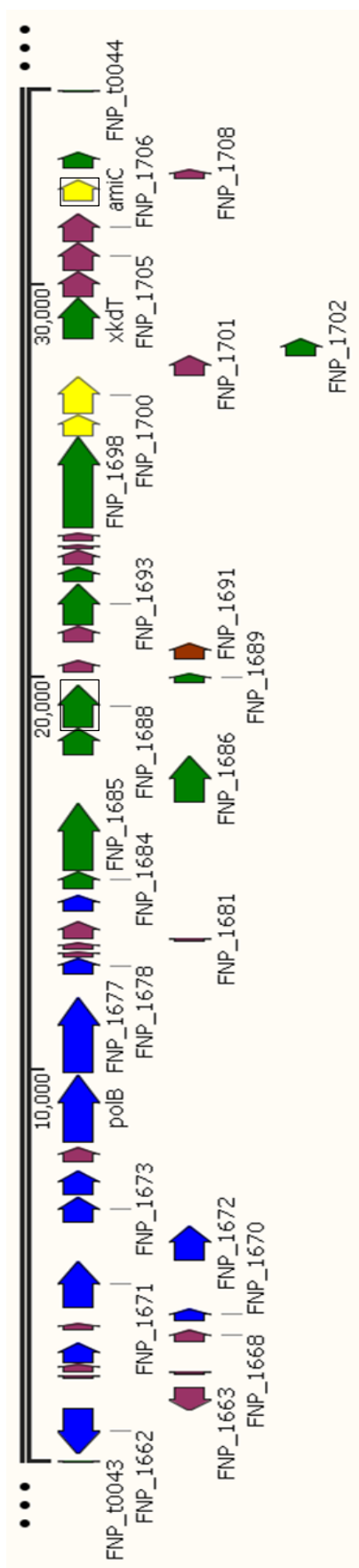


Figure 3.2 Genomic structure of putative prophage of *Fusobacterium nucleatum polymorphum* ATCC 10953 (phiFNP1). PhiFNP1 is located between two tRNA (FNP_t0043 and FNP_t0044) at either end of prophage boundary coding regions. The DNA of genes in boxes were used in primers designs.

- Protein Coding Sequence Annotation
- Replication and regulation module
 - Structural module
 - Lysis module
 - Hypothetical protein

```

>FNP_t0043
GCACTCATAGCTCAATTGGATAGAGCATCTGACTTCGGATCAGAGGGTTGTGGGTTCA
AGTCCTACTGGG
>FNP_t0044
GCATCTGTGGCTCAATTGGATAGAGCATCTGACTACGGATCAGAGGGTTGTGGGTTTCG
ACTCCTGCCAGG

```

Figure 3.3 FNP_t0043 and FNP_t0044 sequences that share direct repeat sequences (red colour letters).

As can be seen in Figure 3.2 and Table 3.1, the genes identified in this genome include three major phage clusters. The first locus (left segment, blue coded genes) represent genes involving in phage integration and DNA replication represented by a putative bacteriophage integrase (FNP_1662), a bacteriophage helicase (FNP_1671), bacteriophage endonuclease (FNP_1672), bacteriophage antirepressor (FNP_1673 and FNP_1667), NTP-binding protein (FNP_1674), DNA-directed DNA Polymerase II (FNP_1676) and HNH endonuclease domain protein (FNP_1683), all genes associated with presence of a temperate lysogenic bacteriophage. The second cluster are genes encoding phage structural proteins (right segment, green coded genes) represented mainly by bacteriophage terminase small subunit and large subunits (FNP_1684, FNP_1685), bacteriophage portal protein (FNP_1686), bacteriophage head capsid and packing protein (FNP_1688, FNP_1689), bacteriophage tail sheath (FNP_1693), bacteriophage tail protein (FNP_1698).

Table 3.1 Names and proposed function of phiFNP1 genes blast hits.

#	CDS_POSITION	BLAST_HIT
1	2023949..2023973	attL GCTCAATTGGATAGAGCATCTGACT
2	complement(2024189..2025301)	PHAGE_Strept_O1205_NC_004303: putative integrase; FNP_1662; phage(gi23455849)
3	complement(2025285..2025833)	hypothetical protein; FNP_1663
4	2026091..2026192	hypothetical protein; FNP_1664
5	2026189..2026266	hypothetical protein; FNP_1665
6	2026263..2026469	hypothetical protein; FNP_1666
7	2033885..2035804	bacteriophage antirepressor; FNP_1667

8	2027004..2027339	hypothetical protein; FNP_1668
9	2027332..2027514	hypothetical protein; FNP_1669
10	2027558..2027881	PHAGE_Thermo_THSA_485A_NC_018264: VRR-NUC domain-containing protein; FNP_1670; phage(gi397912645)
11	2027878..2029083	PHAGE_Thermo_THSA_485A_NC_018264: SNF2-related protein; FNP_1671; phage(gi397912655)
12	2029076..2030008	PHAGE_Bacill_virus_1_NC_009737: Putative endonuclease; FNP_1672; phage(gi155042966)
13	2030056..2030718	PHAGE_Paenib_philBB_PI23_NC_021865: antirepressor protein; FNP_1673; phage(gi526245052)
14	2030756..2031412	PHAGE_Strept_PH15_NC_010945: putative NTP-binding protein; FNP_1674; phage(gi190151434)
15	2031597..2032013	hypothetical protein; FNP_1675
16	2032091..2033854	PHAGE_Enterо_IME_EFm1_NC_024356: DNA polymerase; FNP_1676; phage(gi658310484)
17	2033885..2035804	PHAGE_Lister_P35_NC_009814: gp34; FNP_1677; phage(gi157325399)
18	2036369..2036806	PHAGE_Strept_SM1_NC_004996: gp29; FNP_1678; phage(gi32469460)
19	2036807..2036989	hypothetical protein; FNP_1679
20	2037013..2037204	hypothetical protein; FNP_1680
21	2037206..2037310	hypothetical protein; FNP_1681
22	2037279..2037746	hypothetical protein; FNP_1682
23	2038001..2038411	PHAGE_Clostr_phiSM101_NC_008265: HNH endonuclease domain protein; FNP_1683; phage(gi110804050)
24	2038549..2039034	PHAGE_Bacill_BtCS33_NC_018085: phage terminase small subunit, P27 family; FNP_1684; phage(gi392972711)
25	2039035..2040759	PHAGE_Clostr_phiSM101_NC_008265: putative phage terminase, large subunit; FNP_1685; phage(gi110804033)
26	2040756..2041970	PHAGE_Geobac_virus_E2_NC_009552: putative portal protein; FNP_1686; phage(gi148747730)
27	2041963..2042673	PHAGE_Clostr_phiMMP04_NC_019422: ATP-dependent Clp protease; FNP_1687; phage(gi414090445)
28	2042678..2043784	PHAGE_Bacill_WBeta_NC_007734: putative major capsid protein; FNP_1688; phage(gi85701384)
29	2043796..2044089	PHAGE_Enterо_IME_EFm1_NC_024356: head-tail joining protein; FNP_1689; phage(gi658310466)
30	2044082..2044417	hypothetical protein; FNP_1690
31	2044422..2044841	PHAGE_Clostr_phiMMP04_NC_019422: hypothetical protein; FNP_1691; phage(gi414090449)
32	2044841..2045281	hypothetical protein; FNP_1692
33	2045295..2046359	PHAGE_Clostr_phiMMP04_NC_019422: tail sheath; FNP_1693; phage(gi414090451)
34	2046372..2046803	PHAGE_Clostr_phiMMP04_NC_019422: XkdM-related protein; FNP_1694; phage(gi414090452)
35	2046817..2047206	hypothetical protein; FNP_1695
36	2047209..2047355	hypothetical protein; FNP_1696

37	2047426..2047671	hypothetical protein; FNP_1697
38	2047745..2050096	PHAGE_Lactoc_340_NC_021853: putative tail tape measure protein; FNP_1698; phage(gi526244482)
39	2050111..2050656	PHAGE_Clostr_phiMMP04_NC_019422: peptidoglycan-binding lysin domain protein; FNP_1699; phage(gi414090456)
40	2050666..2051646	PHAGE_Clostr_phiC2_NC_009231: putative hydrolase; FNP_1700; phage(gi134287357)
41	2051639..2052163	hypothetical protein; FNP_1701
42	2052142..2052594	PHAGE_Clostr_phiMMP04_NC_019422: XkdS-related protein; FNP_1702; phage(gi414090460)
43	2052591..2053649	PHAGE_Clostr_phiMMP04_NC_019422: baseplate J-like assembly protein; FNP_1703; phage(gi414090461)
44	2053650..2054306	PHAGE_Clostr_phiMMP04_NC_019422: hypothetical protein; FNP_1704; phage(gi414090462)
45	2054309..2055052	hypothetical protein; FNP_1705
46	2055064..2055777	hypothetical protein; FNP_1706
47	2056091..2056639	PHAGE_Crocei_P2559S_NC_018276: N-acetylmuramoyl-L-alanine amidase; FNP_1707; phage(gi399528661)
48	2056642..2056929	hypothetical protein; FNP_1708
49	2056916..2057365	PHAGE_Erwin_phiEaH2_NC_019929: phage tail assembly-like protein; FNP_1709; phage(gi431810647)
50	2058861..2058885	attR GCTCAATTGGATAGAGCATCTGACT

	Hits against Virus and prophage DB
	Hits against Bacterial DB or GenBank file

The third locus of gene clusters is the lysis module (yellow coded genes) located at the right boundary of the phage structural proteins represented by a peptidoglycan-binding lysin domain protein (FNP_1699), putative hydrolase (FNP_1700) and N-acetylmuramoyl-L-alanine amidase (FNP_1707). Temperate phages usually release their newly formed progenies after environmental induction through lysis enzymes. The lysis genes usually lie adjacent to and at either end of the virion protein genes cluster as is observed in some of the best-characterized tailed phage genomes (Casjens, 2003) and this is what is seen here (genes encode for phage structural proteins).

3.3 Testing for the presence of phiFNP1 in *Fusobacterium nucleatum polymorphum* ATCC 10953

In order to determine and identify the presence of FNP prophage harboured by *F. nucleatum polymorphum* ATCC 10953 laboratory strain and test its presence in oral samples collected from patients with chronic periodontitis, a number of primers specific

to the prophage and FNP ATCC 10953 strain were designed and tested. Hence, the presence of prophage *F. nucleatum polymorphum* ATCC 10953 was tested and compared to a negative control of *F. nucleatum nucleatum* ATCC 25586. Overnight cultures from both strains were grown before chromosomal DNA was extracted (see section 2.3.2). A PCR screen was carried out using DreamTaq Green PCR Master Mix (2 X) polymerase using two primer pairs designed to amplify the *amiC* (FNP_1707) and head capsid (FNP_1688) coding regions within the predicted prophage genome (Figure 3.2, boxed genes). A positive reaction producing bands at 550 bp and 450 bp respectively indicates the presence of this part of the prophage region. This PCR reaction confirmed the presence of both genes (Figure 3.4) in FNP but their absence from FNN, as expected and so indicated the putative prophage genome presence and the utility of these primers. In the rest of the tests, FNP_1688 was used as a sole primer for phiFNP1 identification as it is specific for that prophage and in contrast to the 1707 genes did not lie close to the phage termini and so indicated presence of the full prophage genome.

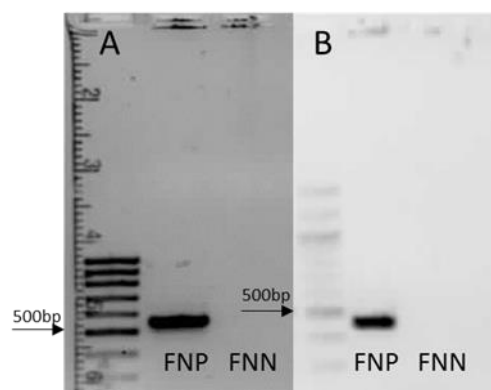


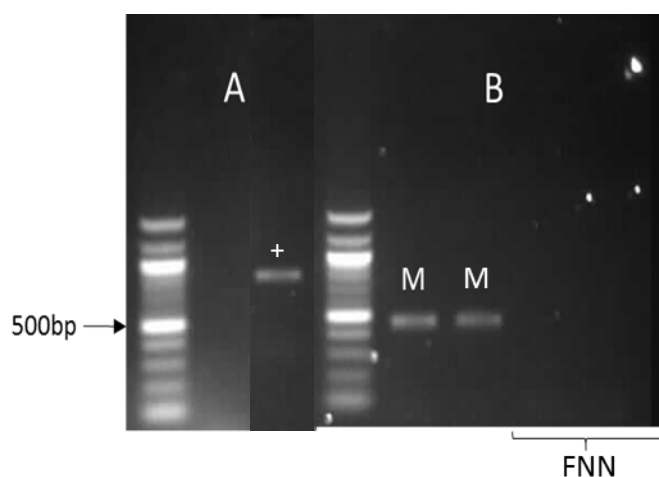
Figure 3.4 PCR screen for the phiFNP1 phage genome. FNP_1707 (A) and FNP_1688 (B) with template DNA from *F. nucleatum subsp. polymorphum* ATCC 10953 (FNP) and *F. nucleatum nucleatum* ATCC 25586 (FNN). Analysis was by TAE-Agarose electrophoresis, with Hyperladder I molecular weight marker used to elucidate the DNA fragment size.

3.4 Induction of phiFNP1 prophage with Mitomycin C

In order to explore if phiFNP1 prophage acts as source of lysogenic conversion or as a source of lateral transfer of other mobile DNA elements or bacterial DNA. An attempt was performed to induce the prophage from the genome of ATCC 1094 strain, and to use the induced phage particles to infect other strains of *Fusobacterium*.

Mitomycin C was used to induce the putative phiFNP1 prophage. Sub-lethal dose of Mitomycin C of 1 µg/ml was tested first to ensure that no bacterial lysis occurred (data not shown) and compared to the control (without Mitomycin C). This antibiotic was added to mid-log phase liquid cultures of FNP bacteria for 5 h before the supernatants were recovered after filtration to remove bacterial cells, ultracentrifugation was performed to pellet the possible phage particles. After that, the pellet was resuspended overnight in sterile nuclease free H₂O at 4°C to recover possible phage particles, and screened for the presence of phiFNP1 prophage using the phage head capsid FNP_1688 primer (Figure 3.5B). In parallel, to assess the presence of any contaminating DNA arising from cell lysis from phiFNP1 (Figure 3.5A), a primer based upon the *rpoB* gene (with PCR product size of 850 bp), a housekeeping gene specific to the *Fusobacterium* chromosome but located away from the predicted prophage was used. For further confirmation to the absence of any vital FNP cells in the supernatants that might interfere with the subsequent infection test, 10 µl was plated on agar plate and showed the absence of any growing FNP cells. In addition, no induction, as assayed by PCR, was observed without addition of Mitomycin C.

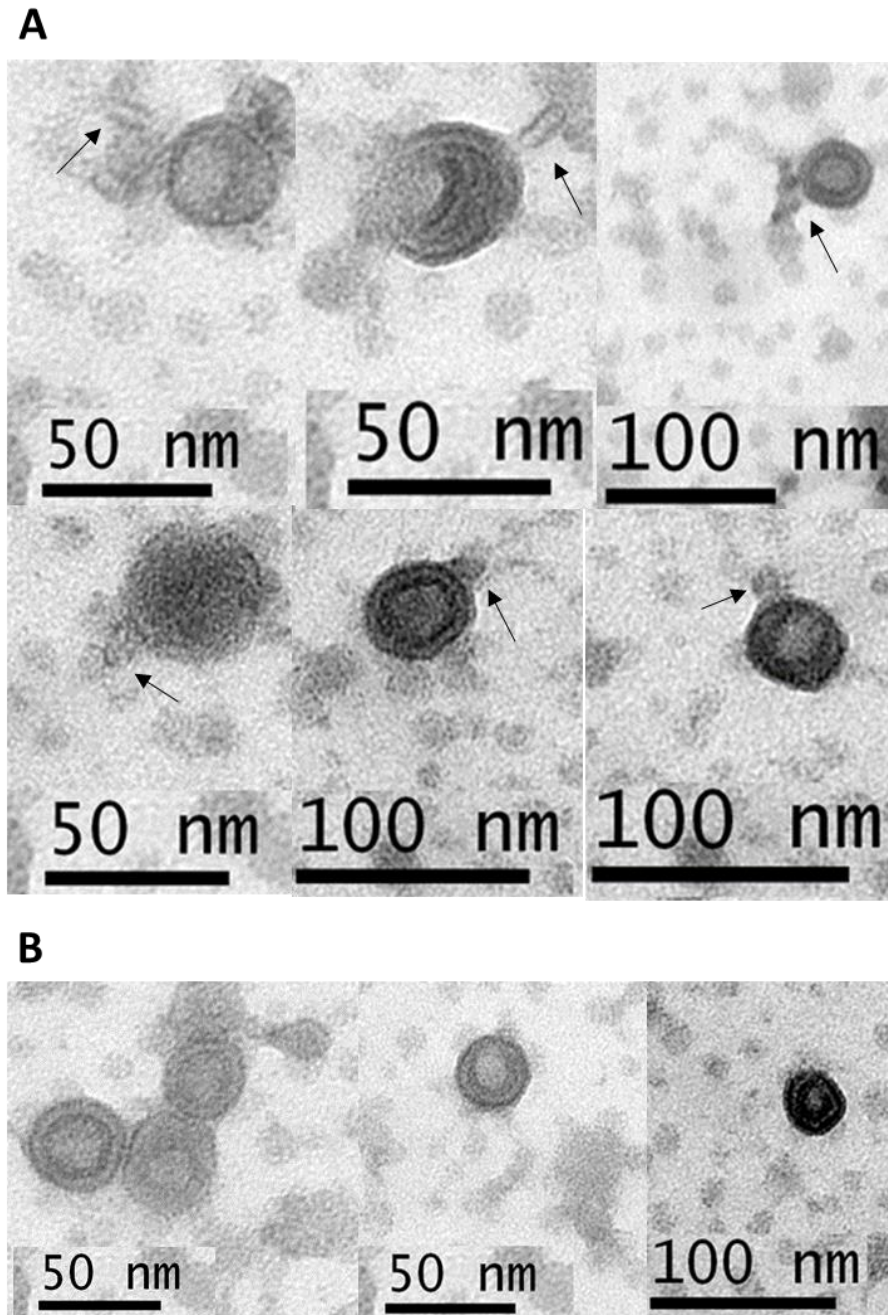
Figure 3.5 PCR screen of phiFNP1 induction from FNP ATCC 10953 cells with



Mitomycin C (1 µg/ml). A) Absence of contaminating FNP DNA from the recovered supernatants (*rpoB* primer) and positive control (+). B) Positive bands (FNP_1688 primer) indicating that the prophage might be induced with Mitomycin C (M) (FNN DNA used as negative control).

The results revealed that, the FNP prophage seems to be induced with Mitomycin C in broth indicated by the presence of positive PCR products in the recovered supernatants as seen in Figure 3.5B. However, when we used a primer set specific for a chromosomal FNP gene (*rpoB*) (Figure 3.5A) on the same Mitomycin C supernatants, there was no FNP DNA detected which indicates that no cell lysis had occurred and the low level of phage induction was not due to Mitomycin C induced cell lysis.

As these data seemed to indicate induction of prophage from the FNP chromosome we investigated whether we could see fully formed phage particles in these supernatants. Sample pellets were resuspended in ammonium acetate after ultracentrifugation (see section 2.4.1) and viewed via transmission electron microscope (TEM) using negative staining. As can be seen in Figure 3.6A and B, two groups with round particles of different sizes ranged about 25-60 nm average size in diameter were visualised throughout the samples. Round head particles with tail like fibers of 10-40 nm were identified from the first group (Figure 3.7A), while the second group have double enveloped particles without visible tails that resembled extracellular bacterial vesicles as can be seen in Figure 3.6B.

Figure 3.6 Transmission electron microscope (TEM) imaging of enriched suspension

induced from FNP ATCC 10953 by Mitomycin C. A) Potential induced phage. Black arrows indicate potential small tails. B) Other particle types.

If there are vital phage particles in the resultant supernatants, they should be capable of recognising and infecting *Fusobacterium* cells (their usual host) and may integrate into the bacterial genome as prophage or undergo lytic cycling. The uncontaminated supernatant that harboured the prophage (Figure 3.5B) was used to infect fresh mid log phase of a number of clinical and lab strains of *Fusobacterium* strains namely: *F. nucleatum polymorphum* Shef2- which we tested and was phage negative, *F.*

animalis Shef2, *F. animalis* Shef3, and *F. nucleatum nucleatum* ATCC 25586, in addition to its original host (ATCC 10953) in broth for 24 hours to allow for the adsorption of the phage particles to the suitable host cells. Of note here is that the tRNA-Arg sequence in Figure 3.3 is identical to sequences in strain 25586. The resultant cells were plated on agar plate and allowed to grow for five days. Checking for the presence of the prophage was performed using PCR after genomic DNA extraction from the infected cells. No band was associated with the tested strains DNA of the infected cells using FNP_1688 primer (primer specific to the prophage) as shown in Figure 3.7. In addition, the phage supernatant was also spotted on a fresh lawn of host strain using the agar overlay method and observation for plaques was monitored that would indicate a successful lytic infection. In these experiments, no plaques were observed from spotted supernatant either, indicating that the induced particles might not have the ability for integration into the chromosome of the tested strains in the form of temperate phage. Overall, phiFNP1 seems to potentially be induced from the chromosome of FNP 10953 apparently without cell lysis as reflected by the phiFNP1 DNA positive PCR amplification and absence of its host DNA in the induced samples. However, we could not observe viable phage infection towards any lab and clinical *Fusobacterium* strains tested.

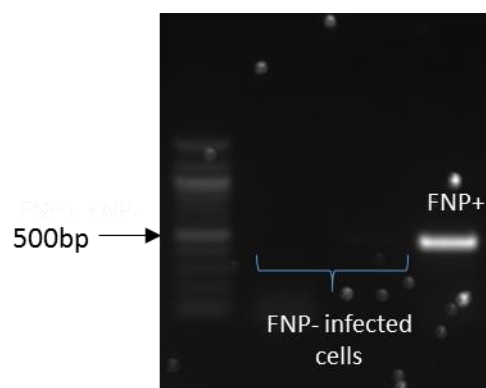


Figure 3.7 Infection of *Fusobacterium* cells (FNP) with Mitomycin C induced supernatants. No band present for the phiFNP1 prophage using FNP_1688 primer in the infected cells indicating its absence from the bacterial DNA (FNP ATCC 10953 DNA used as positive control FNP+).

3.5 The occurrence of *Fusobacterium nucleatum polymorphum* and its prophage in clinical plaque samples

In order to assess whether FNP 10953 clones but also, more importantly, how prevalent carriage of the phiFNP1 prophage was in the human population, we collected clinical plaque samples from 45 patients attending for treatment at the Periodontal Clinic, Charles Clifford Dental Hospital. After suspension in PBS, whole DNA was extracted from each sample (according to methods section 2.2.1). Two samples were collected at each visit from the same patient (one sample from a healthy site and one sample from a diseased site) at three subsequent visits (the total number from each patient through the entire course of treatment was six) as can be seen in Figure 3.8. Figure 3.9 illustrates plaque sampling.

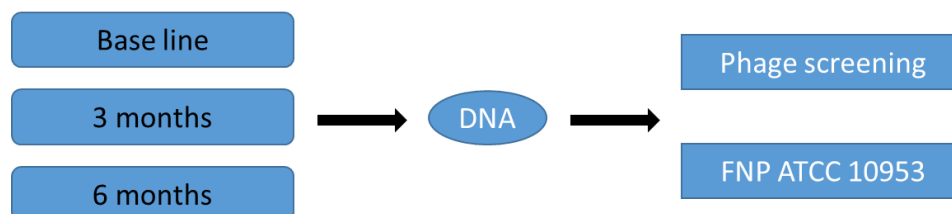


Figure 3.8 Diagram showing the flow chart for phiFNP1 and FNP ATCC 10953 screening from patient.



Figure 3.9 Collection of plaque sample from diseased site of the patient.

Samples were considered positive for phiFNP1 prophage if both primer sets yielded positive PCR reactions from the plaque DNA extracted from the same site in the same patient; this was done to eradicate false positive results. Example amplification gels for both the FNP_10953 specific *rpoB* and prophage phiFNP1 (FNP_1788, head capsid) specific primer sets are shown in Figure 3.10. However, it is highly unlikely that these primers gave false positive results given the anaerobic nature of this organism (i.e. cannot likely come from the environment). Finally, both primers were sensitive in detection of DNA down to 0.0001 ng/ μ l of FNP ATCC 10953 using standard curve slopes (7900HT Fast Real-Time PCR Detection System, Applied Biosystems), which is equal to about 4 bacterial cells of *Fusobacterium* as calculated by dividing the DNA concentration by the predicted genomic weight of *Fusobacterium nucleatum* of 2.32×10^{-6} (Ammann *et al.*, 2013).

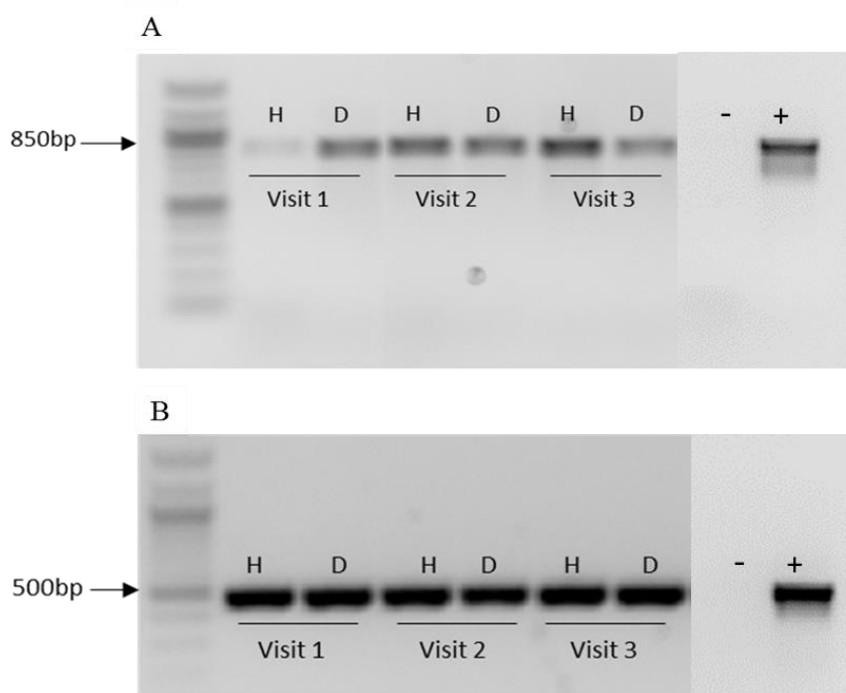


Figure 3.10 A) Positive bands PCR screening for healthy (H) and diseased (D) sites from three visits of the same patient. A) *rpoB* primer and B) FNP_1688 primer. 4 μ l of DNA was used in PCR reaction. Negative control (-) and FNP ATCC 10953 DNA was used as positive control (+).

The results revealed that about half of the patients tested harbour the phiFNP1 DNA as 23 patients (out of 45 patients screened) displayed positive results indicating that phiFNP1 is common among in clinical plaque samples from the oral cavity (Table 3.2). The results were distributed as follow: ~50% of the tested diseased sites were positive (positive in 23 out of 45 patients), while only 26.6% of the samples from healthy sites were positive (12 patients were tested positive out of 45).

Table 3.2 Screening results for phiFNP1 and FNP from 45 patients attending the periodontal departments for treatments at the School of Clinical Dentistry..

	Sites tested	Patients
Healthy sites	135	12/45 (26.6%)
Diseased sites	135	23/45 (50%)
Total	270	23/45 (50%)

The identifications of the phiFNP1 and its FNP ATCC 10953 strain was consistent throughout the treatment in positive sites, in another meaning, if one site showed positive band at the first visit sample collection, the second and the third plaque samples yield the same result from the same site, whether the treatment was performed or not at the second or third visit and vies versa. This is also true for negative patients as screening still yield negative results for the presence of the phage throughout the treatment subsequent screening visits.

However, there were inconsistencies between the diseased and healthy sites in the same patient in whom diseased sites showed positive results. In 23 patients with diseased sites having the presence of phiFNP1, only 12 (approximately 50%) were positive at healthy sites. This could be related to the fact that less amount of DNA was extracted from the plaque samples obtained from healthy sites that might give false negatives, which were in range of 1.2-7.3 ng/ul compared to 2-19 ng/ul obtained from diseased sites. However, this might also reflect that the amount of phiFNP1 prophage might be lower in healthy sites. Hence, measuring the number of phiFNP1 with specific primer set using qPCR and standard curve method might be a better strategy to be applied in future tests. Finally, the largest finding is that phiFNP1 is common among clinical plaque sample obtained from patients having chronic periodontitis.

3.6 Investigation of the phiFNP1 lysis module as a therapeutic

Phage produce lytic enzymes at the end of lytic cycle, referred to as endolysins to facilitate their escape from the host, if the gene encoding the potential enzyme is cloned, the protein could be used to degrade peptidoglycan and kill bacterial pathogens i.e. used as a potential antimicrobial (Fischetti, 2008, Fischetti, 2010).

The genome of phiFNP1 prophage harbours three potential lysis genes named peptidoglycan-binding lysin domain protein (FNP_1699), putative hydrolase (FNP_1700) and N-acetylmuramoyl-L-alanine amidase (FNP_1707) as described previously in section 3.2 and illustrated in Figure 3.11.

3.6 Investigation of the phiFNP1 lysis module as a therapeutic

Phage produce lytic enzymes at the end of lytic cycle, referred to as endolysins to facilitate their escape from the host, if the gene encoding the potential enzyme is cloned, the protein could be used to degrade peptidoglycan and kill bacterial pathogens i.e. used as a potential antimicrobial (Fischetti, 2008, Fischetti, 2010).

The genome of phiFNP1 prophage harbours three potential lysis genes named peptidoglycan-binding lysin domain protein (FNP_1699), putative hydrolase (FNP_1700) and N-acetylmuramoyl-L-alanine amidase (FNP_1707) as described previously in section 3.2 and illustrated in Figure 3.11.

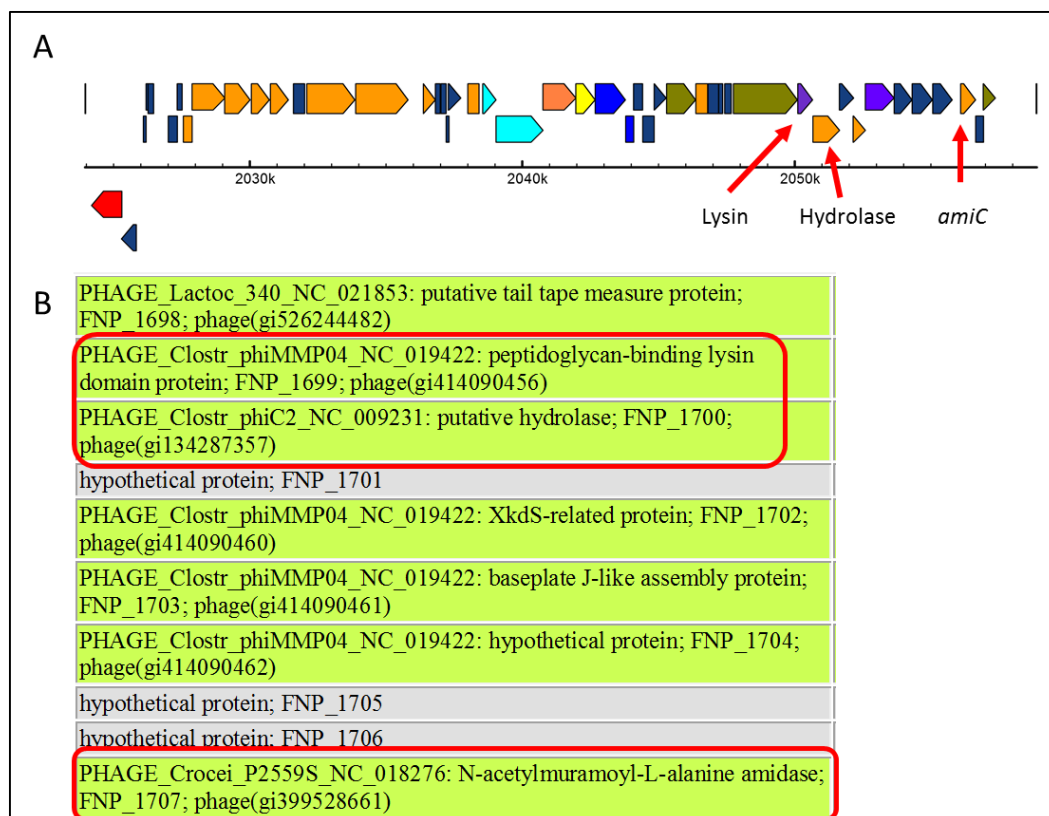


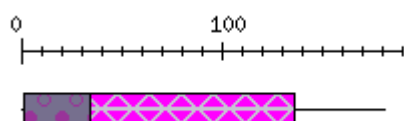
Figure 3.11 PhiFNP1 lysis module investigation. A) The position of the lysis module genes within the FNP prophage (red arrows), B) Snapshot for the FNP blast hits showing the potential lysis module numbers within the prophage genome (red boxes).

In order to look for any conserved domains within the sequence of the lysis module, each of the amino acids sequence of the three genes were placed into online web server ProDom (<http://prodom.prabi.fr/prodom>). ProDom is a protein domain family database constructed automatically by clustering homologous segments. The source protein sequences are non-fragmentary sequences derived from UniProtKB (Swiss-Prot and TrEMBL databases). The results of each domain are shown below in Figure 3.12.

FNP_1699

SUBNAME: FULL=PUTATIVE UNCHARACTERIZED FULL=PEPTIDOGLYCAN-BINDING LYSM
PHAGE DOMAIN HYDROLASE WALL XKDP

Length = 102 out of 181



Score = 384 (152.5 bits), Expect = 7e-36

Identities = 79/102 (77%), Positives = 79/102 (77%)

```

Query: 34 EFTTIDGNTLNXXXXXXXXXXXXXXXXXXXXXXXXXXXXVSFLNFKEPKYYVKKFFEKYRDLKLP 93
        EFTTIDGNTLN                               VSFLNFKEPKYYVKKFFEKYRDLKLP
Sbjct: 34 EFTTIDGNTLNLIGGKGLKKKFSFSSFFPSKLYSFVVSFLNFKEPKYYVKKFFEKYRDLKLP 93

Query: 94 VRIIIVDKYQVILNMLCRYNFTYNFRDRAGDIPYTLTDITEYI 135
        VRIIIVDKYQVILNMLCRYNFTYNFRDRAGDIPYTLTDITEYI
Sbjct: 94 VRIIIVDKYQVILNMLCRYNFTYNFRDRAGDIPYTLTDITEYI 135

```

FNP_1700

SUBNAME: FULL=PUTATIVE HYDROLASE UNCHARACTERIZED PHAGE WALL CELL
 FULL=PHAGE XKDQ PBSX

Length = 37 out of 326



Score = 183 (75.1 bits), Expect = 7e-15

Identities = 37/37 (100%), Positives = 37/37 (100%)

```

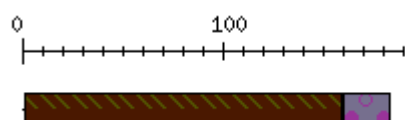
Query:   215 TENKGAI RTIGQE QDTKSIEKYGKLQQVVTLDEKEFS 251
        TENKGAI RTIGQE QDTKSIEKYGKLQQVVTLDEKEFS
Sbjct:   215 TENKGAI RTIGQE QDTKSIEKYGKLQQVVTLDEKEFS 251

```

FNP_1707

SUBNAME: HYDROLASE FULL=N-ACETYLMURAMOYL-L-ALANINE EC=3.5.1.28 AMIDASE

Length = 23 out of 182



Score = 104 (44.7 bits), Expect = 0.0001

Identities = 23/23 (100%), Positives = 23/23 (100%), Gaps = 13/23 (56%)

```

Query:   160 KFSIISDVVNL FVNFIVDTVKEV 182
        KFSIISDVVNL FVNFIVDTVKEV
Sbjct:   160 KFSIISDVVNL FVNFIVDTVKEV 182

```

Figure 3.12 Amino acids blast search for the lysis module of PhiFNP1.

The resulting bioinformatics searches (Figure 3.12) revealed the presence of conserve hydrolase domain in each of the three-lysis module genes, which came in line with the previous bioinformatics prediction performed in section 3.2. FNP_ 1699 and FNP_1700 revealed an uncharacterised hydrolase domain, while FNP_1707 revealed an uncharacterised hydrolase amidase domain, homologues of which are commonly found in phage genomes (Romero *et al.*, 2004). In the case of the predicted N-acetylmuramoyl-L-alanine amidase (FNP_1707 or *amiC*), these enzymes are often involved in the degradation of the peptidoglycan at the terminal stage of phage reproduction cycle. AmiC enzymes are capable of lysis of bacterial cell wall peptidoglycan, hydrolyzing the amide bond between the sugar and peptide in this structure as in Figure 3.13. In contrast to phage amidases, bacterial *amiC* amidase proteins are thought to play a role in cleaving the septum to release daughter cells after cell division, as occurs for *Neisseria gonorrhoeae*, *i.e.* an *amiC* mutant did not fully separate but grew as clumps (Garcia and Dillard, 2006).

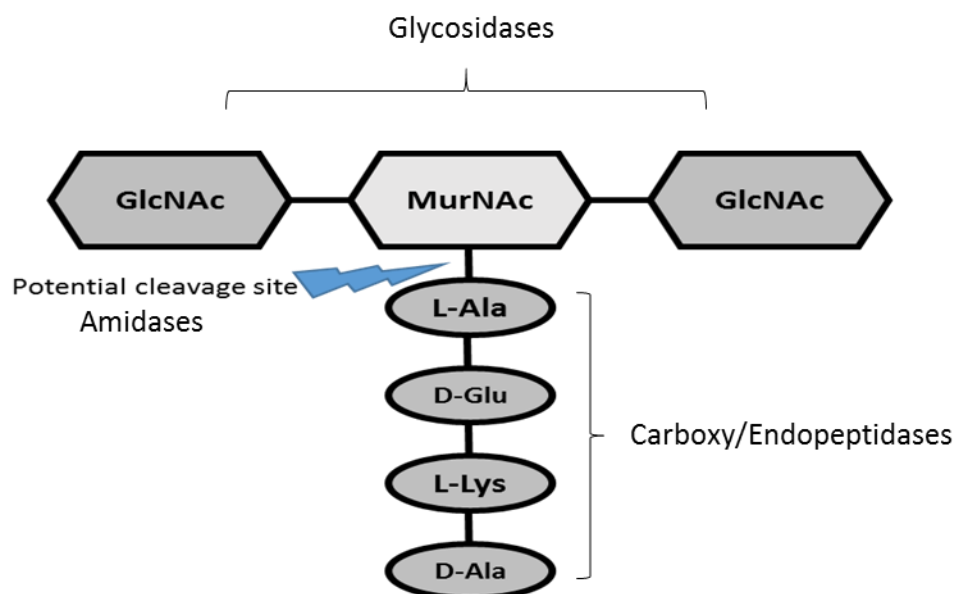


Figure 3.13 Endolysins cleavage activity towards bacterial PG sites. Adapted from (Oliveira *et al.*, 2013).

Based on endolysins having muralytic activity towards bacterial PG (the bond of the PG on which the enzymes act), four types of endolysins have been identified: I- lysozymes and II- transglycosidases act on the glycosidic bond that links the amino sugars in the cell wall, and III- amidases and IV- endopeptidases act on the amide and peptide bonds of the cross-linking oligopeptide stems and interpeptide bridges (Young 1992, lossener, 2005, Fischete 2010) (Figure 3.13).

In order to investigate the activity of the predicted proteins of the FNP lysis module as potential antimicrobial agents *Fusobacterium* strains and other periodontal pathogens strains, it was decided to clone and purify the genes encoding these enzymes, and characterise their action. This had similarly been done by other groups for an amidase identified endolysin from *P. aeruginosa* autolysin *amiB* and *S. aureus* virulent phage plyTW lysin (Scheurwater *et al.*, 2007, Loessner *et al.*, 1998).

3.6.1 Cloning of phiFNP1 lysis module genes

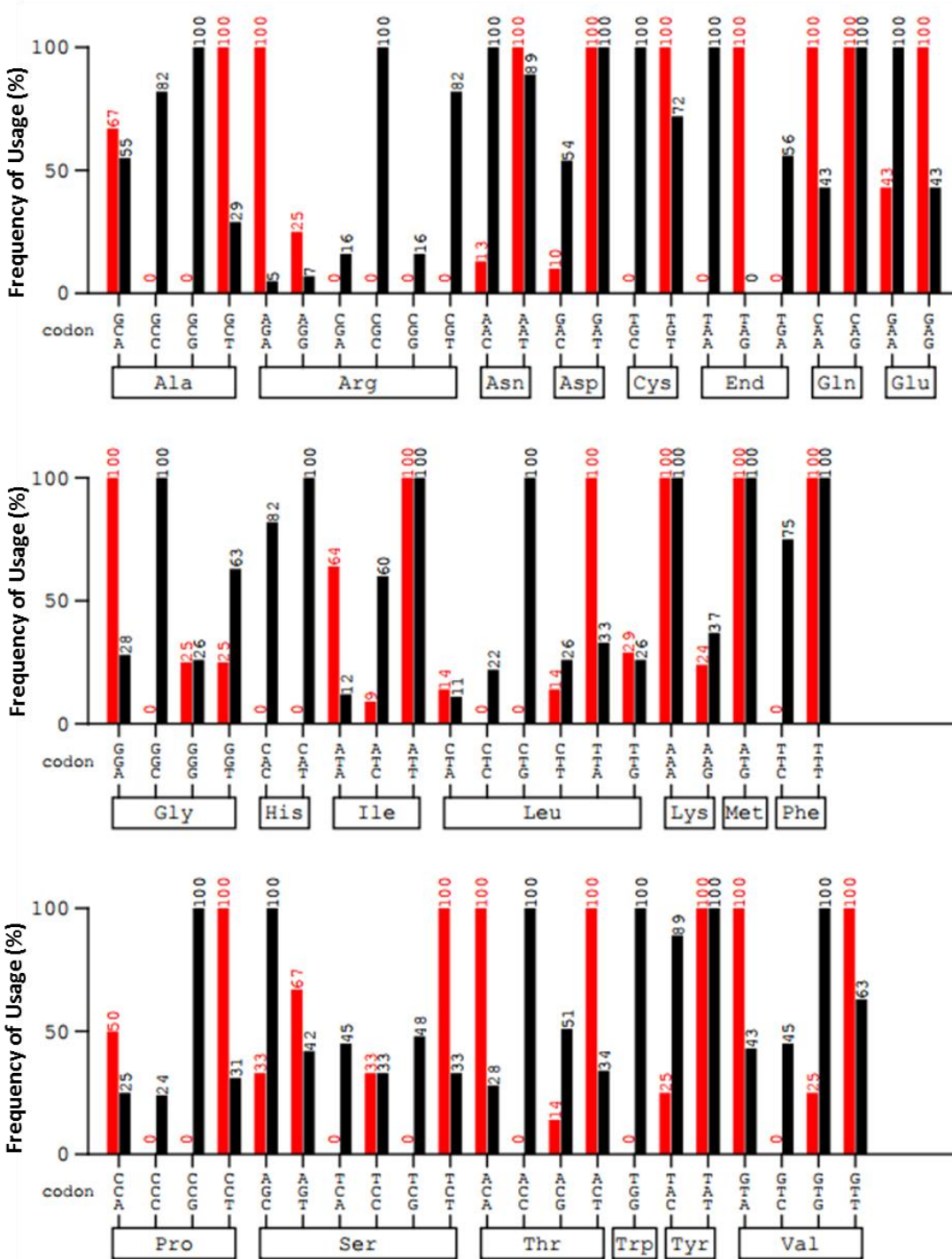
As a first step to assess activity and antimicrobial capability of these three putative lysis proteins they were first either synthesised as linear DNA fragments by Invitrogen GeneArt (FNP_1699 and FNP_1700), while a previous student (Arati Satyal Nepal) from the Stafford group subcloned similarly synthesised FNP-1707 into pGEX-4T-3 plasmid.

The nucleotide sequence of FNP_1699 and FNP_1700 obtained from *Fusobacterium nucleatum polymorphum* (ATCC 10953) with the GenBank number: CM000440.1 from the NCBI (<https://www.ncbi.nlm.nih.gov>) was downloaded and compatible restriction sites with *E.coli* pET15b or pGEX4T3 expression vectors (Figure 3.15, Figure 3.19, and Figure 3.21) i.e. *NdeI* [CATATG] and *BamHI* [GGATCC] were added at the 5' end and *XhoI* [CTCGAG] at the 3' end.

However, before synthesis we applied a codon optimization algorithm (GeneArt) since the codon usage profile of FNP ATCC 10953 and *E. coli* sequence are very different. To visualise the differences in codon usage of FNP_1699 and FNP_1700 in both FNP ATCC 1093 and *E. coli*. The native sequence of both genes codons were compared to the codon preference in *E. coli*, using the Graphical Codon Usage Analyser (GCUA), freely available at <http://gcu.schoedl.de/index.html>. FNP_1699 was shown to possess a mean difference of 50.05%, between FNP ATCC 10953 frequency of codon usage and frequency of *E. coli* codon usage, while for FNP_1700 was 44.23% compared to *E. coli* codon usage which seems to be very high (this can be observed from Figure 3.14 and 3.15). The synthesised FNP1699 and FNP1700 DNA product were cloned into pJET1.2 blunt vector to obtain multiple inserts copies.

A) FNP_1699

Mean difference: 50.05 %



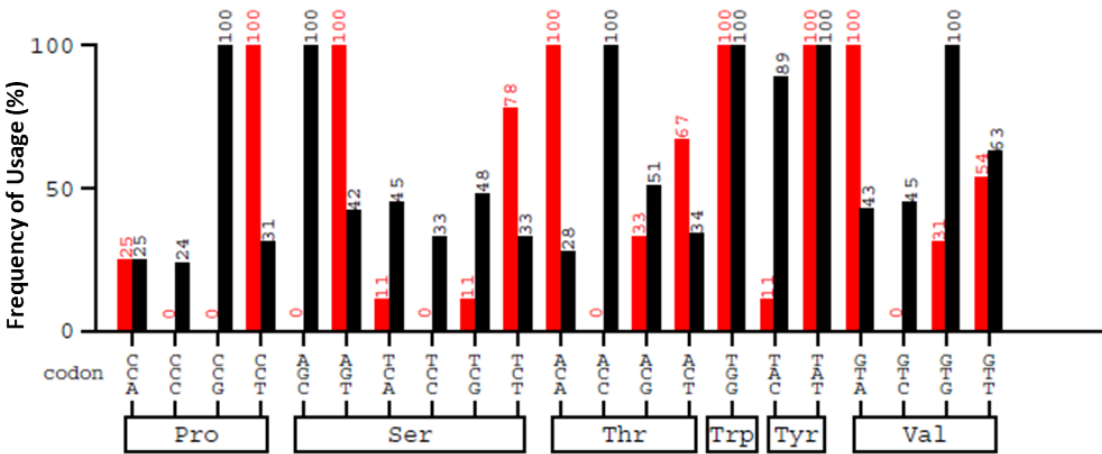
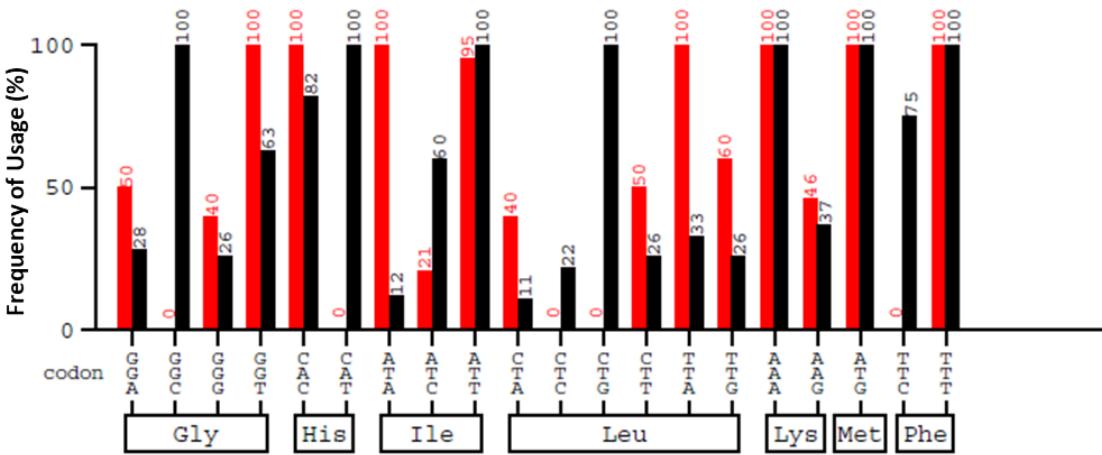
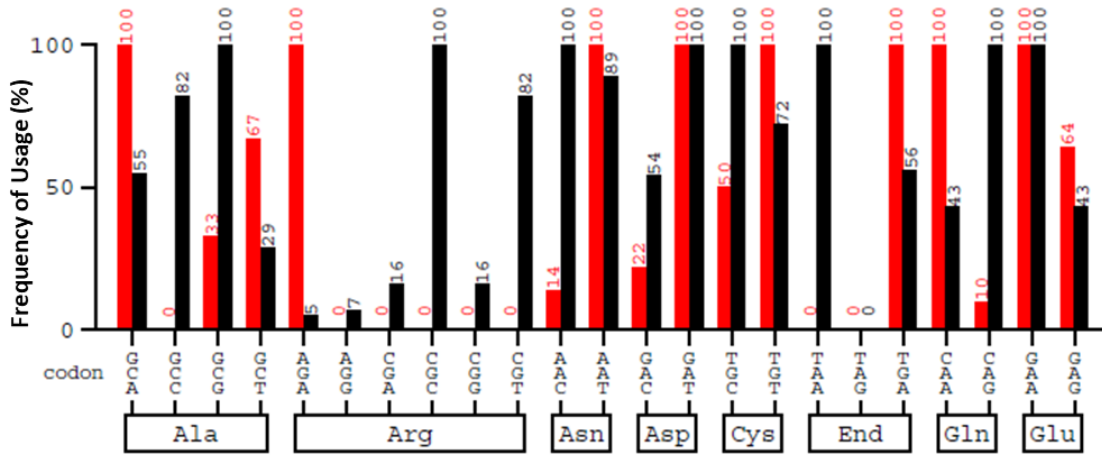
B

	1	10	20	30	40	50	60
BO	ATGAAAATATA TTTATAGCTGAGAAATAATGGAGAAACGGAGATAGTTGCATCCAGTT						
AO	ATGAAAATCTACTTTATCGCCGAAATAACGGCGAAACCGAAATTGTTGCAATCCGGTT						
	70	80	90	100	110	120	
BO	GTACAAAATATGAGGTTATGAATTGTGATACAACTGATGAGGAGTTACAACTATTGAT						
AO	GTTCAGAACATCGAAGTTATGAATTGTGATACCACGATGAAGAATTACACCATTGAT						
	130	140	150	160	170	180	
BO	GGTAACACATTAATTTAATTGGAGGAAAGGGGTTAAAAAGTTTCTTTTTCCTCTTTT						
AO	GGTAATACCTCAATCTGATTGGTGGTAAAGGCCGAAAAAATTCAGCTTTAGCAGCTTT						
	190	200	210	220	230	240	
BO	TTTCCTAGCAAAATATATAGTTTGTGAGITTTCTTAAITTTAAAGAGCCAAATATTAT						
AO	TTTCCGAGCAAACTGTATAGCTTTGTGAGCTTCTCAACTTTAAAGAACCAGAAATATTAC						
	250	260	270	280	290	300	
BO	GTIAAATTTTTGAGAAATATAGAGATTTAAAAATACCAGTAAGAATATATTGTAGAC						
AO	GTGAAATTCTTGAAAAATATGGGACCTGAAACTGCCGTTTCGTATTATCATTGTGGAT						
	310	320	330	340	350	360	
BO	AAATATCAGGTATATTGAATATGCTATGTAGATATAATTTTACATACAATTTTAGAGAT						
AO	AAATATCAGGTATCCTGAATATGCTGTGCCGCTATAACTTTACCTAATTTCCGTGAT						
	370	380	390	400	410	420	
BO	AGGGCAGGAGATATCCATACACATGGATATTACGAATATATTTTCCATTAATAAG						
AO	CGTGCCTGGTATATTCCTGATACCTGGATATTACGAATATATCCTGCCGATTAACAAA						
	430	440	450	460	470	480	
BO	ACAACTGCACCATTGAATCTAAATAACCTAAAAACACAAAAGATAATACAAATATTACT						
AO	ACCACCGCACCATTGAAAGCAACAACCGAAAAATACCAAAGACAACACCAACATCACG						
	490	500	510	520	530	540	
BO	AAAGATAAGAAAACAAAAATAAAAAATAAATAAAGATAATGCTAAATAAAAAACCTAAA						
AO	AAAGACAAAAAAACAAAATCAAAAAATAAATCAAAGATAACGCCAACAAAAACCTAAA						

BO AAGTAG
AO AAATGA

C) FNP_1700

Mean difference: 44.23 %



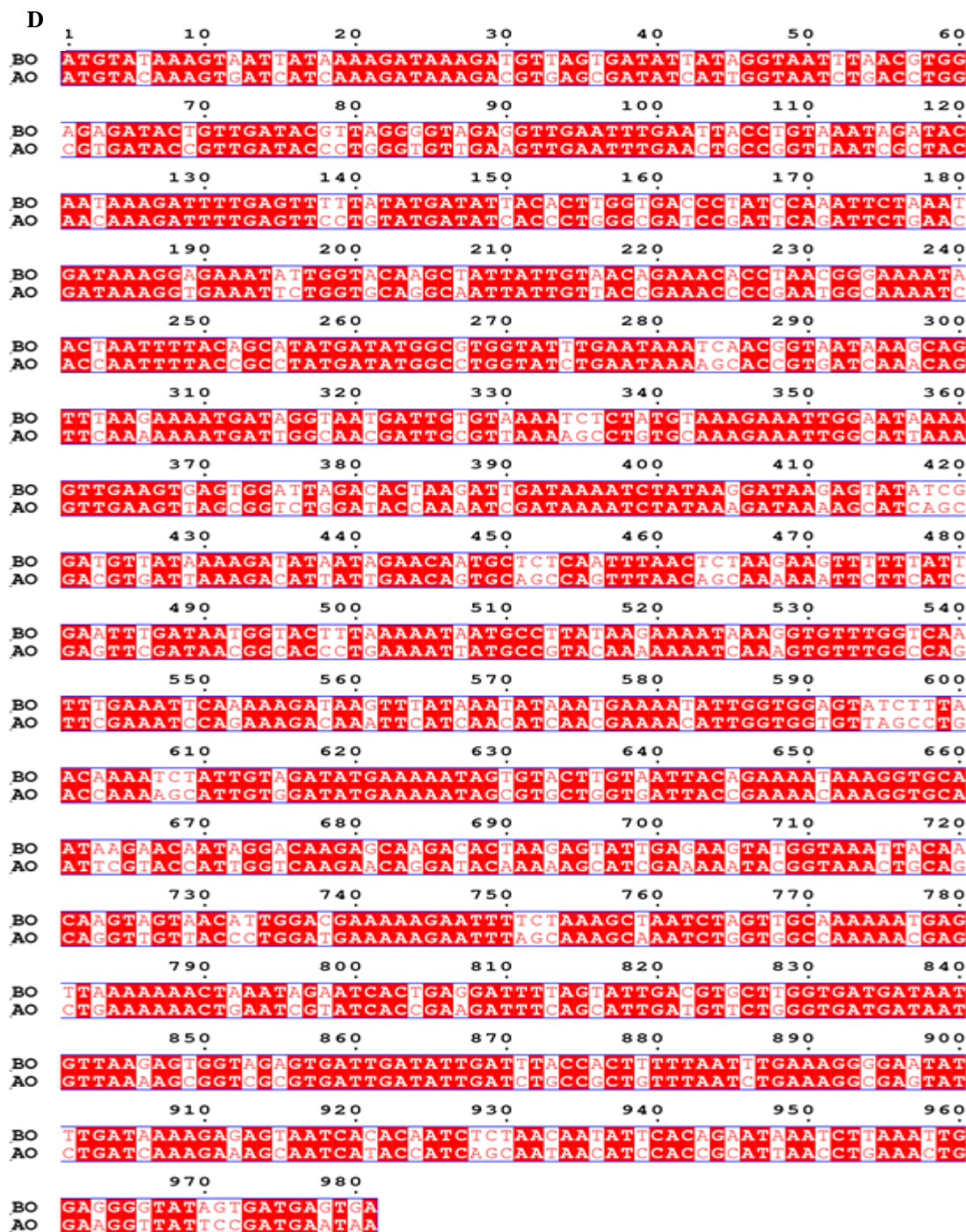


Figure 3.14 Codon optimisation of FNP_1699 and FNP_1700. A) and C) Comparison of codon utilisation between FNP ATCC10953 and *E. coli* For FNP_1699 and FNP_1700 respectively. Nucleotide sequences for both genes from FNP ATCC 10953 were compared against the *E. coli* genome to assess the frequency each codon is used with, using the GCUA (<http://gcu.schoedl.de/index.html>). Red= frequency (%) of a given codon used in FNP ATCC 10953 and black=frequency (%) of a given codon used in *E. coli*. B) and D) Nucleotide sequence of both genes before (BO) and after (AO) codon optimisation. The light colour boxes indicate nucleotide change.

Sequence name / optimized for
FNP-1699/ Escherichia coli

ORF	Protected sites	Protected areas	Motifs to avoid
13-558 [ATG...TGA]	1-6 NdeI [CATATG] 7-12 BamHI [GGATCC] 559-564 XhoI [CTCGAG]		NdeI [CATATG] BamHI [GGATCC] XhoI [CTCGAG]

1.	CATATGGGATCC	M K I Y F I A E N N G E T E I V A I P
70.	GTTGTT CAGA ACATCGAAGTTATGAATTGTGATACCACCGATGAAGAATTCACCACCATTTGATGGTAAT	V V Q N I E V M N C D T T D E E F T T I D G N
139.	ACCCTGAATCTGATTGGTGGTAAAGGCCTGAAAAAATTCAGCTTTAGCAGCTTTTTCCGAGCAAACTG	T L N L I G G K G L K K F S F S S F F P S K L
208.	TATAGCTTTGTGAGCTTCTGAACCTTAAAGAACCAGAAATATTACGTGAAATTCCTCGAAAAATATCGC	Y S F V S F L N F K E P K Y Y V K F F E K Y R
277.	GACCTGAAACTGCCGGTTTCGTATTATCATTGTGGATAAATATCAGGTGATCCTGAATATGCTGTGCCGC	D L K L P V R I I I V D K Y Q V I L N M L C R
346.	TATACTTTACCTATAATTTCCGTGATCGTGCCGGTGATATTCCTGATACCTGGATATTACCGAATAT	Y N F T Y N F R D R A G D I P Y T L D I T E Y
415.	ATCTGCGGATTAACAAACCACCGCACCGATTGAAAGCAACAAACCAGAAAAATACCAAGCAACACC	I L P I N K A T T A P I E S N K P K N T K D N T
484.	AACATCACGAAAGACAAAAAACAAAAATCAAAAACAAAAATCAAAGATAACGCCAACAAAAAACCTAAA	N I T K D K K T K I K N K I K D N A N K K P K
553.	AAATGACTCGAG	K *

Sequence name / optimized for
FNP-1700/ Escherichia coli

ORF	Protected sites	Protected areas	Motifs to avoid
13-993 [ATG...TAA]	1-6 NdeI [CATATG] 7-12 BamHI [GGATCC] 994-999 XhoI [CTCGAG]		NdeI [CATATG] BamHI [GGATCC] XhoI [CTCGAG]

1.	CATATGGGATCC	M Y K V I I K D K D V S D I I G N L T
70.	TGGCGTGATACCGTTGATACCTGGGTGTTGAAGTTGAATTTGAACTGCCGGTTAATCGCTACAACAAA	W R D T V D T L G V E V E F E L P V N R Y N K
139.	GATTTTGAGTTCCTGTATGATATCACCTGGGGCATCCGATTCAGATTCTGAACGATAAAGGTGAAATT	D F E F L Y D I T L G D P I Q I L N D K G E I
208.	CTGGTG CAGGCAATTTATTGTTACCGAAACCCGAAATGGKAAAATCACCAATTTTACCGCCTATGATAG	L V Q A I I V T E T P N G K I T N F T A Y D M
277.	GCCTGGTATCTGAATAAAAAGCACCGTGATCAAAACAGTTCAAAAAAATGATTGGCAACGATTGCGTTAAA	S L C K E I G I K V E V S G L D T K I D K I Y
346.	AGCCTGTGCAAAGAAATTTGGCATTAAAGTTGAAGTTAGCGGTCTGGATACCAAAATCGATAAAATCTAT	K D K S I S D V I K D I I E Q C S Q F N S K K
415.	AAAGATAAAGCATCAGCGACGTGATTAAGACATTATTGAACAGTGCAGCCAGTTTAAACAGCAAAAAA	F F I E F D N G T L K I M P Y K K I K V F G Q
484.	TTCTTCATCGAGTTCGATAACGGCACCTGAAAAATATGCCGTACAAAAAATCAAAGTGTGGCCAG	F E I Q K D K F I N I N E N I G G V S L T K S
553.	TTCGAAATCCAGAAGACAAAATTCATCAACATCAACGAAAACATTGGTGGTGTAGCCTGACCAAAAGC	I V D M K N S V L V I T E N K G A I R T I G Q
622.	ATTGTGGATATGAAAAATAGCGTGCTGGTGTACCCGAAAACAAAGGTGCAATTCGTACCATTTGGTCAA	E Q D T K S I E K Y G K L Q Q V V T L D E K E
691.	GAACAGGATACAAAAAGCATCGAAAAATACGGTAAACTGCAGCAGGTTGTTACCTGGATGAAAAAGAA	F S K A N L V A K N E L K K L N R I T E D F S
760.	TTTAGCAAAGCAAATCTGGTGGCCAAAAACGAGCTGAAAAAATGAAATCGTATCACCGAAGATTTGAGC	I D V L G D D N V K S G R V I D I D L P L F N
829.	ATTGATGTTCTGGGTGATGATAATGTTAAAAGCGGTGCGGTGATTGATATTGATCTGCCGCTGTTAAT	L K G E Y L I K E S N H T I S N N I H R I N L
898.	CTGAAAGGCGAGTATCTGATCAAAGAAAGCAATCATACCATCAGCAATAACATCCACCGCATTAACTG	K L E G Y S D E *
967.	AAACTGGAAGGTTATTCGGATGAATAA	CTCGAG

Figure 3.15 Snapshot for the final optimized nucleotide sequence of FNP_1699 and FNP_1700. The restriction enzymes *NdeI* [CATATG] and *BamHI* [GGATCC] were added to the beginning of the sequence while *XhoI* [CTCGAG] (yellow boxes) and a stop codon (*) were added at the end.

3.6.1.1 Cloning into pJET 1.2 vector

pJET1.2 vector is a versatile cloning plasmid that possesses a lethal restriction enzyme gene which when disrupted by ligation of a DNA insert into the cloning site results in formation of viable colonies, but in the absence of an insert is lethal to the *E. coli* cell. After ligation with T4 ligase, the resultant plasmids are immediately transformed into *E. coli* DH5 α competent cells and plated onto LB agar containing ampicillin. The resulting colonies are picked carefully, subjected to PCR amplification using pJET1.2 primers (see section 2.3.3) and plasmid clones related to positive colony were extracted and sent to a sequencing facility (GATC biotech, Germany) to ensure that the insert harbors the correct sequence (data not shown).

Purification of pJET1.2-FNP1699 and pJET1.2-FNP1700 was performed with the aid of a plasmid mini prep kit followed by double digestion with *NdeI-XhoI* and *BamHI-XhoI* for each vector separately, to clone in pET15b or pGEX-4T3 respectively. Upon successful digestion with *NdeI-XhoI* and *BamHI-XhoI*, bands were released as demonstrated below in Figure 3.16 and Figure 3.17 alongside the vector bands of 2.97 Kbp, PCR fragments with correct sizes were excised with the aid of a sterile scalpel and purified with PCR gel and clean kit.

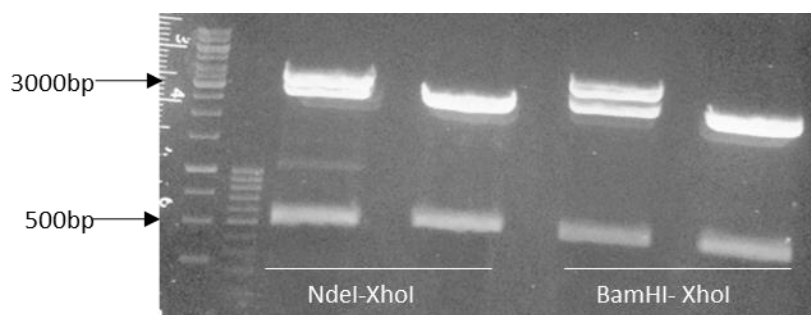


Figure 3.16 Restriction digestion of pJET1.2-FNP1699. Two prospective pJET1.2-FNP1699 clones were digested with *NdeI-XhoI* (left) and *BamHI-XhoI* (right) respectively. Uncut plasmid is seen at 3500 bp with the linearised plasmid at 3000 bp and the released FNP1699 insert at 565 bp. Hyperladder I and II molecular weight markers were used to elucidate the DNA fragment size respectively.

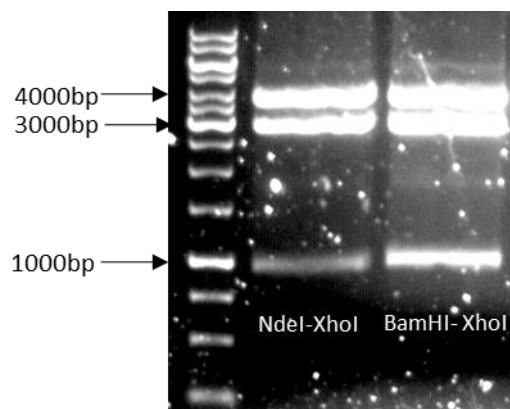


Figure 3.17 Restriction digestion of pJET1.2-FNP1700. The FNP1699 was digested with *NdeI-XhoI* and *BamHI-XhoI* respectively. The linearised vector size is 2974 bp while the incomplete digested vector-insert will be higher at approximately 4000 bp and the insert of FNP1700 at 1000 bp (upper band in the first and second lane).

3.6.1.2 Cloning into pET15b

In order to express the FNP1699 and FNP1700 protein at high levels in *E. coli* it was required to clone the coding sequence into a suitable expression vector. Both genes of interest were removed from the pJET1.2 plasmid through restriction enzymes *NdeI* and *XhoI* in order to transfer it into the expression vector, pET15b, which is detailed in Figure 3.18. Prior to the cloning of resultant FNP1699 and FNP1700 DNA fragments, the vector was dephosphorylated with alkaline phosphate CIP (NEB) to avoid pET15b self-ligation. The vector pET15b possesses a T7 promoter that is highly inducible in *E. coli* λ DE3 lysogen strains to control the expression of the plasmid and with the use of *NdeI* and *XhoI* restriction nucleases could accommodate the gene insert such that it would contain an N-terminal His-tag for later purification of the expressed recombinant protein.

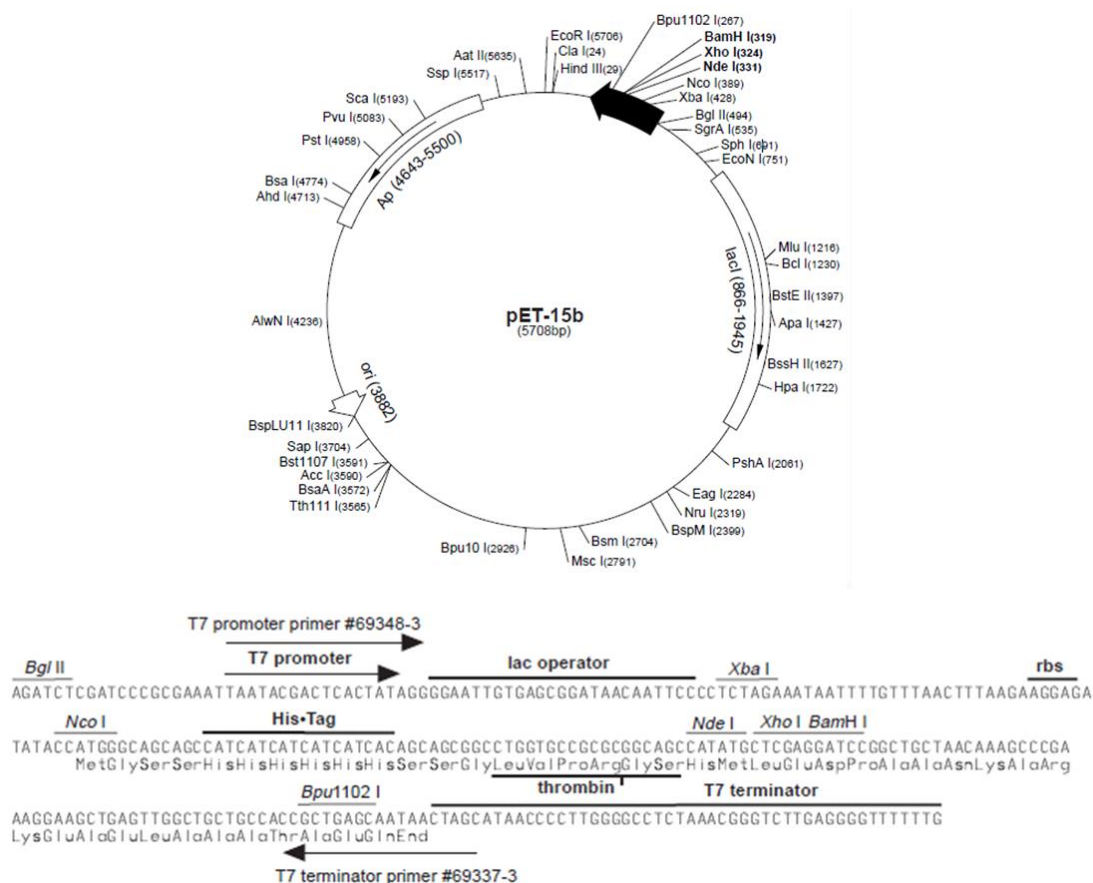


Figure 3.18 pET15b vector map and cloning details. The pET15b vector contained *NdeI* and *XhoI* restriction sites such as to allow for the insertion of FNP1699 and FNP1700 DNA fragment in the correct orientation.

The double digested pET15b and gel purified FNP1699 and FNP1700 extract were ligated using T4 DNA-ligase before transformation into *E. coli* DH5 α competent cells and cultured overnight on LB ampicillin selective plates (pET15b contains ampicillin resistance). The resultant colonies were picked, subjected to PCR amplification using T7 primer and plasmid clones related to positive colony were extracted and sent to a sequencing facility (GATC biotech, Germany) (Figure 3.19).

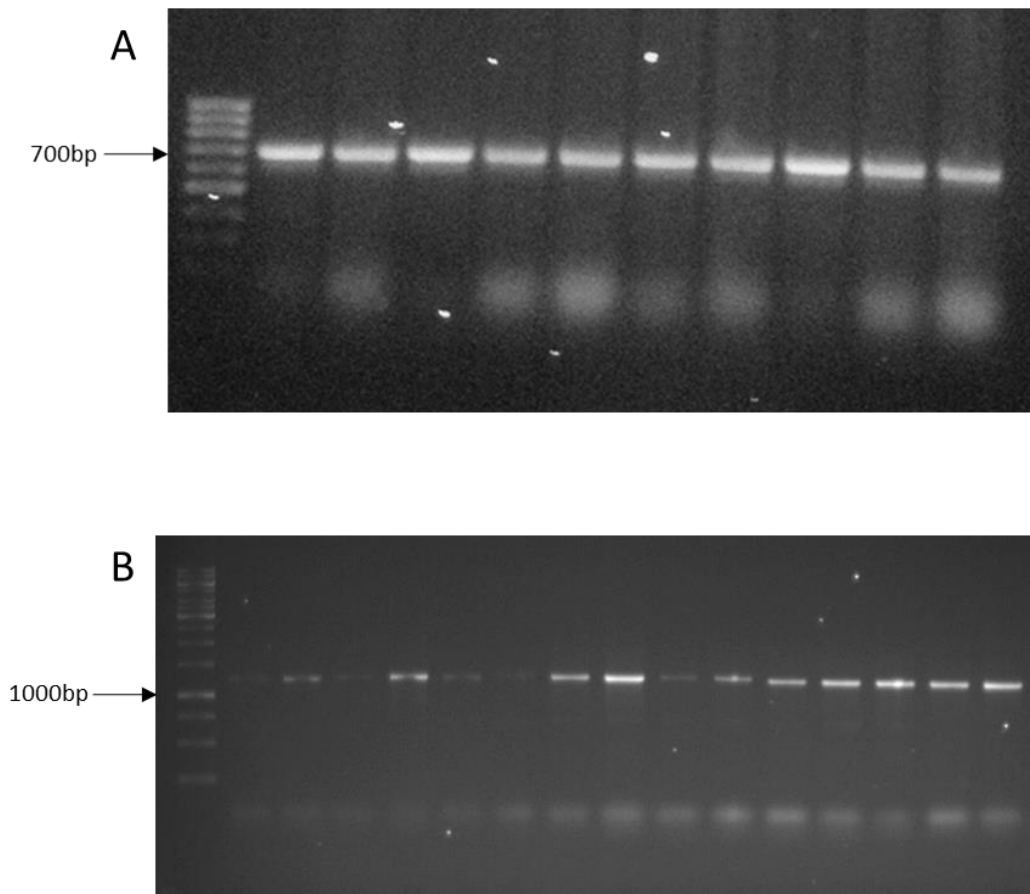


Figure 3.19 PCR screen of pET5b-FNP1699 and 1700 DNA from different colonies. (A) 10 colonies screened positive for pET15b-FNP1699 indicated by 785 bp (565 bp insert+200 bp T7 primer extension) and (B) 16 colonies screened positive for pET15b-FNP1700 indicated by 1200 bp (1000 bp insert+200 bp T7 primer extension).

The results revealed that the cloning was successful as the inserts came at the correct expected size, and the sequencing came back 100% identical with both synthesised gene and with an in-frame 6-Histidine tag.

3.6.1.3 Cloning into pGEX vector

In order to increase the chance to produce recombinant protein expression in a soluble form, the FNP1699 and FNP1700 DNA fragment encoding region were also cloned into pGEX-4T-3, an expression vector which attaches a glutathione S-transferase (GST) tag to the recombinant protein expressed and again is IPTG inducible as shown below in Figure 3.20. This technique often increases the solubility of proteins since the fusion protein - GST is highly soluble, and has proven successful in our laboratory for *Tannerella* genes (Phansopa *et al.*, 2015). Both genes of interest were removed from the

pJET1.2 plasmid through restriction enzymes *Bam*HI and *Xho*I this time, in order to transfer it into the expression vector pGEX-4T-3. Prior to the cloning of the resultant FNP1699 and FNP1700 DNA fragments, the vector was again dephosphorylated with alkaline phosphate CIP (NEB) to avoid plasmid self-ligation.

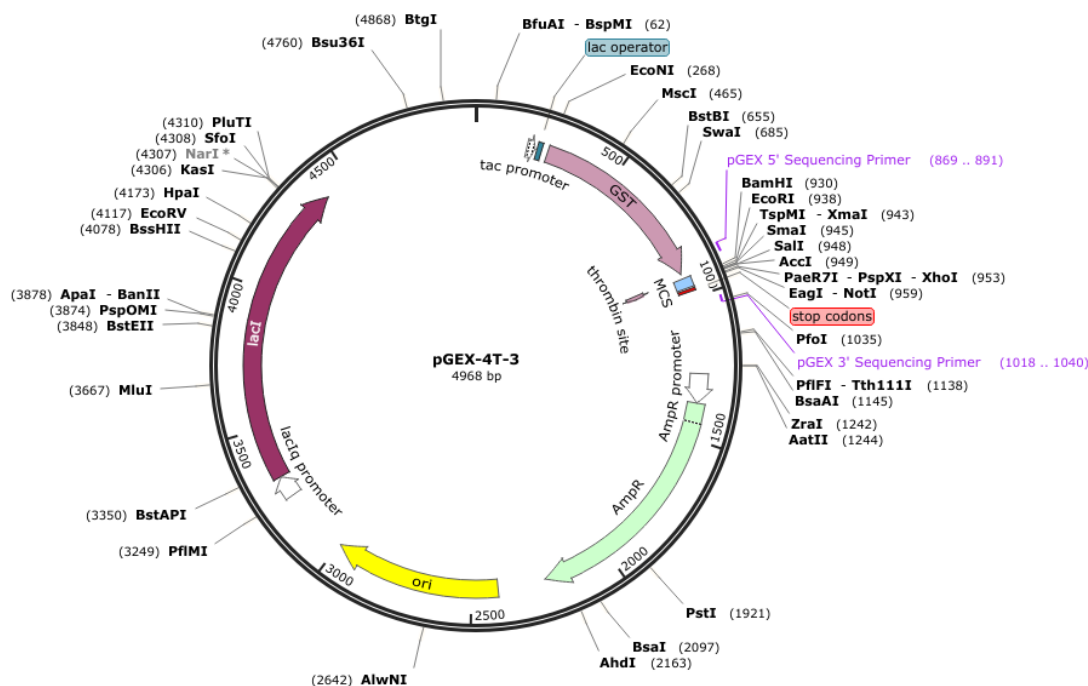


Figure 3.20 pGEX-4T-3 vector map and cloning details. The pGEX-4T-3 vector contained *Bam*HI and *Xho*I restriction sites such as to allow for the insertion of FNP1699 and FNP1700 DNA fragment in the correct orientation.

The double digested pGEX-4T-3 and gel purified FNP1699 and FNP1700 DNA extract were ligated using T4 DNA-ligase before transformation into *E. coli* DH5 α competent cells and cultured overnight on LB ampicillin selective plates. Colony PCRs were performed on the resultant colonies using pGEX primer and the resulting band of correct length were excised and sequenced, this was done to ensure that the insert harbors the correct DNA fragment sequence (Figure 3.21).

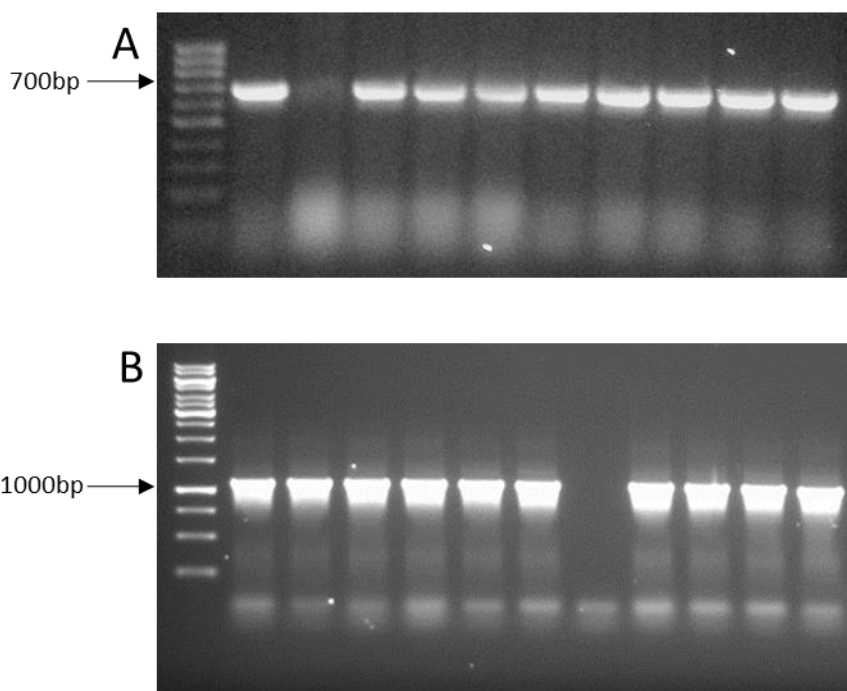


Figure 3.21 PCR screen of pGEX-4T-3-FNP1699 and 1700 DNA. (A) pGEX-4T-3-FNP1699 indicated by 731 bp (565 bp insert+166 bp pGEX primer extension) and pGEX-4T-3-FNP1700 (B) indicated by 1166 bp (1000 bp insert+166 bp pGEX primer extension).

The results revealed that the cloning to be successful and the sequencing came back positive and 100% identical with both synthesised genes.

3.6.2 Overexpression of FNP lysis module genes

3.6.2.1 FNP_1707 protein overexpression and solubility

FNP_1707 was cloned previously into a pET expression vector and proved insoluble by a previous student (Arati Satyal Nepal) from the Stafford group. It was thus decided to clone it into another type of expression vector that might increase its solubility. The *FNP_1707* was cloned by the same student into the plasmid vector pGEX4T3-*amiC* and was provided to me. The plasmid vector pGEX4T3-*amiC* has transformed into *E. coli* strain DH5 α (cloning strain) before extraction using ISOLATE Plasmid Mini Kit (BIOLINE). After that, transformation was performed into expression strains BL21(λ DE3). pGEX vector carries a T7 highly inducible promoter so as to over-express the cloned gene. Attempts to heterogeneously overexpress *amiC* in *E. coli* BL21(λ DE3) with 1 mM IPTG at 37°C for 5 h were made. Samples were taken at 0, 2, 4 and 5 h after induction with IPTG. In this case, IPTG acts as a mimic form of allolactose which serves

to induce the over expression of protein by binding with the Lac repressor, resulting in activation of *amiC* gene translation (Figure 3.22A).

The SDS-PAGE demonstrated that BL21(λ DE3) *E. coli* strains yielded the expression of the protein (46 KDa) when incubated for 5 hours at 37°C in the LB media. Consequently, protein overexpression was performed in large scale volume of BL21(DE3) at 37°C for 5 h (Figure 3.22B).

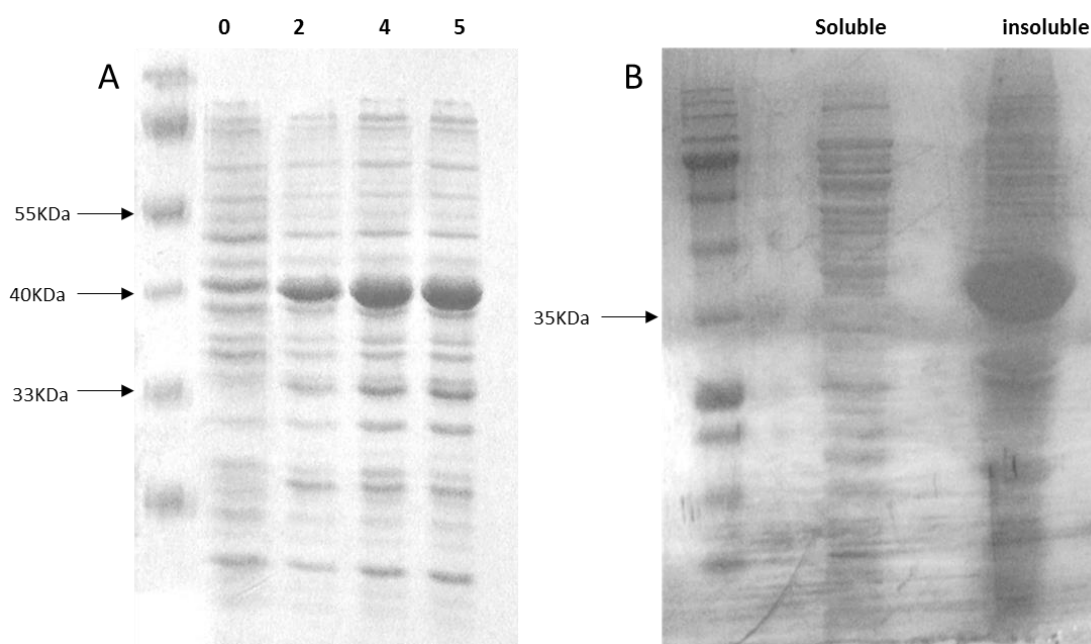


Figure 3.22 *amiC* GST-tag protein overexpression and solubility test. A) pGEX4T3-*amiC* was transformed into electrocompetent *E. coli* strains namely BL21(DE3) and overexpressed by adding 1 mM IPTG in the mid log phase. Uninduced cell represents as a control 0 time, induced represented by 2, 4 and 5 h time. B) BL21(DE3) protein solubility test showing the obtained supernatant (soluble) and pellet (insoluble) after centrifugation of total cell lysate. 15% polyacrylamide gel was used to run the SDS-PAGE.

Solubility of the GST-tagged recombinant *amiC* had to be examined so as to purify the protein in soluble form. The harvested pellet of BL21 were resuspended in binding buffer (50 mM Tris-HCl, 0.5 M NaCl, pH 8.0) and subjected to French Press lysis. The collected supernatant and cell pellet were analysed through SDS-PAGE for BL21 (Figure 3.22B).

The data revealed that the overexpressed *amiC* GST-tagged recombinant protein was insoluble. The heavy band (46 KDa) represented the insoluble protein that was present in the cell pellet. While the light band refers to a small proportion in the soluble protein fraction present in supernatant. However, despite this small amount in the soluble fraction, purification failed (not shown), probably as it was mainly located in the insoluble fraction and we suspect that precipitation occurred during purification also.

3.6.2.2 FNP_1699 lysis protein overexpression and solubility

Upon successful cloning of *FNP_1669*. The pGEX-FNP1699 and pET15b-FNP1699 plasmid vectors were then transformed as described in a previous section (3.6.2.1). Induction with 1 mM IPTG at 20°C overnight was performed, 1ml cell pellets were taken from the two samples before and after induction. After re-suspension of the bacterial pellet in binding buffer, they were subjected to a French Pressure at 1000 psi to release internal proteins while the pellets will contain the insoluble protein. The four samples of uninduced, induced, soluble and insoluble for both pGEX-FNP1699 and pET15b-FNP1699 were analysed via SDS-PAGE (Figure 3.23A and B).

The size of the pGEX-FNP1699 and pET15b-FNP1699 protein was worked out using the ExPASy ProtParam tool (<http://web.expasy.org/protparam/>) and was estimated to be 47 KDa and 22 kDa respectively as the two-plasmids harbour the same inserts, but the pGEX-FNP1699 possess an extra 25 KDa GST tag protein domain. Although, both showed successful overexpression of the indicated protein as shown by the heavy bands in the two induced samples at 47 KDa and 22 KDa respectively and the absence from the un-induced samples, the His-tag (pET15b-FNP1699) showed more protein overexpression than the GST-tagged protein (pGEX-FNP1699) that reside in soluble form.

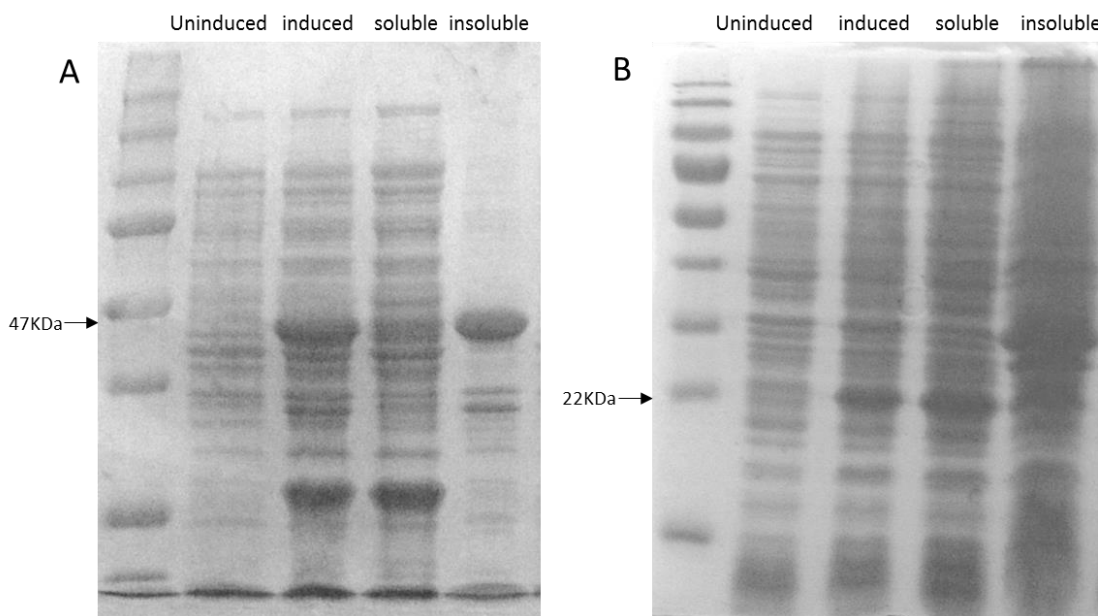


Figure 3.23 FNP1699 GST-tag and His-tag protein overexpression and solubility test. A) FNP1699 GST-tag protein (pGEX-FNP1699) at 47 KDa. B) FNP1699 His-tag protein (pET15b-FNP1699) at 22 KDa. 12% polyacrylamide gel used to run the SDS-PAGE.

Elution and purification for the soluble protein was performed next, pGEX-FNP1699 and pET15b-FNP1699 soluble protein was suspended in binding buffer and subjected to GST and His purification protocols respectively (see section 2.3.11.2 and 2.3.11.1). The GST-tag protein was introduced onto Glutathione affinity resin before elution with 100 mM L-reduced glutathione while His-tag protein was introduced onto a nickel resin before elution with a 300 mM imidazole buffer (Figure 3.24A and B).

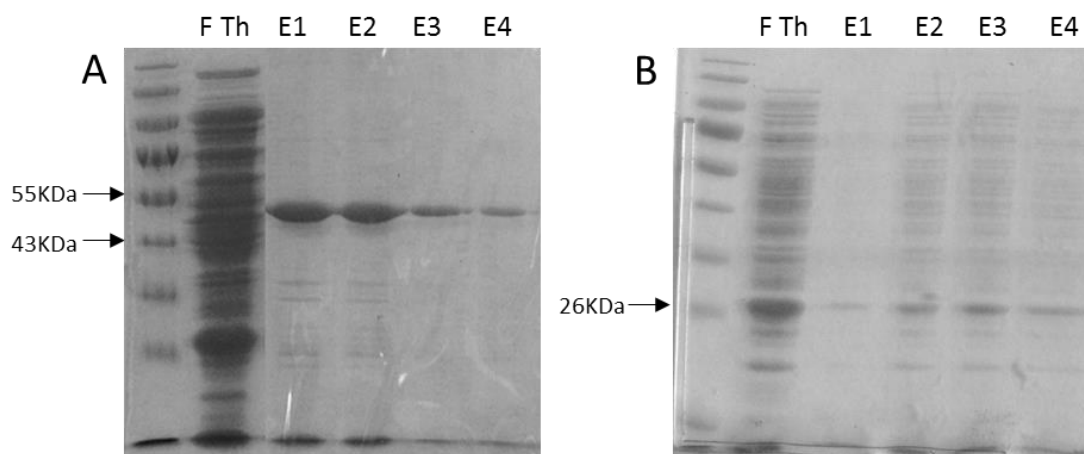


Figure 3.24 FNP1699 GST-tag and His-tag protein elution test. A) FNP1699 GST-tag protein elution fragments at 47 KDa, 12% polyacrylamide gel was used to run the SDS-PAGE. B) FNP1699 His-tag protein elution fragments at 22 KDa, 15% polyacrylamide gel used to run the SDS-PAGE. F Th:flow through, E1-E4:elution fragments.

As can be seen from comparing the different fractions of proteins generated from elution, a small amount of soluble protein was obtained from GST-tag and His-tag protein at 47 KDa and 22 KDa respectively. However, upon dialysis with lower salt buffer, the resulted GST-tag protein was precipitated and returned to an insoluble form (Figure 3.25), this was followed by several trials of dialysis with higher concentrations of salt buffers with new eluted proteins patches with the same results, while the His-tag protein was not pure enough and had many contaminants as revealed from the SDS-page. Since this happened we did not follow up as they are not suitable for further activity test investigation.

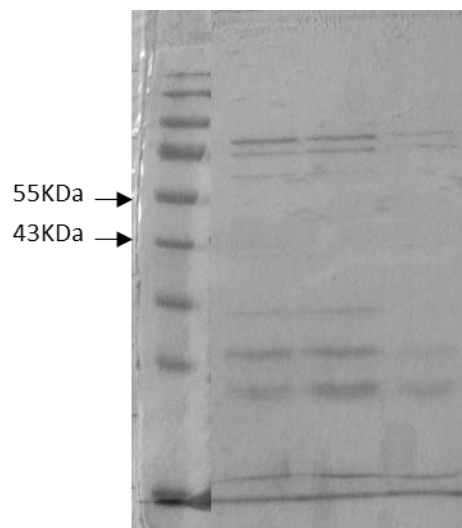


Figure 3.25 Testing FNP1699 GST-tag after dialysis. No band was visualised at 47 KDa after dialysis with 150 mM NaCl buffer, 12% polyacrylamide gel was used to run the SDS-PAGE.

3.6.2.3 Improving recombinant protein production and solubility for FNP_1707 and FNP_1699

Successive attempts were made to reproduce and overexpress both proteins in order to obtain enough quantity of recombinant protein for improving solubility and purification. However, these attempts showed inconsistency in the expression and/or production (several attempts even reveal no expression of target protein) in *E. coli* strain BL21(λ DE3) which might be due to loss of plasmids from the expression strain as a result of plasmid instability (high toxic recombinant protein being produced). It was decided to transform both GST-tagged plasmids that harboured *FNP_1707* and *FNP_1699* into *E. coli* strain C41(λ DE3). The *E. coli* strain BL21(λ DE3) used generally for both prokaryotic and eukaryotic protein overexpression based upon the bacteriophage T7 promoter expression system (the T7 RNA polymerase is produced from the lysogenic λ prophage DE3 under the control of the IPTG-inducible lac UV5 promoter) (Miroux and Walker, 1996).

C41(λ DE3) strain has been used previously in several studies to produce proteins that were either insoluble, expressed poorly, and in cases with unstable plasmid transformation into BL21(DE3) (Masi *et al.*, 2003, Sørensen *et al.*, 2003, Voet-van-Vormizeele and Groth, 2003). *E. coli* strain C41(λ DE3) is a mutant from BL21(λ DE3) that propagated to high density, and continue to produce proteins at improved level

without toxic effects (Miroux and Walker, 1996). Therefore, it was selected for both unstable protein overexpression as shown in Figure 3.26.

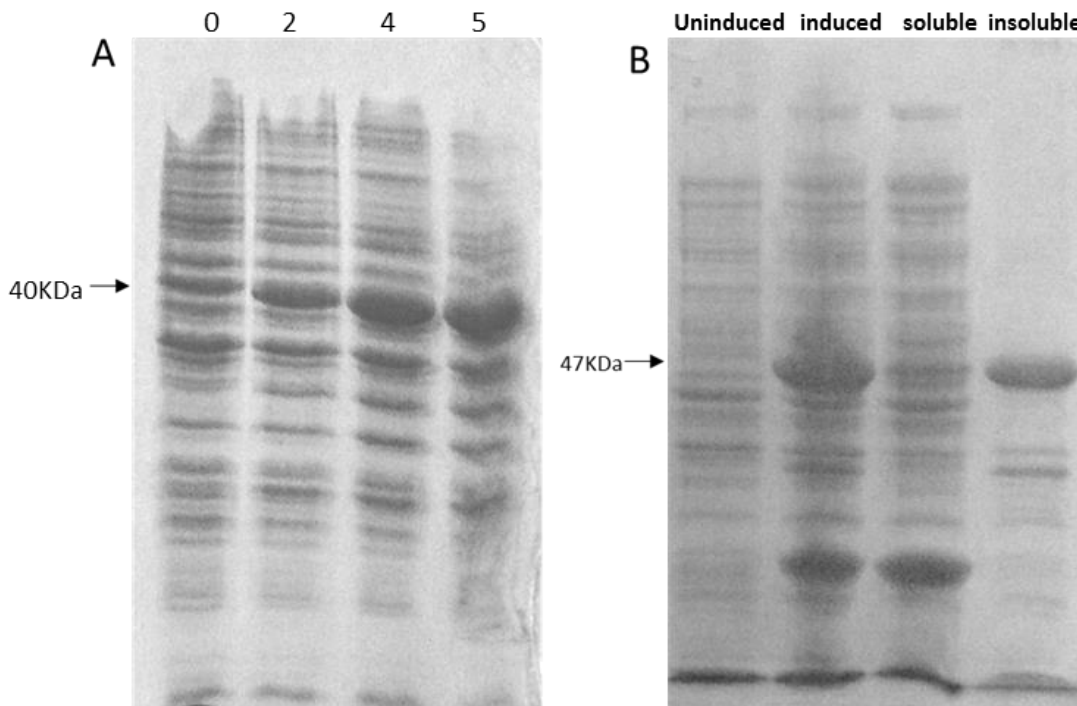


Figure 3.26 FNP_1707 and FNP_1699 GST-tag proteins overexpression in *E. coli* strains C41(λ DE3). A) pGEX4T3-1707 plasmids was transformed into electrocompetent *E. coli* C41(λ DE3) and overexpressed by adding 1mM IPTG in the mid log phase. Uninduced cell represents as a control 0 time, induced represented by 2, 4 and 5 h. B) Overexpression and solubility test of pGEX-FNP1699 protein at 47 KDa. 15% and 12% polyacrylamide gel was used for the SDS-PAGE..

Both FNP_1707 and FNP_1699 GST-tag proteins were overexpressed successfully using *E. coli* strain C41.

If the recombinant protein is expressed faster than they can fold into its native structure, sometimes aggregates will be formed as the result of the reaction of its hydrophobic or sticky partially folded or misfolded regions with other similar proteins (Burgess, 2009). This insoluble form is called an inclusion body of about 0.2-0.5 microns in diameter and the exact mechanism for its formation is not fully understood and differs with different protein being expressed (Singh and Panda, 2005).

Attempts were made to obtain both proteins in active soluble forms using three denaturant agents (N-lauroyl sarcosine, guanidine hydrochloride, and urea) based on

recommendations by Leal *et al.*, (2006) and Burgess, (2009). In all methods, the insoluble protein pellet is resuspended in a suitable denaturant to allow denaturation and solubilisation. Refolding is then performed by dilution of the denatured protein about 60 fold to a point where the protein can refold (flash dilute into refolding buffer). If the denaturation is successful, elution and dialysis can be performed after. As can be seen in Figure 3.27, attempts to resolubilise in a urea and guanidine hydrochloride solutions were successful in denaturation and solubilisation as can be seen by strong bands in Figure 3.27A and B respectively. However, while this was successful for resolubilisation, unfortunately most protein was lost during dialysis due to dilution or aggregate formation due to instability of the solubilised protein when lower salts dialysis buffer was used (our ultimate goal is to produce protein in physiological salt concentration, of 150 mM NaCl).

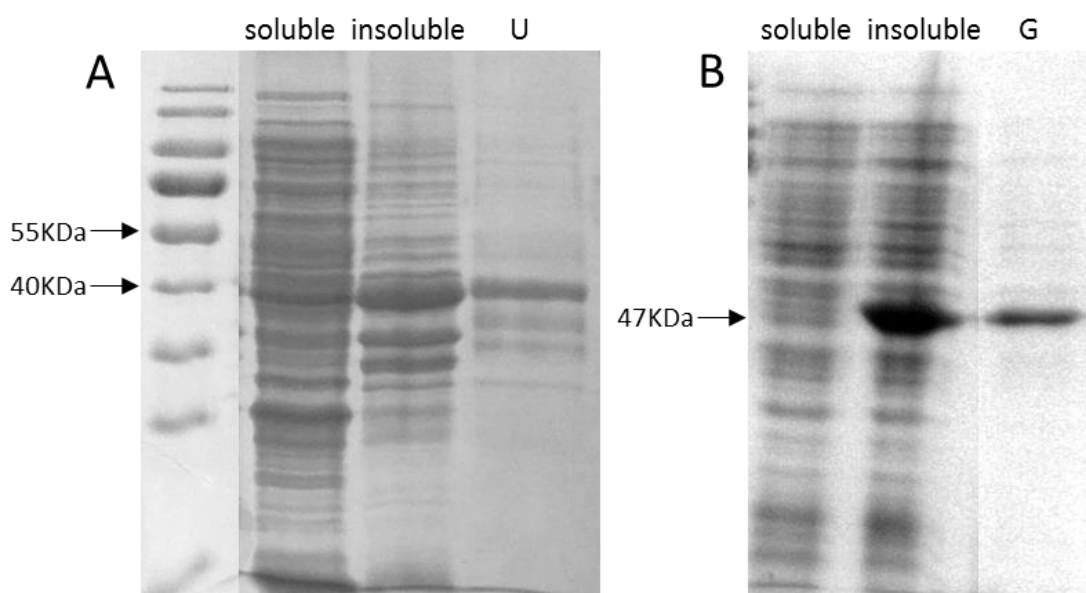


Figure 3.27 FNP_1707 and FNP_1699 GST-tag proteins solubilisation. A) FNP_1707 protein solubilisation with urea (U). B) FNP_1699 protein solubilisation with guanidine hydrochloride (G). 12% polyacrylamide gel was used for SDS-PAGE.

The main problem observed in many refolding attempts is that upon dilution or dialysis of the solubilised recombinant protein to decrease the concentration of the denaturant detergent to lower levels to allow native protein that might have a measurable activity, major precipitation was formed. This might be caused as the sticky regions of the solubilised protein folding again and precipitate, thus it has been stated that refolding of any given protein still presents a significant challenge (Singh and Panda, 2005). As

both FNP_1707 and FNP_1699 proteins overexpression reside mainly in insoluble form, we stopped further purification and went for investigation of the third lysis module *FNP_1700* gene that might give better chance to be overexpressed in soluble form.

3.6.2.4 FNP_1700 lysis protein overexpression and solubility

Upon successful cloning of *FNP_1700*. The pGEX-FNP1700 and pET15b-FNP1700 plasmid vectors was then transformed into the *E. coli* strain BL21(λ DE3) and subjected to overexpression and solubility test protocol of *FNP_1699* as described in previous section (3.6.2.2). The four samples of uninduced, induced, soluble and insoluble for both pGEX-FNP1700 and pET15b-FNP1700 were analysed via SDS-PAGE (Figure 3.30A and B). The size of the pGEX-FNP1700 and pET15b-FNP1700 protein molecular weight estimated to be 62 KDa and 37 kDa respectively. Both showed successful overexpression of the indicated protein as shown by the heavy bands in the two induced samples at 62 KDa and 37 kDa respectively and the absence from the un-induced samples. In addition, the protein resided mainly in the soluble form from both vectors that express the recombinant protein in *E. coli* strain BL21(λ DE3) as shown in Figure 3.28 soluble lane of 62 KDa and 37 kDa respectively.

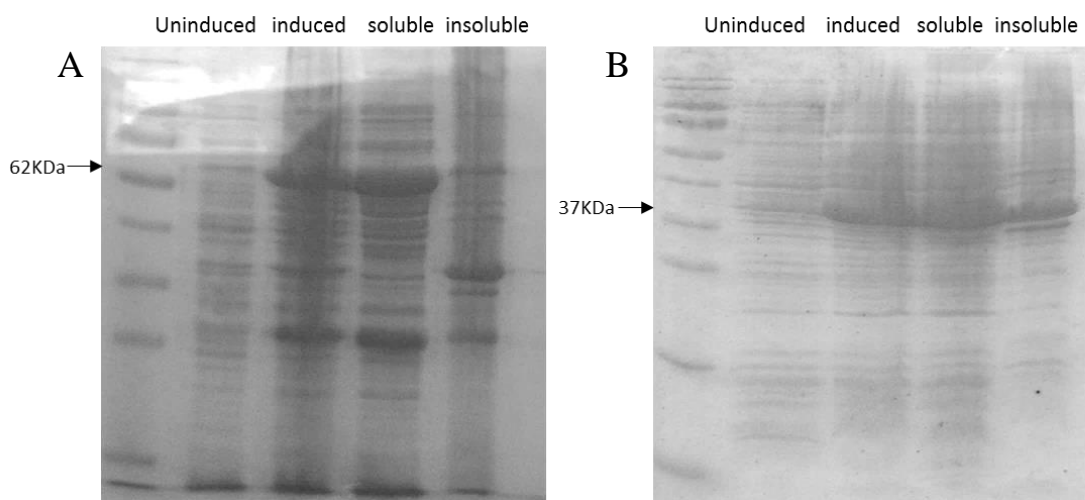


Figure 3.28 FNP1700 GST-tag and His-tag protein overexpression and solubility test. A) FNP1700 GST-tag protein (pGEX-FNP1699) at 62 KDa, 12% polyacrylamide gel was used to run the SDS-PAGE. B) FNP1700 His-tag protein (pET15b-FNP1699) at 37 KDa, 15% polyacrylamide gel used to run the SDS-PAGE.

His-tag purification and elution protocol for the soluble protein from pET15b-FNP1700 was performed next. The His-tag protein was introduced onto a nickel resin

before elution with a 300 mM imidazole buffer. Since this is a competitive binding, the soluble protein will reside into the eluted fractions as shown below in Figure 3.29A.

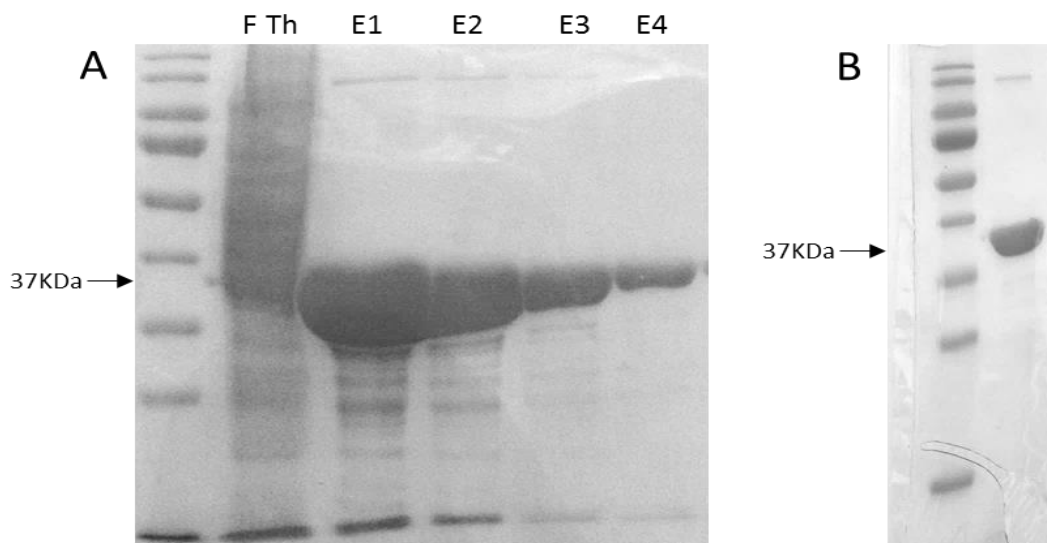


Figure 3.29 FNP1700 His-tag protein elution and dialysis tests. A) FNP His-tag protein elution fragments at 37 KDa. F Th:flow through, E1-E4:elution fragments. B) Dialysis results in more purified protein and absent of most contaminants. 12% polyacrylamide gel used to run the SDS-PAGE.

As can be seen from Figure 3.29A, His-tag protein results in high yield of protein fractions generated from elution at 37 KDa. Dialysis was performed with buffer exchange that contain suitable working concentration of 150 mM NaCl as the high concentration present in elution buffer will interfere with the subsequent protein activity tests. The resulted dialysed protein was stored in 4°C until further test Figure 3.29B.

3.6.2.5 Anti bacterial activity testing of FNP_1700 lysis protein

The dialysed and purified FNP_1700 lysin was measured to be 10 mg/ml using a BCA assay (Pierce BCA assay kit, Thermo-Fisher Scientific). Its antibacterial activity was tested next. To allow the enzyme access to the G-negative peptidoglycan (PGN) through outer membrane (OM), a suitable OM permeablizer (EDTA) was mixed with the FNP_1700 hydrolyase in a final concentration of 0.05 mM. This concentration of EDTA was used to overcome the OM and promote the penetration of several endolysins of muralytic activity on the peptidoglycan of a broad range of G-negative bacteria, namely OBPgp279 (*Pseudomonas fluorescens* phage OBP), PVP-SE1gp146 (*Salmonella enterica* serovar Enteritidis phage PVP-SE1) and 201phi2-1gp229 (*Pseudomonas*

chlororaphis phage 201phi2-1) (Walmagh *et al.*, 2012). First attempt was done by spotting 10 ul of FNP_1700 lysin (with EDTA) onto a 0.7% BHI top agar that contain a lawn of FNP ATCC 10953 and incubation overnight in anaerobic incubator at 37°C. Clearance in the top agar at point of spotting compared to a control of 0.5 mM EDTA only, mean that the mixture of enzyme and EDTA prevent the growth of bacteria and indicate the antibacterial activity of the endolysin. However, no clearance were observed at the points of spotting for both the mixture and the control also, indicating that bacterial growth was not affected. The FNP ATCC 10953 has a mid-log phase of growth about 8 h (Figure 3.30) and usually need 24 h to form a uniform lawn in top agar. Bacterial growth might be returned to normal after enzyme inactivity and its effect might not be visualised with slow growing bacteria, this is supported by the fact that most endolysin-bacterial interaction were tested till 30-60 min (Walmagh *et al.*, 2012, Gong *et al.*, 2016).

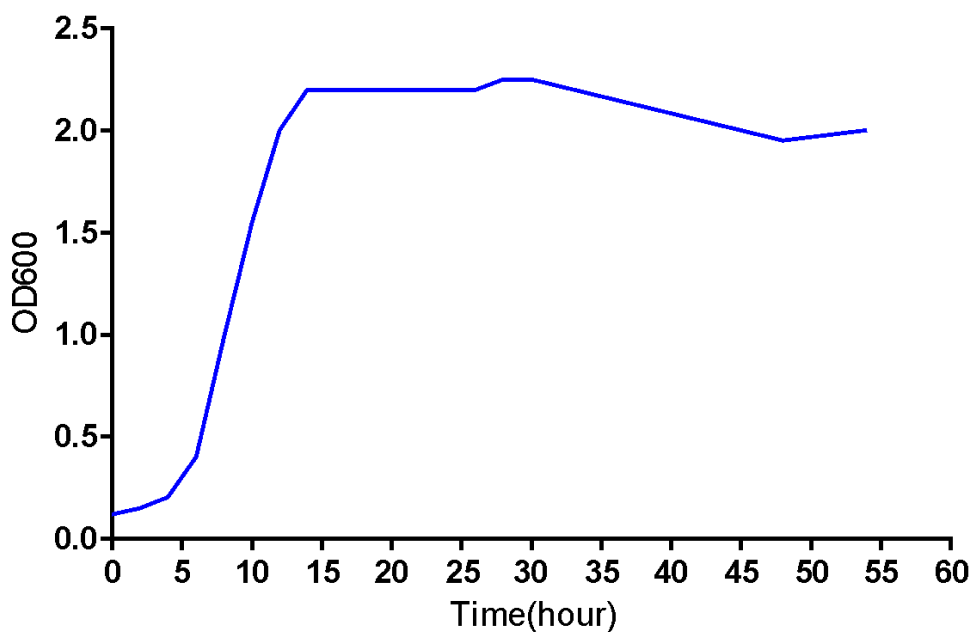


Figure 3.30 Growth curve of FNP ATCC 10953 in broth medium. Fresh bacterial cultures were inoculated broth of BHI with additions of 0.5% yeast extract (YE) (Oxoid, UK), 5.0 µg/ml haemin (Sigma, UK), 1.0 µg/ml cysteine (ICN Biomedicals Ltd, UK) and 2.0 µg/ml menadione sodium bisulphate (vitamin K) (Sigma, UK), from overnight growth to a starting OD₆₀₀ of 0.085 before the growth was measured. Each record represents the mean of three replicates of the same sample. Records were taken across various time points to assess growth rate.

Next FNP_1700 hydrolyase activity was tested against whole FNP bacterial suspension in PBS (Walmagh *et al.*, 2012, Gong *et al.*, 2016) and changes in the turbidity were monitored over time by measuring optical density at OD₆₀₀ every 1 min for 30 min with 2 s circular shaking before each reading in plate reader spectrophotometer (Tecan infinite 200, Austria). As can be seen in Figure 3.31, there was no decrease in turbidity of the enzyme treated bacterial suspension, instead there was slight increase in turbidity measurement reading and there was no significant difference in counting the CFU spotted on FA agar plate compared to the control.

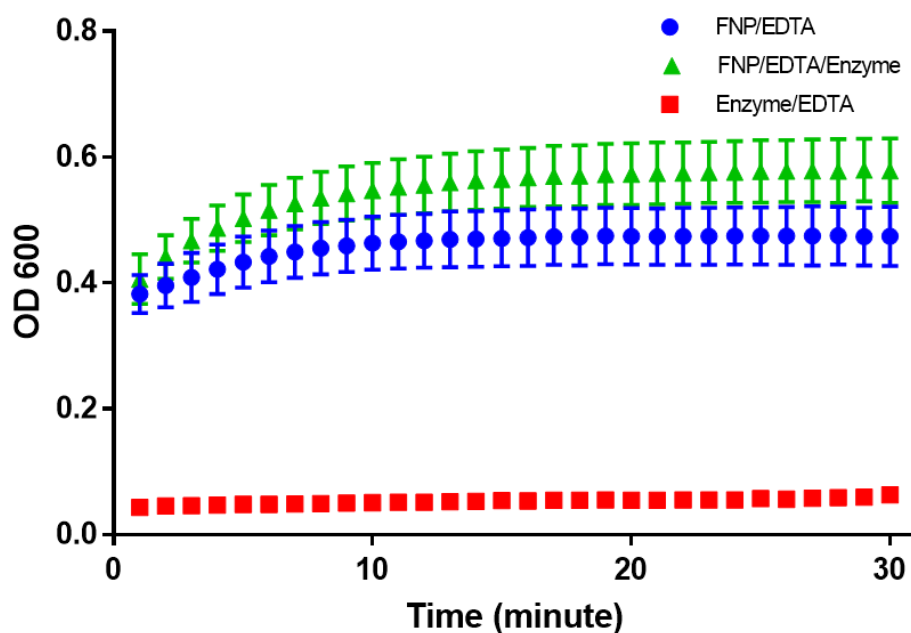


Figure 3.31 FNP_1700 lysin–bacterial activity assay. FNP_1700 (40 $\mu\text{g/ml}$)/0.5 mM EDTA was incubated with 10^8 FNP cells in PBS at 37°C in 100 μl final volume and OD₆₀₀ measured over time in a plate reader.

Despite its lack of antimicrobial activity, and in order to assess the enzymatic efficacy of the FNP_1700 lysin, we performed peptidoglycan degradation assays. Since there is no *Fusobacterium nucleatum polymorphum* ATCC 10953 peptidoglycan available commercially for purchasing, we purchased *Staphylococcus aureus* peptidoglycan (PGN), a G-positive cell wall peptidoglycan to see if any changes in OD could be detected that could reflect the protein activity. In this test, the purified lysin was added to the PGN (0.6 mg/mL) suspended in phosphate buffer (the final concentration of

FNP_1700 lysin is 40 $\mu\text{g}/\text{mL}$), and the mixture was incubated at 37°C. OD₆₀₀ was measured every 1min for total of 58 min in a plate reader. Lysozyme was included as positive control, FNP_1700 lysin alone is the negative control while PGN alone is the control (Figure 3.32A). A decrease in turbidity reading means solubilisation of insoluble PG and positive activity of the enzyme (Hash, 1967). The graph demonstrates that the OD reading decreased over time in FNP_1700 lysin treated *S. aureus* peptidoglycan as did the lysozyme control. However, the decrease in OD of FNP_1700 lysin/PGN is slightly confusing given that the FNP1700/PGN starting OD was higher at time = 0.

In order to also test activity on a G-negative PGN (which has an altered structure compared to *S. aureus*, the same experiment was repeated with commercial *E. coli* K12 PGN. The OD of the treated FNP_1700 lysin/PGN increased instead of decreasing with time (Figure 3.32B).

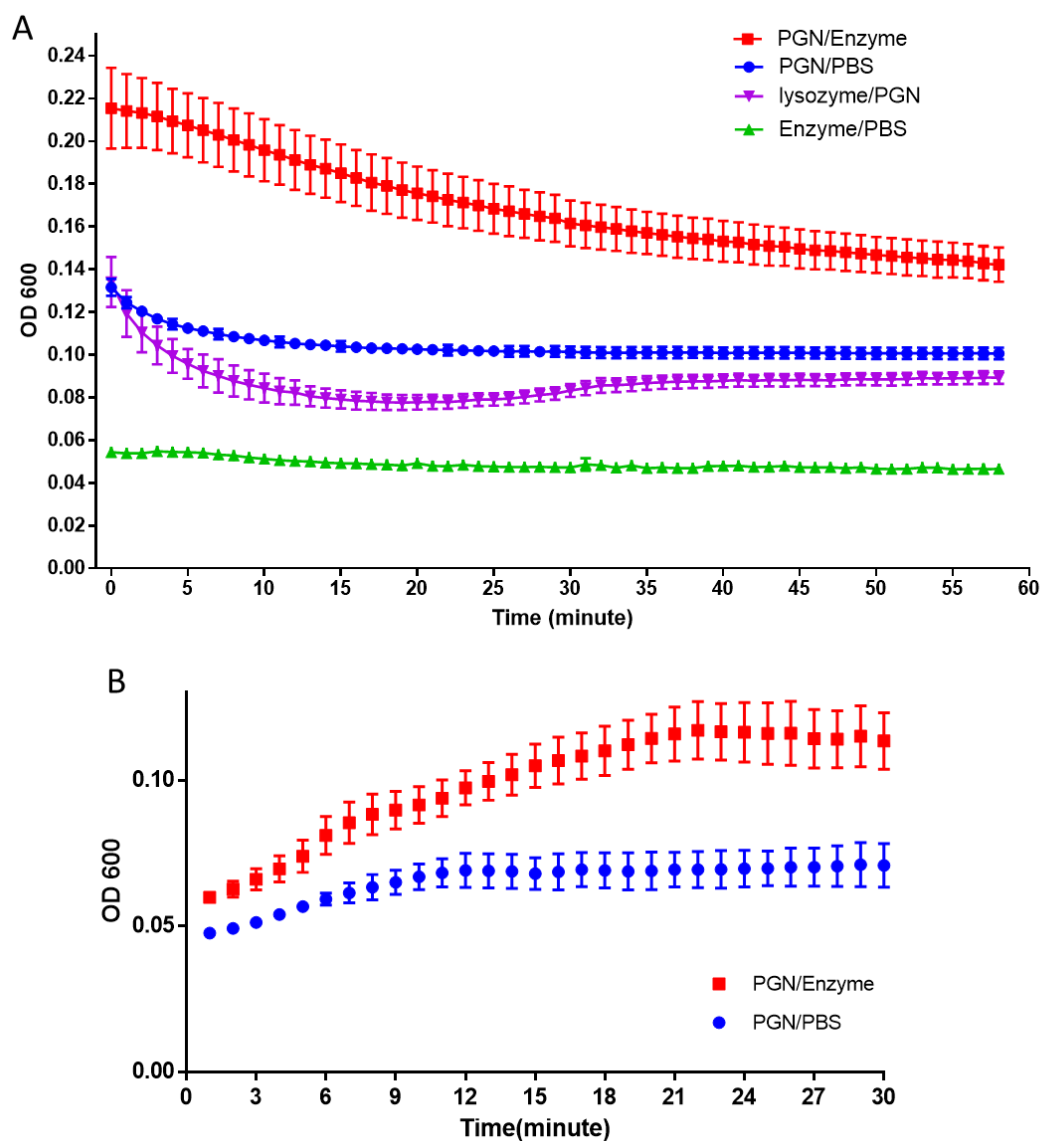


Figure 3.32 Peptidoglycan degradation assays of FNP_1700 lysin. A) FNP_1700 lysin (40 $\mu\text{g/ml}$) with *S. aureus* peptidoglycan (PGN) (0.6 mg/mL) and B) FNP_1700 lysin (20 $\mu\text{g/ml}$) With *E. coli* K12 PGN (0.25 mg/ml). OD₆₀₀ measured over time in a plate reader at 37°C.

To further investigate the potential activity of FNP1700, zymogram was performed as described in section 2.3.15 and shown in Figure 3.33.

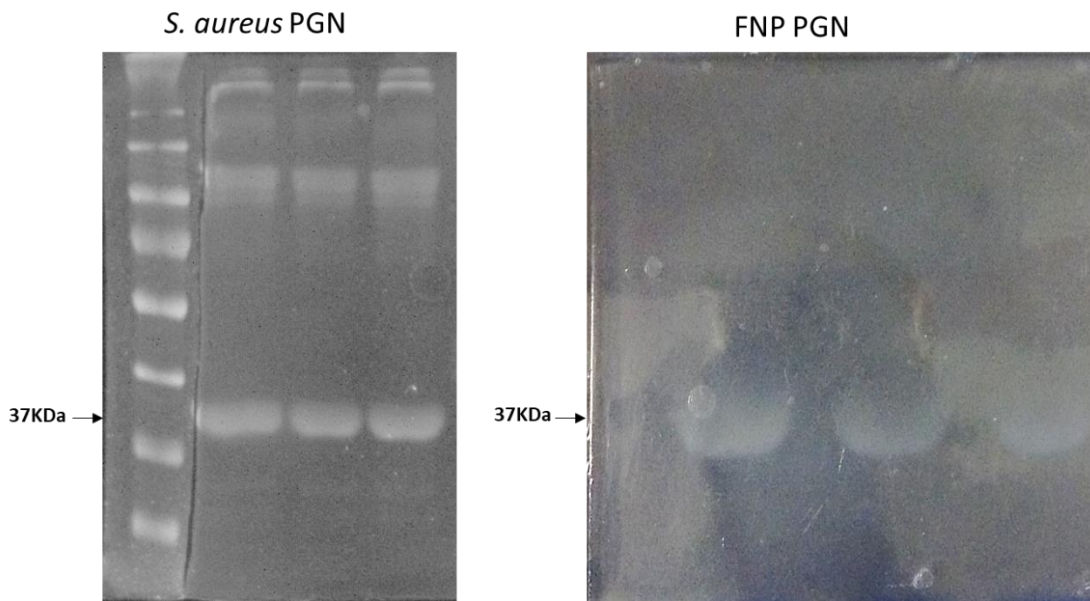


Figure 3.33 Zymogram analysis of FNP_1700 lysin for both *S. aureus* and FNP ATCC 10953 PGN. Purified enzyme were subjected zymogram analysis using 0.1-0.2% PGN. No clear zones in the gel stained with methylene blue were observed but bands related to expected protein size can be visualised at 37 KDa.

The results of zymography did not show zones of clearance in the blue background of the stained gels, instead bands of protein could be seen related to FNP_1700 lysin size for both bacterial PGN as can be seen in Figure 3.34.

In summary, the antimicrobial activity of FNP_1700 lysin was tested, which showed increase in OD reading towards FNP ATCC cells. This was followed by testing its activity towards G-positive and G-negative commercial PGN, while it showed decrease in OD reading regarding *S. aureus* PGN, it does not confirmed by zymography. As we run out of time, the decision was made to go through isolation of bacteriophage targeting oral and endodontic pathogens from human and environmental samples and fully characterise them in order to be applied as antimicrobials.

3.7 Discussion

3.7.1 Bioinformatic exploration of *Fusobacterium nucleatum polymorphum* ATCC 10953 (FNP) prophage

The first aim of this chapter was to characterise a potential prophage present in the genome of the ‘orange complex’ periodontal pathogen *Fusobacterium nucleatum polymorphum* ATCC 10953 that was revealed by genome sequencing (Karpathy *et al.*, 2007) and explore its potential as a source of lysogenic conversion of selective advantage to the bacterial host and/or as a source of lateral transfer of other mobile DNA elements or bacterial DNA. To address this aim, the full chromosome sequence of *Fusobacterium nucleatum polymorphum* (ATCC 10953) with GenBank number: CM000440.1 was analysed using the online web server: PHAST (PHAge Search Tool) (Zhou *et al.*, 2011), a phage searching tool <http://phast.wishartlab.com>. The program is designed to rapidly and accurately identify, annotate and graphically display prophage sequences within bacterial genomes. This was followed by manual annotation using the Basic Local Alignment Search Tool (NCBI) (Altschul *et al.*, 1990).

A prophage like genetic element (phiFNP1) was identified during the genomic analysis of *Fusobacterium nucleatum polymorphum* (ATCC 10953) and is represented by genes immediately downstream of tRNA-Arg3 (t0043, 5' of FNP1662) and tRNA-Arg4 (t0044, 3' of FNP1712) that was arranged in modular form. They include genes involving in phage integration and DNA replication, phage structural proteins, and a lysis module. The integration and DNA replication module harboured gene that encodes for an integrase enzyme (FNP_1662) which usually functions to allow the short phage genome to attach at a specific site to the host bacterium genome (called *attL* and *attR*) and are usually highly conserved in terms of primary amino acid sequence (Groth *et al.*, 2004). Bacteriophage integrase FNP_1662 amino acids BLAST search revealed a specific domain of tyrosine based site-specific integrase of INT_ICEBs1_C_like (cd01189) similar to *Bacillus subtilis* conjugative transposon ICEBs1 integrase, that can be excised and transferred to various recipients as a result of stress (Lee *et al.*, 2007). It also can be carried by non-phage structures such as in plasmids, pathogenicity islands and integrons, thus integrases can not be considered as enough proof to its complete existence as prophage, but it is certainly indicative of this (Casjens, 2003). The same argument can be applied to DNA regulatory genes due to the fact that non-prophage bacterial homologues to nearly all these genes can be recognised. However their occurrence together in this

putative prophage genome is certainly highly suggestive of a complete prophage (Lewis *et al.*, 1998). In contrast to the first locus, the presence of genes that are encoding the phage morphogenetic genes is considered to be a true indication of prophage existence in the host bacterial genome, and the cornerstone for that is the identification of the large terminase subunit and portal protein (Casjens, 2003). The genes ordering observed here are found in nearly every tailed temperate phage. In addition, an amino acid BLAST search for conserved domains of the predicted head capsid protein (FNP_1688) revealed a specific hit for those in phage major capsid protein of HK97 family (TIGR01554) found in *E. coli* bacteriophage HK97, *Bacillus subtilis* bacteriophages phi-105, and *Salmonella* Bacteriophage P27. This model represents one of several analogous families lacking detectable sequence similarity.

3.7.2 Induction of FNP prophage with Mitomycin C

In order to understand if phiFNP1 temperate phage was functional or merely a pseudophage of genetic remnant in the chromosome, I attempted to induce it using Mitomycin C in an attempt to isolate it, view the induced particles using TEM negative staining, and infect other clinical and lab strains and study the change in its pathogenicity.

Mitomycin C has been used to induce the synthesis of temperate phages from *Yersinia* strains (Popp *et al.*, 2000) and phages or phage-like particles from G-positive dairy *Streptococcus* strains (Huggins and Sandine, 1977). In addition, it is categorised as antibiotic derived from *Streptomyces caespitosus* that inhibits DNA synthesis. It reacts covalently with DNA, *in vivo* and *in vitro*, forming crosslinks between the complementary strands of DNA. This interaction prevents the separation of the complementary DNA strands, thus inhibiting DNA replication (Ueda and Komano, 1984). The TEM negative staining technique consists of staining the virus particles with electron dense material, to introduce contrast. Uranyl acetate was used in this study to stain the phage particles as it was proved previously to be a potent phage stain in numerous studies (Huxley and Zubay, 1960). Putative phages appeared as negative translucent particles against a dark background- positive staining of phage heads occur because uranyl acetate has strong affinity to dsDNA phages result in black stained capsids (Kutter and Sulakvelidze, 2004). The *rpoB* primer set was chosen to assess the presence of any contaminating DNA arising from cell lysis from phiFNP1 because it is very specific to FNP and possesses no specificity to other *Fusobacterium* species while 16S rRNA primer is specific to a range of *Fusobacterium* species.

If phiFNP1 prophage could infect or integrate into the genome of *Fusobacterium polymorphum* strains that lack the temperate phage, the presence and expression of new virulence genes could be studied by comparing to its phage free strain. Although positive bands related to the phiFNP1 were shown in the PCR screen using specific primers after induction with 1 µg/ml Mitomycin C, the TEM images did not show any clear fully formed morphology of tailed phage or polyhedral head particles, while some particles possessed small protrusions that might represent small tails such as those present in several podoviridae, it was not conclusive. Instead, variously sized round particles with potential double membranes were present in large numbers as in Figure 3.6B. These particles might be phage or could be outer membrane vesicles (OMVs) similar to those identified from *P. aeruginosa* and many other G-negative bacteria of different sizes bilayered MV of 50-150 nm (Kadurugamuwa and Beveridge, 1996). The amount of OMVs from *P. aeruginosa* were positively associated with exposure to gentamycin (antibiotics) and they were filled with periplasmic components i.e. peptidoglycan hydrolases. While no lysis of FNP ATCC 10953 cells was associated with this possible induction of the particles it is possible that the cells stayed intact with progeny production, as is the case for some single stranded DNA filamentous bacteriophages, whose newly formed progenies are released by a secretion-related mechanism that maintains bacterial cell integrity (Russel, 1995) or in certain enveloped mycoplasmaviruses in which budding of the newly formed progenies with host cell outer membrane in order to be elaborated occur (Maniloff *et al.*, 1980). However, this does not explain the presence of DNA belonging to phiFNP1. On the other side, Seaman *et al.* (1964) showed that different sizes of oval PBSX prophage heads could be induced from *Bacillus subtilis* alone (heads only) or associated with tails. They are genetically defective and unable of self-reproduction in the recipient strains (they can infect other strains of *Bacillus subtilis* but they do not produce new progenies and do not produce plaques in spot testing on a lawn of the host strains), though they harbour DNA similar to the host DNA which might explain the presence of positive PCR reaction towards phage DNA in our experiments. Later reports identify the DNA to be approximately 13 Kbp that were belonged to *Bacillus subtilis* (Haas and Yoshikawa, 1969, Anderson and Bott, 1985). Although, they are adsorbed to the surface of their host strains, their DNA seems not to be injected which might explain why we could not identify the phiFNP1 genome from the clinical and laboratory strains that were infected by the induced particles (Okamoto *et al.*, 1968). However, DNA extraction and sequencing of the induced particles from phiFNP1 was not performed in

this study and should be recommended for future investigations to identify the nature of the particle contents.

The particles from the Mitomycin C treated lysates were incapable of infecting in broth and double layer plaque assay other clinical and laboratory *Fusobacterium* that we isolated from patients in Sheffield and which we also showed were negative for possessing the PhiFNP1 phage.

The FNP prophage bioinformatics reveals the presence of several genes that encode for tail proteins (Table 3.1) namely FNP_1689 (head-tail joining protein), FNP_1693 (tail sheath), FNP_1698 (tail tape measure protein), FNP_1703 (base plate J-like assembly protein and FNP_1709 (phage tail-like assembly protein). However, there may be a defect in these tail proteins that made them not assembled in correct order to form the tails and join the heads particles later on during head tail assembly and thus improper formation of complete phage particles. In tailed phage, it is the tail of the phage that first contacts bacterial host and is likely responsible for primary recognition and adsorption to specific receptors on the bacterial membrane host (Casey *et al.*, 2015b). This is in agreement with Mmolawa *et al.* (2003) who mentioned that tail genes of ST64B phage isolated from *Salmonella enterica* Serovar Typhimurium DT 64 were not expressing that render the phage defective and no visible tail was identified in TEM micrographs. They suggested that the presence of virulent fragments of genes within tail genomes might cause the phage defective in tail region. Figueroa-Bossi and Bossi (2004) identified that mutation in certain tail operon gene region results in reactivation of ST64B phage. However, this was possible by comparing the sequence of the defective phage with similar active one unlike *Fusobacterium* as no active prophage could be isolated and sequenced that is capable of infecting other *Fusobacterium* strains. One recent study mentions the induction, sequencing and isolation of 2 phages from *F. nucleatum subsp. animalis* strain 7-1, a highly invasive isolate from the human gastrointestinal tract (Cochrane *et al.*, 2016). However, both were defective and incapable of produce plaque in a simple plaque assay. In addition, the TEM micrographs did not show fully formed phage particles, despite claims to the contrary in the manuscript. A previous study by Machuca *et al.* (2010) mentioned the isolation of active phage capable of lysogeny and infection of other oral *Fusobacterium* strains, hence partial sequencing of small 500 bp DNA fragment was sequenced and showed more than 90% nucleotide sequence identity to gp3 and gp4 structural protein-encoding genes of *P. acnes* phages. Thus, I, and others believe that it represents a contaminant sequence from oral *P. acnes* phage and not a true

Fusobacterium phage sequence (Brüggemann and Lood, 2013). Although phiFNP1 genome sequences annotation did not ultimately identify virulence associated genes within it, several of its genes coded for hypothetical proteins of unknown function, and it is possible that these predicted genes are involved in virulence mechanisms that not been identified till now. The virulence encoded genes located inside the prophage genome usually appear to be remnants from previous bacterial host and some proved to be encode for virulence factors in *S. enterica* prophages (McClelland *et al.*, 2001). Nevertheless, we have still obtained valuable information concerning the predicted gene content of the FNP prophage.

3.7.3 Testing for the occurrence of *Fusobacterium nucleatum polymorphum* and its prophage in clinical plaque samples.

In order to investigate the clinical important of phiFNP1 prophage and the FNP ATCC strain, clinical plaque samples from deep periodontal pockets (diseased sites) and healthy sites collected from cases of patients attending the periodontal departments for treatments at the School of Clinical Dentistry were screened by extracting DNA and doing qualitative pcr for presence or absence phiFNP1 and its FNP ATCC strain. The DNA extracted from the plaque samples were in the range of 1.2-28 ng/ul, but both for ease of assay and since we were only looking for a qualitative assessment of phiFNP1 carriage we designed an assay where we used a set, but consistent volume of extracted DNA. While this has limitations, it does not enable the quantification of gene (or transcript) numbers which are proportional to the starting template concentration (Smith and Osborn, 2009), i.e. each sample can have differing concentrations of DNA based on differing amounts of plaque collected in the samples, we felt that it provided a simple and robust method to establish how prevalent this phage was in our patient population. During an optimisation phase we established 4 µl as the optimal level of DNA sample to detect the DNA by PCR in this qualitative PCR assay. It is worth mentioning at this stage that the same plaque samples were used in another recently published study for investigation of a novel predictive biomarker profile for the outcome of periodontal treatment (Gul *et al.*, 2017). In which universal 16S rRNA primers and those specific for *F. nucleatum*, *P. gingivalis* and *T. forsythia* were used to count their numbers in response to treatment. The result of that study indicates that *F. nucleatum* cell numbers were not significantly different in health or disease or after treatment, while the reverse was true for *P. gingivalis* and *T. forsythia* (Gul *et al.*, 2017).

The results revealed that the phiFNP1 prophage and its strain are common among the disease sites of patients suffering from periodontal disease (half of the patients screened positively from diseased sites) and they are not just present in a lab strain isolated previously. However, half of the patients screened negatively for both which is in agreement with (Moore and Moore, 1994), as he mentioned that the most common subspecies in the gingival crevice is *F. nucleatum* subsp. *vincentii* followed by *F. nucleatum* subsp. *nucleatum* and finally and less common is the *F. nucleatum* subsp. *polymorphum* in an isolation ratio of 7:3:2. In contrast, Kim *et al.* (2010), reported that *F. nucleatum* subsp. *polymorphum* is the most frequently isolated subspecies in the Korean oral cavity. They regarded that to the difference in the geographical ethnic groups and their different eating habits, various methods being used and the sampling size difference. Metagenomic sequencing could be also applied to identify different *Fusobacterium* species and most importantly the diversity of phages within subgingival plaque samples (Ly *et al.*, 2014) that we recommend for the future study.

A second interesting finding is that if the patient screened positively in the first visit before treatment, that result will be still consistent throughout the successive 2 visits (after treatment). This finding assumes that once the bacterial strain is established in a diseased site and or sites, it will persist even after treatment and the treatment outcomes even when it is positive will not end in pathogenic strain complete elimination and removal from the mouth of patients suffering from chronic periodontitis. This finding is in agreement with research conducted on animal models that mention anti-inflammatory treatments suppress the periodontal bacterial load (Hasturk *et al.*, 2007, Eskin *et al.*, 2012, Moutsopoulos *et al.*, 2014) and not completely eliminate them. In addition, this is further supported by the fact that synergistic and dysbiotic selection of bacterial community initiated by certain pathogens such as *P. gingivalis* are behind periodontitis (Hajishengallis and Lamont, 2012, Abusleme *et al.*, 2013). They can act at low levels of abundance, as mentioned in mucosal keystone pathogens hypothesis (Hajishengallis *et al.*, 2012). The presence of FNP ATCC 10953 in healthy sites is not surprising (in about half of the patients that their diseased sites were positive), as *F. nucleatum* is one of the G-negative species always identified in biofilm plaque of healthy sites and its numbers increase distinctly in diseased sites (Moore and Moore, 1994, Becker *et al.*, 2002). Hence, it is considered as an intermediate colonizer bridging the attachment of early commensals of the tooth and epithelial surface with late pathogens (Kolenbrander, 2000) that might explain why it is not found in all healthy sites of positive diseased patients as their

presence in identified form might be occur not so early. Testing for the phiFNP1 and its' host strain in a future study in plaque samples of healthy people and compare it to similar once from healthy sites of patients having chronic periodontitis is recommended. In addition, in light of this study, the distribution and occurrence of other periodontal associated pathogenic bacteria should be tested which harbour known inducible prophages from samples obtained from the dental plaque of diseased and healthy sites of patients having chronic periodontitis before and after treatment and correlate the results to the sites that responded to treatment, like phages from *A. actinomycetemcomitans* such as in the study performed in patients having prepubertal periodontal destruction (Preus *et al.*, 1987).

3.7.4 Investigation of the phiFNP1 lysis module as a source of therapeutic antimicrobial proteins

Bioinformatics revealed that the genome of phiFNP1 prophage harbours three potential lysis genes named peptidoglycan-binding lysin domain protein (FNP_1699), putative hydrolase (FNP_1700) and N-acetylmuramoyl-L-alanine amidase (FNP_1707). However, the bioinformatics of FNP prophage did not reveal the presence of an obvious gene that encode for holin. Holin is a protein that enable passive diffusion of endolysin into the periplasmic space thus rendering the former act on hydrolysing bacterial PG (Young, 2002, Reddy and Saier, 2013, Savva *et al.*, 2014). However, new systems other than the holin-endolysin cell lysis system has been reported in bacteriophage, such as Lys44 reported from *Oenococcus oeni* phage fOg44 (São-José *et al.*, 2000). In this system, the endolysin is produced with an N-terminally located signal-arrest-release (SAR) sequence that is cleaved by the proteolytic activity of periplasmic protease LepB, and released into the bacterial periplasm. More recently Frias *et al.* (2013) reported that the lysin Svl from the pneumococcal phage SV1 is able to carry out holin-independent killing and the choline containing teichoic acid (TA) was responsible for endolysin transport.

The recognised prophage genes that encode for lysis could potentially be an antimicrobial protein that would target *Fusobacterium nucleatum*. This could be employed as part of phage therapy in the combat of this periodontal disease. To date, the potential antimicrobial efficacy of *Fusobacterium* phage endolysins have not been

studied. In order to assess their antimicrobial activity, the potential lysin genes were either cloned by PCR (FNP_1707) or synthesised as linear DNA fragments by Invitrogen GeneArt (FNP_1699 and FNP_1700). The method of codon optimisation has proved very useful in recombinant protein production, both in the literature (Rosano and Ceccarelli, 2009) and in our own laboratory (unpublished data) where enzyme have been transformed from insoluble proteins to soluble active enzymes as a result of codon optimization using this method. In these cases, the aim is to obtain a high yield of protein from synthetic genes whilst the encoded amino acid sequence of the synthesized nucleotide sequence remains identical to that encoded by the native original DNA sequence (Figure 3.15). This was necessary as the GC content and codon usage of FNP differed markedly and this was an approach used in the lab for the *Tannerella* NanH sialidase. As a result the final synthetic genes had altered DNA sequence in comparison to the original gene but identical primary amino acid sequences (Figure 3.15). In addition, the final nucleotide sequences for both genes were in-frame checked by ExPASy translate online tool (web.expasy.org/translate) with 6-Histidine tag (pET vector) and gst-tag (pGEX vector) and, showing changes in nucleotide but not amino acid sequence for both sequences.

Via these methods I managed to express and purify successfully one of the three recognised phiFNP1 prophage genes lysis module (FNP_1700) in soluble form and then began to examine its potential as an antimicrobial. It had no antimicrobial activity towards FNP bacteria. Despite that, I went to test FNP_1700 lysin enzymatic activity (peptidoglycan degradation assays) against commercial cell wall of G-positive (*Staphylococcus aureus* peptidoglycan) and G-negative (*E. coli* K12 peptidoglycan). Again, no FNP_1700 lysin activity was obtained from these experiments.

Endolysin is an enzyme that is encoded by bacteriophage that hydrolyse and digest the bacterial cell wall PG at the end of the phage infection cycle. This occurs in order to release the newly formed and packed phage particles carried out by the double strand DNA viruses in a process called lysin-mediated breakdown of PG (Young *et al.*, 2000, Young, 2014, Lood *et al.*, 2015). The endolysins of bacteriophages infecting G-positive bacteria harbour endolysins that contain at least one catalytic and one cell wall binding domain arranged in a modular form in nature (Fischetti, 2010, Sudiarta *et al.*, 2010). Regarding the lysis modules of FNP ATCC 10953 prophage, all the three identified lysis genes do not harbour a cell wall binding domain (CBD), this is not surprising as most endolysins of phages infecting G-negative bacteria contain only a catalytic domain (Cheng *et al.*, 1994). This obviously will end with broader effective

host-range of spectrum as endolysins of G-negative bacteria will not be necessarily obligated to certain bacteria that match with its CBD (Loessner *et al.*, 2002, Hermoso *et al.*, 2003, Fischetti, 2008). However, it was stated that deletion of CBDs results in a significant decrease (Morita *et al.*, 2001) or complete loss (Loessner *et al.*, 2002, Zimmer *et al.*, 2002) of the enzymatic activity of different endolysins that highlight the need for CBD. Hence, the G-negative bacteria have an outer membrane that shielding the peptidoglycan from the lethal action of external endolysin with high-affinity binding domain comparing to G-positive bacteria (Briers *et al.*, 2007).

FNP_1699 and FNP_1707 were proved to be insoluble, which places a limitation for investigating their potential lysis activity. This might be due to recombinant protein being produced in solo form by *E. coli*, while in the actual phage infection cycle more than one protein from the lysis module are produced in parallel at the same time that might have positive affect on each other. Several studies mention that the transcription of phage lytic genes started at an early stage of infection, and continue through out different stages of infection (Duplessis *et al.*, 2005, Dedrick *et al.*, 2013, Nguyen and Kang, 2014). This is further supported by the study of Briers *et al.* (2007) which showed that deletion of the N-terminal PBD of KZ144 and EL188 endolysins resulted in insoluble catalytic domains, emphasising the important of PBD in enzyme folding and activity. Furthermore, several endolysins were proven to be formed without activity then later to be activated at a certain time point to initiate the lysis of the host cell membrane. The first and best studied example is represented by PlyC, an endolysin produced by streptococcal C1 phage. PlyC oligomer is formed by the association of PlyCA (bear the catalytic domain) with PlyCB (that possess the cell wall binding ability). Interestingly, PlyCA alone shows no lytic activity in the absence of PlyCB (McGowan *et al.*, 2012). Another example is represented by depolarisation of the bacterial cytoplasmic membrane that occurs by the pinholins (Young, 2002). Pinholins, forms very small dimension holes in the cytoplasmic membrane of the host that lead to leakage of protons leading to the disruption of proton motive force (PMF), and thus resulting in the depolarization of membrane (Park *et al.*, 2007, Pang *et al.*, 2010, Pang *et al.*, 2013). In addition, when the purified phage fOg44 endolysin Lys44 is added to *Oenococcus oeni* culture, no activity was observed and lysis do not occur unless nissin added (a membrane-disrupting agent) (Nascimento *et al.*, 2008). The formation of disulphide bond between Cys13 and Cys44 activates the P1 endolysin (Xu *et al.*, 2005) is another example. However, not all process that activate endolysin are known till now such as in case of coliphage 21 endolysin (R²¹), the

formation of the catalytic triad inside the periplasmic space is unknown till now (Sun *et al.*, 2009b). However, the results were conflicting and left us with the assumption that the potential FNP_1700 endolysin might exhibit low activity towards *S. aureus* PG but not towards *E. coli* PG. However, FNP_1700 endolysin might be naturally produced in an inactive form and might need another enzyme from the lysis module to be fully active such as FNP_1699 (predicted to be peptidoglycan-binding lysM phage domain, see section 3.6). Thus, the cloning of lysis module enzymes such as FNP1700 and FNP1699 in the same vector is suggested for future study, which might improve the solubility of the later and improve the activity of the former at the same time. In addition, to improve the solubility of FNP1707 and FNP1699, the fusion of cloned protein with maltose binding-protein (MBP) is suggested also, which showed proper folding of the attached partner (cloned protein) into its biologically active conformation and thus improve solubility that were much superior to GST-tagged protein for five fused partners (Kapust and Waugh, 1999).

3.8 Conclusions

Bioinformatics for the whole genome sequence of *Fusobacterium nucleatum polymorphum* ATCC 10953 revealed the presence of a complete prophage as predicted by phage searching tool. However, the phiFNP1 prophage seems to be defective, as it could not infect other *Fusobacterium* strains. Hence, several of its genes coded for hypothetical proteins of unknown function, and it is possible that these predicted genes are involved in virulence mechanisms that have not been identified until now and still we get valuable information from studying the phiFNP1 prophage. *Fusobacterium nucleatum polymorphum* ATCC 10953 and phiFNP1 prophage occurrence are common in patients suffering from periodontal disease. Once the pathogenic bacterial strain established in diseased site and or sites, it will persist even after treatment and the treatment outcomes even when it is positive will not end in pathogenic strain complete elimination and removal from the mouth of patients suffering from chronic periodontitis. Finally, one of three recognised prophage genes within phiFNP1 prophage lysis module has been successfully cloned and expressed by *E. coli* in soluble form. Though its activity as antibacterial was not confirmed, it needs to be further explored as phage endolysins against *Fusobacterium* have not been identified yet and may aid in the treatment of periodontal diseases and other *Fusobacterium* infection associated disease such as FadA

adhesin positive *Fusobacterium nucleatum* that are found to promote colorectal carcinogenesis (Rubinstein *et al.*, 2013).

**Chapter 4: Isolation of lytic
Bacteriophage targeting endodontic and
oral associated pathogens from oral and
wider environments**

4.1 Introduction

The aim of the work in this chapter was to attempt to isolate bacteriophage targeted against a range of periodontal, endodontic and other oral associated bacterial pathogens and subsequently go on to characterise them as potential therapeutic agents. As mentioned in the introduction, bacteriophage are the most numerous organisms on earth and are found in abundance in almost all environments inhabited by bacteria (Hendrix *et al.*, 1999). The oral cavity is no exception, it is an environment rich in bacteria with estimation of more than 1000 taxa and over 500 species present, of which around 50% are culturable (Dewhirst *et al.*, 2010). These bacteria are the cause of the two major oral disease affecting our teeth and supporting tissues, namely caries (or cavities) and gum disease- characterised by reversible gingivitis and more chronic and serious periodontal disease (Hardie, 1992) (see section 1.1). As outlined in section 1.3, if cavities in our teeth progress to enter the tooth pulp or even break out of the tooth apex, this leads to apical abscesses that after initial treatment may not resolve due to the presence of small numbers of hard-to-eradicate bacteria such as *E. faecalis*.

Given that these infections, although not classical, are caused by dysbiotic microbial biofilm communities, that are by their nature hard to treat and eradicate. In some cases influenced in this dysbiosis by a small handful of ‘keystone’ species, the possibility of using targeted therapy against the most influential of these species has become attractive. In addition, in the case of recalcitrant endodontic infections and localized aggressive periodontitis there are strong associations with one-species, namely *E. faecalis* (Dahlen *et al.*, 2000) and *A. actinomycetemcomitans* (Fine *et al.*, 2007) both of which can be difficult to eradicate via normal means. One possibility for novel targeted treatment of these infections might be the isolation of bacteriophage targeted against these pathogens. However, to date cataloguing or indeed isolation of oral cavity derived or those phage that target oral strains has met with little success, and in reality the best existing evidence phage in the oral cavity is from metagenomic studies (Ly *et al.*, 2014). However, these have rarely been observed visually, and even more rarely isolated (Hitch *et al.*, 2004).

Given the evidence of the presence of phage in the oral metagenome (Ly *et al.*, 2014) (accepting that a proportion of this might be from prophages) and following the logic that they should be present, one aim in this chapter was the cataloguing and attempted isolation of phage from oral samples against oral pathogens. We also took the

novel approach of attempting isolation against new, i.e. limited lab adaptation, clinical strains from periodontal patients in Sheffield and Baghdad. In addition, given its traditional use for such studies, we also sourced phage from a rich wastewater source as a known habitat of phage.

If isolated, we then aimed to go on to characterise these phage in terms of morphological characterisation, phage genome characterisation, phage-host range determination, One step growth, infection cycle, adsorption rate, biofilm eradication on biofilm and infection models. We also attempt to investigate the molecular determinants of the strain specificity of these phages.

Specific Aims:

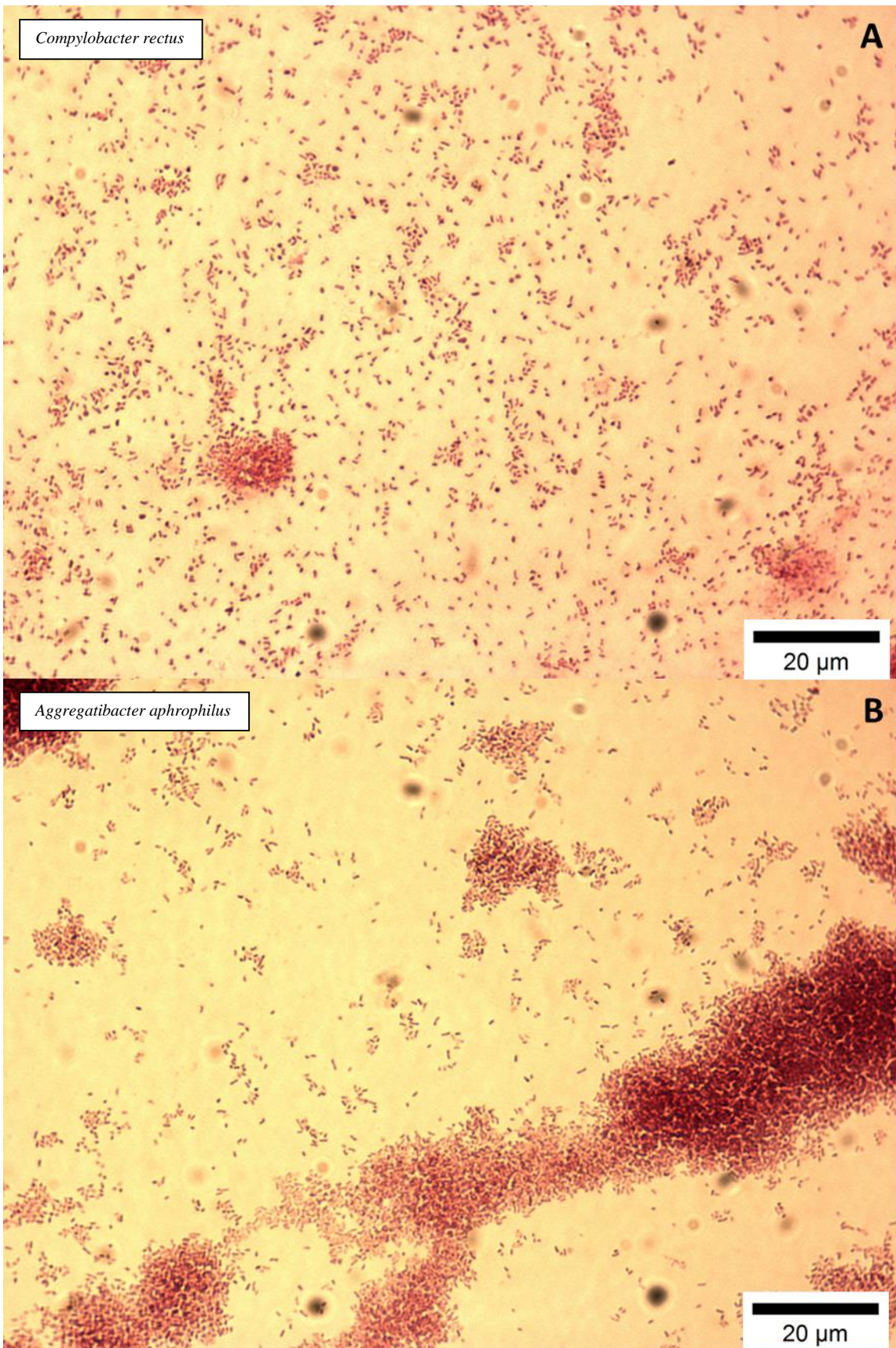
- 1. Isolation of new clinical strains of periodontal pathogen *A. actinomycetemcomitans*.**
- 2. Cataloguing of phages from the oral cavity of patients attending periodontal department in UK and IRAQ by TEM.**
- 3. Cataloguing of phages from Sheffield wastewater by TEM.**
- 4. Attempted isolation of phage against isolated strains, a range of endodontic *E. faecalis* strains and other periodontal associated clinical strains.**
- 5. Characterisation of *E. faecalis* phages in both biofilm model and animal model.**

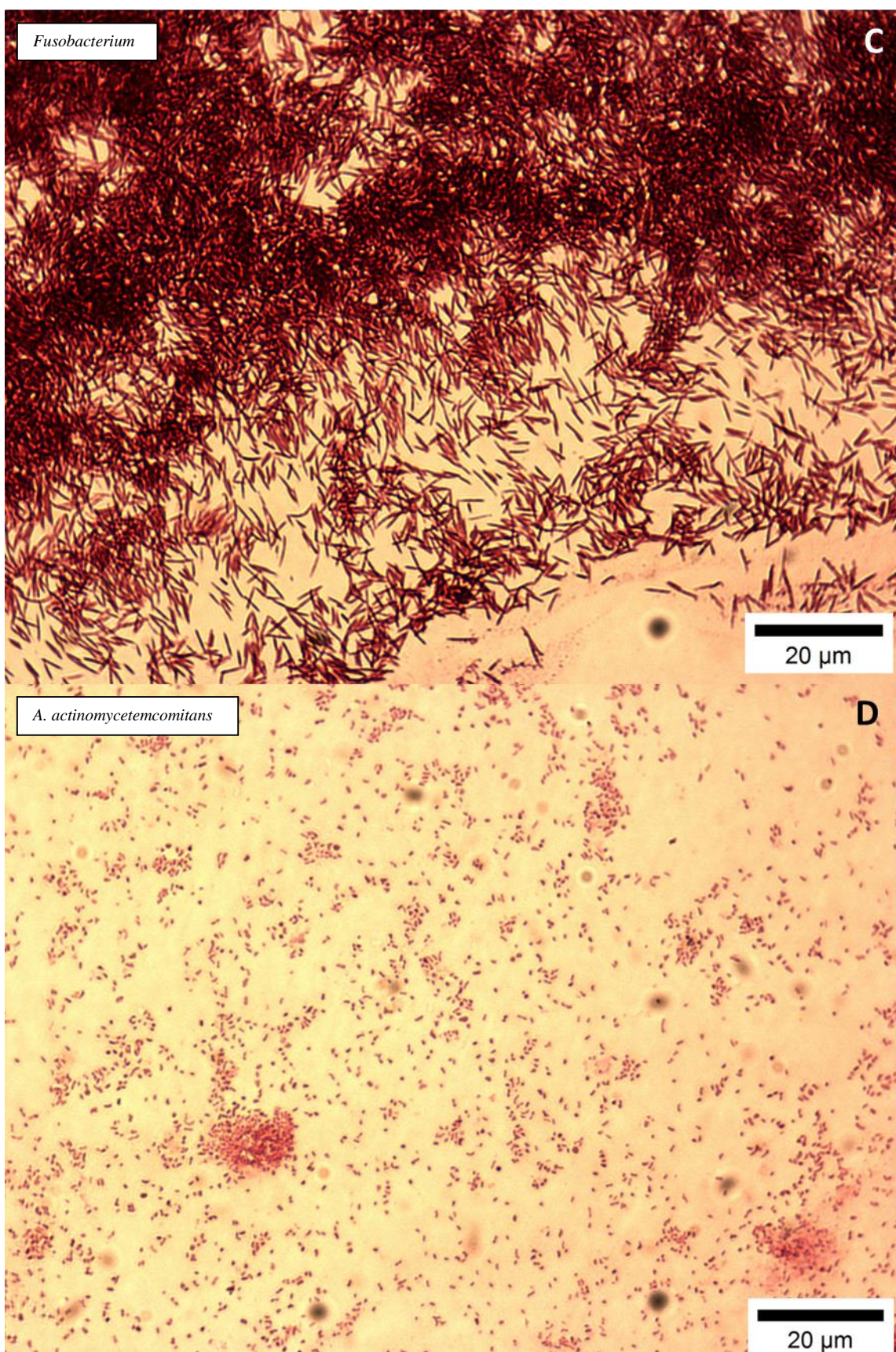
4.2 Isolation of clinical strains of *Aggregatibacter actinomycetemcomitans*

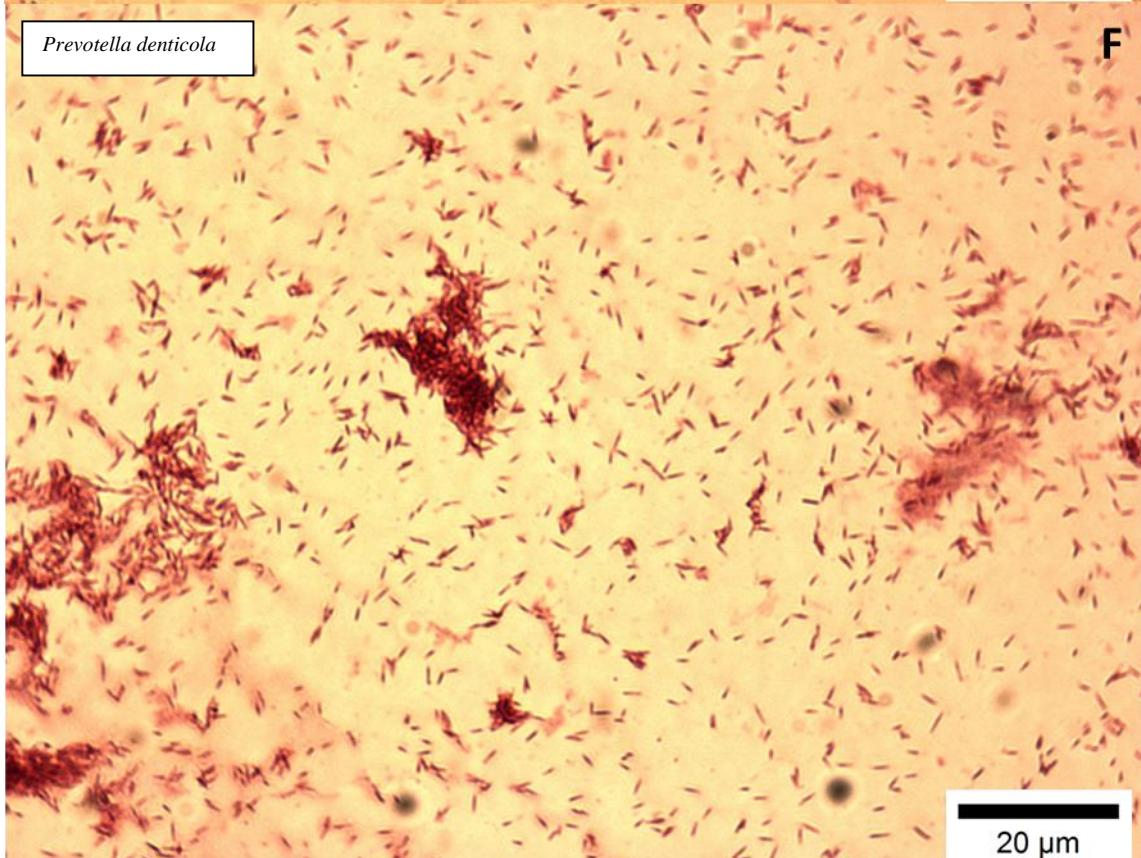
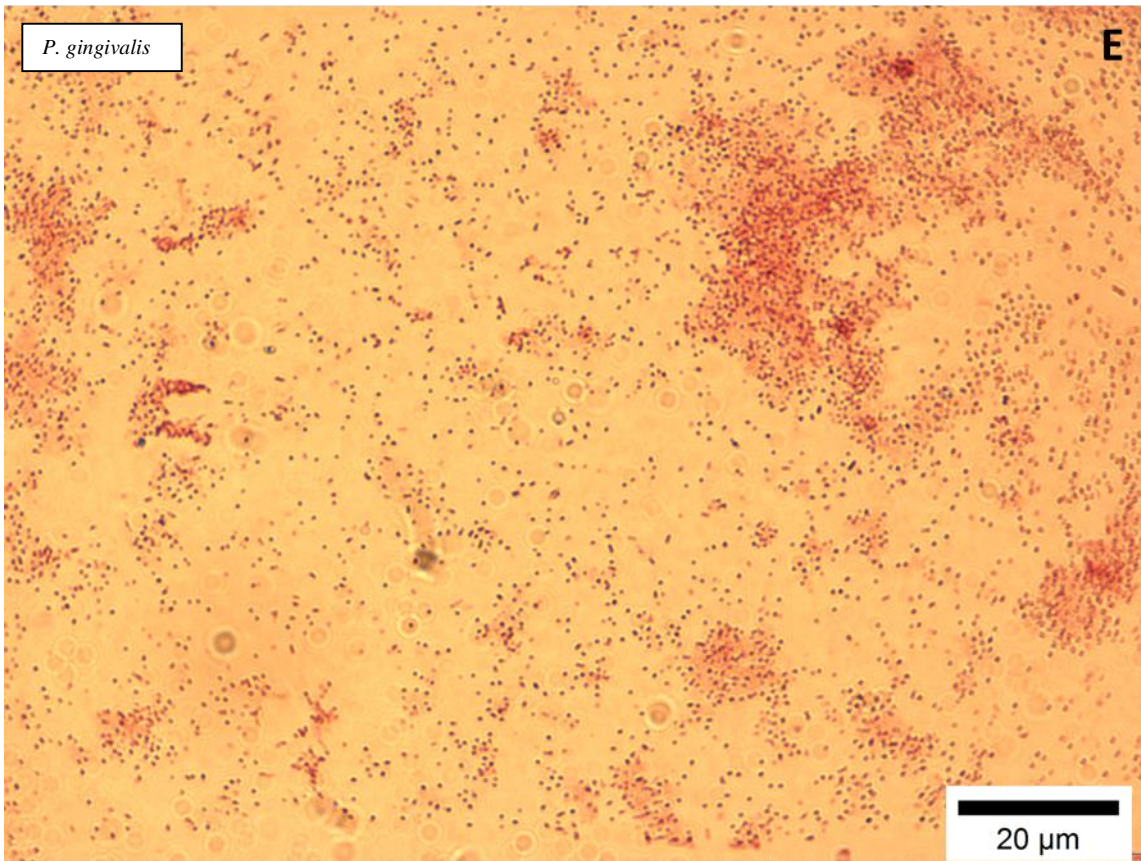
In order to gain novel and fresh (non-lab adapted) strains of periodontal pathogens, and in this case specifically the causative agent of localized aggressive periodontitis (previously known as juvenile periodontal disease) (Fine *et al.*, 2007), a disease strongly associated with this organism, an attempt was made to isolate *Aggregatibacter actinomycetemcomitans* (previously known as *Actinobacillus actinomycetemcomitans*) strains from deep pockets of patients attending the Periodontology Clinic at the Charles Clifford Dental Hospital, Sheffield, UK using TSBV (tryptic soy-serum-bacitracin-vancomycin) selective media according to the methodology used by (Slots, 1982).

In the case of other colony types, the best growing strains with differing morphologies were picked for subsequent plating out of colonies onto fresh agar to single colony for 3-4 passages, samples of the strains were frozen in BHI/glycerol (80%-20%) and stored at - 80°C. Once colonies were isolated, DNA was extracted and the Universal 16S ribosomal rRNA primers 27F and 519R that used to amplify the 16S ribosomal gene which is commonly used for molecular typing of bacterial spp before sequencing and comparisom to the NCBI GenBank database using BLASTN search (Goodfellow and Stackebrandt, 1991).

Using this method, a range of clinical isolates were obtained namely three strains of *Campylobacter rectus*, two *Aggregatibacter aphrophilus*, and two *Fusobacterium spp.* (Gram stains are illustrated in Figure 4.1A-D) while the star shape colony of *A. actinomycetemcomitans* (four strains) were differentiated from the other colonies such as the cotton-wool appearance of *Fusobacterium* as can be seen in Figure 4.1G-J. In addition, other clinical strains used as indicator strains for bacteriophage isolation were also Gram stained to assure their purity (Figure 4.1E-F). Some of these clinical strains namely *Porphyromonas*, *Prevotella* and *Fusobacterium* (Table 2.1) were isolated by PhD student Sarhang Gul from the same source of plaque samples, as indicated. All of these strains were used in subsequent studies in attempts to isolate phage against these strains.







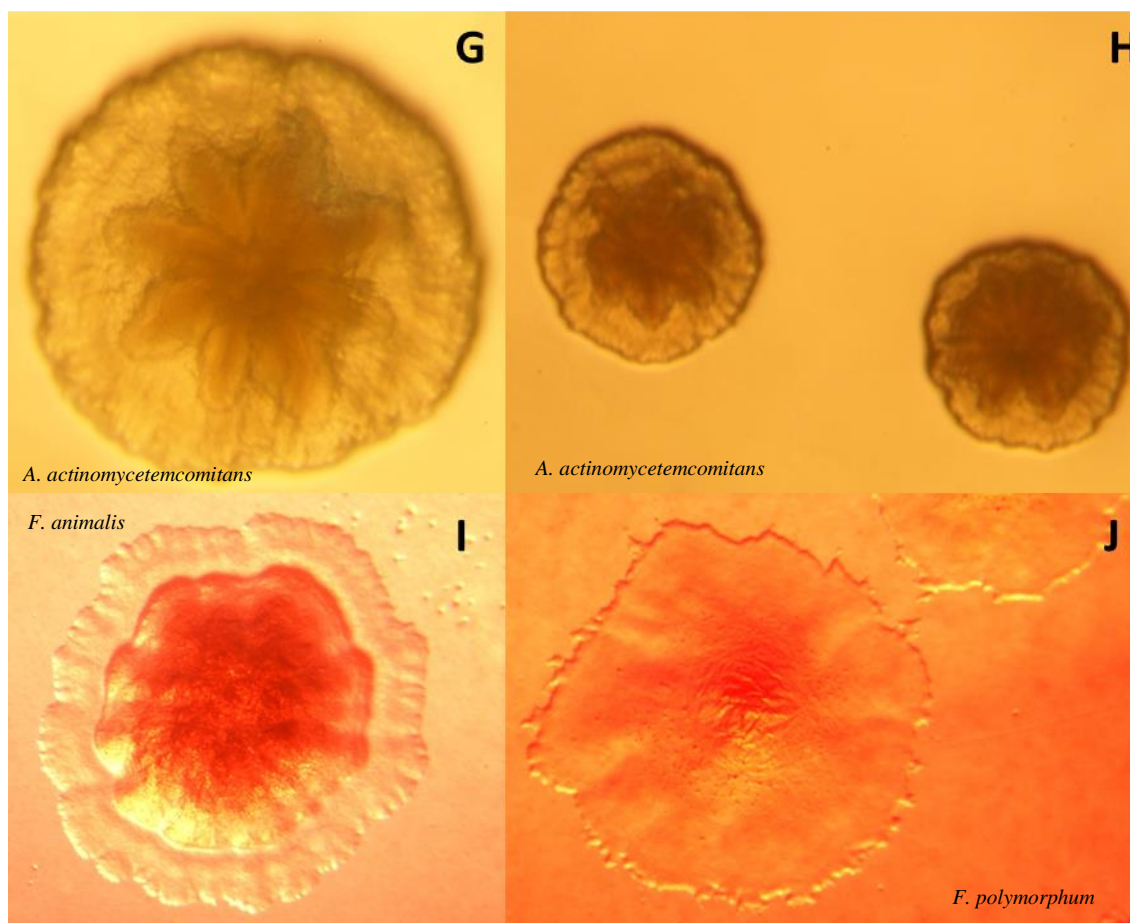


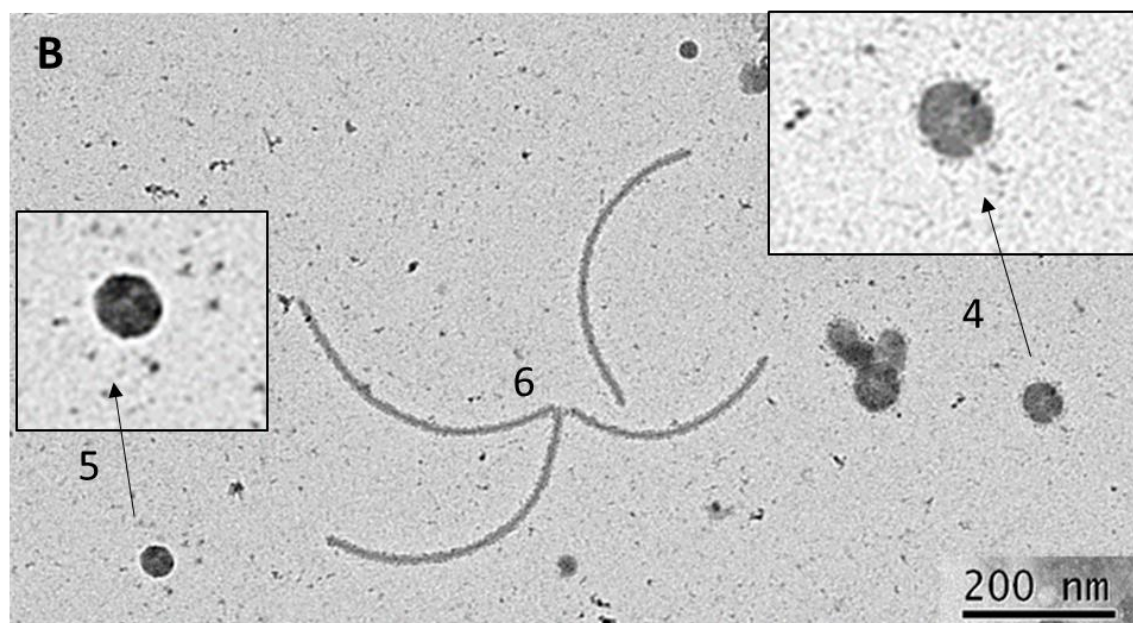
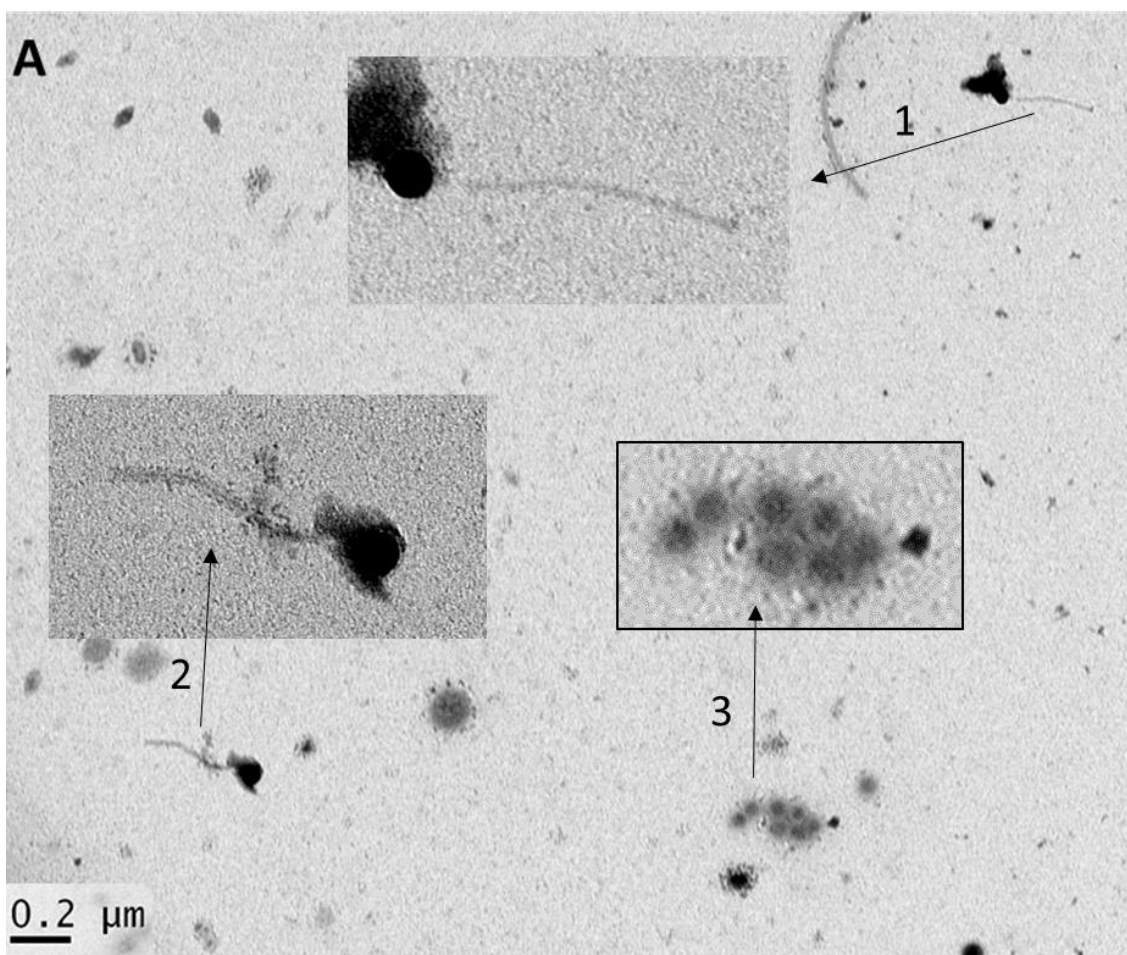
Figure 4.1 Gram stain and colony morphology of some oral clinical isolates. Oral clinical strains were isolated from the plaque samples of patients attending the Periodontology Clinic at the Charles Clifford Dental Hospital, Sheffield, UK. Gram stain of A) *Compylobacter rectus*, B) *Aggregatibacter aphrophilus*, C) *Fusobacterium*, D) *A. actinomycetemcomitans*. E) *P. gingivalis* Shef21 and F) *Prevotella denticola* Shef22. G) and H) The star shape colonies morphology of *A. actinomycetemcomitans* as seen in stereomicroscope, colony morphology of I) Shef2 and J) *F. polymorphum* Shef3.

4.3 Investigation of morphological diversity of bacteriophage within oral samples by direct electron microscopy

Given that limited evidence exists of intact bacteriophage particles in the oral cavity we first set out to examine whether phage could be visualised from saliva and eluted from plaque of both healthy volunteers and from periodontal clinic patients. In order to achieve this, ethical approval was obtained (STH 19056, appendix 1 and 2) to

facilitate the collection of whole mouth sub and supra gingival plaque samples as well as saliva of patients suffering from chronic periodontitis. In addition, another ethical approval was obtained from College of Dentistry, Al-Mustansiriya University; Baghdad, Iraq (my sponsorship university) to collect whole mouth plaque samples from patients attending the periodontology clinics (Appendix 4). Plaque samples from 21 Sheffield patients (mixed in one tube) and 50 from Iraqi patients (mixed in one tube), were processed and concentrated as described in section (2.2.2 and 2.2.5), 2 grids from each concentrated Iraqi and Sheffield samples were screened under TEM. For salivary samples 5 mM of DTT was added in each tube so as to cleave sulphide bond present in mucus of saliva to recover possible phage particles and to reduce viscosity. The supernatant was filtered through a 0.45 μm syringe filter. Finally, in order to recover the phage particles from suspensions, samples were then centrifuged 35,000 $\times g$ for 90 min to pellets the phage particles. The pellets that harbour the possible phage particles were then carefully suspended overnight in 4°C with 2 ml of SM buffer (so as not to cause phage damage by immediate and heavy resuspension).

These samples were then stained as described in (section 2.4.7) using 2% (wt/vol) uranyl acetate pH4 on carbon-coated copper grids as can be seen Figure 4.2 A-E. The electron micrographs show the presence of several phage particles scattered within the processed plaque of both Sheffield and Iraqi samples. Most of the identified phages have apparent non-contractile tails, which putatively belong to the family Siphoviridae as illustrated in Figure 4.2 (1, 2, 9, 10, 11, 12, 13). However, phage particles with short tails are also identified that mostly belong to the family Podoviridae as seen in Figure 4.2 (4, 5). Both family are within the order *Caudovirales* based upon tail morphology that have a third family of contractile tail named *Myoviridae*. Cubic phage particles (Figure 4.2 7, 8) with no obvious tail could also be identified that either lost its tail during processing or belong to the family *Tectiviridae*. In addition, filamentous (6) and enveloped like phages (3) could also be identified. In summary, many phage like particles had been visualised which reflect the richness and diversity of bacteriophage that is harboured in the dental plaque samples obtained from patients having chronic periodontitis.



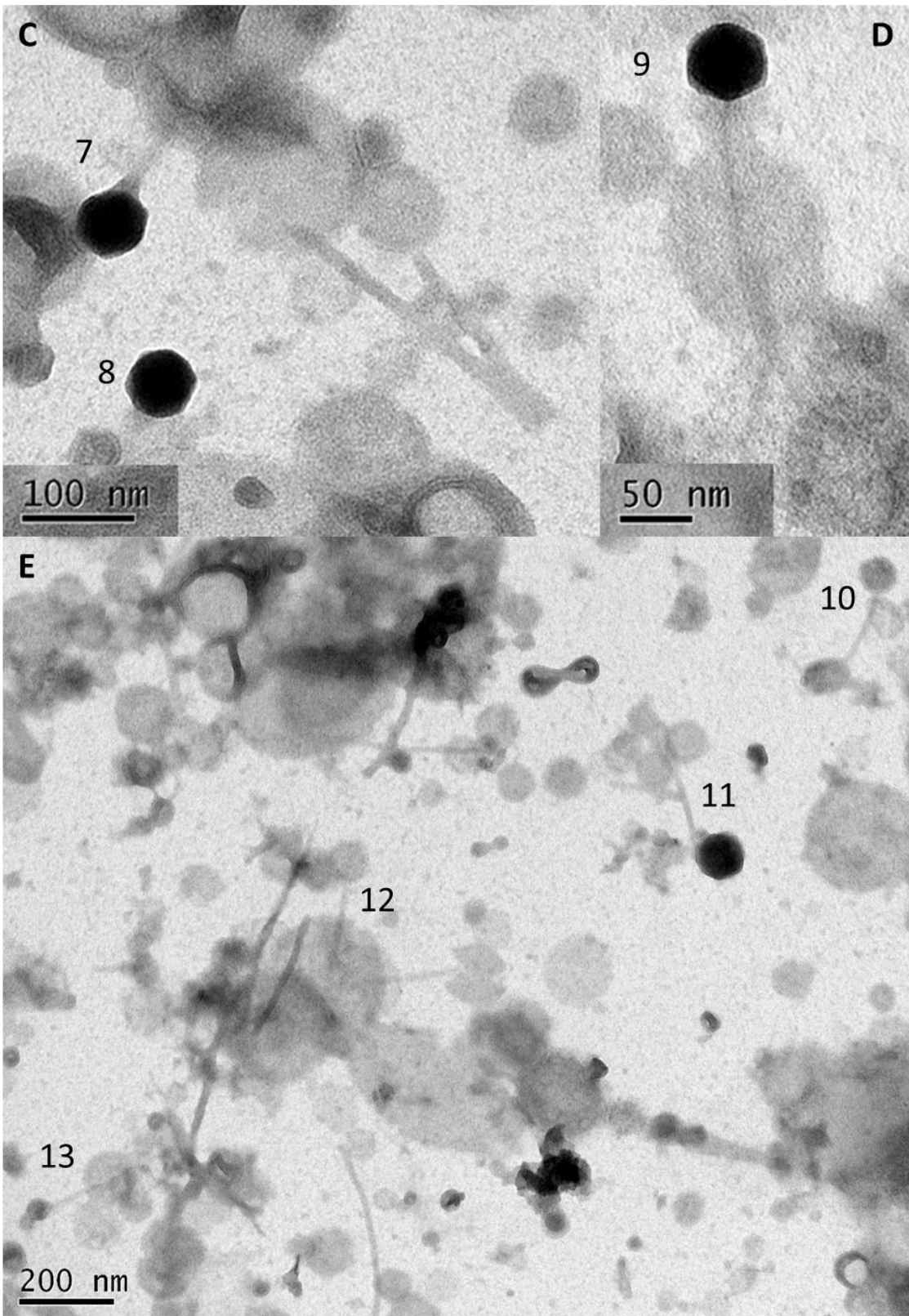


Figure 4.2 Electron micrographs of bacteriophages in plaque samples from Sheffield samples (A and B) and Iraqi plaque samples (C, D, E). Possible phage particles of non-contractile tails that belong to the family Siphoviridae (1, 2, 9, 10, 11, 12, 13). Bacteriophage like particles with short tail that mostly belong to the family Podoviridae (4, 5). Both families are with order Caudovirales that possess a third additional family of

long contractile tail named Myoviridae. Cubic phages particle with no obvious tail (7, 8), possible filamentous (6) and enveloped phages (3). Note that some phage particles pictures were enlarged for better illustration.

4.4 Phages observed in Sheffield wastewater

A third possible main source of bacteriophage was also included in order to increase the chances for bacteriophage isolation especially towards *E. faecalis* oral strains, as wastewater was reported to be rich in *Enterococcus* species (Bahirathan *et al.*, 1998, Graves and Weaver, 2010) that provide rich host source for bacteriophage infection and multiplications. The Sheffield wastewater collected by PhD student Afifah Abd Rahim (Pennine Water Group) was also scanned for bacteriophage and compared to those in oral samples. 8 liters of wastewater in total were filtered, processed and concentrated before samples were screened under TEM.

The identified phages were a mixture of morphologically different particles. At least 24 morphologically different phages could be identified in one carbon grid that the concentrated sample of wastewater adsorbed to and examined under the TEM. The sample showed traces of phages mainly with isometric heads, long or short contractile and noncontractile tails. All three families of Siphoviridae (Figure 4.3 and 4.4), Myoviridae (Figure 4.5) and Podoviridae (Figure 4.6 A and B) could be identified. In addition, cubic phages could also be identified (Figure 4.6 C).

The isometric phages of Siphoviridae family identified mostly had icosahedral heads shape as shown in Figure 4.3 with variable tail length (used mainly to differentiate between them). However, Siphoviridae with isometric elongated heads, variable tail length (Figure 4.4 A, B and D) and irregular head (Figure 4.4 C) were also been identified. In total, at least 10 different phages in Siphoviridae family could be recognized based upon morphology.

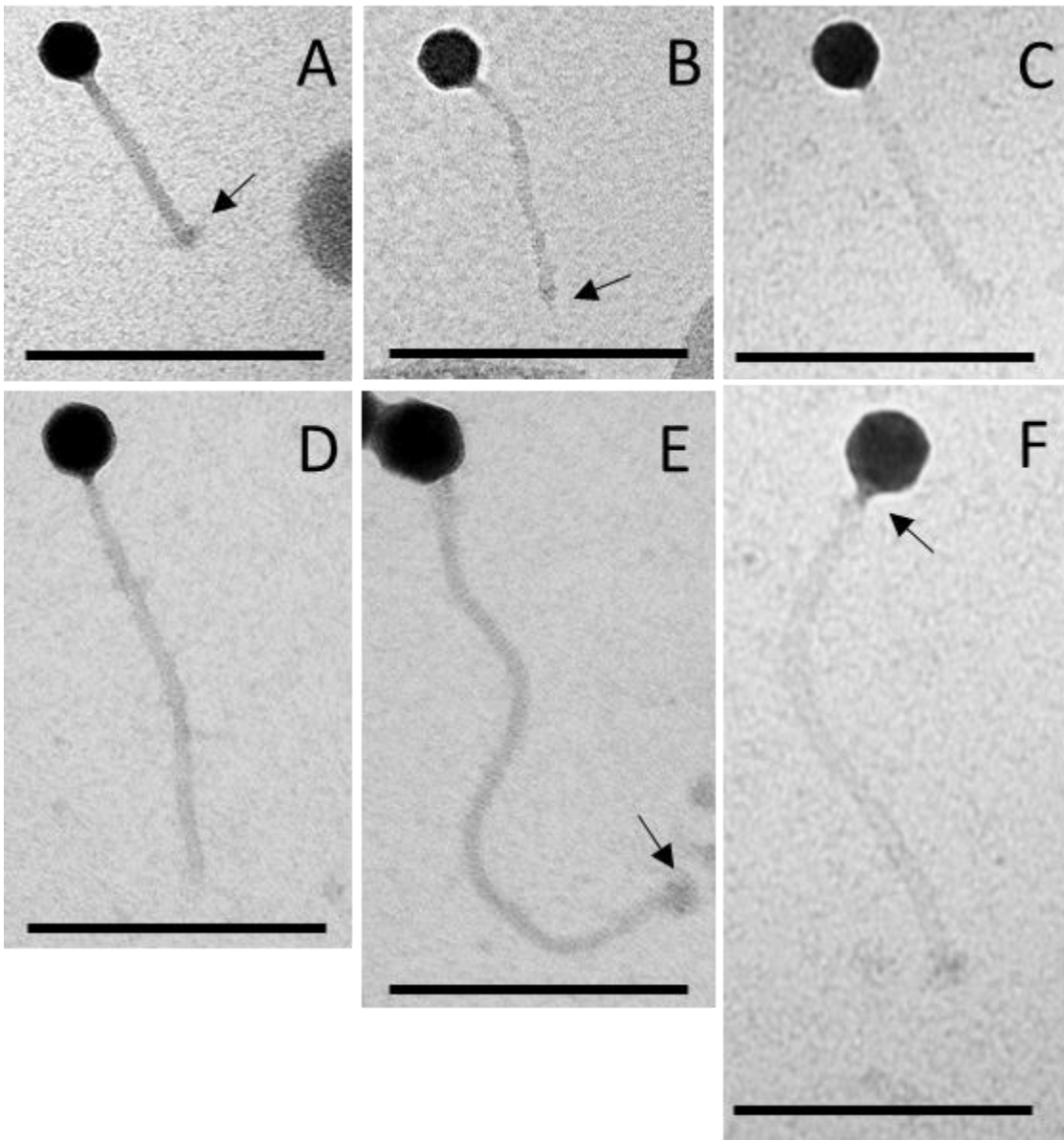


Figure 4.3 Electron micrographs of bacteriophage from wastewater that belong to the family *Siphoviridae*. Each phage particle is composed of icosahedral head and non-contractile flexible long tail. (Bar 200nm). Arrows indicate, base plate (A and E), tail spike (B), visible neck (F).

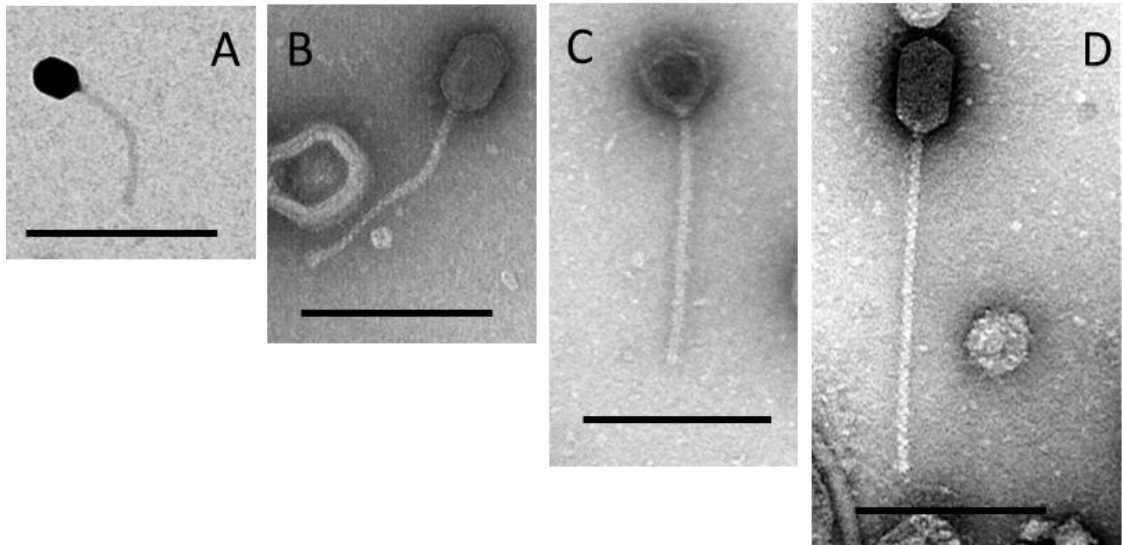


Figure 4.4 Electron micrographs of bacteriophage from wastewater that belong to the family Siphoviridae; show elongated and variable head morphology. (Bar 200nm).

The most variation in phages morphology were identified in wastewater belong to Myoviridae family, as they show more diversity in head shapes morphology (being mostly isometric) in addition to variable tail length and shapes as can be seen in Figure 4.5. Both uncontractile (Figure 4.5 A, D and H) and contractile (Figure 4.5 I) tail position were observed, in addition some phages showed variable tail sheath position within the central tail (Figure 4.5 J, K and L). Tail sheath usually surround the central non contractile tail and by contraction during infection will drive the phage tail tube through the outer membrane of the bacterial host, thus creating channel for the viral genome delivery as in T4 bacteriophage (Aksyuk *et al.*, 2009). In total, about 12 phage morphologies that belong to this family were observed.

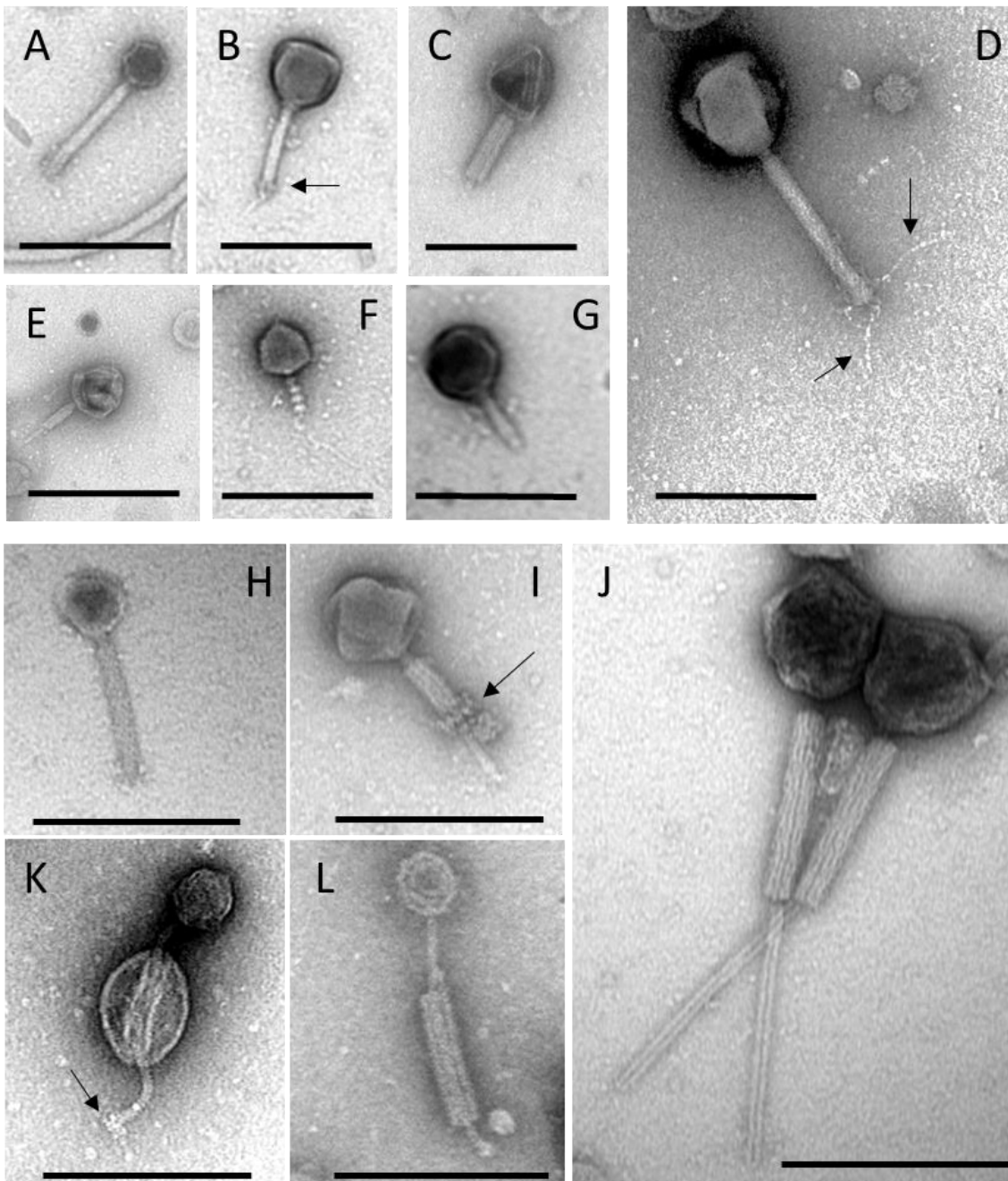


Figure 4.5 Electron micrographs of bacteriophage from wastewater that mostly belong to the family Myoviridae. Each phage particle is composed of head and contractile tail. Variable head morphology and double tail sheath are visible in most pictures. (Bar 200nm). Arrows indicate, base plate (B, I, K), tail fibres (D).

On another hand, two phages morphology that belong to the third family of Podoviridae were observed in the sample of wastewater which reflect the low diversity of this family (Figure 4.6 A and B). Finally, possible cubic phages were also recorded as can be seen in Figure 4.6 C.

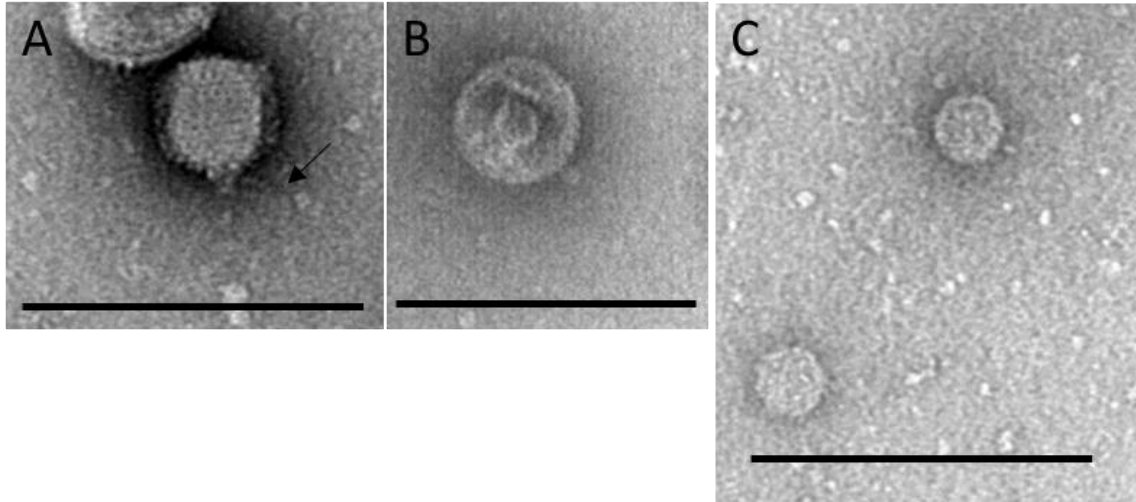


Figure 4.6 Electron micrographs of bacteriophage from wastewater that mostly belong to the family Podoviridae (A and B), cubic like phage (C). (A) Head fibre is visible (arrow). (Bar 200nm).

The electron micrographs revealed some fine structure of nearly all phages. Base plates could be observed as seen in Figure 4.3 A, E and Figure 4.5 B, I, K. Tail spike (Figure 4.3 B). A visible neck that join the head and tail (Figure 4.3 F). Tail fibres (Figure 4.5 D and Figure 4.6 A).

An interesting observation about phage behaviour could also be recorded represented by adsorption of a group of several similar morphology phages together at the head region as illustrated in Figure 4.7 A and B. While Figure 4.7 C and D show the adsorption of phage to a wastewater debris at the tail end, which reflect that phages always explore the media for a possible host through its tail.

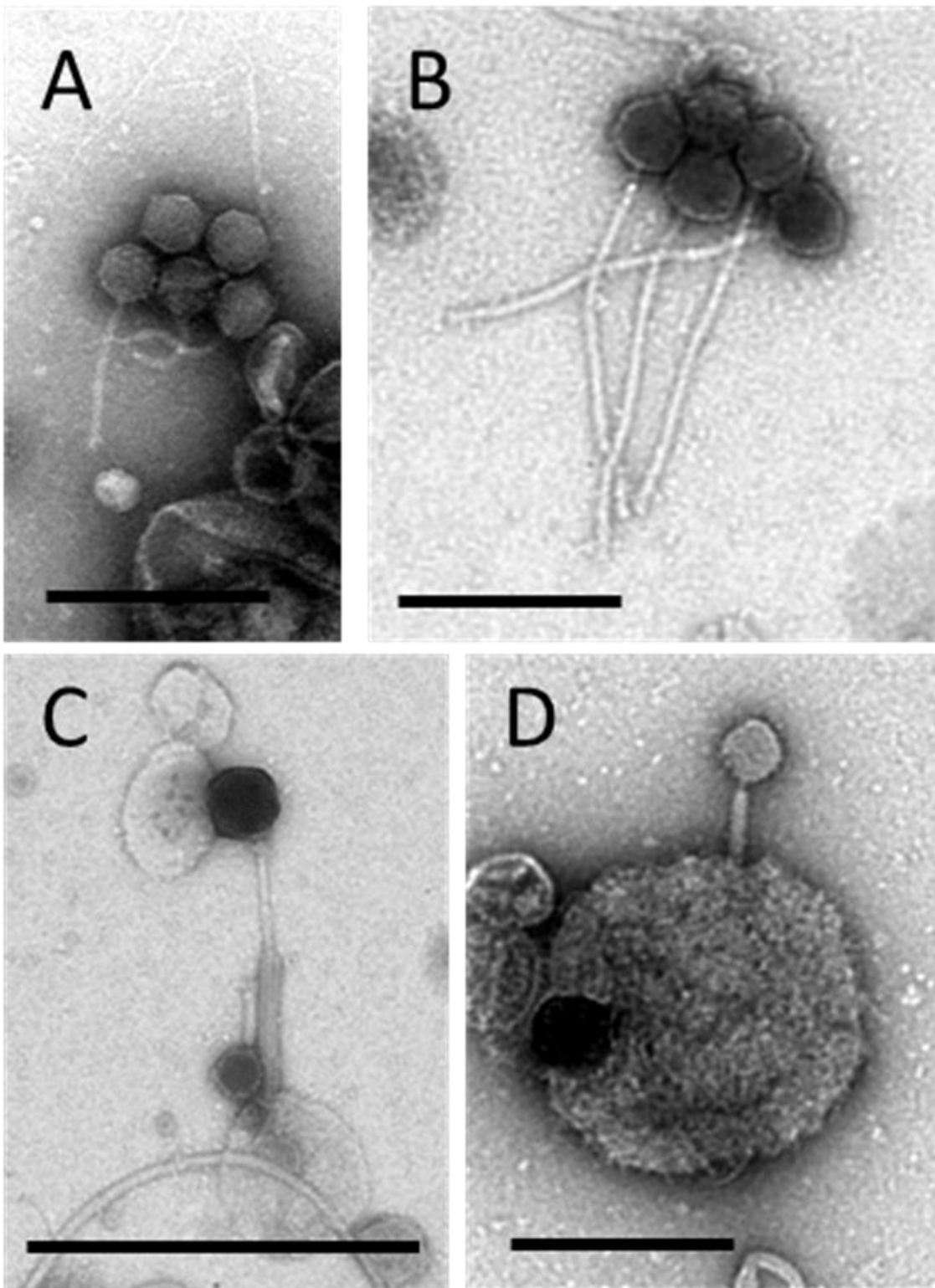


Figure 4.7 Electron micrographs of bacteriophages from wastewater. (A and B) Group of similar morphology phages attached to each other at the head region. (C and D) phage particle attached to debris at the tail end. (Bar 200nm).

4.5 Isolation of virulent bacteriophage

4.5.1 Isolation of bacteriophage targeted towards periodontal associated pathogens

Several attempts were conducted to isolate bacteriophage targeting pathogens associated with periodontal disease and periodontal pathogens (Table 2.1) using concentrated samples from Sheffield wastewater, Sheffield and Baghdad plaque, saliva and dental chair drains. However, no visible plaques that indicate successful isolation were obtained after enrichment and/or direct spotting on double layer agar.

4.5.2 Isolation of bacteriophage targeted towards endodontic associated pathogens

Despite the failure to isolate phage against periodontal associated pathogens, we then tested our samples against a range of clinical *E. faecalis* strains that had been used as target for bacteriophage isolation. They were isolates from oral origin, either directly from endodontic infections or mouthwash of patient receiving endodontic treatment, and from oral lesions which we sourced from a range of oral microbiology labs in Europe. We wish to thank Professor Wim Crierlaard (ACTA, University of Amsterdam, NL) and Professor Gunnar Dahlen (Department of Oral Microbiology and Immunology, Institute of Odontology, Sahlgrenska Academy, University of Gothenburg, Sweden) for donating the *Enterococcus* clinical and lab strains (Table 2.5). Again, no successful phage isolation was obtained from the concentrated plaque samples, chair drain and saliva (used as possible phage sources). Despite that, using Sheffield wastewater showed successful phage isolation results. It was collected by University of Sheffield Pennine Water Group (by PhD student Afifah Abd Rahim) and we processed it as described in Materials and methods (section 2.2.4 and 2.2.5). The wastewater was collected from a treatment plant in Sheffield area, UK. The plant treats both industrial and domestic wastewater with the capacity of 185,000 P.E. (population equivalent). The wastewater had been through sieving to remove any large solids but not treated chemically or biologically.

Phage plaques were first identified by spotting the suspended solution (Figure 4.8A) on top agar lawns of a range of orally isolated clinical strains of *E. faecalis* (Table 2.5). 10 µl of processed sample were spotted on lawn of *E. faecalis* (for example OS16), the spotted samples either produce several small spots of clearance or one large clearance, and other samples do not produce any clearance. One plaque was picked and mixed with the same host in double layer plaque assay, an immature plaques were start to be visible after 3 h of incubation and mature plaques were visible after 24 h (Figure 4.8B and C).

This process was repeated 3 times to ensure purity. Finally, single, well-isolated plaques were excised and suspended in SM buffer and stored in 4°C for further testing. Via this method phages against several *E. faecalis* strains were obtained successfully followed by identification and characterisation.

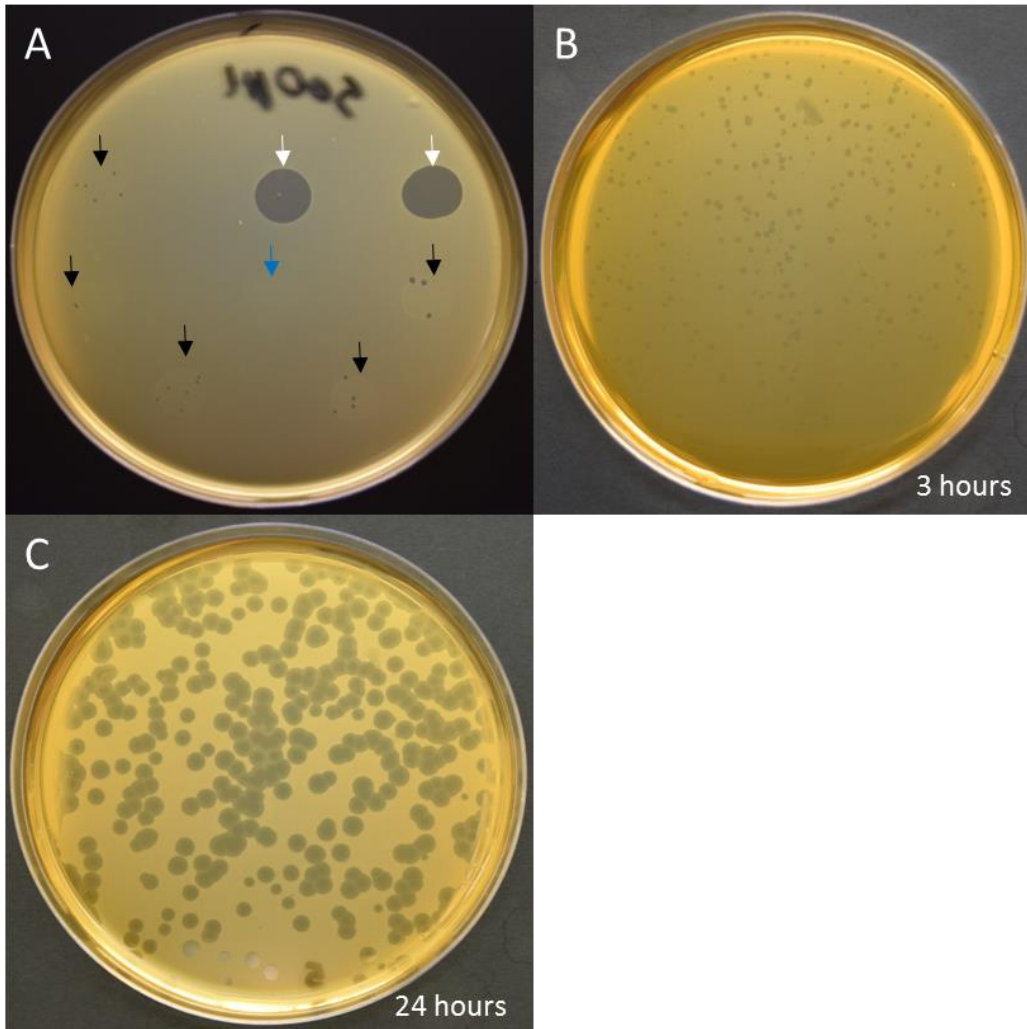


Figure 4.8 Phage isolation procedure. A) 5-10 μ l of processed sample were spotted on lawn of *E. faecalis* bacteria (OS16), some produce several small spots of clearance (black arrows), one large clearance (white arrows), and no clearance (blue arrow). One plaque was picked and mixed with the same host in double layer plaque assay, B) Immature plaques were start to be visible after 3 h of incubation, C) Mature plaques were visible after 24 h.

4.5.2.1 Bacteriophage isolation, plaque morphology and EM morphology analysis

As outlined in Figure 4.9, a total of five distinct bacteriophage named phiSHEF 2, 4, 5, 6, and 7 were obtained that infect various *E. faecalis* strains. phiSHEF2 was isolated using strain OS16, while phiSHEF 4 was isolated using the EF3, strain EF2 was used to isolate phiSHEF 5 (all are oral clinical strains isolated from oral rinse of endodontic patient), while phiSHEF 6 and 7 were isolated using the oral lesion derived clinical strain OMGS3919. Another phage named phiSHEF 3 was also isolated. However, it possesses many similarities to phiSHEF 2 with exceptions that will be discussed later in this chapter.

Three distinct plaque morphologies were identified when infecting *E. faecalis* strains with the isolated phages. Firstly, a plaque with 3-4 mm diameter surrounded by a thin rim of secondary lysis of 1mm (phiSHEF 2, 5, 6 and 7), 2 mm diameter central plaque surrounded by haloes of larger secondary lysis (phiSHEF 4), while the third morphology observed had a small pin hole sized plaques of 1 mm diameter without distinct secondary lysis (phiSHEF 7+OG1RF). It has been observed both here and in the literature that the shape and plaque morphology are both phage and indicator strain dependant. The same phage was shown to produce two different plaque morphologies when the host strain was changed, for example phiSHEF 7 produced a plaque diameter of 3-4 mm with OMGS3919 host strain, while a pin hole plaque was formed if OG1RF strain used as host strain as shown in Figure 4.9 (phiSHEF 7 and phiSHEF 7+OG1RF).

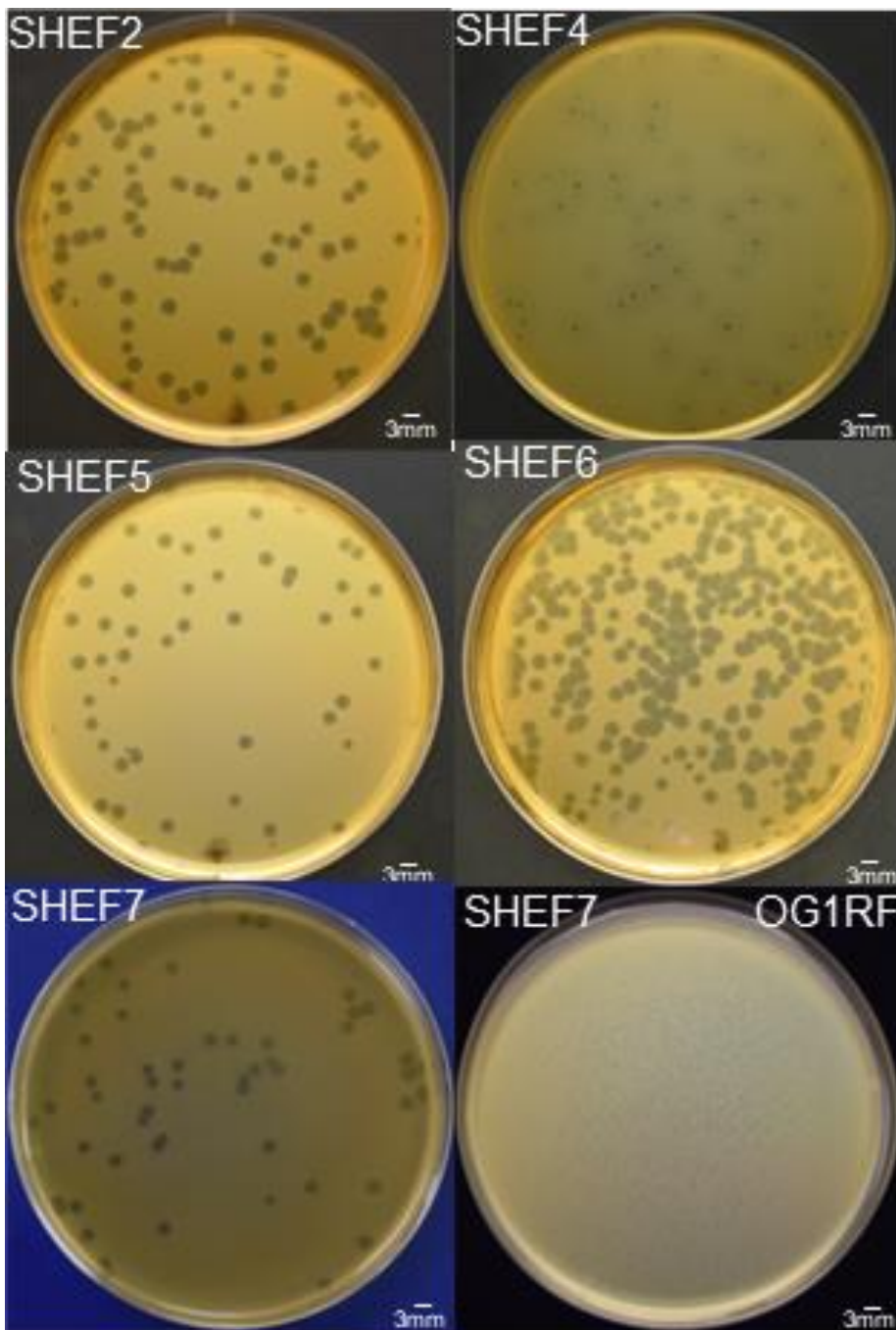


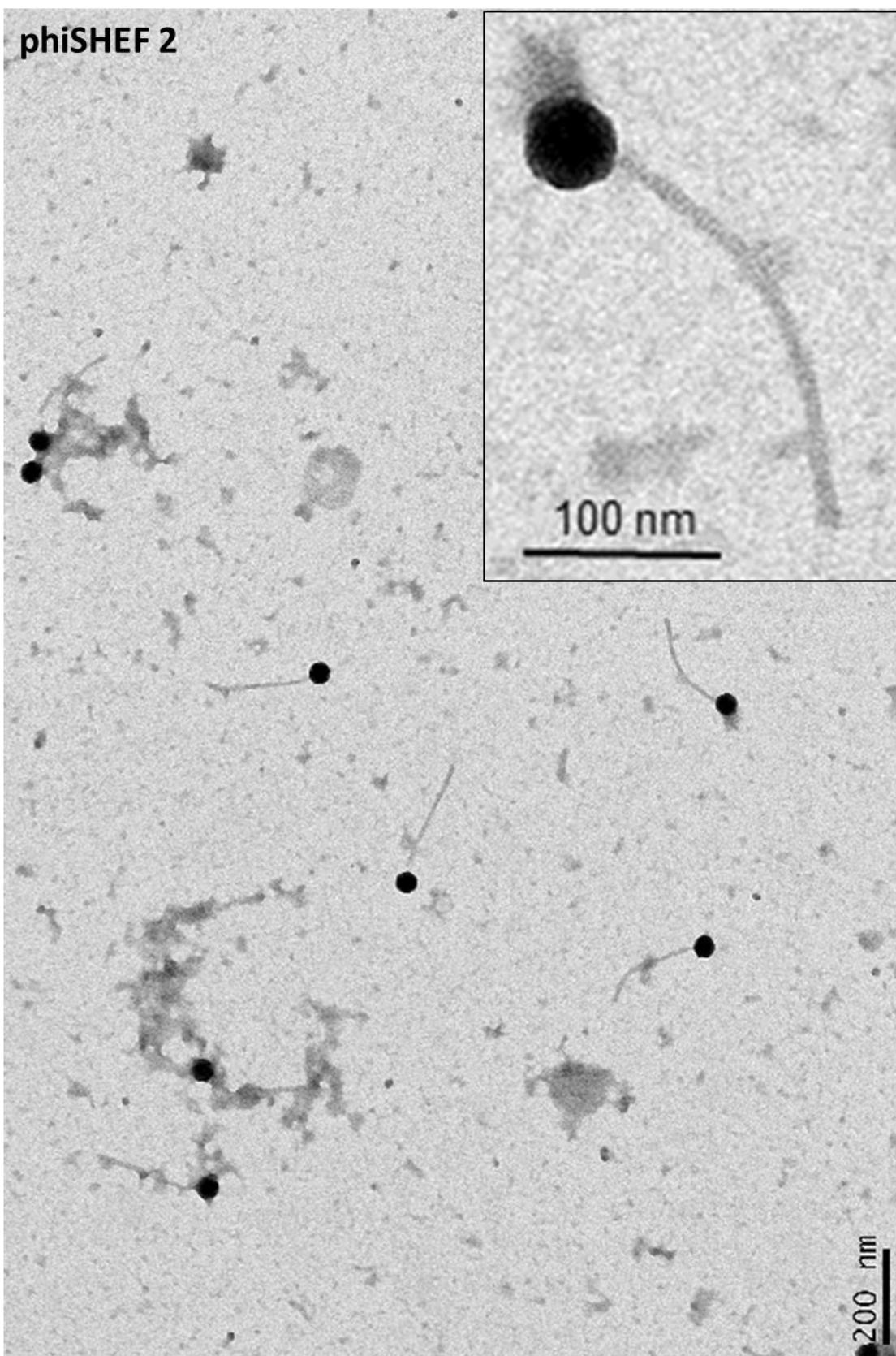
Figure 4.9 Isolation of *E. faecalis* bacteriophages and plaque morphology. PhiSHEF 2 was isolated using strain OS16, while phiSHEF 4 was isolated using the EF3, strain EF2 was used to isolate phiSHEF 5 (all are oral clinical strains isolated from oral rinse of endodontic patient), while phiSHEF 6 and 7 were isolated using the oral lesion derived clinical strain OMGS3919. Three distinct different plaque morphology were observed on DL agar. PhiSHEF 2, 5, 6 and 7 produce plaques of 3-4 mm diameter surrounded by thin rime of secondary lysis. PhiSHEF 4 produce 2 mm diameter of central plaque surrounded by large haloes of lysis. PhiSHEF 7 phage on the host OG1RF produce pin hole sized plaques of 1 mm diameter.

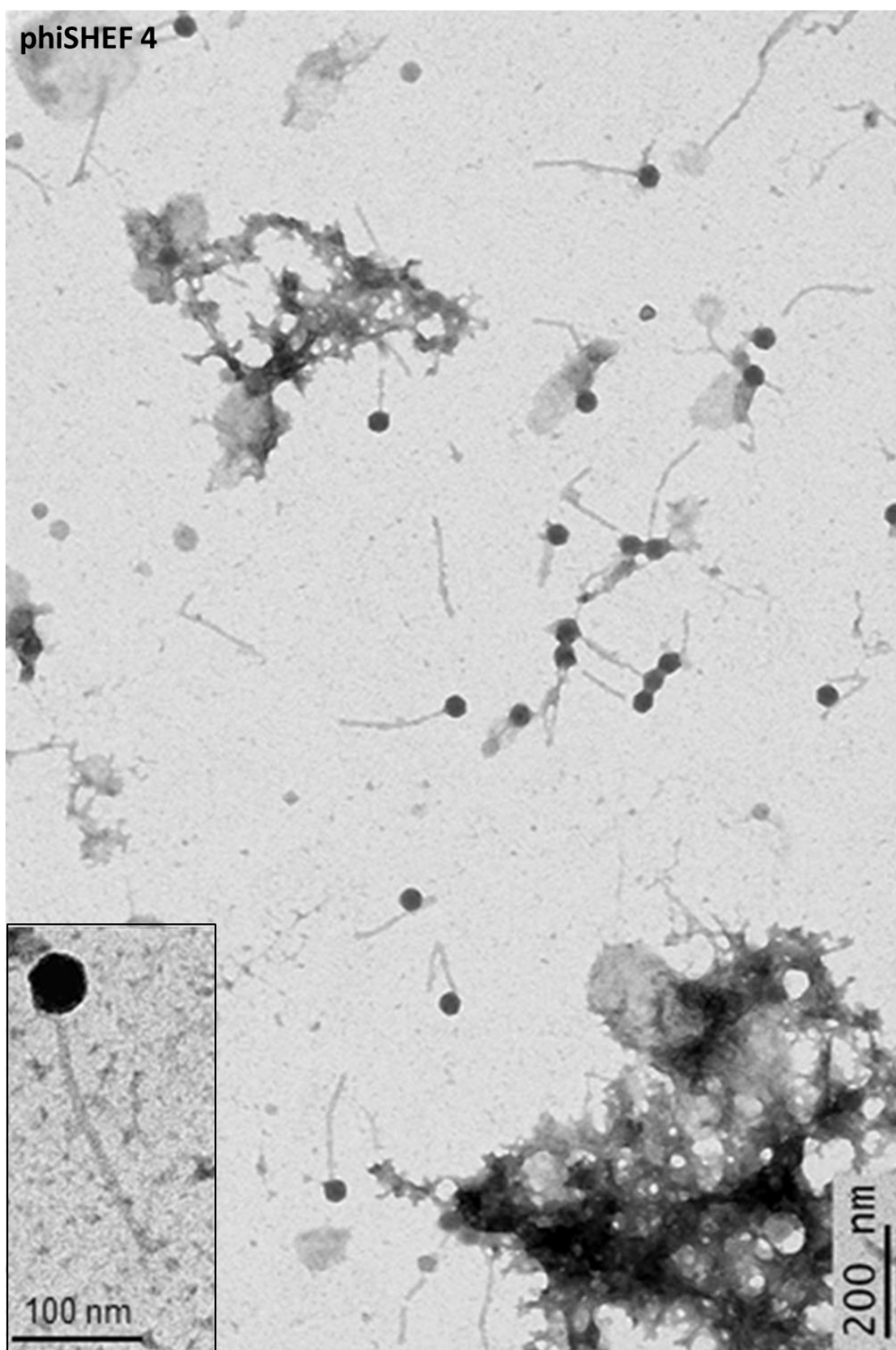
As seen in Figure 4.10, transmission electron microscopy analysis revealed that all phiSHEF bacteriophages had an isometric head and an apparently non-contractile long tail ranging in size from 200-250 nm depending on the phage in question (see Table 4.1). In general the isometric heads diameters ranged from approximately 41-46 nm in diameter. According to the guidelines of the International Committee on Taxonomy of Viruses (ICTV, 2005), phiSHEF bacteriophages apparently are classified as belonging to the family Siphoviridae (order Caudovirales) based upon tail morphology (Ackermann, 2007).

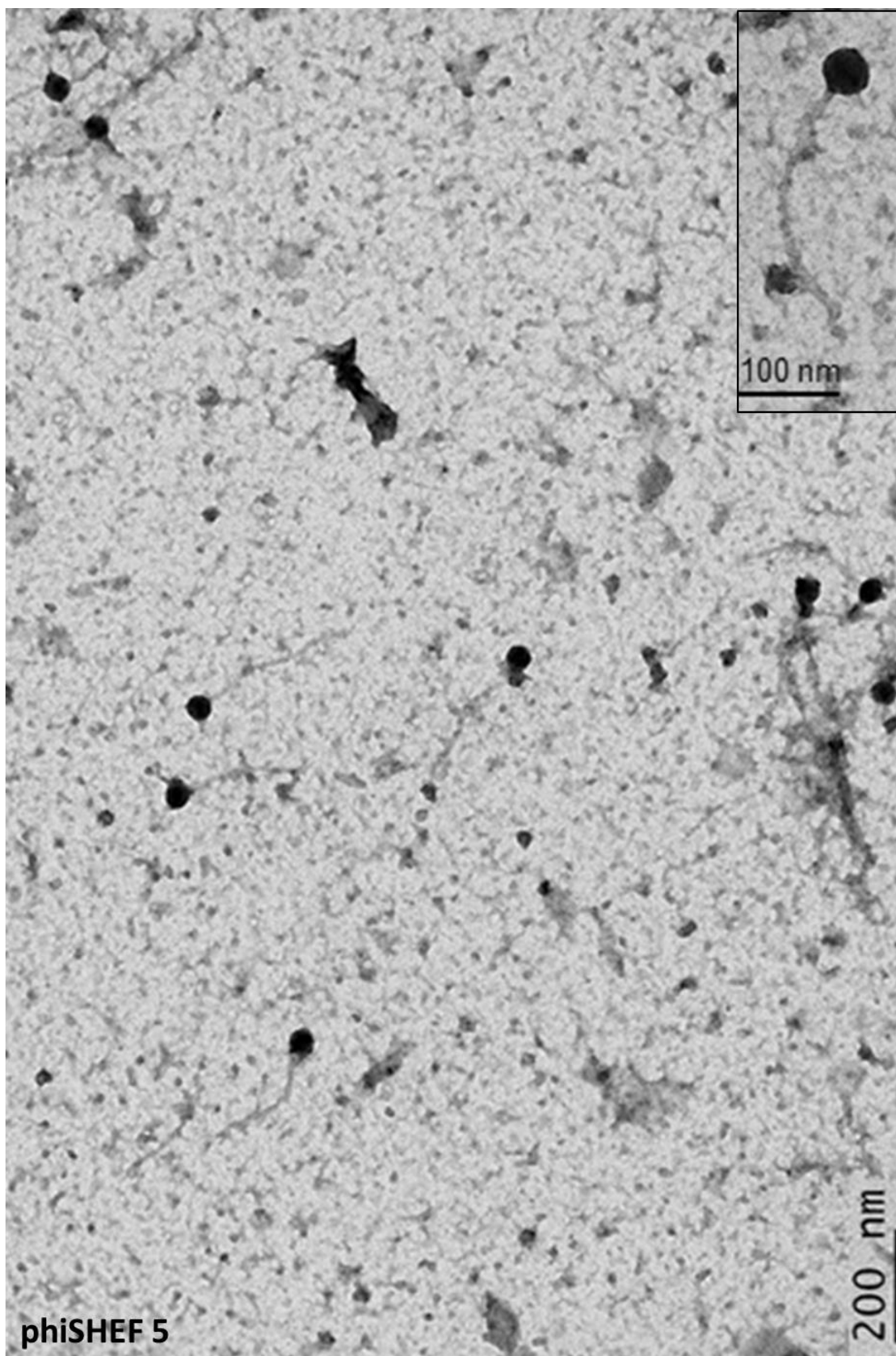
Table 4.1 The head and tail dimensions for the isolated *E. faecalis* phages.

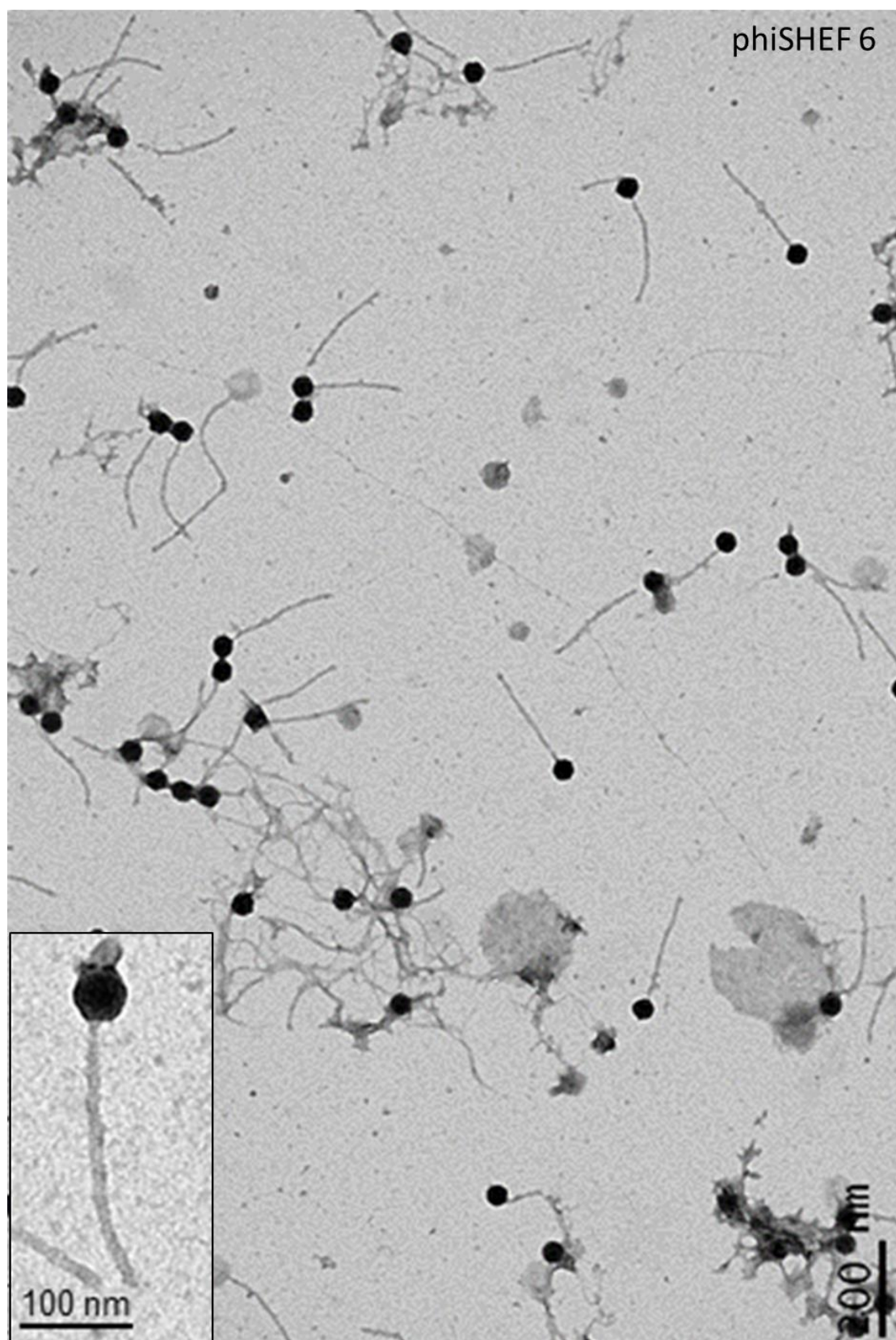
Phage	Mean Head diameter (nm)	SD \pm (nm)	Tail length	SD \pm (nm)
SHEF2*	42.34	1	231	1.3
SHEF4	45.60	1	199.4	0.8
SHEF5	44.32	0.9	240.5	1.5
SHEF6	45.81	0.4	250.6	3
SHEF7	41	0.1	230	2.4

*Three of the phage particles were measured for each phage type and the mean value was used for calculating the dimension.









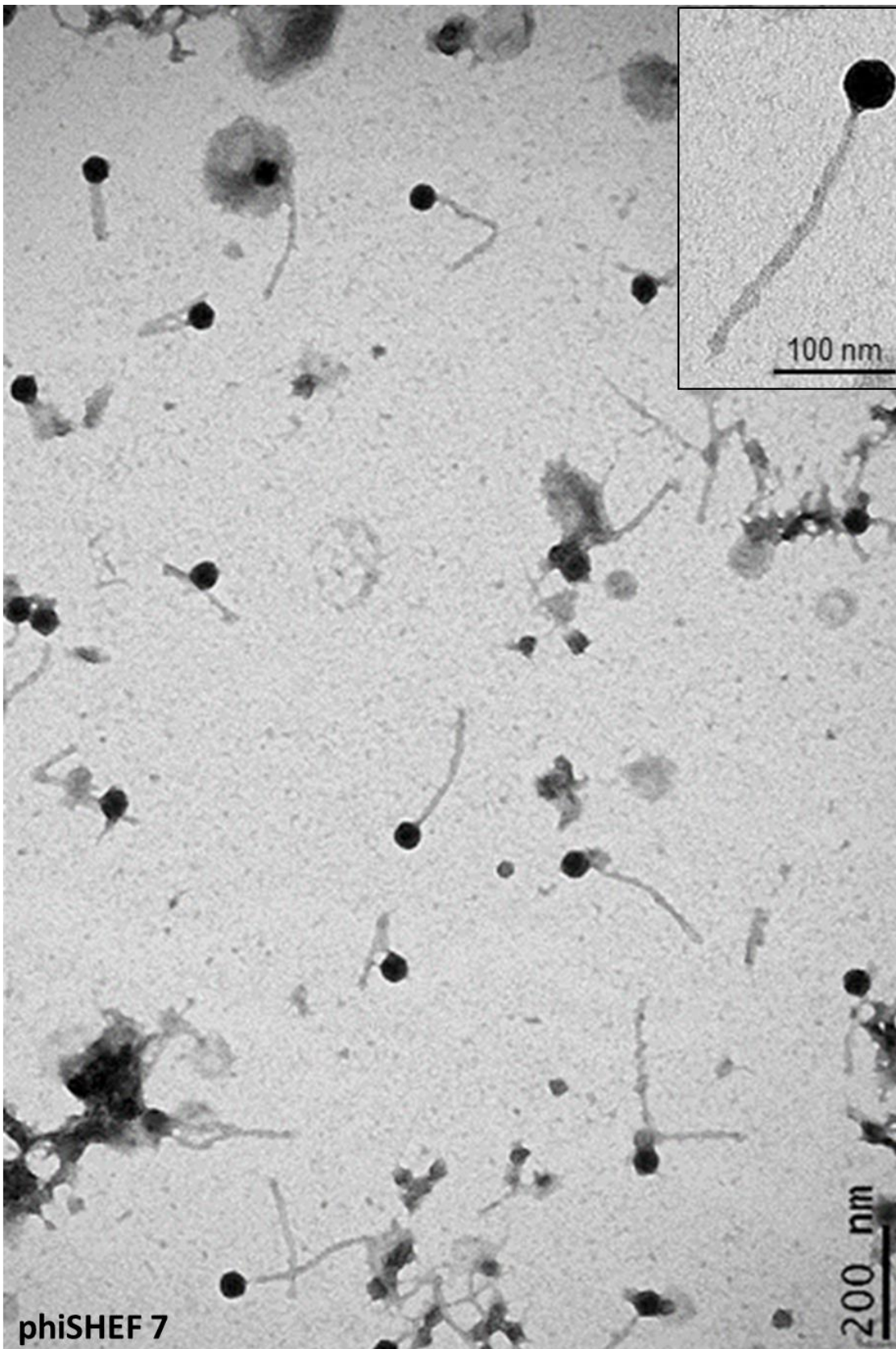


Figure 4.10 Transmission electron micrographs of SHEF phage particles. Phages were negatively stained with 0.2 % uranyl acetate. The image revealed that phage phiSHEF belongs to Siphoviridae family. They have an isometric head and long

segmented non-contractile tail. Three of the phage particles were measured for each phage type and the mean value was used for calculating the dimension. One phage particle from each phage was enlarged for better illustration.

4.5.2.2 Characterisation of isolated phages

To establish and confirm that these five phages were in fact distinct from each other restriction fragment length polymorphism (RFLP) analysis was performed. In order to extract phages chromosomal DNA, 200 ml of exponential growth phase indicator bacteria were infected with each phage at MOI of 0.01 for 3-4 h, the clear broth was subjected to Polyethylene Glycol (PEG 8000) precipitation (see section 2.4.6), followed by treatment with 10 µg/ml DNase and RNase in order to remove contaminating DNA, and further treatment with 100 µg/ml of proteinase K was performed to degrade the enzymes. Removal of proteins from phage nucleic acids were achieved by extraction with phenol: chloroform: isoamyl alcohol (25:24:1) (as described in section 2.4.11) and the final phage chromosomal DNA was dissolved with sterile milli-Q-water. In order to evaluate which of the restriction enzymes was an efficient cutter of phage genomic DNA to produce phage map, an initial attempt to subjected to use phiSHEF 2 DNA to restriction digestion with several enzymes such as *AfeI*, *EcoRI*, *DpnI*, *HindIII*, *AgeI*, and *NedI* and the digested products were separated by 1% agarose gel electrophoresis (section 2.4.12). As can be seen in Figure 4.11, *HindIII* and *NedI* restriction enzymes was an efficient phage genome DNA cutter, the decision was made to go with *HindIII* for all other phiSHEF phages in RFLP tests.

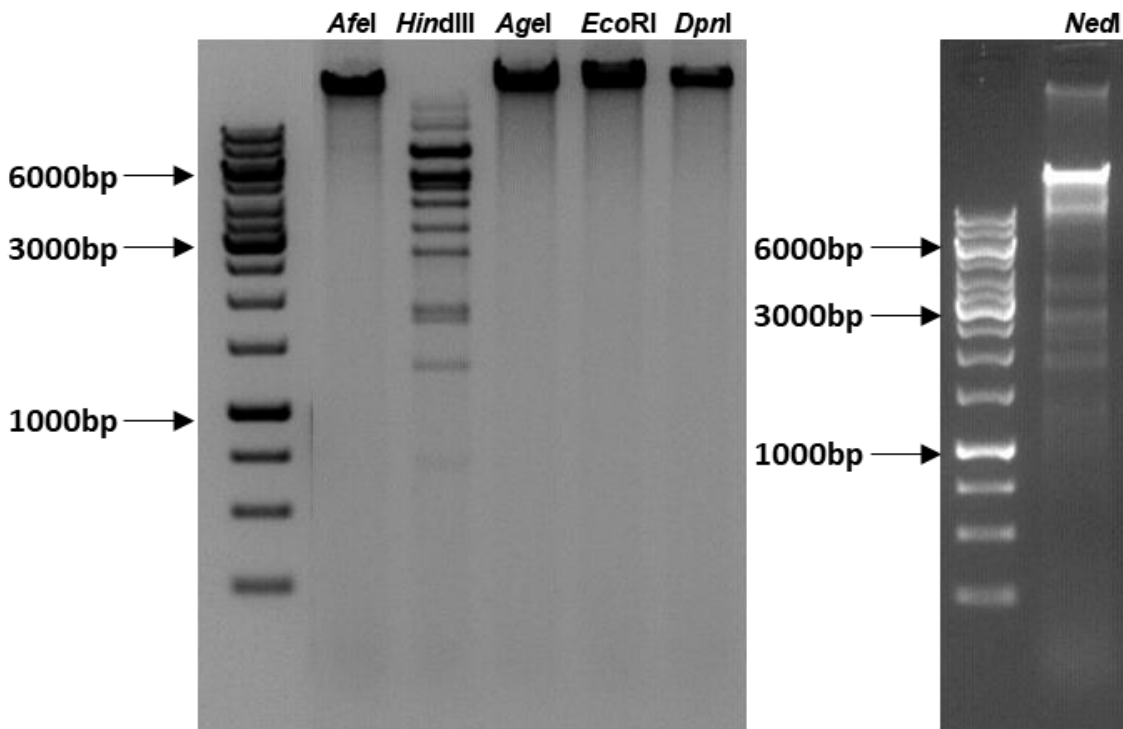


Figure 4.11 Restriction fragment length polymorphism (RFLP) of phiSHEF 2. Chromosomal DNA digestion by several restriction endonuclease enzymes, *HindIII* and *NedI* were capable of phage genome digestion. The digested products were separated by 1% agarose gel electrophoresis (15x15 cm) in 1x TBE buffer running at 90 volts for 4 h to determine the map and genomic size of bacteriophage.

The restriction profiles indicate that these five phages were genetically different, corresponding to differences in their host-range- see later (in fact we isolated several other phage which displayed identical RFLP patterning and protein profile that were discarded at this stage). Furthermore, digestion of extracted DNA with restriction enzymes and DNase I indicated that that all were double stranded DNA viruses. By annotating these fragment sizes and adding their cumulative masses we estimated that the phage indicative genome sizes in the range 39-43 kb, a size in-keeping with expectations (Figure 4.12A).

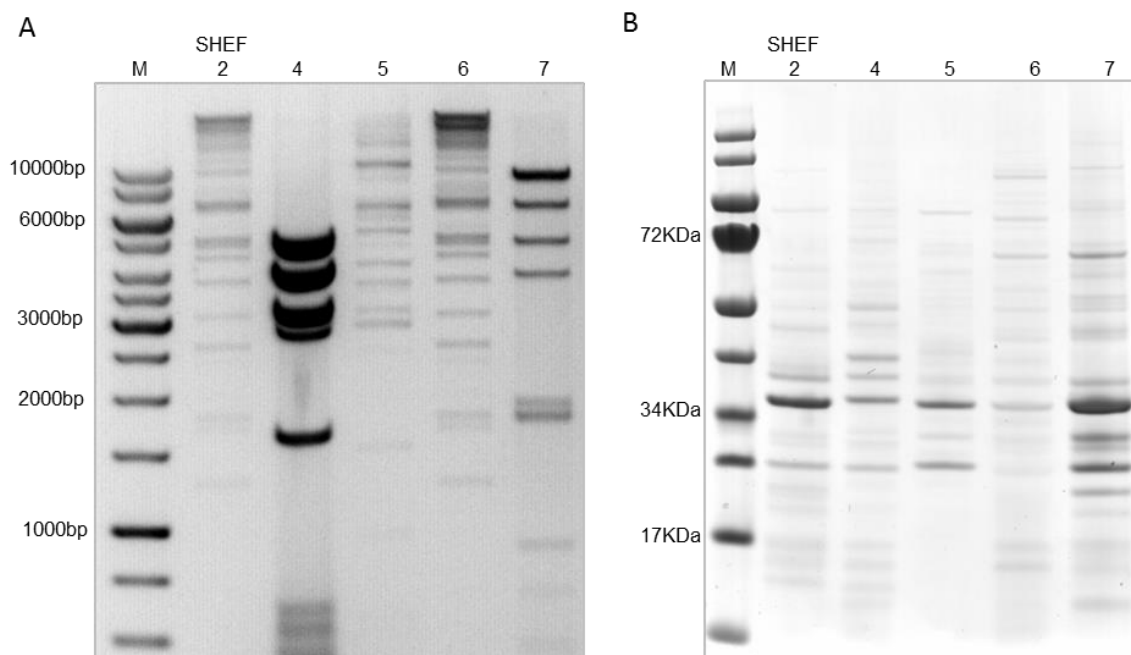


Figure 4.12 Restriction fragment length polymorphism (RFLP) of extracted phage chromosomal DNA and protein profile for phiSHEF phages. A) PhiSHEF phages genome DNA profiles digestion by restriction endonuclease *Hind*III. Phages genome sizes reside in the range 39-43 kb. B) Virions protein profiles of phiSHEF on the SDS-PAGE. A large protein band was conserved in all phages of about 36 KDa.

To further characterise these phages, phage particles from PEG 8000 concentrated phage stock was mixed with equal volume of chloroform in order to separate the phage particles from PEG 8000 (section 2.4.9). Followed by mixing 50 μ l from the upper layer (10^{11} - 10^{13} PFU/ml) with 50 μ l of SDS-PAGE loading buffer, 10 μ l volume of lysate was loaded directly (after heating at 95°C for 7 min) onto 4-12% and subjected to analysis by SDS-PAGE, again confirming that five separate phage were present based on their alternative protein profiles. As expected, given that the phage has largely similar structures both among and across phyla the protein profiles between these strains were more similar than their DNA profiles with the most prominent band in all cases a 36 KDa band. In short, we confirmed that we isolated five distinct phages against *E. faecalis* in the family Siphoviridae (Figure 4.12B).

For identification of the major 36 KDa band, the band from phiSHEF 2 (because it is one of the early isolated phages and it exhibits a wide host range as shall be mentioned later, section 4.4.2.4) was cut from the gel and proteomic technique of ‘in gel digestion’ performed as described in mass spectrometry in material and method section (2.4.10). After comparing against the full genome sequence of phiSHEF 2 (fully annotated fasta amino acid file format derived as part of this project, see section 4.4.2.3), a protein sequence coverage of 28% identified this 36kDA band as the putative phage capsid protein (one of the phage structural head module) as illustrated in Figure 4.13. This is not surprising as phage head is a significant part of the phage particle.

Protein sequence coverage: 28%

Matched peptides shown in **bold red**.

```

 1 MSRQELMEQA QTLTSEGKLD EAEKAMQEIK ALDEEKPKKEE RAVDNKDEEK
 51 PEEEAQAEAA KDEPKKEPKK EAKKEEPKKEE RSKAKPETDVE EPKEEPKKEE
101 KKEKRSLEQK GEENMEKVIL DGKEVENKEV RGFLEYLRSK ETRALPESFE
151 GVKSADASAI IPEEIIITKAK MLPETVVDLR NMITRQKVTH AMGKYPILKA
201 NEAVLATVEE LKKNPDLEGP AFEEVKYEVE TYRGQIAVAE EALQDSDDDL
251 SGIIRHIQR QGLNTANKAI VAKLKTATAV AATSIDDLKT QVNTGFDPAY
301 NLEFIVSQSF FNALDQMKDA NGRYLLEDDI KAQSGKSLLG RKVTVLADKL
351 IGTADGDKVA FLGQPDFAFV FFDRVDITVR WVEHQYYGQV LAVAMRFDCV
401 VVDRKNAGKYI TLTPAP

```

Figure 4.13 Snap shot from MASCOT search results of the 36 KDa protein band analysis of phiSHEF 2 phage. 50 peptide matches were obtained (24 non-duplicate and 26 duplicate) giving 28% protein sequence coverage of phage capsid protein of phiSHEF 2.

4.5.2.3 Genome organisation of phiSHEF 2, 4 and 5.

In order to analyse further the genome of the isolated phages i.e. genome size, genome modules distributions, and most important to understand the nature of phages, whether they are lytic or lysogenic (through the absence of genes associated with lysogenic cycle such as integrase). PhiSHEF 2, 4, and 5 phages DNA were sent for full chromosome sequencing at (MicrobesNG, Birmingham, UK) as described earlier in section 2.4.13. The sequence results were received in two basic formats namely: FASTA (contains the nucleotide sequence in one or several nodes) and GBK (contains an automated annotation performed using Prokka). Analysing the FASTA formats revealed

that phiSHEF 2 composed of one main node/contig and 12 small unrelated nodes, while phiSHEF 4 sequence has only one main node, and phiSHEF 5 has one main and two unrelated small nodes. The main node from each phage was further analysed using the online web server: PHAST, a phage searching tool as well as Artemis. The results of the analysis revealed that their genome size range from 40.9-41.3Kbp with GC percentage of about 34.55-34.75% as illustrated in Table 4.2.

Table 4.2 PhiSHEF 2, 4, and 5 characterisation. The main nucleotide sequence of each phage was analysed by PHAST online program.

Phage	Region length (Kbp)	ORF	Region position	GC percentage
SHEF 2	41.3	68	266-41607	34.55%
SHEF 4	40.9	63	160-41070	34.71%
SHEF 5	41.2	69	105-41334	34.75%

Next, the annotated GBK files were visualised by SnapGene® Viewer 1.1.3 Software and further analyses on an amino acid sequence level performed using the Mauve align software tool. Images of phiSHEF 2, 4, and 5 genome organisations and protein features were generated as shown in Figure 4.14 and Table 4.3, 4.4, and 4.5 respectively and have been deposited for phiSHEF 2, 4 and 5 at NCBI with GenBank reference numbers MF678788, MF678789, and MF678790 respectively.

The organization of the phiSHEF 2, 4 and 5 genomes coding regions are divided into two halves transcribed in opposite directions (Figure 4.14). The genome sizes of these three phage were approximately 41 kilobase pairs (Kbp)- i.e. in agreement with our RFLP estimations and, placing them as moderate genome length as compared to other *Enterococcus* phages. Each genome was assembled into one large contig with low read mapping coverage at the 5' and 3' ends with no clear edges at the ends of the contigs, this suggested circularity of terminally redundant permuted linear genomes. As with most phages, the genomes are arranged in a modular form, which include modules for DNA packaging, structural components, cell lysis (rightward transcribed genes) and a module for regulation and replication (left ward transcribed genes) as shown in Figure 4.14A

(colour coded). As is typical for bacteriophage, there is little noncoding DNA between these genes, suggesting that there is a single transcript for each set of genes. Although each one exhibits a different host range, they have high similarity among them at the primary amino acid level (aa) suggesting that these phages might have recently diverged, for example phiSHEF 2 is 94% identical to phiSHEF 5 with query coverage of 81%, while harbouring 92% similarity to phiSHEF 4 with query coverage of 77% using BLASTp (Figure 4.14B, mauve align comparisons). The results of phiSHEF 2, 4 and 5 genomes analysis using PHAST program showed high identity to the complete sequence of the enterococcal bacteriophages EfaCPT1 GenBank accession no. (NC_025465), IME-EF3 (NC_023595.2), IME-EF4 (NC_023551.1) and vB_IME196 (NC_028990) respectively. Finally, the same analysis reveals the absence of putative gene that encoded integrase, which indicate that they are likely to be lytic in nature as evidenced by our isolation method which favoured lytic viruses.

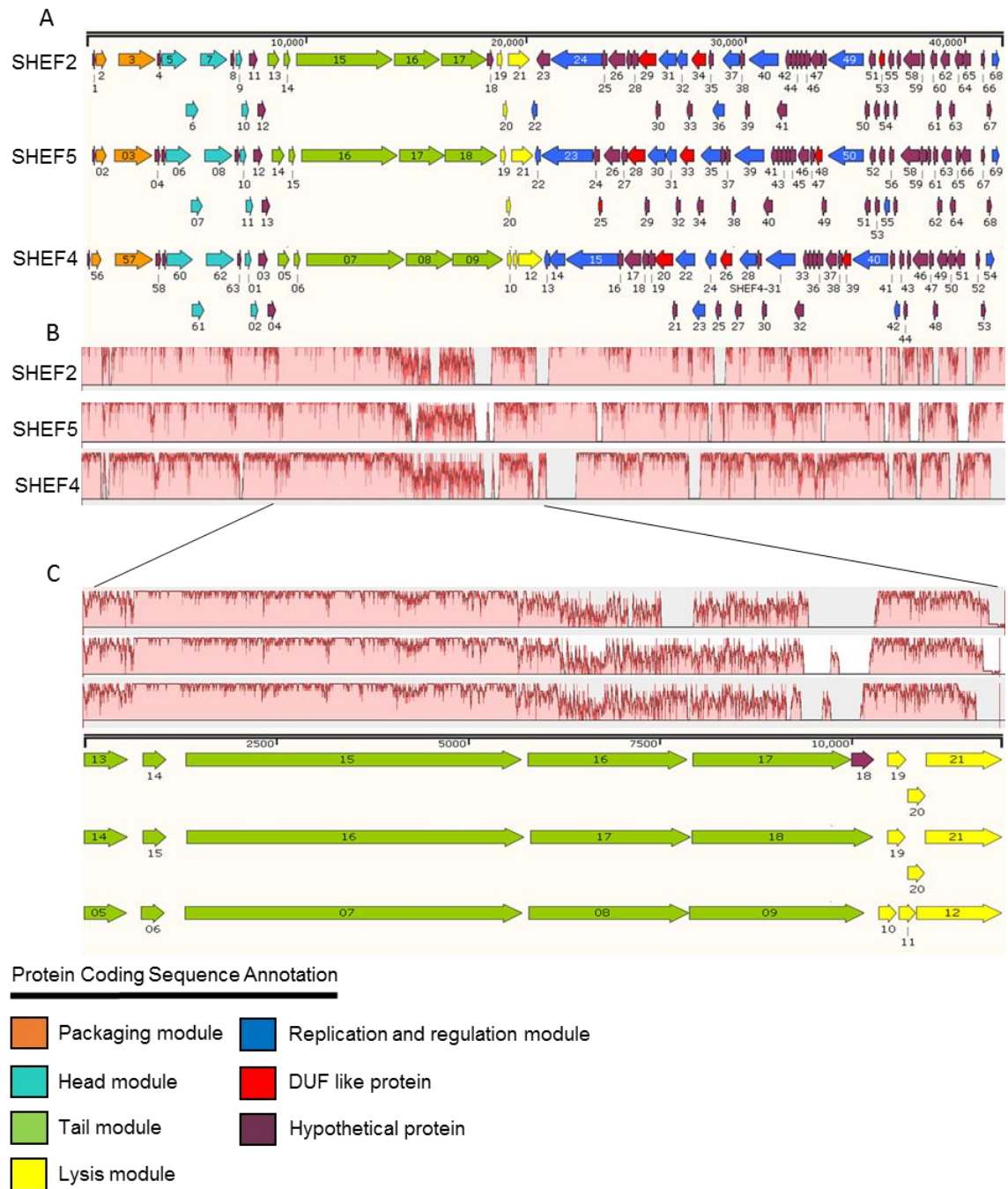










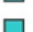

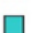







































































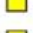

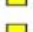



























































Figure 4.14 A) Genome organization of *E. faecalis* lytic phages phiSHEF 2, phiSHEF 5, and phiSHEF 4 respectively. Images produced using SnapGene® Viewer 1.1.3 Software. B) Snap shot of aa comparison of phiSHEF genomes by Mauve multiple genome alignments Version 2.4.0. C) Enlarged section of genome and mauve align for the tail and lysis module organization. Areas that are completely white were not aligned and probably contain sequence elements specific to a particular genome. The height of the similarity profile corresponds to the average level of conservation in that region of the genome sequence.

Table 4.3 Names and proposed function of phiSHEF 2 annotated genes.

Feature	Location	Size (bp)			Type	
1	266 .. 418	153			CDS	hypothetical protein
2	433 .. 906	474			CDS	Phage terminase, small subunit
3	1443 .. 3167	1725			CDS	Phage Terminase
4	3237 .. 3401	165			CDS	hypothetical protein
5	3406 .. 4557	1152			CDS	Phage portal protein
6	4544 .. 5107	564			CDS	Caudovirus prohead protease
7	5177 .. 6427	1251			CDS	Phage capsid family
8	6553 .. 6753	201			CDS	hypothetical protein
9	6797 .. 7093	297			CDS	gp6-like head-tail connector
10	7065 .. 7400	336			CDS	Phage head-tail joining protein
11	7397 .. 7804	408			CDS	hypothetical protein
12	7801 .. 8166	366			CDS	hypothetical protein
13	8242 .. 8808	567			CDS	Phage major tail protein
14	9003 .. 9314	312			CDS	tail tape measure chaperone
15	9571 .. 13,941	4371			CDS	Chromosome partition Smc
16	14,024 .. 16,105	2082			CDS	Phage tail protein
17	16,176 .. 18,233	2058			CDS	Prophage endopeptidase tail
18	18,242 .. 18,535	294			CDS	hypothetical protein
19	18,713 .. 18,958	246			CDS	hemolysin XhIA
20	18,973 .. 19,209	237			CDS	Bacteriophage holin
21	19,206 .. 20,192	987			CDS	Autolysin
22	20,274 .. 20,501	228			CDS	Glutaredoxin-like protein NrdH
23	20,498 .. 21,097	600			CDS	hypothetical protein
24	21,160 .. 23,451	2292			CDS	DNA polymerase
25	23,487 .. 23,711	225			CDS	hypothetical protein
26	23,782 .. 24,489	708			CDS	hypothetical protein
27	24,567 .. 24,818	252			CDS	hypothetical protein
28	24,819 .. 25,115	297			CDS	hypothetical protein
29	25,116 .. 25,934	819			CDS	DUF1351
30	25,924 .. 26,112	189			CDS	hypothetical protein
31	26,088 .. 26,864	777			CDS	Beta-lactamase superfamily

Feature	Location	Size (bp)			Type	
32	26,875 .. 27,354	480			CDS	HNH homing endonuclease
33	27,351 .. 27,572	222			CDS	hypothetical protein
34	27,574 .. 28,173	600			CDS	DUF3310
35	28,330 .. 28,554	225			CDS	hypothetical protein
36	28,529 .. 29,047	519			CDS	HNH endonuclease
37	29,001 .. 29,741	741			CDS	DNA primase/polymerase
38	29,754 .. 29,951	198			CDS	hypothetical protein
39	30,014 .. 30,190	177			CDS	hypothetical protein
40	30,187 .. 31,482	1296			CDS	SNF2 family N-terminal/helicase
41	31,475 .. 31,864	390			CDS	hypothetical protein
42	31,848 .. 32,084	237			CDS	hypothetical protein
43	32,087 .. 32,296	210			CDS	hypothetical protein
44	32,299 .. 32,508	210			CDS	hypothetical protein
45	32,510 .. 32,671	162			CDS	hypothetical protein
46	32,673 .. 32,945	273			CDS	hypothetical protein
47	32,994 .. 33,437	444			CDS	hypothetical protein
48	33,510 .. 33,698	189			CDS	hypothetical protein
49	33,787 .. 35,367	1581			CDS	D5 N terminal like/primase
50	35,462 .. 35,659	198			CDS	hypothetical protein
51	35,656 .. 35,895	240			CDS	hypothetical protein
52	35,892 .. 36,107	216			CDS	hypothetical protein
53	36,104 .. 36,331	228			CDS	X878 like protein
54	36,328 .. 36,546	219			CDS	hypothetical protein
55	36,546 .. 36,767	222			CDS	hypothetical protein
56	36,767 .. 36,907	141			CDS	hypothetical protein
57	36,904 .. 37,065	162			CDS	hypothetical protein
58	37,221 .. 37,931	711			CDS	hypothetical protein
59	38,008 .. 38,142	135			CDS	hypothetical protein
60	38,445 .. 38,708	264			CDS	hypothetical protein
61	38,705 .. 38,890	186			CDS	hypothetical protein
62	38,890 .. 39,297	408			CDS	hypothetical protein
63	39,294 .. 39,506	213			CDS	hypothetical protein
64	39,544 .. 39,909	366			CDS	hypothetical protein
65	39,923 .. 40,240	318			CDS	hypothetical protein
66	40,744 .. 40,947	204			CDS	hypothetical protein
67	41,030 .. 41,236	207			CDS	hypothetical protein
68	41,236 .. 41,607	372			CDS	HNH endonuclease

Table 4.4 Names and proposed function of phiSHEF 4 annotated genes.

Feature	Location	Size (bp)			Type	
01	7314 .. 7610	297			CDS	gp6-like head-tail connector
02	7582 .. 7917	336			CDS	Phage head-tail joining protein
03	7914 .. 8321	408			CDS	hypothetical protein
04	8318 .. 8683	366			CDS	hypothetical protein
05	8762 .. 9322	561			CDS	Phage major tail protein
06	9500 .. 9811	312			CDS	TAIL TAPE MEASURE CHAPERONE
07	10,068 .. 14,438	4371			CDS	tape tail measure protein
08	14,521 .. 16,596	2076			CDS	putative minor tail protein
09	16,602 .. 18,869	2268			CDS	putative minor tail protein
10	19,052 .. 19,297	246			CDS	hemolysin XhIA/DUF1267
11	19,311 .. 19,544	234			CDS	Bacteriophage holin
12	19,547 .. 20,644	1098			CDS	Bifunctional autolysin precursor
13	20,737 .. 20,961	225			CDS	Glutaredoxin-like protein NrdH
14	20,962 .. 21,648	687			CDS	Modification methylase DpnIIB
15	21,711 .. 24,002	2292			CDS	putative DNA polymerase
16	24,037 .. 24,261	225			CDS	hypothetical protein
17	24,332 .. 25,042	711			CDS	hypothetical protein
18	25,120 .. 25,368	249			CDS	hypothetical protein
19	25,369 .. 25,665	297			CDS	hypothetical protein
20	25,666 .. 26,484	819			CDS	DUF1351 LIKE PROTEIN
21	26,474 .. 26,662	189			CDS	hypothetical protein
22	26,638 .. 27,450	813			CDS	Beta-lactamase superfamily
23	27,404 .. 27,925	522			CDS	NUMOD4 motif
24	27,937 .. 28,416	480			CDS	HNH homing endnuclease
25	28,413 .. 28,619	207			CDS	hypothetical protein
26	28,621 .. 29,127	507			CDS	DUF3310
27	29,291 .. 29,539	249			CDS	hypothetical protein
28	29,490 .. 30,233	744			CDS	DNA primase/polymerase
29	30,245 .. 30,433	189			CDS	hypothetical protein
30	30,492 .. 30,668	177			CDS	hypothetical protein
31	30,665 .. 31,960	1296			CDS	SNF2 family N-terminal domain
32	31,953 .. 32,342	390			CDS	hypothetical protein
33	32,326 .. 32,559	234			CDS	hypothetical protein
34	32,562 .. 32,771	210			CDS	hypothetical protein
35	32,773 .. 32,934	162			CDS	hypothetical protein
36	32,936 .. 33,220	285			CDS	hypothetical protein
37	33,353 .. 33,814	462			CDS	hypothetical protein
38	33,890 .. 34,078	189			CDS	hypothetical protein
39	34,119 .. 34,466	348			CDS	DUF1140 LIKE PROTEIN

































































































































































































	Location	Size (bp)			Type	
40	34,557 .. 36,137	1581			CDS	putative primase
41	36,233 .. 36,430	198			CDS	hypothetical protein
42	36,427 .. 36,639	213			CDS	transcriptional regulator
43	36,636 .. 36,860	225			CDS	hypothetical protein
44	36,860 .. 37,000	141			CDS	hypothetical protein
45	36,997 .. 37,152	156			CDS	hypothetical protein
46	37,264 .. 37,887	624			CDS	hypothetical protein
47	37,968 .. 38,177	210			CDS	hypothetical protein
48	38,174 .. 38,359	186			CDS	hypothetical protein
49	38,359 .. 38,766	408			CDS	hypothetical protein
50	38,803 .. 39,168	366			CDS	hypothetical protein
51	39,185 .. 39,583	399			CDS	hypothetical protein
52	40,097 .. 40,300	204			CDS	hypothetical protein
53	40,342 .. 40,548	207			CDS	hypothetical protein
54	40,548 .. 40,919	372			CDS	HNH endonuclease
55	232 .. 384	153			CDS	hypothetical protein
56	399 .. 872	474			CDS	Phage terminase, small subunit
57	1469 .. 3193	1725			CDS	Phage Terminase large subunit
58	3282 .. 3548	267			CDS	hypothetical protein
59	3586 .. 3789	204			CDS	hypothetical protein
60	3794 .. 4945	1152			CDS	Phage portal protein
61	4932 .. 5495	564			CDS	Caudovirus prohead protease
62	5565 .. 6818	1254			CDS	Phage capsid family
63	6943 .. 7143	201			CDS	hypothetical protein

Table 4.5 Names and proposed function of phiSHEF 5 annotated genes.

Feature	Location	Size (bp)			Type	
01	265 .. 417	153			CDS	hypothetical protein
02	432 .. 905	474			CDS	Phage terminase, small subunit
03	1278 .. 2999	1722			CDS	Phage Terminase/large subunit
04	3088 .. 3354	267			CDS	hypothetical protein
05	3392 .. 3595	204			CDS	hypothetical protein
06	3600 .. 4751	1152			CDS	Phage portal protein
07	4738 .. 5301	564			CDS	Caudovirus prohead protease
08	5371 .. 6624	1254			CDS	major capsid protein
09	6747 .. 6968	222			CDS	hypothetical protein
10	6982 .. 7278	297			CDS	gp6-like head-tail connector
11	7250 .. 7585	336			CDS	Phage head-tail joining protein
12	7582 .. 7989	408			CDS	hypothetical protein
13	7986 .. 8351	366			CDS	hypothetical protein
14	8427 .. 8993	567			CDS	Phage major tail protein
15	9188 .. 9499	312			CDS	tail tape measure chaperone
16	9756 .. 14,126	4371			CDS	putative tail tape measure SMS
17	14,206 .. 16,281	2076			CDS	Phage tail protein/minor
18	16,293 .. 18,647	2355			CDS	putative minor tape protein
19	18,825 .. 19,070	246			CDS	hemolysin XhIA/DUF1267
20	19,085 .. 19,321	237			CDS	Bacteriophage holin class II
21	19,318 .. 20,304	987			CDS	Autolysin/ENDOLYSIN
22	20,388 .. 20,615	228			CDS	Glutaredoxin-like protein NrdH
23	20,678 .. 22,969	2292			CDS	putative DNA polymerase
24	23,005 .. 23,277	273			CDS	hypothetical protein
25	23,255 .. 23,413	159			CDS	EFP-GP141
26	23,504 .. 24,208	705			CDS	hypothetical protein
27	24,286 .. 24,537	252			CDS	hypothetical protein
28	24,538 .. 25,356	819			CDS	DUF1351 protein
29	25,346 .. 25,534	189			CDS	hypothetical protein
30	25,510 .. 26,286	777			CDS	Beta-lactamase superfamily
31	26,297 .. 26,776	480			CDS	HNH homing endonuclease
32	26,773 .. 26,979	207			CDS	hypothetical protein
33	26,981 .. 27,580	600			CDS	DUF3310 PROTEIN
34	27,737 .. 27,985	249			CDS	hypothetical protein
35	27,936 .. 28,811	876			CDS	DNA primase/polymerase
36	28,824 .. 29,012	189			CDS	hypothetical protein
37	29,026 .. 29,223	198			CDS	hypothetical protein
38	29,285 .. 29,461	177			CDS	hypothetical protein
39	29,458 .. 30,753	1296			CDS	SNF2 family N-terminal domain

Feature	Location	Size (bp)			Type	
40	30,746 .. 31,135	390			CDS	hypothetical protein
41	31,119 .. 31,352	234			CDS	hypothetical protein
42	31,355 .. 31,564	210			CDS	hypothetical protein
43	31,567 .. 31,776	210			CDS	hypothetical protein
44	31,778 .. 31,939	162			CDS	hypothetical protein
45	31,941 .. 32,219	279			CDS	hypothetical protein
46	32,343 .. 32,786	444			CDS	hypothetical protein
47	32,859 .. 33,047	189			CDS	hypothetical protein
48	33,087 .. 33,404	318			CDS	DUF1140
49	33,398 .. 33,604	207			CDS	hypothetical protein
50	33,693 .. 35,273	1581			CDS	D5 N terminal like
51	35,374 .. 35,574	201			CDS	hypothetical protein
52	35,571 .. 35,810	240			CDS	hypothetical protein
53	35,807 .. 36,022	216			CDS	hypothetical protein
54	36,019 .. 36,237	219			CDS	hypothetical protein
55	36,230 .. 36,451	222			CDS	TRANSCRIPTIONAL REGULATOR
56	36,448 .. 36,672	225			CDS	hypothetical protein
57	36,672 .. 36,827	156			CDS	hypothetical protein
58	36,986 .. 37,813	828			CDS	hypothetical protein
59	37,815 .. 38,132	318			CDS	hypothetical protein
60	38,204 .. 38,356	153			CDS	hypothetical protein
61	38,446 .. 38,655	210			CDS	hypothetical protein
62	38,652 .. 38,837	186			CDS	hypothetical protein
63	38,837 .. 39,244	408			CDS	hypothetical protein
64	39,241 .. 39,465	225			CDS	hypothetical protein
65	39,478 .. 39,690	213			CDS	hypothetical protein
66	39,712 .. 40,146	435			CDS	hypothetical protein
67	40,634 .. 40,837	204			CDS	hypothetical protein
68	40,917 .. 41,123	207			CDS	hypothetical protein
69	41,123 .. 41,494	372			CDS	HNH endonuclease

All phiSHEF phages share a similar distribution pattern for DNA packaging and head morphogenesis (Figure 4.14, orange coded genes), i.e. packaging module preceding head assembly via predicted terminase. The small subunit terminase recognizes and binds to the phage DNA site, while the large subunit usually delivers the enzymes needed to cleave concatemeric phage DNA at *cos* sites to allow packaging of the DNA into phage heads (Fujisawa and Morita, 1997, Sun *et al.*, 2012). The predicted head module (Figure 4.14, turquoise coded genes) harbours genes encoding portal proteins (for genome injection into host cells), prohead protease maturation, head capsid proteins and head-tail adaptor proteins. Based on the absence of two extra head-tail adaptor proteins we suggest phiSHEF phages are more related to EfaCPT1 than IME-EF3 type phage. These genes are followed by tail and tape-measure proteins (Figure 4.14, green coded genes) and a lysis module (Figure 4.14, yellow coded genes) containing putative haemolysin Xh1A,

putative holin and endolysin genes, which are very highly conserved in these phage (95-98%aa, 95-96%aa and 80-97%aa respectively). PhiSHEF 2 and 5 contain an endolysin with a predicted C-terminal ZoocinA_TRD (pfam16775) superfamily of lytic exoenzyme target recognition domain that differs in this C-terminal end from the phiSHEF 4 endolysin, which have SH3b (smart00287) domain of bacterial SH3 domain homologues superfamily (pfam08460) (Figure 4.15).

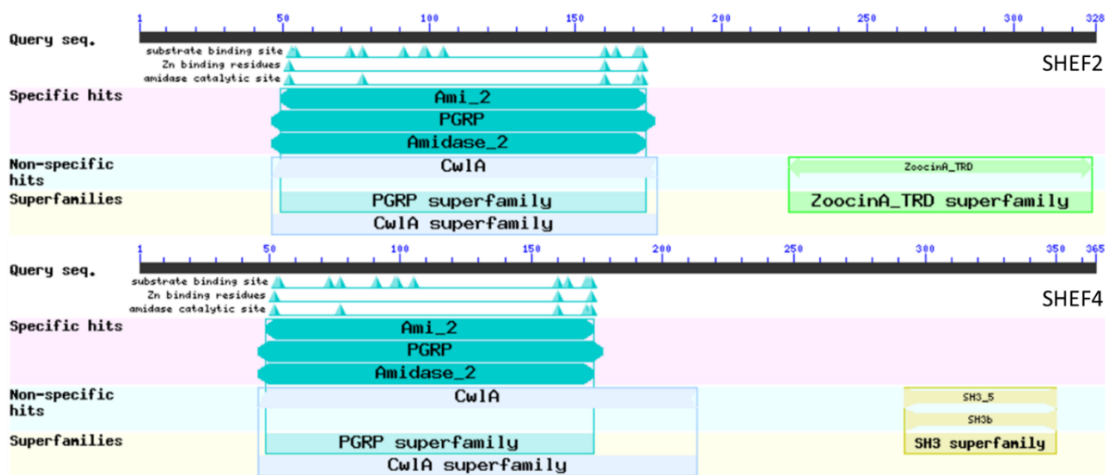


Figure 4.15 Snap shot from NCBI conserved domains for phiSHEF 2 and phiSHEF 4 endolysins.

The replication and regulation module are also clustered and ordered identically, with a few exceptions. PhiSHEF 4 encodes for an adenine-specific methyltransferase (modification methylase DpnIIB) which is absent from phiSHEF 5. At the same position in phiSHEF 2, the bioinformatics reveal two hits for a homologue of DNA modification protein of *Polaribacter* phage P12002L and an acetyltransferase of uncultured Mediterranean phage uvMED, all of which are putatively involved in modification of phage DNA (a well-known strategy to protect viral DNA on injection into the host). In addition, phiSHEF 4 and 5 harbour a transcriptional regulator encoding gene (gene number 42 in Figure 4.4 and number 55 in Figure 4.5 respectively) that is absent from phiSHEF 2 suggesting that all three employ slightly different modes of post-replication and DNA modification that might be key for survival of the DNA during infection cycle.

During infection, it is the tail of the phage that first contacts bacterial host and is likely responsible for primary recognition and adsorption to specific receptors on the bacterial membrane host (Casey *et al.*, 2015a). Due to the fact that phiSHEF 2, 4 and 5

exhibit different host ranges we examined the predicted primary aa sequence of their tail gene locus by using Mauve (Figure 4.14C) to align the genomes and revealed that the first three tail genes have high similarity (81-100% at primary aa). In contrast, alignments of the fourth tail gene (first minor tail gene) (Figure 4.14B, gene number 16 from phiSHEF 2) reveal that only the first 130aa (out of 695 aa) share similarity which represent an N-terminal highly conserved domain of a siphovirus G-positive bacteria tail component (pfam05709), while still retaining some conserved motifs, then the sequence starts to diverge after 130 aa (Figure 4.16A). However, it does retain some other small regions of strong homology, which might represent structural homology rather than sequence homology. For the fifth tail gene (second minor tail gene) (Figure 4.14B, gene number 17 from phiSHEF 2) a similar situation exists but with about 175 aa at the N-terminal end sharing similarity (out of 800 aa) with a family of proteins potentially involved in host specificity and annotated as a phage anti-receptor (TIGR01665) in the databases, while another small section matches a phage tail endopeptidase (pfam06605) then it starts to diverge as in previous gene (Figure 4.16B).

A

	1	10	20	30	40	50	60
SHEF2_16	MKENY	NFLRSFTFDG	KETSHLFQIAKVN	VPFLSKDND	FFQIGNTDGKHFNR	TRLGDFAIS	
SHEF4_8	MKENY	NFLRSFTFDG	METS	HLFQIAKVN	IPFLSKDND	YYTVGNTDGKHFNR	TKLGDYSIS
SHEF5_17	MAENY	NFLRSFTFDG	KETSHLFQIAKVN	IPFLSKDND	FFTVGNTDGKHFNR	SKLGEYSIS	
Sipho/Phi_dom 70							
SHEF2_16	IDGFIISDNS	GMTVSQTKD	ALVKIINSDEPKR	LILDQMPDRYF	NAIFTGTE	EYDATDTKY	
SHEF4_8	IDGFIISDNS	KMSVSKTKD	ELVKIINSDEPKR	LILDLEFPDRYF	SAIFS	GTQEYDATDTKY	
SHEF5_17	IDGFIISDNS	GMTVSE	TKDELVKIINSDEPKR	LILDLEFPDRYF	NAIYS	GTQEYDATDTKY	
130							
SHEF2_16	TPFTL	TFDVPDALAHQ	IEASNFNNV	ITKNSNMVLD	SNFERK	DQYKPAQLAIEKQGE	SN
SHEF4_8	TPFTL	TFDVPDALAHQ	IEPSGYTNV	ITINENLV	IDSEFKD	IRKYYKPW	TVKLVEDNNGSS
SHEF5_17	TPFTL	TFDVPDALAHQ	INPAGFTNV	KSNKLIYDSEY	TKINQY	LKPWVKV	LPEKRLNS
190							
SHEF2_16	VLSC	DFTAGIPAY	YTDNSTPH	QAWFFYDAY	YRRMNL	DLEVGQTV	GFQAKV
SHEF4_8	IIRG	DFSTSRP	TGF.YSVN	WDEAWFQMNAY	TRRIK	DLTVG	TKV..KAS
SHEF5_17	VIGAD	DFTS	SGVPFDYDK	NSTKQAWFQMNQ	YTRRMIP	DLKVG	DRV..VAG
250							
SHEF2_16	PDKTAE	LILMEWADN	PIRKYTHV	IQMPNEVKD	.WTL	LYFKTITIKSPETT	GLSMNFGLYG
SHEF4_8	FENNGK	LIVBEWGIN	PTRILERE	HEVVIPATESD	TFT	TRYTIDTTIKNKDTQ	AINLAFGSI
SHEF5_17	ADIAGR	LIVBEWGDAP	LRILKR	RHTRDIPKGTTE	.WTH	FYLDIKLESPNVK	GINFQYSAEG
300							
SHEF2_16	DHVS	SGDICE	PMFALDT	KAPMTYQKSL	IELRKELK	VVNN	GTYSKAYPRFS
SHEF4_8	NFTI	VDFSK	PMLSIN	PAEPFTY	VPSETALTEN	LLVSN	NGTYRTPYRYT
SHEF5_17	SEF	SVAYAR	PYMYL	LNPE	TGTYVPSE	FQYTENIT	IQNKGTYSKAYPTYT
360							
SHEF2_16	VNKN	GDILQFGN	PEEVDY	TEQTRTETV	QWLD	FWGPNL	PENMVQNS
SHEF4_8	INDK	GNILQFGN	PNDVDV	ATS	LKVE	TVKWWDFWGD	TLGEEW
SHEF5_17	VDG	KGNV	LQFGYPAEKDY	IEKTKVETV	KWDFWGN	KPLDD	FRINE
420							
SHEF2_16	PNLVD	GTLMN	TKD	VDSVVPNFT	.GEKTDV	WHGPTAVVPITAP	STNDRT
SHEF4_8	PNVFS	GTFD	MAKNP	DDVTPFT	TPNTGT	GYWHGPTSM	LAPPANS
SHEF5_17	PNIFD	GTID	MFLDPNS	ATPVFG	.SAND	OYWHGPTSMVAI	IPPS
480							
SHEF2_16	NYKDN	PPMAHLE	FMIGD	TAGN	PVIINTL	FRDSL	LYSTNHTI
SHEF4_8	YSKI	.QAMGR	VE	MNLQD	VNGKAV	MSVVF	FRDSTAD
SHEF5_17	YSNSP	QAMGR	VE	FNLD	TAGEY	VMGAV	FRDSTIT
540							
SHEF2_16	NTKLE	INIER	TE	TYIKWRL	ASIKGINK	YDNV	VVDNYIFTY
SHEF4_8	NGWRE	VTLER	WS	DKIV	WRLSQIK	SLAPND	NVHVGNEFKY
SHEF5_17	NGWRE	INLER	LG	DKLV	WRLCSIK	SINQ	FDNV
600							
SHEF2_16	NFRANQ	VMV	TD	AKLR	WLN	VKHIK	DVRN
SHEF4_8	NKLV	MSVSD	VKIR	WRD	SVTTN	VKNIF	QDGD
SHEF5_17	SNLH	ILMD	IS	DAK	MRW	KDTP	YLQ
660							
SHEF2_16	WEAF	R	LDV	GEHE	I	LPFY	SSWALQ
SHEF4_8	WEK	F	R	LE	LD	T	ITP
SHEF5_17	WEK	F	V	L	P	I	GETV
Sipho_dom3							

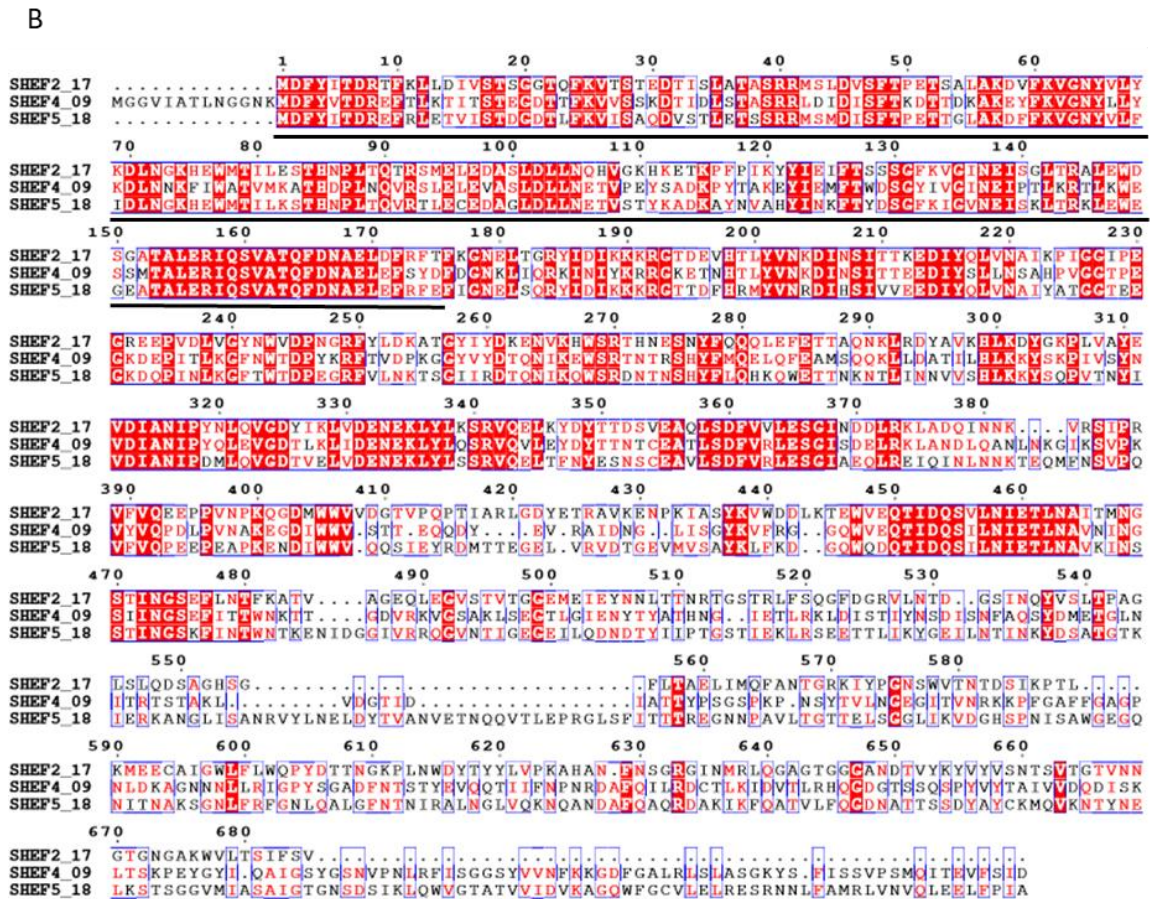


Figure 4.16 Multiple sequence alignment of fourth and fifth tail genes of phiSHEF phages produced by Multalin online program. A) Alignments of the fourth tail gene (first minor tail gene) reveal that only the first 130 aa (out of 695 aa) share similarity which represent an N-terminal of highly conserved domain of a siophvirus G-positive bacteria tail component (pfam05709) then it starts to diverge (underlined black line), while still retaining some conserved motifs (underlined blue line). B) The fifth tail gene (second minor tail gene) with about 175 aa at the beginning share similarity (out of 800 aa) that involve in host specificity protein of phage anti-receptor (TIGR01665) and smaller domain of phage tail endopeptidase (pfam06605) then it starts to diverge as in previous gene (underlined black line). High similarity (red font).

4.5.2.4 Determination of phage host-range

Having isolated a range of novel phage against *E. faecalis* and characterized them both morphologically and three in terms of their genome sequence we next investigated their biological host-range capacity. Host-range was tested qualitatively using the soft agar overlay method test at MOI 0.1 to detect visible plaques. Host-range tests show that

the phiSHEF 2 phage has the broadest host-range with capacity to lyse 9 out of 13 *E. faecalis* indicator strains tested, followed by phiSHEF 6 and 7 while phiSHEF 5 and 4 possesses the lowest host-range (lysis of 3 and 2 strains respectively). All five phiSHEF bacteriophages were specific to *E. faecalis* (Table 4.6) as none of them were capable to produce visible plaques towards an *E. faecium* strain (E1162), or towards other periodontal associated pathogens used in this study (Table 2.1).

Table 4.6 Phage-host range of phiSHEF phages. PhiSHEF 2 exhibits the widest host range followed by phiSHEF 6, 7, 5, and 4 respectively.

strain/phage	SHEF2	SHEF4	SHEF5	SHEF6	SHEF7
OS16	+	-	+	+	+
ER3/2s	+	-	-	+	+
EF1	-	-	+	-	-
EF2	-	+	-	-	-
EF3	-	+	-	-	-
EF54	+	-	-	+	+
OMGS 3197	+	-	-	+	-
OMGS 3198	+	-	-	-	-
OMGS 3885	+	-	-	+	-
OMGS 3919	+	-	-	+	+
OG1RF	+	-	-	+	+
V583	+	-	+	-	-
JH2-2	-	-	+	-	-
Total	9	2	4	7	5

4.5.2.5 PhiSHEF 3 phage

In addition to the phage indicated above, several other phage were also isolated, that are both less well characterised and in some cases were not distinguishable from our current pool of phage, either by RFLP or SDS-PAGE profile. However, there was one very interesting exception to this occurrence, namely the isolation of phiSHEF 3 phage. This was also isolated from our wastewater samples using the oral clinical strain OS16 (same host used to isolate phiSHEF 2).

The initial genome digestion, plaque morphology and micrograph appeared identical to phiSHEF 2 (Figure 4.17). PhiSHEF 2 and 3 DNA were subjected to restriction digestion with *Hind*III and the restriction profiles indicate that they are sharing the same genome map as seen in (Figure 4.17A), phiSHEF 3 produce plaque diameter of 3-4 mm morphology (Figure 4.17B) and phage head diameter~41 nm and tail length of ~235 nm (Figure 4.17C) which is seems to be similar to phiSHEF 2.

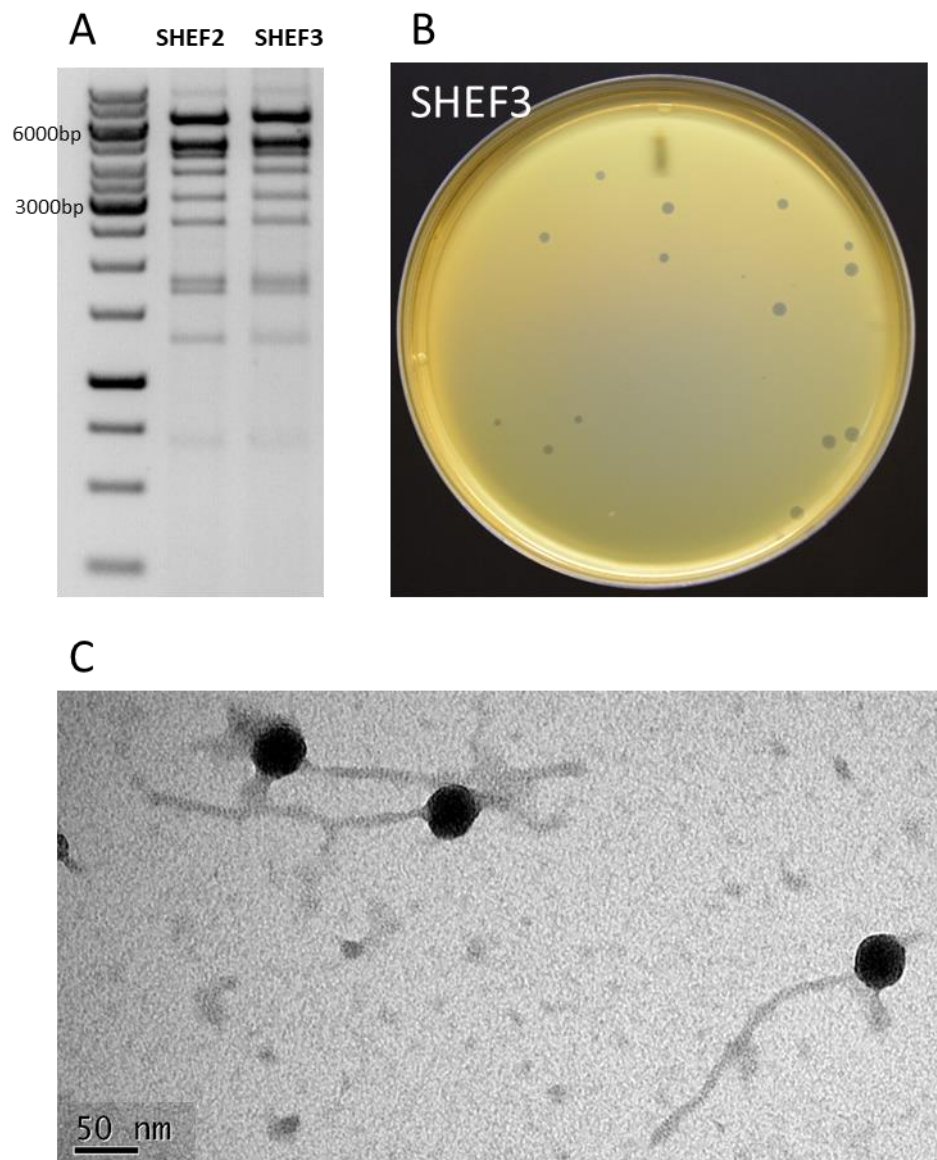


Figure 4.17 Characterisation of phiSHEF 3 phage. A) phiSHEF 2 and phiSHEF 3 sharing similar genome map, B) phiSHEF 3 plaque morphology diameter of 3-4 mm, C) Transmission electron micrographs of phiSHEF 3 which revealed that it belongs to the Siphoviridae family of head and long non contractile tail.

However, further characterisation revealed that it possessed a slightly different host-range compared to phiSHEF 2, as phiSHEF 3 was able to infect *E. faecalis* non-oral clinical strain U92304 while phiSHEF 2 was not (Fig 4.18A). In contrast, phiSHEF 3 was not able to infect *E. faecalis* oral strain OMGS3198 that phiSHEF 2 was able to. In contrast, they share the same host-range profile for the rest of the 8 strains. In addition, and possibly very importantly, the SDS_PAGE protein profile revealed differences between them, as two high molecular weight bands at around ~60 and 65KDa are present in the profile of phiSHEF 3 and not phiSHEF 2 (Figure 4.18B, indicated by arrows). This suggested differences at the genome level that result in production of two altered proteins compared to phiSHEF 2, and are probably contained on *HindIII* fragments since *HindIII* based RFLP patterning was unable to differentiate the phage. Therefore, we decided to send phiSHEF 3 for full genome sequence, in order that we could compare it to the phiSHEF 2 genome sequence, and potentially define the reason for this alteration in host-range. Unfortunately, upon analysing SHEF3 sequence as described in section 4.4.2.3, the sequence was incomplete and missing several sections related to tail modules as can be seen in Figure 4.18C, this section represent the nucleotide sequence from 37500bp until 41725bp (about 4225bp) at the end of the sequenced phiSHEF 3. Through the genome comparisons with fully annotated GBK file of sequenced genome of phiSHEF 2, tail gene number 15 with size of 4371 (Figure 4.14 and Table 4.3) that encode tail chromosome partition protein *smc*, seems to be unidentified and/or corrupted which make the comparisons unachievable. However, this part could be amplified using PCR primers from annotated ends of the phiSHEF 3 ends and several other primers could be designed upon the received PCR sequence until the full missing area identified which is suggested for future work.

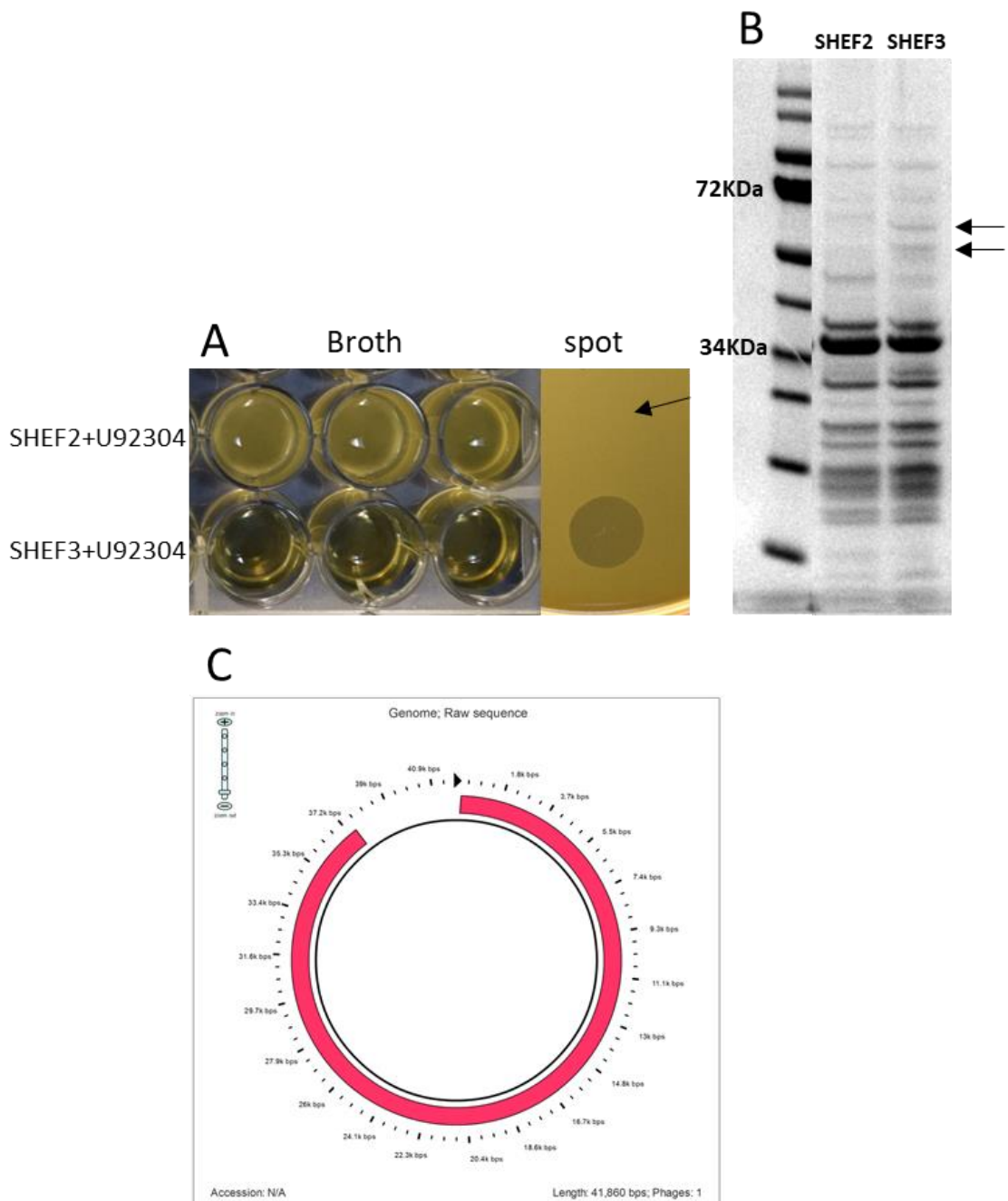


Figure 4.18 Further characterisation of phiSHEF 3. A) PhiSHEF 3 is sensitive to *E. faecalis* U92304 as revealed from the elimination of that strain in broth and in spotting test while phiSHEF 2 is not (arrow indicates that no clearance is produced from phiSHEF 2 spotting). B) Virions protein profiles of phiSHEF 2 and 3 on the 12% SDS-PAGE. Arrows indicate the presence of extra bands belong to phiSHEF 3. C) Snap shot from PHAST program of the sequenced phiSHEF 3 showed the unannotated (absence of continuous red line) nucleotide sequence from 37500 bp until 41725 bp (about 4225 bp) at the end of the sequenced phiSHEF 3.

4.5.2.6 Molecular determination of phage adhesion for phiSHEF 2, 6, and 7

Previous studies indicated that several *E. faecalis* phages (and indeed from other bacteria) adhered to the surface of G-positive bacteria via their extracellular polysaccharide capsule material (Monteville *et al.*, 1994, Tremblay *et al.*, 2006, Teng *et al.*, 2009, Casey *et al.*, 2015a, Duerkop *et al.*, 2016). Therefore, we endeavoured to investigate whether this was the case for any of our isolated phage. One limitation to such a study is the availability of genetically altered strains that contain defined mutations in *Enterococcus* polysaccharide (EPS) genes that have also been well characterised phenotypically. Fortunately, these were available for the strain OG1RF which is the most studied of the *E. faecalis* strains via collaboration with Dr S Mesnage, department of molecular biology and biotechnology in Sheffield. *E. faecalis* OG1RF is a laboratory-generated strain of the non-antibiotic resistant human oral isolate OG1 (Gold *et al.*, 1975). OG1RF produces a cell wall polymer of rhamnopolysaccharide that is known as the enterococcal polysaccharide antigen (Hancock *et al.*) composed of rhamnose, N-acetylglucosamine, N-acetylgalactosamine, glucose, and galactose which together with wall teichoic acid forms the secondary wall polysaccharides (Hancock *et al.*, 2003, Teng *et al.*, 2009). The OG1RF *epa* locus is composed of 18 highly conserved genes (*epa A* to *R*) followed by a variable region of about 13 genes (Xu *et al.*, 1998) as illustrated in Figure 4.19A. Within this locus, the *epaB* gene is known to encode a glycosyl transferase that mediates allocation of the major rhamnose component of Epa and is considered key to Epa composition while the variable region encodes decoration genes that are believed to modulate rhamnopolysacchride, but are as yet uncharacterised (Teng *et al.*, 2009, Palmer *et al.*, 2012).

In order to investigate the effect of disruption of *epa* locus genes on phage sensitivity, a mutant of *epaB* and several mutants and complemented strains of the Epa variable region of OG1RF_11720, 11715 and 11714 were infected with phiSHEF phages (Figure 4.19A black arrows). In order to perform these analyses we had to choose phage that infected wild type OG1RF, namely phiSHEF 2. In addition, phiSHEF 6 and 7 were also capable of infecting both strains when incubated with the *epaB* mutant (Figure 4.19B), the phage showed no infection in both spot and double layer agar tests, this mean that the EpaB dependent EPS was important for successful infection of OG1RF by phiSHEF 2, 6, and 7. This is further illustrated in TEM micrographs as seen in Figure

4.19C, where phiSHEF 2 showed to be adsorbed to both but plaques of clearance only appeared with OG1RF and absent in case of Epa mutant strain.

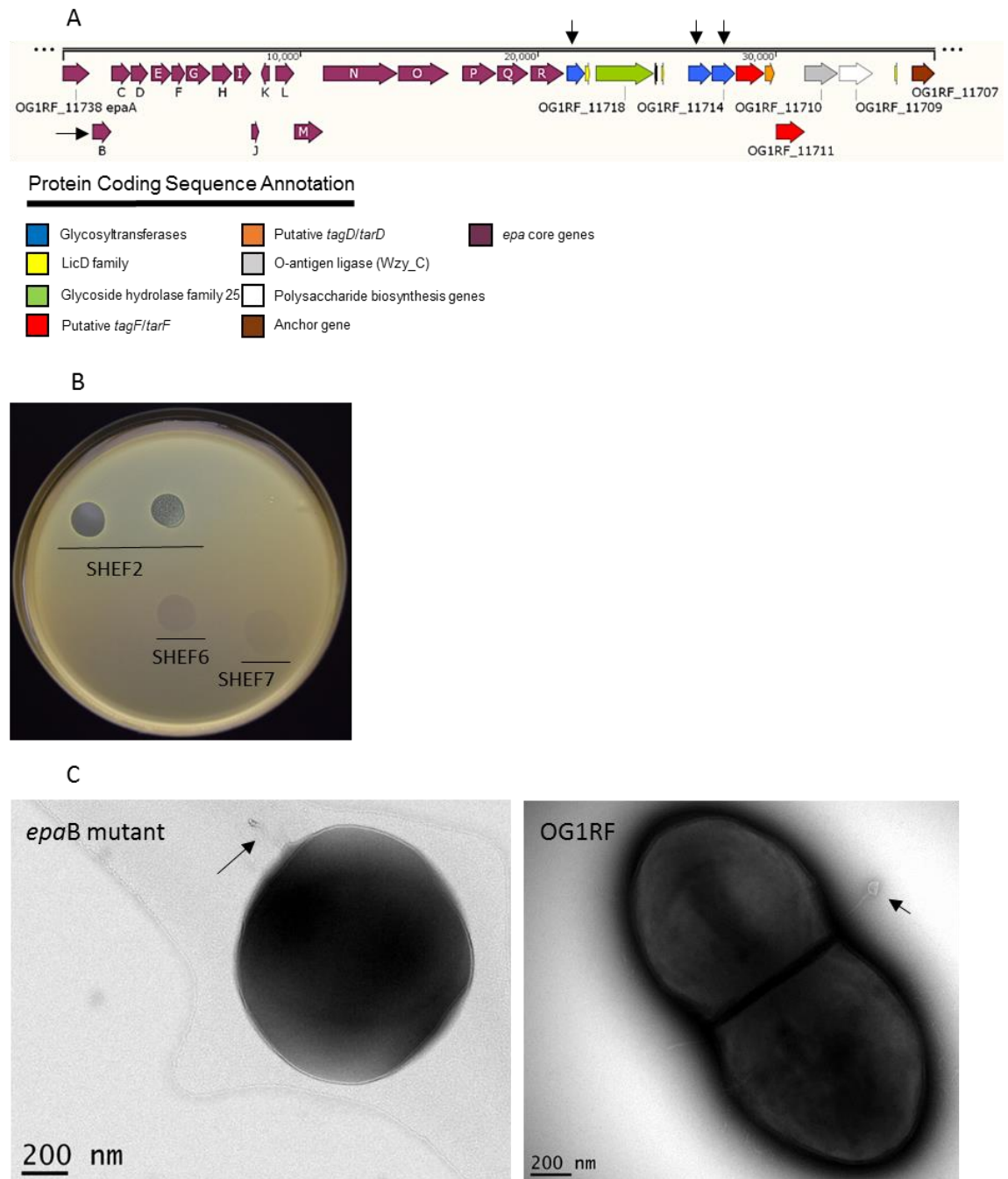


Figure 4.19 Molecular determination of phiSHEF phages adhesion. A) The OG1RF Epa locus is composed of 18 highly conserved genes (*epa* A to R) followed by a variable region of 13 genes (variable colour coded) (Teng et al 2009), arrows indicate location of the mutants. **B)** Spot testing of SHEF phages on OG1RF lawn in DL agar, OG1RF were sensitive to three of SHEF phages tested namely phiSHEF 2, 6, and 7 though it lost its sensitivity when mutations in Epa were tested. **C)** TEM showed that adsorption of

phiSHEF 2 phage (arrow) to both OG1RF (spent head) and *epaB* mutant (tail without head).

Similarly, the phage was incubated with mutants of the variable region (OG1RF_11720, 11715 and 11714) and complemented versions of the variable region. Furthermore, when the mutants of the variable regions were complemented, they all regained sensitivity to all of the tested phages and produce plaques in DL agar. Interestingly, when we complement the OG1RF_11715 with plasmid encoding the function of OG1RF_11714 (both encoded predicted glycosyltransferases), the mutants do not retain sensitivity unless it is complemented with the original plasmid that hold OG1RF_11715 function which might indicate that its function cannot be substituted with gene predicted to perform the same function. Taken together these data indicate that the overall structure of the EPS is key to infection with these phages (Table 4.7).

Table 4.7 Sensitivity of phiSHEF phages to *E. faecalis* OG1RF and mutants.

Strain/Phage	SHEF2	SHEF4	SHEF5	SHEF6	SHEF7
OG1RF	+	-	-	+	+
OG1RF <i>epaB</i>	-	-	-	-	-
OG1RF_11720	-	-	-	-	-
OG1RF_11720C	+	-	-	+	+
OG1RF_11715	-	-	-	-	-
OG1RF_11715C	+	-	-	+	+
OG1RF_11714	-	-	-	-	-
OG1RF_11714C	+	-	-	+	+
OG1RF_11714C*	-	-	-	-	-

epa core locus (*epaB* mutant), mutants and complements (C) in variable region. OG1RF_11715 complemented with plasmid encoding the function of OG1RF_11714 (C*).

As phiSHEF 2, 6 and 7 were not able to lyse Epa mutants of OG1RF. We then set out to investigate for one of these phage phiSHEF 2 (since it had the broadest host-range), whether this lack of infection might be due to exclusion from adsorption by loss of the Epa saccharide or whether phiSHEF 2 might be adsorbing successfully but not able to bind to a secondary component to produce a productive infection cycle.

To dissect if this lack of infection was due to poor adsorption to the cell surface or lack of progression to a productive infection, or a combination of both, we performed a series of experiments examining both adsorption to the cell surface but also phage progeny produced. Using an adsorption assay where phage were incubated with target strains OG1RF (WT) and mutants for 10min before harvesting of cell-free phage via centrifugation and filtration, we observed that about 2-4 fold less phage adsorbed to the mutants as illustrated in Table 4.8. However, this reduction does not explain the complete lack of infection by phiSHEF 2, as evidenced by the number of progeny after incubation with WT reaching 1×10^{11} pfu/ml from an inoculum of 2×10^6 pfu/ml, while with the mutants strains this actually reduced dramatically to less than even original inoculum, reflecting that all phages that adsorbed over a 24 h period, none had proceeded to lytic infections. This evidence was further supported when we added 0.28 M NaCl, a treatment known to interfere with electrostatic phage-bacterial interactions but not harm cell viability (we tested this here also) and released further still infective phages particles that were already adsorbed to the mutants surface (but not injecting its DNA inside the host cytoplasm). In addition, there are differences in the number of released infective phages that were adsorbed to the cells surface between mutants *epaB* (core region) and mutants from the variable region such as OG1RF_11720, being much less from the later (only 700 phage particles released) which might mean that they are not involved in strong phage-host interaction in the later (still strong). The same for OG1RF_11715 (700 phage particles released) but not with OG1RF_11714 (8000 phage particles released). On the other hand, this might also be due to that injection of the phage genome occurs after adsorption but not reached inside bacterial cell cytoplasm to continue a successful phage cycle and the remaining released phage particles are not infective anymore, which reflect the low numbers in OG1RF_11720 and OG1RF_11715. In general, this indicates that they might be involved in 2-stage interactions for productive infection (reversible and irreversible) while the substrates and products of these enzymes are not fully characterised but the data do imply 2-stages to the injection process.

In order to exclude the possibility of phage progenies entrapment inside the host cells that could not lyse the host membrane and escape for any reason, cells suspensions were treated with chloroform to lyse the cells, this resulted in no further release of viable phage particles. In addition, samples from both infected wild type and *epaB* mutant at 30 min post infection were examined under TEM, micrographs taken revealed the adsorption of phiSHEF 2 phage to both cell surfaces (Figure 4.19C). However, more round bacterial cells shape of *epaB* and OG1RF_11720 mutants could be visualised when examined under the TEM (Figure 4.20).

Table 4.8 Molecular determination of Epa mutants of OG1RF.

	OG1RF	<i>epaB</i>	OG1RF_11720	OG1RF_11715	OG1RF_11714
Input PFU/ml	2×10^6	2×10^6	2×10^6	2×10^6	2×10^6
After 24 h PFU/ml	1×10^{11}	2.7×10^5	4×10^4	1.2×10^4	1.5×10^4
0.28 M NaCl PFU/ml		1.4×10^5	700	700	8000
Adsorption after 10 min	50%	17%	17%	12%	14%

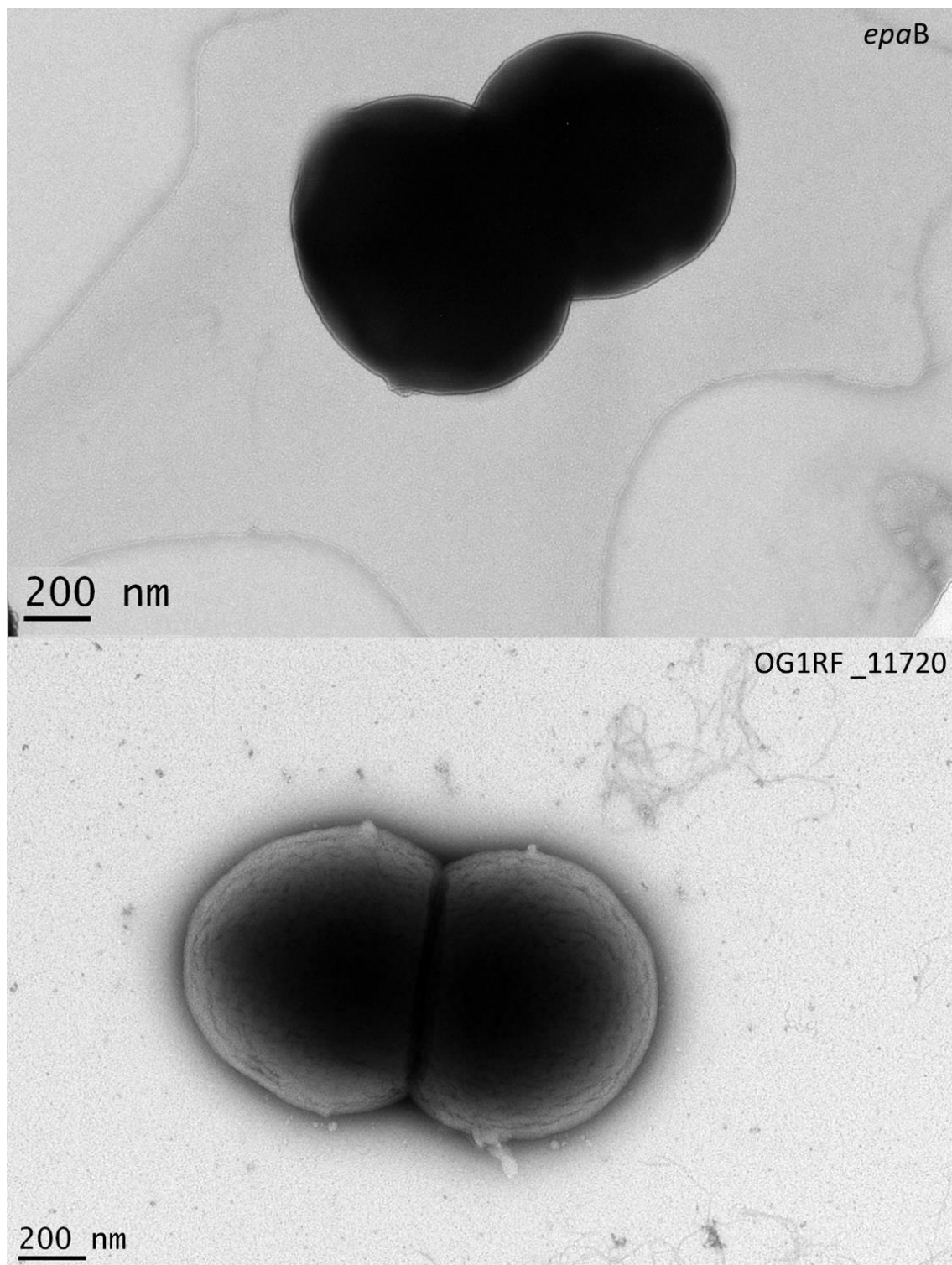


Figure 4.20 Transmission electron micrographs of *epaB* and OG1RF_11720 mutants, round bacterial cells outline could be visualised.

4.5.2.7 One step growth, infection cycle and adsorption rate

We then proceeded to a more in depth characterisation of the wide spectrum host range bacteriophage phiSHEF 2. Using the orally isolated clinical strain OS16 (isolated from mouthwash of endodontic patient). Firstly, we performed a one-step growth experiment to establish the eclipse period (average time to produce the first mature intracellular phage), latent period (average time to cell lysis) and burst size (the average number of phage released at cell lysis), which showed phiSHEF 2 as a highly efficient *E. faecalis* targeting phage with an eclipse period of only 10 min, a latent period of only 30min (broadly in agreement with Figure 4.21A, and a burst size of 9.3 PFU, i.e. 9-10 phages produced per bacterial cell infection cycle. The plateau phase was reached after 75 min, following a 45 min burst period. Next, infection cycles of phiSHEF 2 was performed at different MOI with the OS16 host. PhiSHEF 2 was capable of OS16 elimination in a dose dependant manner, as the higher the phage titre the faster drop in OD of the growing bacteria till clearance of the broth occurs, the time needed ranged between 60 min at higher MOI down to 120 min at the lowest MOI tested (Figure 4.21B) which means that higher numbers of phage particles available at the time of infections will result in infections and elimination of most cells at the same time. In addition, we examined adsorption parameters of this phage with the *E. faecalis* strain OS16, and found that saturation of adsorption was reached after 10 min (Figure 4.21C). This adsorption is illustrated in Figure 4.22 where a TEM taken of cells at 30 min post infection illustrates adsorbed phage that seem to have injected DNA (spent heads are seen on the surface) but the cell is still intact.

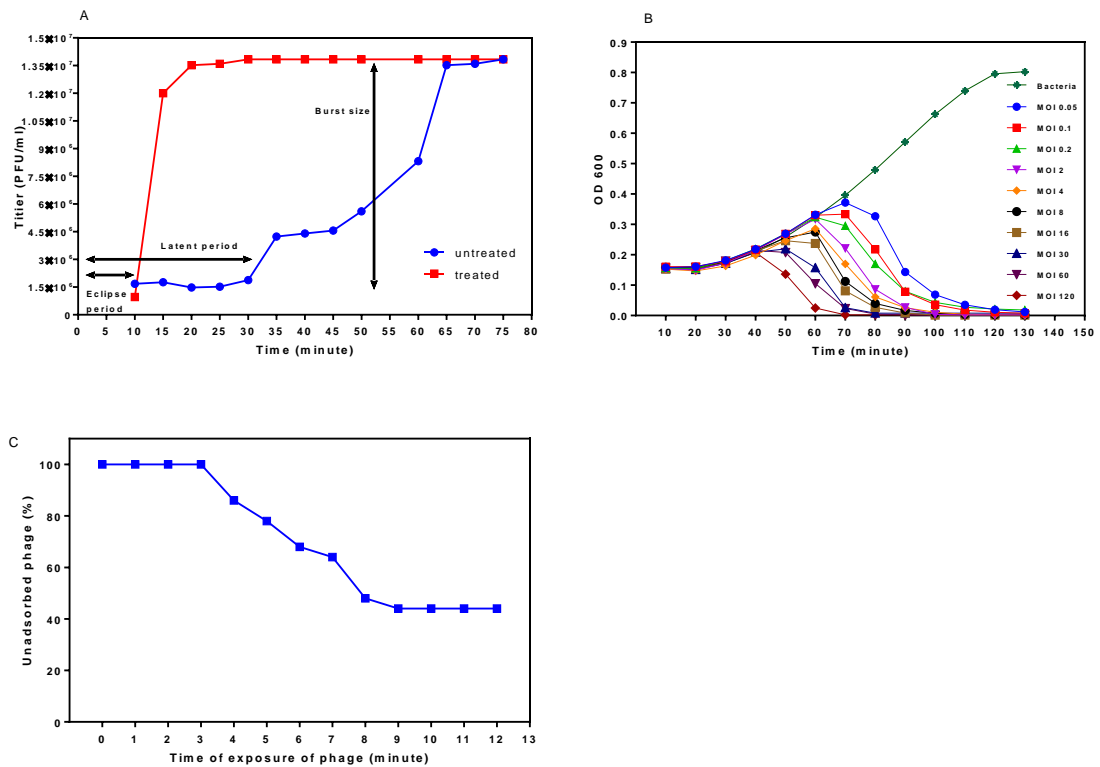


Figure 4.21 One step growth, infection cycle and adsorption rate of phiSHEF 2. A) One-step growth curve of phiSHEF 2 phage with the OS16 clinical strain host. The two sets of data represent samples treated with and without chloroform. lysis of the bacterial host happens too quickly result in a low burst size of about 9.3 though few numbers of phage particles will be made. B) Infection cycle that showed the dose dependence manner of phiSHEF 2. C) Adsorption of phiSHEF 2 phage to OS16 host strain occurs very fast as 60% of the phage particles were adsorbed within 9-10 min.

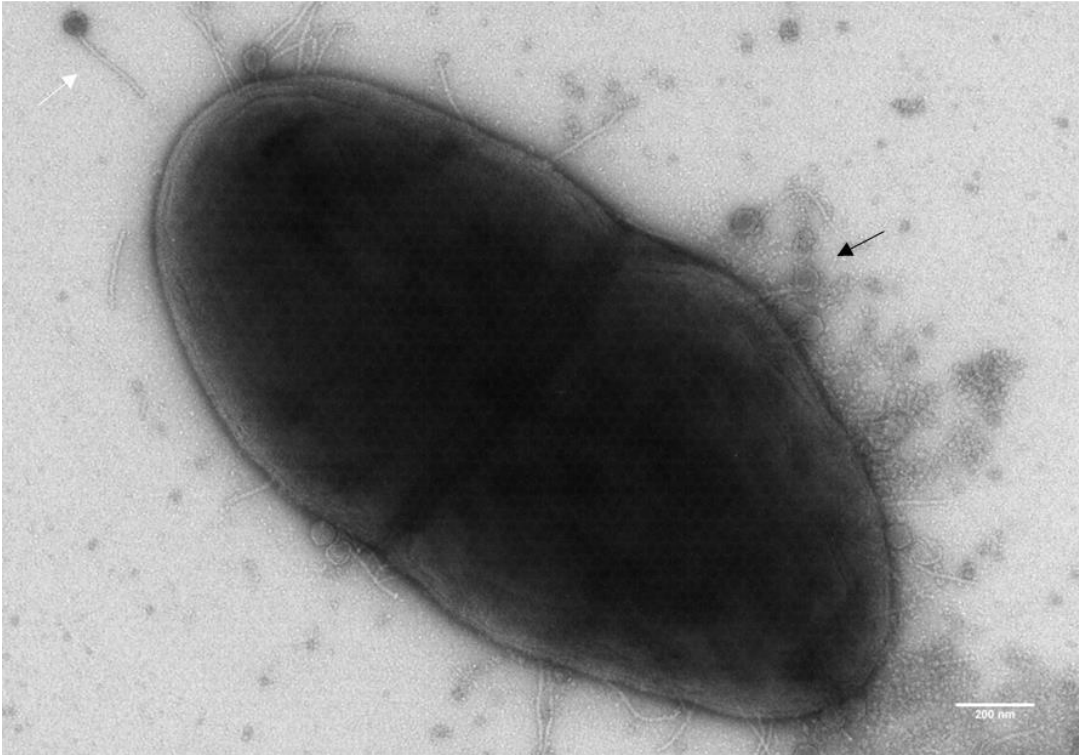


Figure 4.22 Transmission electron micrographs taken of cells at 30 min post infection with phiSHEF 2. Adsorbed phage that seem to have injected DNA (black arrows: spent heads are seen on the surface of *E. faecalis* OS16 strain) or still unadsorbed (white arrow) but the cell is still intact.

4.5.2.8 Ability of phiSHEF 2 to clear biofilms of *E. faecalis*

Given that most bacteria in nature and in clinical infections reside in biofilms (Hall-Stoodley *et al.*, 2004, Høiby *et al.*, 2011) we tested the ability of phiSHEF 2 to eradicate pre-formed biofilms of *E. faecalis* *in vitro*. However, we first tested biofilm growth potential of three *E. faecalis* strains (OS16, ER3/2s and EF54) and established that EF54 formed the strongest one-day biofilms on abiotic plastic surfaces (data not shown), and was thus chosen for these tests. Biofilm tests where phiSHEF 2 was introduced to the biofilm both after 24 h (young biofilm) and 144 h (mature biofilm) revealed that phiSHEF 2 is capable of complete elimination of *E. faecalis* mature or immature biofilm ($p < 0.0001$) using a crystal violet based assay (Figure 4.23A). As phiSHEF 2 phage was capable of eliminating the biofilm formed on abiotic surfaces and as a previous study mentioned that *E. faecalis* endodontic isolates were rich in biofilm associated *esp* gene (surface adhesin gene) (Sedgley *et al.*, 2005a), we tested its efficiency

to eradicate biofilm formed on natural mineralised tooth root surfaces and quantify it through a resazurin metabolic assay. The blue and nonfluorescent resazourin is reduced by cellular activity (oxygen intake through bacterial cells metabolism) to pink colour highly fluorescent resorufin which is further reduced to nonfluorescent hydroresorufin (O'brien *et al.*, 2000) as illustrated in Figure 4.23B. The results reveal a significant reduction ($p < 0.0001$) in emission of samples infected with phiSHEF 2 phage treated EF54 biofilm from tooth surfaces (blue colour unreduced solution) compared to the untreated group which showed higher emission (higher cellular activity) and pink colour solution (Figure 4.23B). In addition, more biofilm of *E. faecalis* colonies was observed (Figure 4.24) along the walls of the root canal (stereomicroscope images) and on the tooth dentin surface (light microscope images).

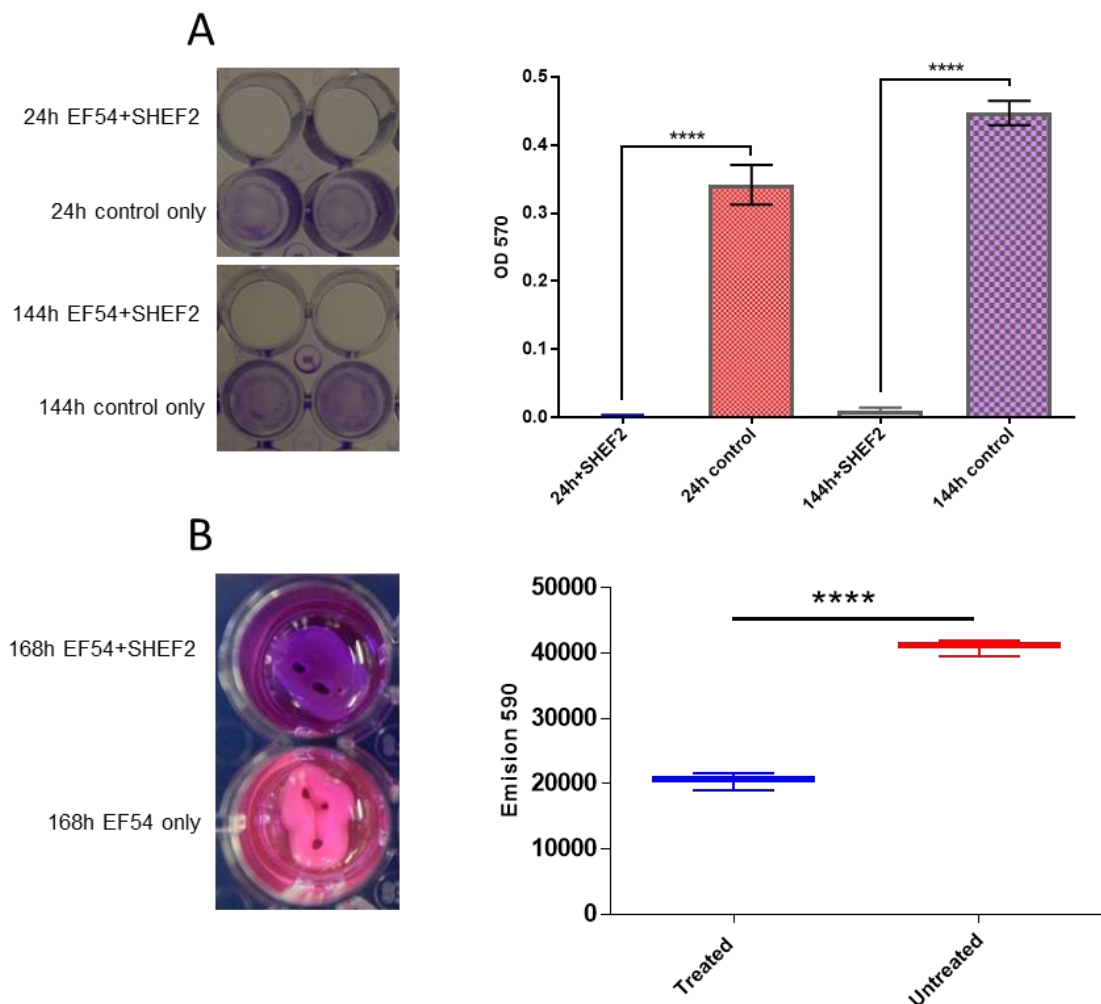


Figure 4.23 Biofilm assay on polystyrene plates and tooth root slices. A) Polystyrene plates: left) representative part of microtiter plate with *E. faecalis* biofilm after resolubilization of crystal violet used to stain the formed biofilm (initial and mature biofilm). The upper wells represents phage treated biofilm in which phiSHEF 2 phage

were added to *E. faecalis* after the required time incubation. Lower wells represent untreated biofilm with more intense coloration (thicker biofilm formation), right) OD₅₇₀ readings of one (initial) and six (mature) days biofilm assay of the treated versus untreated respectively. PhiSHEF 2 phage significantly eliminate the biofilm when added and almost no biofilm were detected in the treated groups. B) Tooth root slices: left) The upper well represent the phiSHEF 2 treated group while the lower pink colour well represent the reduced resazurin to the fluorescence resorufin by *E. faecalis* cellular activity, right) the addition of phiSHEF 2 phage significantly reduced 7 days biofilm formation as represented by OD₅₉₀ emission readings. Student's t-test was used to compare between treated and untreated groups.

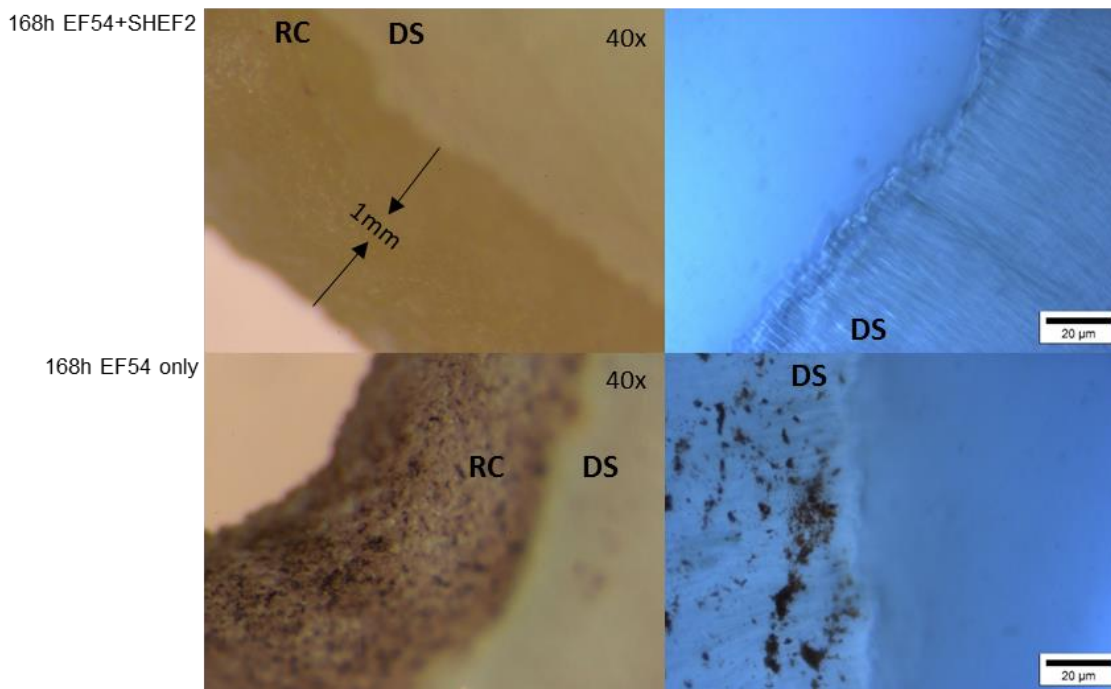


Figure 4.24 Stereo microscope and light microscope images of treated and untreated *E. faecalis* biofilm on root surface slices. Stereo microscope (upper and lower left images) and light microscope (upper and lower right images), upper images represent phiSHEF 2 treated group with no obvious *E. faecalis* colonies, while the lower images (untreated) showed the biofilm of *E. faecalis* colonies scattered on the root canal (RC) and dentinal surface (DS) respectively.

4.5.2.9 Zebrafish as *in vivo* model for phage treatment evaluation

In clinical settings *E. faecalis* is known to be a common cause of septicaemia while there is a well-established link between dental procedures and certain systemic infections such as association of endocarditis with release of oral bacteria into the bloodstream (Li *et al.*, 2000). Therefore, we decided to test phiSHEF 2 in an established model of *E. faecalis* systemic infection (Prajsnar *et al.*, 2013), namely the use of zebrafish embryo infection model. In these studies a strain of *E. faecalis*, which phiSHEF 2 can lyse were used to infect zebrafish, namely the oral clinical strains OS16.

This experiment was performed through collaboration with a visiting PhD student, Magdalena Widziolek who performed all the injections, records and statistics. Zebrafish (n = 40) were injected with *E. faecalis* OS16 with 30,000 CFU (Colony Forming Units), which was then allowed to spread through the embryo circulation for two hours. Phage were then injected next at an MOI of 20 (about 6×10^5 phage particles) at 2 h post infection (no = 20) with photographs taken and vital signs (heart beat and blood circulation) recorded every 24 h for three days (72 h) as shown in Figure 4.25. When embryos were infected with *E. faecalis* OS16 alone (in the absence of any bacteriophage (control group)), only 12% of the embryos survived at the end of 72 hpi as can be seen from the survival curve Figure 4.24A. Examination for the presence of unhealthy looking fish which displayed pericardiac oedema, yolk sac and eyes abnormalities as well as spine curving were evaluated every 24 h for three days also.

Two extra separated groups of fish were also microinjected systemically into the Duct of Cuvier of dechorionated larvae with PBS and phiHEF 2 phage. This is very important as the effect of phage injection should be monitored and evaluated to be safe to the fish and not cause any extra side effects compared to its control (PBS in this case) that interfere with the overall results of the treated group. The results revealed that no signs of infection were visualised when injected with phiSHEF 2 which reflect that delivery of phage alone was safe.

However, most changes occur during the first 24 hpi, with the majority of the fish (72%) displaying decreasing vital signs, i.e. heart rate which was annotated as 'sick' (Figure 4.24B). After 48 hpi, most of the sick fish had died (68%) while the mortality rate is increased to 85% at the end of 72 hpi as illustrated in Figure 4.24C and 4.24D.

Concerning the treated group, the efficiency of the treatment started to be observed after 24 hpi as all the fish that were treated with phage had survived (only 13% were sick compared to 72% sick fish from *E. faecalis* infection). At the end of 72 hpi, 89% of fish were survived (80% healthy and 9% ill) while only 11% from the phage treated group were died due to infection (Figure 4.24D and 4.24E). In conclusion, treatment of OS16 infected fish with phiSHEF 2 phage increased the survival rate from 12% (control) to 88% (treated) and the results were statistically significant as $p < 0.0001$ (student's t-test).

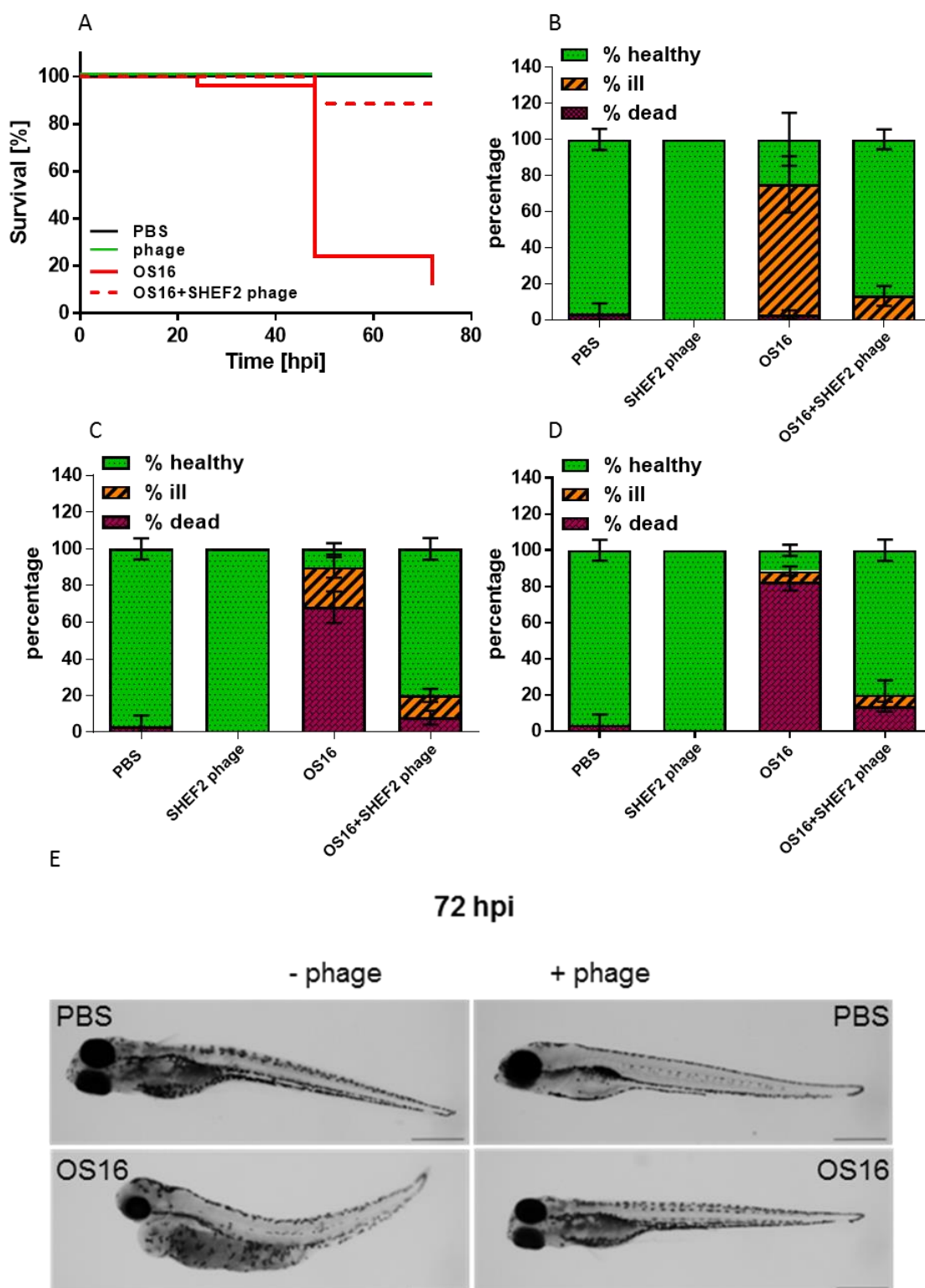


Figure 4.25 Animal model of phage-bacterial interaction. Zebrafish larvae were injected with *E. faecalis* OS16 strains at a dose of 30 000 CFU at 30 hpf (hours post-fertilisation) and after 2 hpi (hours post-infection) larvae were injected again with phiSHIF 2 phage at a MOI of 20. Fish were monitored for survival and disease development for up to 72 hpi. Kaplan-Meier plot shows that phage therapy was very successful for *E. faecalis* OS16- infected larvae as it significantly increased fish survival

from 12% for phage-untreated fish to 88% for phage-treated larvae by 72 hpi (A). B) 24 hpi, C) 48 hpi, D) 72 hpi. Vast majority of *E. faecalis* OS16 infected but phage-untreated larvae, developed progressive signs of systemic disease as soon as 24 hpi, in contrast to phage-treated fish, most of which remain healthy (B-D). E) Unhealthy looking *E. faecalis* OS16-infected fish displayed pericardiac oedema, yolk sac and eyes abnormalities as well as spine curving in contrast to phage-treated larvae which remain healthy throughout the experiment and showed appearance comparable to PBS-injected control fish. Scale bar 500 μm .

4.6 Discussion

4.6.1 Isolation of new clinical strains of periodontal pathogen *A. Actinomycetemcomitans*

We set out first to isolate strains namely *A. actinomycetemcomitans* from the oral cavity in order to use in phage infection, several clinical strains were isolated successfully (Shef30, Shef31, Shef32, and Shef33). This was performed to expand our library of clinical strains that been associated with periodontal infection, thus if phage been isolated using them as template for infection (indicator strains), it could be used as antibacterial therapy that might aid in treatment of periodontal disease. In addition to the isolated strains of *A. actinomycetemcomitans*, several other strains could also be detected that were also grown on TSBV selective medium but the star shaped colonies and subsequent 16S rRNA confirmed the isolation of *A. actinomycetemcomitans*. This selective media was enriched with 10% horse serum instead of blood to suppress hemin-requiring *Haemophilus* and since the growth of *A. actinomycetemcomitans* can be repressed *in vitro* by oral streptococcal species, Bacitracin was added (in addition it suppresses other G-positive oral bacteria). The TSBV selective medium suppresses growth of most oral species and permits the recovery of *A. actinomycetemcomitans* that can be isolated based upon colony morphology- characteristic star shape. However, this medium will support the growth of fusobacteria and G-negative anaerobic motile rods (Slots, 1982).

4.6.2 Cataloguing of phages from the oral cavity of patients attending periodontal department in UK and IRAQ

In order to investigate the morphological diversity of bacteriophage within oral samples obtained from patients that attending the periodontal department in Iraq and UK, direct electron microscopy was used to view the samples. TEM is widely used as a method of choice for phage geography, ecology investigation, and identification (Ackermann and Nguyen, 1983). Due to the small sizes of phages, they can only be directly visualised with significant magnification. In addition, some bacteria are not cultivable under the lab conditions, thus their corresponding phages could not be identified using DL plaque technique but direct visualisation will provides through perception into the morphological diversity of phage populations within sample without depend on certain host (Demuth *et al.*, 1993).

Reports for the direct visualisation of human gingival plaque by Electron Microscope has been identified the presence of bacteriophage as early as 1975 (Halhouli and Colvin, 1975). It describes head particles hexagonal in shape of about 50 nm in diameter attached to “fine fibres” referring to a tail. Yet, processing and concentration of the samples for bacteriophage identification were not performed, as the plaque samples were placed under the TEM without phage concentration step. After 2 years, Brady *et al.* (1977) describe “tailpieces” that attached to hexagonal bacteriophage-like particles that clumped between bacteria in dental plaque. Recently, techniques such as metagenomics were used to characterise phage communities within dental plaque followed by filtering out obvious phage reads through comparing it to the bacteriophage database (Ly *et al.*, 2014, Naidu *et al.*, 2014). Ly *et al.* (2014), established that large communities of viruses that inhabited saliva, biofilms composed largely of bacteriophage. *Siphoviridae* bacteriophages were mainly dominated in saliva and supragingival plaque samples of healthy and periodontal diseased groups while *Myoviridae* bacteriophages were dominated in subgingival samples of diseased group only and significantly higher than healthy group. The use of new metagenomic sequencing is possible due to low plaque biomass available, which render final sample quite not adequate even after processing and concentration (Edlund *et al.*, 2015). In our study, we recorded a high distribution and diversity of phage particles within the concentrated plaque samples in both Iraqi and Sheffield plaque samples; with observation of both groups TEM micrographs revealed that *Siphoviridae* family were more dominant in samples from Iraq but displayed less bacteriophage diversity within the samples. However, this might be due to the fact that

amount of supragingival plaque from Iraqi patients were much higher (observed at the time of collection) than those collected from Sheffield patients and they are stored and transported differently.

In this study, the presence of a range of phage were observed in the two main families of Siphoviruses and Podoviruses in electron microscope micrographs in addition to possible cubic, enveloped, and filamentous like virus particles from the plaque samples that been obtained from supra and sub gingival plaque of chronic periodontitis cases patients. However, (Ly *et al.*, 2014) reported the identification for the all tailed three families using metagenomic sequencing. As we can exclude the processing and concentration method used in this study as the cause (wastewater sample reveal the presence of the three families that will describe later, which indicate the successful methodology used), we could estimate that the new sequencing methods is more sensitive but temperate phage might be also recorded, that might be actually represent a defective integrated phages which lost their capacity to excise from bacterial genome. This data shows that there are various phages morphology that inhibited the oral cavity in ethnically diverse populations. This is expected because the isolation of bacteriophage sourced from the oral cavity targeting oral and non-oral pathogenic bacteria has been described against a range of spp. i.e.; *Actinomyces viscosus* (Tylenda *et al.*, 1985), *Enterococcus faecalis* (Bachrach *et al.*, 2003), *Proteus mirabilis* (Hitch *et al.*, 2004), *Fusobacterium nucleatum* (Machuca *et al.*, 2010), *Aggregatibacter actinomycetemcomitans* serotype b (Castillo-Ruiz *et al.*, 2011) and *Neisseria meningitidis* (Aljarbou and Aljofan, 2014). In contrast, in this study the presence of bacteriophage within the sourced samples were performed first followed by isolation trials.

4.6.3 Cataloguing of phages from Sheffield wastewater

We also went to investigate the morphological diversity and distributions of bacteriophage from samples obtained from Sheffield wastewater. Great morphological variability was detected in the phage collections from Sheffield wastewater. Similar results were obtained for phage identification from various studies with several specific examples in the literature, e.g. Limestone Creek wastewater treatment plant (South Carolina, USA). With exceptions, phages were more diverse in Sheffield wastewater as cubic phages were not described in earlier papers (Ewert and Paynter, 1980). In addition, it does not differentiate between contractile and non-contractile phages ratio. We could observe about equal distribution of both families in Sheffield wastewater. However, direct

microscopic study of phages morphology from rumen of sheep and cattle samples mention that phages with contractile tails were the most frequent (Klieve and Bauchop, 1988). In contrast, the reverse ratio were estimated in lake water from Yaquina Bay, Oregon (Torrella and Morita, 1979), a water sample from the North Atlantic (Frank and Moebus, 1987) and Lake PluBsee in the northern part of Germany (Demuth *et al.*, 1993). Phages diversity may have great impact on the density and distribution of their hosts in wastewater as in marine (Suttle and Chan, 1993) and freshwater (Phlips *et al.*, 1990) environments, suggesting a major role as a powerful regulation mechanisms. The average size of the phages observed in the Sheffield wastewater samples of 37 to 95 nm (head diameter) which is less than previously described range found for 662 bacteriophages from diverse habitats (Reaney and Ackermann, 1982), while the tail length of 5 to 450 nm in our study were in line with it.

Studies that focused on recording phage morphological diversity within natural samples were also performed through pre-enrichment with known numbers of bacteria before having the TEM micrographs (Hidaka and Fujimura, 1971, Ogata *et al.*, 1980). Ackermann and Nguyen (1983) enriched sewage water with 35 *E. coli* strains, and the phages within enrichment cultures were studied in the electron microscope. They contained about 10 varieties of morphologically different particles most of which belong to corresponded enterobacterial phage species. However, it shall not reflect the actual phage inhabitant distribution within a certain sample as the number of phages specific to the enriched bacterial strain will overcome the others. Studies concerning direct visualization of whole bacteriophage population in wastewater without bacterial host enrichment are very limited (Ewert and Paynter, 1980). In this study, we focused on direct visualisation of bacteriophage communities in wastewater samples without any enrichment.

We could estimate the abundance of phages in Sheffield wastewater that infect *E. Coli* and *Enterococcus* as research indicate that both bacteria have the ability to multiply in such environments (Whitman *et al.*, 2003). In addition, there counts are high in wastewater and sludge (Lasobras *et al.*, 1999, Mignotte-Cadiergues *et al.*, 2002, Mandilara *et al.*, 2006). Mandilara *et al.* (2006) found a strong correlation between the number of *E. coli* bacterial indicators and the presence of their coliphages. Finally, evidence that show coliphages are capable of infection and multiplication in water environments (Grabow *et al.*, 1984, Borrego *et al.*, 1990) further support our assumption,

placing bacteriophage as strong tool in controlling the bacterial community within wastewater.

4.6.4 Isolation of phage against isolated strains, a range of endodontic *E. faecalis* strains and other periodontal associated clinical strains

4.6.4.1 Isolation of phage towards periodontal associated clinical strains

The initial attempt to isolate phage against periodontal pathogens were performed using concentrated samples of saliva and dental chair drain on a host of type strains (also could be called indicator strains) of *F. polymorphum* ATCC 10953 and *F. nucleatum* ATCC 25586. This was followed by expanding studies to test infection of oral clinical strains of *Fusobacterium*, *Porphyromonas* and *Prevotella* isolated from the dental plaque of patients having chronic periodontitis in Sheffield (Table 2.1). As bacteriophages are very specific to their hosts (as mentioned previously in section 1.3.1), expanding the indicator strains will obviously increase the chances to isolate possible phage. Another reason to include these strains is that, if isolation was achieved, that phage will be specific towards pathogens associated with periodontal disease and might be used as potential therapy (obviously because the indicator strains were from real disease sites). Isolation of bacteriophage from oral salivary samples was shown to be possible previously in our labs by the Stafford group targeting *E. faecalis* (G Stafford, unpublished) but unfortunately it was lost due to improper storage. Clinical isolates of *A. actinomycetemcomitans* (Table 2.1) were also included in the library of indicator strains for phage isolation since phage that infect various strains of *A. actinomycetemcomitans* were mentioned previously such as PAA84 (Loftus and Delisle, 1995) and Aaphi23 (Resch *et al.*, 2004). Both enrichment and direct spotting were performed to isolate bacteriophage (see section 2.4.3 and 2.4.4). In the enrichment method, the sample which might harbour the potential phage was added to the broth that contain mid-log phase of single indicator strain, this will allow the low phages numbers that are specific to that indicator strain to multiply and increase in numbers. This was followed by filtering to remove the bacteria to leave only phage particles suspended in the broth and thus providing suitable starting phage sample to work with. In order to screen for possible phage, that sample will be used either mixed with the same host in double layer agar or directly spotted on the host. On the other hand, the second method of spot pipetting involves the spotting of small amount (5-10 µl) from the processed sample on 0.4-0.7% top layer agar that contains a single lawn of indicator host. In both ways, the presence of visible clear zone in the top agar (plaque) will represent a

potential successful isolation. Later trials to isolate bacteriophages involved the addition of processed samples obtained from supra and sub gingival plaque and processed samples from wastewater, as they were rich in phage particles as visualised in TEM (see section 4.3 and 4.4). However, as mentioned in the start of this section, no bacteriophages capable of infecting periodontal pathogens were isolated. Phage targeting *Fusobacterium* spp., *Prevotella* spp., and *P. gingivalis* have not been isolated and characterised previously in the literature except one that infected *Fusobacterium* spp. (Machuca *et al.*, 2010). However, its published small genome fragment believed to be a contaminant sequence from oral *P. acnes* phage and not a true *Fusobacterium* phage sequence (Brüggemann and Lood, 2013). Some periodontal pathogens such as *Fusobacterium* had not been associated to date with phage transduction or well known conjugation and natural transformation mechanisms (Han *et al.*, 2007, McGuire *et al.*, 2014) which is in part related to the various restriction-endonuclease systems that *Fusobacterium* species harbor which may cleave foreign DNA irrespective of the extent of methylation (Lui *et al.*, 1979). Bacteria also can act to degrade phage DNA that does not convey the corresponding methylation configuration via the action of restriction endonucleases that recognise and destroy foreign DNA (restriction-modification). (Forde and Fitzgerald, 1999, Coffey *et al.*, 2001). In addition, bacteria that harboured clustered, regularly interspaced short palindromic repeats with cas genes (CRISPR-cas) showed immunity to foreign phage infections and vice versa (Palmer and Gilmore, 2010). For example, V583 (which does not harbour the CRISPR-cas system), has a genome that harbours approximately 25% of acquired DNA (Polidori *et al.*, 2011).

4.6.4.2 Isolation of phage towards endodontic associated clinical strains of *E. faecalis*

Isolation of bacteriophage targeted towards endodontic *E. faecalis* clinical strains were possible using processed wastewater samples. The *E. faecalis* clinical strains were isolates from oral origin, either directly from endodontic infections or from the mouthwash of patients receiving endodontic treatment, and from oral lesions which were sourced from a range of oral microbiology labs in Europe. Six distinct tailed bacteriophage that belong to the Siphoviridae family as reflected from TEM micrographes named phiSHEF 2, 3, 4, 5, 6, and 7 were isolated. In general, our overall aim is to prepare a bacteriophage cocktail that contain several broad spectrum phages target towards different oral clinical strains of *E. faecalis*. This cocktail could be used as preventive measure in the form of a mouth wash prior to endodontic treatment sessions

or as intracanal irrigation in failed endodontic treated teeth to decrease the bacterial load of *E. faecalis* associated with infection in addition to preparing a library that harbour new and updated *E. faecalis* phages. This could be performed throughout isolation and characterisation of new wide spectrum phages like phiSHEF 2. In order to reach our goals, characterisation for the isolated phages were performed followed by the establishment of a biofilm model and animal model to test the efficiency of these phages to eliminate *E. faecalis* infection.

In the oral cavity, enterococci show prevalence in oral infection of 3.7 to 35% in periodontitis (Rams *et al.*, 1992, Souto and Colombo, 2008, Sun *et al.*, 2009a) and participating in oral mucosal lesions infections (Dahlén, 2009, Dahlen *et al.*, 2012). In addition, *E. faecalis* plays a role in endodontic failure and is often isolated from the obturated root canal system. The results of two studies showed that the vast majority of human chronic endodontic infection isolates were *Enterococci* (Dahlen *et al.*, 2000, Love, 2001). One reason this might be the case is that there is evidence that they can live and survive in the presence of several commonly used root canal antiseptic irrigants (e.g., sodium hypochlorite) (Spratt *et al.*, 2001), tolerate prolonged periods of starvation (Figdor *et al.*, 2003), form biofilm (Mohamed *et al.*, 2004) and acquire antibiotic resistance (Leclercq, 1997, Hunt, 1998). Moreover, anatomical variation and complexities of the tooth root canal and tooth related structures make it more selective towards bacteria that can withstand depleted nutritional levels (Nair *et al.*, 2005). All these distinct features make *E. faecalis* an exceptional survivor and place a limitation to the current chemomechanical procedure to resolve the issue. Finally, it is probably the cause behind many failed root canal treatments and outlines an urgent need for a new antimicrobial therapy (Khalifa *et al.*, 2016).

Successful attempts were made previously to isolate lytic *E. faecalis* phages using indicator strains of animal origin (Son *et al.*, 2010b, Fard *et al.*, 2010b), non-oral human isolates and lab strains (Uchiyama *et al.*, 2008a, Li *et al.*, 2014, Khalifa *et al.*, 2015a, Khalifa *et al.*, 2015b). In order to investigate the potential of phage therapy towards oral infections elimination and estimate the capability of such new antibacterial therapy, we successfully isolated and characterise six *E. faecalis* phages designated as phiSHEF 2, 3, 4, 5, 6 and 7 using an isolates from oral lesions and endodontic *E. faecalis* clinical isolates. The full chromosome of three phiSHEF phages were sequenced and annotated (phiSHEF 2, 4 and 5). PhiSHEF 4 and 5 exhibited a narrow host range compared to phiSHEF 2, 6 and 7. This might be due to the difference in the bacterial cellular target molecule for

phage adsorption between these phage and due to the fact that some bacterial strains express different types of surface molecules that are not found in the all the isolates (Gu *et al.*, 2014). PhiSHEF 3, possessed similar digested genome map of phiSHEF 2 but exhibited a different protein profile and host range.

Bioinformatics revealed that their genome size ranged from 40.9-41.3 Kbp with a GC percentage of about 34.55-34.75%. The organisation of the phiSHEF 2, 4 and 5 genome coding regions are divided into two halves transcribed in the opposite direction and that the genomes are arranged in a modular form, which include modules for DNA packaging, structural components, cell lysis (rightward transcribed genes) and a module for the regulation of the DNA replication (left ward transcribed genes). In addition, the same analysis revealed the absence of a putative gene encoding integrase, which indicate that they are likely to be lytic in nature as evidenced by our isolation method that favoured lytic viruses. Although each isolated phage exhibits a different host range, they have high similarity at the primary amino acid level (aa), suggesting that these phages might have recently diverged.

The host cellular receptor protein called PIP (phage infection protein) is proved to play an important role in phage DNA injection in G-positive bacteria as in prolate-phages (Geller *et al.*, 1993, Monteville *et al.*, 1994, Garbutt *et al.*, 1997). However, both bacterial receptor and phage adhesin PRP are important in making the phage host variation and with the PIP_{EF} receptor being identified (Duerkop *et al.*, 2016), our goal was therefore to place a site into possible tail genes that might play a role in phiSHEF phages-bacterial host recognition. Analysing their tail genome module revealed the presence of two genes that might participate in host specificity selection based on several facts: phiSHEF 2, 4 and 5 exhibited different host range and regarding amino acids level, genes 4 and 5 are the only genes in the tail locus that sharing less than 50% identity in aa level. While the N-terminal part of these two genes is highly conserved among them, the C-terminal show amino acids variable region (VR). (Duplessis and Moineau, 2001), show practically a similar trait in *Streptococcus thermophilus* phages as the N-terminal part of (ORF18) are highly conserved while changing the C-terminal variable region of phage DT1 with the C-terminal variable region from phage MD4 changed the host specificity accordingly. After that, Stuer-Lauridsen *et al.* (2003) suggested that ORF31 of phage BIL67 is one in a set of genes that participate in G-positive phage-host determinant based to a similarity to another ORF110 in phage C2 of *Lactococcus lactis*. The later ORF110 product found by immunogold electron microscopy was located at the tip of the phage

tail. Both ORFs are sharing the N-terminal and then diverging to form a variable region as in phiSHEF tail locus genes 4 and 5 (Lubbers *et al.*, 1995). Moreover, blast search of the tail gene 4 shows 27% aa similarity to tail fibre protein of *Lactobacillus* bacteria i.e. phage Lrm1 of *Lactobacillus rhamnosus* (Durmaz *et al.*, 2008). Overall, our suggestions here regarding the importance of both genes build upon their location at the tail locus, their assortment pattern of homology to phages of different G-positive bacterial and putative blast hits similarity to host specificity protein in the phage data base. Our vision will open the way for further investigation of phage host specificity and adhesion of G-positive bacteria. Finally, we suggest the genome sequence for phiSHEF 3, 6 and 7 phages, having both sequenced and annotated, proper compares of their genomes to the previously sequenced phiSHEF 2, 4 and 5 should be performed next.

The lysis module of phiSHEF phages delineated the presence of a putative protein haemolysin gene Xh1A (Pfam10779). Both haemolysin and holin encodes putative proteins that can aggregate to form structures in the inner membrane which in turn allow the endolysin out from the cytoplasm to degrade the cell wall and thus control the timing of lysis during phage infection (Longchamp *et al.*, 1994, Krogh *et al.*, 1998), thus expression of both protein Xh1A and holin is necessary to establish effective host cell lysis of *B. subtilis*.

PhiSHEF 2 phages endolysin lytic enzyme contain two domains: N-terminal catalytic domain and a C-terminal binding domain. The catalytic domain class type amidase being the same in all the three sequenced phiSHEF 2 phages, which is the most identified enzyme at the present time (Kutter and Sulakvelidze, 2004). Hence, the C-terminal half of the molecule which binds to a substrate in the host cell wall are different among them. ZoocinA_TRD (found in phiSHEF 2 and 5) is the target recognition domain of zoocin A, an exoenzyme secreted by *Streptococcus equi* subspecies *zooepidemicus* 4881 that has potent antibacterial activity against a range of streptococci including the pathogens *Streptococcus pyogenes* and *Streptococcus mutans* (Chen *et al.*, 2013). On the other hand, SH3b domains (phiSHEF 4) contain the target recognition site of another lysis exoenzyme called Lysostaphin, which is secreted by *Staphylococcus simulans* biovar *staphylolyticus*. Lysostaphin is active against the pathogen *Staphylococcus aureus* (Gargis *et al.*, 2010). Notably, both enzymes have different spectrum of susceptible bacteria. We could estimate due to the variability at the C-terminal among putative phiSHEF endolysins (TRD and SH3b recognition site) modules, indicates that the internal

host cell membrane recognition plays also a central role in diverse biological processes of endolysin-receptor interactions.

Adsorption of the tailed phage to the host surface membrane comes through the interaction between the attachment site on the phage tail and the host surface molecules (Casey *et al.*, 2015a). This may involve two main steps, such as initial reversible binding by tail adhesin with proper phage tail positioning, followed by irreversible binding of a different tail protein to secondary receptor molecule (Monteville *et al.*, 1994, Duplessis and Moineau, 2001, Spinelli *et al.*, 2006). The receptors of G-positive bacteria might be peptidoglycan elements, implanted teichoic acids, lipoteichoic acids, and associated protein (Geller *et al.*, 1993, Wendlinger *et al.*, 1996, Garbutt *et al.*, 1997, Stuer-Lauridsen *et al.*, 2003).

The enterococcal cell wall in general is composed of peptidoglycan layer (PG) that located above the lipid bilayer membrane. Like other related G-positive organisms, their PG and cell membrane decorated with a variety of polysaccharides and proteins (Archibald *et al.*, 1993, Bhavsar and Brown, 2006). Polysaccharides, teichoic acids, and surface-anchored proteins are directly chained to the cell wall PG through covalent linkages, while lipoteichoic acid and lipoproteins are anchored to membrane lipids envelope (Coyette and Hancock, 2002, Huycke and Hancock, 2011). Previous study shows that G-positive phages of *L. lactis* adsorb initially to a greater extent to rhamnose moieties of the cell wall carbohydrate, and in order to obtain a productive phage infection, adsorption to both the cell wall carbohydrates and the plasma membrane of the host are mandatory (Geller *et al.*, 1993, Monteville *et al.*, 1994, Babu *et al.*, 1994). Mutants in the *epa* main and variable locus showed lower adsorption rate of phiSHEF 2 phage than the wild type OG1RF when measured at 10 min after infection (17%, 17%, 12%, 14% compared to 50% of wild type as shown in Table 4.8. In addition, small phage numbers were counted from the free supernatant of the mutants strains 24 h after infection which were less than even the original input of 2×10^6 PFU/ml compared to high phage yield count for the wild type of 1×10^{11} PFU/ml. Whether it is not adsorbed at all or freed due to weak adhesion to the mutant cell surface, lead us to assume that Epa of *E. faecalis* function is important in phage recognition and adsorption to the bacterial host surface. Duerkop *et al.* (2016), showed that in-frame deletion of EF0858 (an integral membrane protein encodes PIP_{EF}) in *E. faecalis* V583 chromosome was resistant to phage VPE25 infection but not required for initial phage adsorption. Furthermore, PIP_{EF} is conserved in *E. faecalis* including OG1RF and harbours a 160-amino-acid hypervariable region (hpr).

A mutation in this cell wall protein hpr by the bacterial cell may result in developing phage resistance by disabling phage DNA entry. This leads us to the suggestion that unsuccessful infection of phiSHEF 2 to the *Epa* mutants cells of OG1RF might be related to disruption at the mechanism that delivers the phage DNA inside the cytoplasm across PG and plasma membrane in order to switch lytic phage infection cycle. This is in agreement with Teng *et al.* (2009), as they suggested that replacement of rhamnose with mannose in the *epaB* mutant in the overall sugar composition has an effect on the structure or integrity of the cell envelope of OG1RF. This suggestion came after TEM observation, which showed that *epaB* mutant cells result in a more round cell shape as compared to the more oval-shaped cells of wild-type. We observed the same shapes during cells screening under the TEM, however, we acknowledge that the TEM preparation itself may have altered cell morphology (Figure 4.19C and 4.20).

One of the phages isolated in this study, named phiSHEF 2 exhibited a wide host-range against oral *E. faecalis* oral clinical isolate, and thus was chosen to be further characterised. The results show that it is an efficient killer as lysis starts to occur shortly after infection, represented by the latent period of only 30 min in a one step growth experiment (Figure 4.21A). In addition, phiSHEF 2 adsorbs quickly to the cell surface as 60% of the phage particles are adsorbed within less than 9 min. However, it has a low burst size of 9.3 PFU compared to the other isolated Enterococcal phage- e.g. IME-EFm1 (Wang *et al.*, 2014). In contrast to phiSHEF 2 phage, IME-EFm1 could infect *E. faecium* isolates and did not infect any of the tested *E. faecalis*, and *vice versa*. Furthermore, looking into the behaviour of phiSHEF 2 in one step growth, low numbers of phage particles will be made if the lysis of the bacterial host happens too quickly and this might be the case here with a short latency and only 10 progenies released per event (Abedon, 1990) as in some podoviridae phages which show a short latent period and small burst sizes (Ashelford *et al.*, 1999). Due to the time limit, we suggest to repeat all phiSHEF 2 characterisations using different oral *E. faecalis* strain as phage-characterisation is both phage-strain dependant. In addition, it is important to characterise all the other isolated phiSHEF phages in a similar.

4.6.5 Biofilm models

Many studies have been done to assess the capability of *E. faecalis* to form biofilm *in vitro* and concluded that 15-80% of the clinical isolates are biofilm formers (Baldassarri *et al.*, 2001, Prakash *et al.*, 2005, Di Rosa *et al.*, 2006). Previous studies were also done to establish phage infection model to compete non-oral *E. faecalis* in animal, EF24c phage was capable of competing the *E. faecalis* infection and saving the mice model from abdominal infection (Uchiyama *et al.*, 2008b). EFDG1 was isolated using V583 strain and its host-range tested mainly using *E. faecalis* clinical strains isolated from urinary tract infections. In an *ex-vivo* of root canal model, EFDG1 was capable of eliminating *E. faecalis* colonisation of their root model and it reduce the number of bacterial tested significantly (Khalifa *et al.*, 2015a).

We aimed to set up a good model to test killing of *E. faecalis in vitro* in this study both in abiotic surface and tooth root slices biofilm, thus we chose a strain that was a good biofilm former namely EF54. In addition, it is identified previously as strong biofilm forming *E. faecalis* and it is capable of primary attachment and biofilm formation on abiotic surfaces of clinical devices (Toledo-Arana *et al.*, 2001). First, we tested elimination of biofilm on an abiotic surface which revealed that one and six days' biofilm of EF54 is efficiently and almost completely removed when phiSHEF 2 phage added. In addition, this lytic bacteriophage is capable of 7 days mature biofilm elimination from natural mineralized slices of the tooth root surfaces as estimated by resozarin metabolic assay which can be implicated in failed root canal therapy as adjunctive therapy to reduce the biofilm bacterial load associated with *E. faecalis* infection. Crystal violet was not used in this test because it might stain the tooth dentin structures with different intensity, in addition to bacterial cells biofilm, that might cause errors in reading after stain extraction. These data also reflect that phiSHEF could eliminate stationary phase *E. faecalis* as we assume that biofilm in that state. We suggest the testing of the treatment outcome of combined phage plus root canal dressing such as calcium hydroxide and compare it to either treatment in both abiotic surface and animal teeth model against chronic *E. faecalis* infection and abscess. In addition, adding extra variables such as collagen, serum, and level of acidity to test if the phage treatment still effective or might cause some retardation and/or inhibition, this is in order to improve the efficiency of phage formula such as the media that carry the phage suspensions. Regarding tooth model, we suggest testing an even longer biofilm time in mineralised tooth root surface, which might resemble persistence root canal infection and a longer phage incubation time also. Furthermore,

testing the ability of isolated and characterised phiSHEF phages in competing non-oral *E. faecalis* clinical isolates that were shown to adhere to and form biofilms on chronic instrument and device associated infections such as urethral stents and catheters, and against isolated strains that cause serious and life threatening systemic infections such as bacteraemia patients with defective immune systems.

4.6.6 Infection in an animal model- Zebrafish

Zebrafish larvae were established previously as an *in vivo* model for observing *E. faecalis* pathogenesis using model strain (Prajnsnar *et al.*, 2013). It is considered as a powerful module because it provides the advantage of monitoring the fish vital signs throughout the *E. faecalis* infection process and divide the observations into three major parts as healthy, ill and dead fish. Zebrafish were used previously as model for phage treatment to reduce the negative effect of vibriosis infection in larviculture by adding the phage and bacteria directly to the fish media (Silva *et al.*, 2014). The author considers it as inexpensive and simple approach by directly supplying phages to the fluid media. We could not prove that, as our initial trial using addition of phage to the tank media was unsuccessful to eradicate *E. faecalis* infection by adding phiSHEF 2 phage to the Zebrafish media. This could be due to differences in the pathogenicity of the bacterial strains used in both studies. Though we went for injecting the zebrafish directly with bacteria first, allowing it to disseminate for two hours then injecting the fish with phage after that.

Comparing the phage efficiency towards decreasing the mortality rate of *E. faecalis* oral clinical strains, reveals that phiSHEF 2 treatment was successful in reducing mortality of OS16-infected embryos. Out of 72% ill fish from 24 hpi, 68% were killed in OS16 strains infections at the end of second day (48 hpi). Through combining this with the one step growth infection cycle *in vitro* results, we observed that phiSHEF 2 could eliminate OS16 infection very fast and prevent the increase in *E. faecalis* cell numbers and thus allow the fish to survive and clear the infection. Data also showed that fish not dying from phage injection and the release of peptidoglycan as a result of bacterial lysis did not kill the fish. Here, we considered for the first time phage-oral clinical *E. faecalis* isolate treatment in zebrafish larvae and our results reveal that the zebrafish is a novel, successful model for testing phage efficiency towards *E. faecalis* infection. We suggest the testing the capability of phiSHEF 2 phages to eliminate *E. faecalis* infection in other animal model for example in induced abscess in mouse teeth and compare it to control

group. Furthermore, biofilm elimination should be visualized and quantified by Scanning Electron Microscope SEM after teeth are extracted.

4.7 Conclusions

Various phage like particles with different morphology were visualised by direct electron microscopy from oral and wastewater samples, which reflect the richness and diversity of bacteriophage within those samples. Six bacteriophages were isolated from concentrated wastewater named (phiSHEF2, 3, 4,5,6,7) that belong to the Siphoviridae family. They were specific to *E. faecalis* and had genome sizes ranging from 39-43kb. Full chromosome sequences of phiSHEF 2, 4 and 5 alongside biological evidence revealed that they are lytic bacteriophage which place them as suitable candidate for therapy. We tested the ability of these phage to eradicate biofilm from abiotic surfaces and a extracted natural tooth root slices model while also showing that they are able to rescue Zebrafish embryos from *E. faecalis* systemic oral clinical stain infection. Finally, we established that the extracellular Exopolysaccharide of *E. faecalis* was the bacterial docking target of these phage and they are probably involve in 2-stage infection. We suggest that these or other bacteriophage might be novel adjuncts to current endodontic therapy to eradicate recalcitrant biofilm and antibiotic resistant *E. faecalis*.

Chapter 5: Summary, Final Discussion and Future Prospects

5.1 Summary of major findings

The data presented in this thesis has contributed to the characterisation of a putative prophage present in the G-negative periodontal-associated pathogen *Fusobacterium nucleatum polymorphum* ATCC 10953. Identification of the prophage lysis gene module, and studied the possible ways of its expression to characterise its' activity. In addition, attempts were made to isolate lytic bacteriophage targeted against endodontic and oral associated pathogens from human and wastewater, characterise the isolated phages, and establish an *in vitro* model for phage-bacterial infection in order to develop them for treatments.

5.1.1 Chapter 3: Characterisation of a putative *Fusobacterium nucleatum polymorphum* ATCC 10953 prophage

- Bioinformatics for the phiFNP1 phage that has harboured in the genome of *Fusobacterium nucleatum polymorphum* ATCC 10953 was arranged in modular form. They include genes involving in phage integration and DNA replication, phage structural proteins, and a lysis module. The cornerstone for phiFNP1 prophage identification is the presence of genes that encode for structural proteins such as terminase subunits and portal protein (Casjens, 2003). In addition, the phiFNP1 is located between two tRNA coding regions that form direct repeats at either end of prophage boundary (FNP_t0043 and FNP_t0044). They share the same direct repeat sequence of 5' GCTCAATTGGATAGAGCATCTGACT 3' that gave the assumption of phiFNP1 prophage site-specific direct repeat, which is very important for future excision.
- Testing for the presence of phiFNP1 in oral samples collected from patients with chronic periodontitis attending for treatment at the Periodontal Clinic, Charles Clifford Dental Hospital revealed that phiFNP1 is common among clinical plaque samples as half of the patients tested harboured the phiFNP1 DNA (23 patients out of 45 patients screened) displayed positive results.
- An attempt was made to induce the phiFNP1 prophage from the genome of *Fusobacterium nucleatum polymorphum* ATCC 10953 strain using Mitomycin C which revealed that phiFNP1 induced from the chromosome of its host cell apparently without cell lysis as reflected by the phiFNP1 DNA positive PCR amplification and absence of its host DNA in the induced samples. However, the Mitomycin C-induced particles were neither capable of producing clear plaques

when spotted on lawns of several lab and clinical *Fusobacterium* strains nor were positive prophage bands were identified from the genome of the infected strains which indicates that they might be defective and incapable of successful phage infection.

- The genome of phiFNP1 prophage harbours three potential lysis genes named peptidoglycan-binding lysin domain protein (FNP_1699), putative hydrolase (FNP_1700) and N-acetylmuramoyl-L-alanine amidase (FNP_1707) as revealed by bioinformatics. One of these three recognised prophage genes within phiFNP1 prophage lysis module was successfully cloned (FNP_1700) and expressed by *E.coli* in soluble form. Its activity as an antibacterial agent needs further exploration as phage endolysins against *Fusobacterium* have not been previewing. These phages may aid in the treatment of periodontal diseases and also other *Fusobacterium* associated disease such as FadA adhesin positive *Fusobacterium nucleatum* that has been found to promote colorectal carcinogenesis (Rubinstein et al., 2013).

5.1.2 Chapter 4: Isolation of lytic bacteriophages targeting endodontic and oral associated pathogens from oral and wastewater

- A range of clinical strains were isolated from the dental plaque of patients with chronic periodontitis using TSBV selective media: namely several strains of *A. actinomycetemcomitans*, *Campylobacter rectus*, *Fusobacterium* spp., and *Aggregatibacter aphrophilus*. In addition, Gram staining and 16S rRNA sequencing was performed to identify the isolated strains. Some of the orally isolated clinical strains were used as indicator strains for bacteriophage isolation in addition to other clinical strains that were previously isolated from the same oral source namely *Porphyromonas*, *Prevotella* and *Fusobacterium*.
- Investigation of morphological diversity of bacteriophage within oral samples by direct electron microscopy revealed many phage like particles, displaying non-contractile tails, which putatively belong to the family Siphoviridae, phage particles with short tails that mostly belong to the family Podoviridae. In addition, filamentous, enveloped phages, and cubic phage particles with no obvious tail could also be visualised. These polyhedral phages either lost its tail during processing or belong to the family Tectiviridae. This reflects the richness and diversity of bacteriophage that were harboured in the chronic periodontal plaque samples, and this is the first study to document this fully.

- Investigation of morphological diversity of bacteriophage within Sheffield wastewater revealed a mixture of morphologically different particles as reflected from the TEM micrographs. At least 24 phage-like particles that belong mainly to all families of tailed phages with different morphologies could be identified. An equal percentage of the main two families (Siphoviridae and Myoviridae) were distributed within the visualised samples followed by Podoviridae phage like particles. However, the most variation in phage morphology in wastewater belong to the Myoviridae family, as they show more diversity in head shape morphology (being mostly isometric) and tail sheath position within the central tail.
- Several attempts were conducted to isolate bacteriophages targeting pathogens associated with periodontal disease using concentrated samples from Sheffield wastewater, plaque, saliva and dental chair drains. However, no visible plaques that indicate successful isolation were obtained after enrichment and/or direct spotting on double layer agar.
- Isolation of bacteriophage targeted towards endodontic associated pathogens were possible using processed wastewater samples. *E. faecalis* clinical strains were used as target for bacteriophage isolation, these strains were isolates from oral origin, either directly from endodontic infections or from the mouthwash of patients receiving endodontic treatment, and from oral lesions which were sourced from a range of oral microbiology labs in Europe.
- Six distinct tailed bacteriophage that belong to the Siphoviridae family named phiSHEF 2, 3, 4, 5, 6, and 7 were obtained that infect various *E. faecalis* strains based upon restriction fragment length polymorphism (RFLP) of extracted phage chromosomal DNA, protein profile, plaque morphology, and host range. They had non-contractile, long tails ranging in size from 200-250 nm depending on the phage in question and head diameters ranging from approximately 41-46 nm in diameter. Three distinct plaque morphologies were identified when infecting *E. faecalis* strains with the isolated phages.
- Full chromosome sequencing of phiSHEF 2, 4, and 5 phages revealed that their genome size ranged from 40.9-41.3 Kbp with a GC percentage of about 34.55-34.75%. Bioinformatics revealed that the organisation of the phiSHEF 2, 4 and 5 genome coding regions are divided into two halves transcribed in the opposite direction and that the genomes are arranged in a modular form.
- All phiSHEF bacteriophages were specific to *E. faecalis* as none were capable of producing visible plaques towards an *E. faecium* strain (E1162), or towards other

periodontal associated pathogens used in this study. In addition, the isolated phages exhibited different host range towards *E. faecalis* strains. They represent a panel of phages that can infect 13 clinical and lab strains both orally and non orally derived. In addition, another phage namely phiSHEF 3, that possessed similar digested genome map of phiSHEF 2 exhibited a different protein profile and host range was isolated.

- Molecular determination of phiSHEF 2, 6, and 7 phage adhesion to genetically altered strains that contain defined mutations in *Enterococcus* polysaccharide (EPS) revealed that they adhered to the surface via their extracellular polysaccharide capsule material leading to the assumption that infection is a 2-stage process. They lost their sensitivity to *epa E. faecalis* mutants. However, they still adsorb to the cell surface but could not produce successful infection cycle.
- Characterisation for the wide host range phiSHEF 2 phage revealed it was capable of *E. faecalis* elimination in a dose-dependant manner. The time needed ranged between 60 min at higher MOI down to 120 min at the lowest MOI tested. In addition, saturation of adsorption of phiSHEF 2 particles was reached after 10min and showed phiSHEF 2 was a highly efficient *E. faecalis* targeting phage with an eclipse period of only 10 min, a latent period of only 30 min, and a burst size of 9.3 PFU.
- PhiSHEF 2 phage is an efficient biofilm killer on abiotic and tooth root surfaces. When phiSHEF 2 was introduced to the biofilm both after 24 h (young biofilm) and 144 h (mature biofilm) revealed that phiSHEF 2 is capable of complete elimination of *E. faecalis* as well as 168 h biofilm formed on natural mineralised tooth root surfaces.
- Here, we considered for the first time the establishment of successful *in vivo* animal model for testing phage towards *E. faecalis* infection. Treatment of *E. faecalis* infected Zebrafish with phiSHEF 2 phage increased the survival rate from 12% (control) to 88% (treated) and the results were statistically significant as $p < 0.0001$. In addition, the results also revealed that no fish were dead or sick when injected with phiSHEF 2 only which suggest that delivery of phage alone was safe.

5.2 General discussion: oral infections control: a target approach

Much recent attention has been made to investigate bacteriophage therapy as an antimicrobial treatment option. This is due to the rise of antibiotic resistance and biofilm associated infection. In the case of difficult to treat infections such as *Pseudomonas aeruginosa* and *Staphylococcus aureus* associated with burn wound infection, phage therapy is now considered an option (Rose *et al.*, 2014). In the United States, the FDA-approved a phase I clinical trial against *P. aeruginosa* and *E. coli* chronic infections, which showed that treatment using a phage cocktail was associated with no adverse reaction (Rhoads *et al.*, 2009). This study led to phase II clinical trials in Europe using phage therapy against chronic otitis externa caused by *P. aeruginosa* infection with successful results (Wright *et al.*, 2009).

Several attempts were made to test the effect of bacteriophage elimination of oral bacterial biofilm either tested *in vitro* on a polystyrene plate or in an *ex-vivo* model of extracted tooth roots. Castillo-Ruiz *et al.* (2011), showed that reduction of bacterial count from polystyrene plate of *A. actinomycetemcomitans* and reduce it to 2.3 log₁₀ after treating an overnight biofilms with Aabphi01-1phage. 48 h old biofilms formed on polystyrene plate of *S. mutans* were challenged with phiAPCM01 that resulted in a reducing the viability of the cells by 5 log₁₀ (Dalmasso *et al.*, 2015). Bacteriophages were also successful in elimination of a biofilm of *E. faecalis* in extracted tooth roots models (Paisano *et al.*, 2004, Khalifa *et al.*, 2015a). Our results also recorded that phiSHEF 2 was an efficient biofilm killer of *E. faecalis* clinical isolate on both an abiotic surface and a tooth root slice model developed in this study. The successfulness of bacteriophages towards bacterial biofilm was attributed mainly to the fact that bacteriophage progenies resulted from infection of upper layer bacterial host of biofilm could penetrate through the successive and deeper layer until complete elimination of the bacterial host and killing and eradication of biofilm (Khalifa *et al.*, 2016). However, research concerning the efficiency of bacteriophage therapy against oral pathogens in animal model is minimal (Szafranski *et al.*, 2017). One study conducted by Uchiyama *et al.* (2008b), describe effectiveness and the safety of using phiEF24C to rescue the mouse model from non oral clinical isolate of VRE *E. faecalis* infection, with the phage introduced by single or multiple doses injected into the peritoneal cavity of the abdomen. In this study, we confirmed the possibility of using bacteriophage as therapeutic potential in animal models for systemic infection to rescue Zebrafish from infection caused by oral clinical isolate of *E. faecalis* OS16. These approaches and efforts will open the way for phage therapy to be

implicated as a solution in combating an oral infection associated with *E. faecalis* and other oral pathogens. Finally, our results also revealed the safety of using phage therapy, as delivery of phages did not kill the fish whether it is delivered alone or after pathogens injection i.e. the massive release of bacterial products such as PGN as a results of phage treatment did not kill the fish.

On the other hand, the use of phage lytic enzymes to control bacterial colonisations *in vivo* on mucosal surfaces of animals were also reported. Nelson *et al.* (2001), showed that lysin derived from streptococcal bacteriophage C1 was effective in elimination of Group A streptococci from the oral mucosal surfaces of heavily colonised mice as no pathogens were detected observed 2 h after lysin treatment. This lytic enzyme was specific to groups A, C, and E streptococci, it possessed no activity against oral streptococci and the author suggested that it could have therapeutic application towards upper respiratory mucosal epithelium infections caused by streptococci. In another study, the pneumococcal bacteriophage lytic enzyme called Pal was effective in the elimination of pneumococcal infection from nasal mucosal surfaces of mice and this lytic enzyme is also effective *in vitro* towards pneumococcal penicillin-resistant strains (Loeffler *et al.*, 2001). Certain limitations should be addressed regarding clinical application of phage lytic enzymes. Phage lytic enzymes might have a short half life, for example phage Cpl-1 enzyme which is specific to 14 strains of *S. pneumoniae* has a half life of 20 min thus repeated dose of the enzyme will be need for complete elimination in the form of constant intravenous infusion in order to be applied systemically (Loeffler *et al.*, 2003). In addition, another issue that accompanied the use of phage lytic enzymes systemically in human and animal for therapeutic purposes is the development of neutralising antibodies because they are large proteins (unlike antibiotics) that stimulate immune response. However, initial research by Fischetti (2004), indicate that anti-Cpl-1 antibodies from a rabbit hyperimmune serum did not block its activity against pneumococcal strain but slow it down to about 50%, indicating that this may not be significant hurdle to use in clinical situations.

Resistance to phage in the form of mutant strains have also been observed in many cases, and although not investigated fully in this study, it is considered as a potential problem that might place a limitation to phage therapy (Summers, 2001). In general, mutants that deliver phage resistance occur by changing the phage receptor on the cell membrane so that phage anti-receptor no longe recognise that host, which is similar to mechanisms that deliver antibiotic resistance (Drake *et al.*, 1998). Smith *et al.* (1983)

conducted a study on animals to treat experimental diarrhea caused by *E. coli* infection, they revealed that no resistant mutants strains could be isolated from the phage treated lambs, few less virulent resistance strain were recovered from treated calves and pigs. This issue could be reduced by using mixtures of phages called a “phage cocktail” that results in increasing the range of targeted bacterial pathogens and decreasing the bacterial resistance (as various phages to the same host adsorb to different membrane receptors) which is very common practice in the former Soviet Union and Poland. Most phage treatment of human infections has been used in these countries contain complex lytic phages and the resistance could not be noticed in real-life trials, even though in laboratory situations resistance is often observed under the stringent selection procedures seen in lab infections. Some of these trials were reviewed by (Abedon *et al.*, 2011) and are illustrated in chapter one Table 1. 2. We did not notice any resistance to phiSHEF phages in biofilm models and also in animal model. A second problem towards phage therapy is the development of neutralising antibody. Phage antibodies were detected towards *S. aureus* phage in 21% of patients examined during a study in Poland and the level of antibodies increased to 54% after treatments, though most patients (27 out of 30) showed no further signs of infection including those with high level of antibody titers (Kucharewicz-Krukowska and Slopek, 1987). In addition, purified phiX174 were used extensively to monitor humoral immune function in immunocompetent and immunocompromised patients without any apparent side effects (Ochs *et al.*, 1993, Fogelman *et al.*, 2000). In conclusion, even when high titers of phage neutralising antibodies are presents or multiple dose are needed, it is possible to use phage therapy in an effective way.

5.3 Future prospects

Bacteriophage are viruses that infect bacteria only. Each virion resemble a complex mobile factory that carries its genome from one host to another to control the production of more new phages. Although they harbour all the information to control their reproduction, their genome have no equipments to produce energy and no ribosomes in order to make protein. Once phage genomes injected successfully inside the bacterial host, it will be exposed to host exonucleases and other restriction enzymes. Therefore, phages have counteracts methods represented by circularize their DNA immediately through their sticky ends or terminal redundancies or mediate the early transcription of certain genes in which their products inhibits the host nuclease such as in T4 bacteriophage (Silverstein and Goldberg, 1976, Amitsur *et al.*, 1987). However, the process of lytic infection is correlated to the host metabolic machinery and its energetic

state at the time of infections such as increasing in phage progenies release rate and numbers of T4 bacteriophage with the increase of bacterial growth rate, while at the same time the eclipse and latent periods decreased (Hadas *et al.*, 1997).

Bacteriophages exhibit diverse susceptibility to various physical and chemical agents such as pH, dryness, UV, detergents, chelating agents, alcohols, and heat. In general, phages are stable in pH of 5-8, susceptible to UV light in the range of 260nm and above but they might still infective as no protein created at this stage, and detergents have less effects on phages than do on bacteria (Kutter and Sulakvelidze, 2004). However, each phage need to be individually characterised in order to be developed for specific treatments. Regarding our study, we could hypothetically develop our isolated phiSHEF phages to be used in oral infection control and treatment either as adjunctive or preventive therapy, these clinical prospects can be summarised by the followings:

A-Mouth wash/foam before and during endodontic treatment (preventive).

B-Irrigation (intra canal irrigation): Chronic infections associated with biofilm and/or antibiotic resistant *Enterococcus* bacteria.

C-Topical applications in non-oral and oral mucosal surfaces infections such as skin infection and infection associated with *Enterococcus* pathogens (antibiotic resistant).

The endodontic treatment procedure involves frequent and alternate use of sodium hypochlorite solution, chlorhexidine solutions, calcium hydroxide, and mineral trioxide aggregate (MTA) at various stages of treatment (Evans *et al.*, 2002, Torabinejad *et al.*, 1995, de Almeida Gomes *et al.*, 2006). The susceptibility and exposure of bacteriophage particles to these various agents should be evaluated first to provide deeper insight into the proper combinations that might be used to obtain the best results. Most of endodontic dental medications mentioned above likely expose the bacteriophage particles to high alkaline range of pH 10.1-12.5 that might result in inactivation; bacteriophages should be exposed to various dilutions with gradual pH values of these material followed by testing the phage counts and viability on their host to identify the lethal dose. However, these values represents the net pH at the time of placement which might be diluted by various agents such as various tissue fluid in the root canal and dentin resulted in lower pH as various pH changes in dental tissues of monkeys were recorded in the range of 7.4-11.1 from various locations of teeth after endodontic treatment with calcium hydroxide (Tronstad *et al.*, 1981). In addition, the pH of aspirated pus from periapical abscesses of human teeth had a range between 6 and 7.3 (Nekoofar *et al.*, 2009), as suitable values for

phage infections, phage delivery or intracanal irrigation with phage suspension could be performed first before the delivery of intracanal medications, which will allow the diffusion and adsorption of the phage particles to its suitable hosts. During clinical endodontic treatment, sodium hypochlorite solution is also used in a concentration range of 0.5–5% (Evans *et al.*, 2002). Phage resistance to sodium hypochlorite were varied in different studies, being as low as 100 ppm (residual free chlorine) of *Lb. helveticus* phage (Quiberoni *et al.*, 1999) to 800 ppm (Marcó *et al.*, 2009) which is higher than that used in dentistry. This also should be addressed in future experiments. Finally, the vehicle which harbour the phage particles suspension should be also investigated and chosen according to the specified application such as proper solution carrier and formulation that might be used in a mouth wash or intracanal irrigation and proper gel or ointment carrier to treat mucosal surfaces infections.

The use of bacteriophage and/or their products (lytic enzymes), may have the opportunity to control or eliminate oral infections because they are shown to reduce or prevent infection caused by these bacteria. In addition to their apparent superiority to eradicate biofilm forming and antibiotic resistant pathogens, they have great potential to decrease the need for antibiotics consumption in routine practice throughout the use of bacteriophages as adjunctive therapy for prophylaxis. However, state of the art biotechnology should be used to purify, produce, and characterise the phage preparations to further ensure the effectiveness and safety of treatments without any unwanted side-effects.

References

- AAGAARD, K., RIEHLE, K., MA, J., SEGATA, N., MISTRETTA, T.-A., COARFA, C., RAZA, S., ROSENBAUM, S., VAN DEN VEYVER, I. & MILOSAVLJEVIC, A. 2012. A metagenomic approach to characterization of the vaginal microbiome signature in pregnancy. *PloS one* **7**: e36466.
- ABEDON, S. T., KUHL, S. J., BLASDEL, B. G. & KUTTER, E. M. 2011. Phage treatment of human infections. *Bacteriophage* **1**: 66-85.
- ACKERMANN, H.-W. 2007. 5500 Phages examined in the electron microscope. *Archives of virology* **152**: 227-243.
- AMMANN, T., BOSTANCI, N., BELIBASAKIS, G. & THURNHEER, T. 2013. Validation of a quantitative real-time PCR assay and comparison with fluorescence microscopy and selective agar plate counting for species-specific quantification of an in vitro subgingival biofilm model. *Journal of periodontal research* **48**: 517-526.
- ANPILOV, L. & PROKUDIN, A. 1984. Preventive effectiveness of dried polyvalent *Shigella* bacteriophage in organized collective farms. *Voенно-meditinskii zhurnal* 39-40.
- BACHRACH, G., IANCULOVICI, C., NAOR, R. & WEISS, E. I. 2005. Fluorescence based measurements of *Fusobacterium nucleatum* coaggregation and of fusobacterial attachment to mammalian cells. *FEMS microbiology letters* **248**: 235-240.
- BACHRACH, G., LEIZEROVICI-ZIGMOND, M., ZLOTKIN, A., NAOR, R. & STEINBERG, D. 2003. Bacteriophage isolation from human saliva. *Letters in applied microbiology* **36**: 50-53.
- BOGOVAZOVA, G., VOROSHILOVA, N., BONDARENKO, V., GORBATKOVA, G., AFANAS' EVA, E., KAZAKOVA, T., SMIRNOV, V., MAMLEEVA, A., GLUKHAREV, I. & ERASTOVA, E. 1992. Immunobiological properties and therapeutic effectiveness of preparations from *Klebsiella* bacteriophages. *Zhurnal mikrobiologii, epidemiologii, i immunobiologii* 30-33.
- BOURGOGNE, A., GARSIN, D. A., QIN, X., SINGH, K. V., SILLANPAA, J., YERRAPRAGADA, S., DING, Y., DUGAN-ROCHA, S., BUHAY, C. & SHEN, H. 2008. Large scale variation in *Enterococcus faecalis* illustrated by the genome analysis of strain OG1RF. *Genome biology* **9**: R110.
- BROOK, I. 1994. Fusobacterial infections in children. *Journal of Infection* **28**: 155-165.
- CASARIN, R., BARBAGALLO, A., MEULMAN, T., SANTOS, V., SALLUM, E., NOCITI, F., DUARTE, P., CASATI, M. & GONÇALVES, R. 2013. Subgingival biodiversity in subjects with uncontrolled type-2 diabetes and chronic periodontitis. *Journal of periodontal research* **48**: 30-36.
- CHAUSHU, S., WILENSKY, A., GUR, C., SHAPIRA, L., ELBOIM, M., HALFTEK, G., POLAK, D., ACHDOUT, H., BACHRACH, G. & MANDELBOIM, O. 2012. Direct recognition of *Fusobacterium nucleatum* by the NK cell natural cytotoxicity receptor NKp46 aggravates periodontal disease. *PLoS pathogens* **8**: e1002601.
- DAHLEN, G., BLOMQVIST, S., ALMSTÅHL, A. & CARLEN, A. 2012. Virulence factors and antibiotic susceptibility in enterococci isolated from oral mucosal and deep infections. *Journal of oral microbiology* **4**.
- DIDILESCU, A., RUSU, D., ANGHEL, A., NICA, L., ILIESCU, A., GREABU, M., BANCESCU, G. & STRATUL, S. 2012. Investigation of six selected bacterial

- species in endo-periodontal lesions. *International endodontic journal* **45**: 282-293.
- DOUGLAS, C. I., NAYLOR, K., PHANSOPA, C., FREY, A. M., FARMILO, T. & STAFFORD, G. P. 2014. Chapter Six-Physiological Adaptations of Key Oral Bacteria. *Advances in microbial physiology* **65**: 257-335.
- EDLUND, A., SANTIAGO-RODRIGUEZ, T. M., BOEHM, T. K. & PRIDE, D. T. 2015. Bacteriophage and their potential roles in the human oral cavity. *Journal of oral microbiology* **7**: 27423.
- EDWARDS, A. M., GROSSMAN, T. J. & RUDNEY, J. D. 2006. *Fusobacterium nucleatum* transports noninvasive *Streptococcus cristatus* into human epithelial cells. *Infection and immunity* **74**: 654-662.
- ELBREKI, M., ROSS, R., HILL, C., O'MAHONY, J., MCAULIFFE, O. & COFFEY, A. 2014. Bacteriophages and their derivatives as bio-therapeutic agents in disease prevention and treatment.
- ELKAIM, R., DAHAN, M., KOCGOZLU, L., WERNER, S., KANTER, D., KRETZ, J. & TENENBAUM, H. 2008. Prevalence of periodontal pathogens in subgingival lesions, atherosclerotic plaques and healthy blood vessels: a preliminary study. *Journal of periodontal research* **43**: 224-231.
- FARD, R. M. N., BARTON, M. D., ARTHUR, J. L. & HEUZENROEDER, M. W. 2010. Whole-genome sequencing and gene mapping of a newly isolated lytic enterococcal bacteriophage EFRM31. *Archives of virology* **155**: 1887-1891.
- FARDINI, Y., WANG, X., TÉMOIN, S., NITHIANANTHAM, S., LEE, D., SHOHAM, M. & HAN, Y. W. 2011. *Fusobacterium nucleatum* adhesin FadA binds vascular endothelial cadherin and alters endothelial integrity. *Molecular microbiology* **82**: 1468-1480.
- FISCHETTI, V. A. 2008. Bacteriophage lysins as effective antibacterials. *Current opinion in microbiology* **11**: 393-400.
- FISCHETTI, V. A. 2010. Bacteriophage endolysins: a novel anti-infective to control Gram-positive pathogens. *International Journal of Medical Microbiology* **300**: 357-362.
- FOGLESONG, M. & MARKOVETZ, A. 1974. Morphology of bacteriophage-like particles from *Fusobacterium symbiosum*. *Journal of bacteriology* **119**: 325-329.
- FUJII, R., SAITO, Y., TOKURA, Y., NAKAGAWA, K. I., OKUDA, K. & ISHIHARA, K. 2009. Characterization of bacterial flora in persistent apical periodontitis lesions. *Molecular Oral Microbiology* **24**: 502-505.
- GARCÍA, P., RODRÍGUEZ, L., RODRÍGUEZ, A. & MARTÍNEZ, B. 2010. Food biopreservation: promising strategies using bacteriocins, bacteriophages and endolysins. *Trends in Food Science & Technology* **21**: 373-382.
- GOODFELLOW, M. & STACKEBRANDT, E. 1991. *Nucleic acid techniques in bacterial systematics*, J. Wiley.
- GOULD, I. M. & BAL, A. M. 2013. New antibiotic agents in the pipeline and how they can help overcome microbial resistance. *Virulence* **4**: 185-191.
- GRIFFEN, A. L., BEALL, C. J., CAMPBELL, J. H., FIRESTONE, N. D., KUMAR, P. S., YANG, Z. K., PODAR, M. & LEYS, E. J. 2012. Distinct and complex bacterial profiles in human periodontitis and health revealed by 16S pyrosequencing. *The ISME journal* **6**: 1176-1185.
- GUL, S. S., GRIFFITHS, G. S., STAFFORD, G. P., AL-ZUBIDI, M. I., RAWLINSON, A. & DOUGLAS, C. W. 2017. Investigation of a Novel Predictive Biomarker Profile for the Outcome of Periodontal Treatment. *Journal of Periodontology* 1-14.
- GUPTA, S., GHOSH, S. K., SCOTT, M. E., BAINBRIDGE, B., JIANG, B., LAMONT, R. J., MCCORMICK, T. S. & WEINBERG, A. 2010. *Fusobacterium nucleatum*-

- associated β -Defensin Inducer (FAD-I) IDENTIFICATION, ISOLATION, AND FUNCTIONAL EVALUATION. *Journal of Biological Chemistry* **285**: 36523-36531.
- HAIJISHENGALLIS, G. & LAMONT, R. J. 2016. Dancing with the stars: how choreographed bacterial interactions dictate nososymbiocity and give rise to keystone pathogens, accessory pathogens, and pathobionts. *Trends in microbiology* **24**: 477-489.
- HAN, Y. 2011a. Oral health and adverse pregnancy outcomes—what’s next? *Journal of dental research* **90**: 289-293.
- HAN, Y. & WANG, X. 2013. Mobile microbiome: oral bacteria in extra-oral infections and inflammation. *Journal of dental research* **92**: 485-491.
- HAN, Y. W. 2011b. 15 *FUSOBACTERIUM NUCLEATUM* INTERACTION WITH HOST CELLS. *Oral microbial communities: genomic inquiry and interspecies communication*.
- HAN, Y. W. 2011c. Can oral bacteria cause pregnancy complications? *Women’s health* **7**: 401-404.
- HAN, Y. W. 2015. *Fusobacterium nucleatum*: a commensal-turned pathogen. *Current opinion in microbiology* **23**: 141-147.
- HAN, Y. W., IKEGAMI, A., CHUNG, P., ZHANG, L. & DENG, C. X. 2007. Sonoporation is an efficient tool for intracellular fluorescent dextran delivery and one-step double-crossover mutant construction in *Fusobacterium nucleatum*. *Applied and environmental microbiology* **73**: 3677-3683.
- HAN, Y. W., IKEGAMI, A., RAJANNA, C., KAWSAR, H. I., ZHOU, Y., LI, M., SOJAR, H. T., GENCO, R. J., KURAMITSU, H. K. & DENG, C. X. 2005. Identification and characterization of a novel adhesin unique to oral fusobacteria. *Journal of bacteriology* **187**: 5330-5340.
- HAN, Y. W., SHI, W., HUANG, G. T.-J., HAAKE, S. K., PARK, N.-H., KURAMITSU, H. & GENCO, R. J. 2000. Interactions between periodontal bacteria and human oral epithelial cells: *Fusobacterium nucleatum* adheres to and invades epithelial cells. *Infection and immunity* **68**: 3140-3146.
- HANCOCK, L. E. & GILMORE, M. S. 2002. The capsular polysaccharide of *Enterococcus faecalis* and its relationship to other polysaccharides in the cell wall. *Proceedings of the National Academy of Sciences* **99**: 1574-1579.
- HANCOCK, R. & BRAUN, V. 1976. Nature of the energy requirement for the irreversible adsorption of bacteriophages T1 and phi80 to *Escherichia coli*. *Journal of Bacteriology* **125**: 409-415.
- HITCH, G., PRATTEN, J. & TAYLOR, P. 2004. Isolation of bacteriophages from the oral cavity. *Letters in applied microbiology* **39**: 215-219.
- JACOB, A. E. & HOBBS, S. J. 1974. Conjugal transfer of plasmid-borne multiple antibiotic resistance in *Streptococcus faecalis* var. *zymogenes*. *Journal of Bacteriology* **117**: 360-372.
- JOHNSON, E. M., FLANNAGAN, S. E. & SEDGLEY, C. M. 2006. Coaggregation Interactions Between Oral and Endodontic *Enterococcus faecalis* and Bacterial Species Isolated From Persistent Apical Periodontitis. *Journal of endodontics* **32**: 946-950.
- KAPLAN, A., KAPLAN, C. W., HE, X., MCHARDY, I., SHI, W. & LUX, R. 2014. Characterization of aid1, a novel gene involved in *Fusobacterium nucleatum* interspecies interactions. *Microbial ecology* **68**: 379-387.
- KAPLAN, C. W., LUX, R., HAAKE, S. K. & SHI, W. 2009. The *Fusobacterium nucleatum* outer membrane protein RadD is an arginine-inhibitable adhesin required for inter-species adherence and the structured architecture of multispecies biofilm. *Molecular microbiology* **71**: 35-47.

- KAPLAN, C. W., MA, X., PARANJPE, A., JEWETT, A., LUX, R., KINDER-HAAKE, S. & SHI, W. 2010. *Fusobacterium nucleatum* outer membrane proteins Fap2 and RadD induce cell death in human lymphocytes. *Infection and immunity* **78**: 4773-4778.
- KARPATHY, S. E., QIN, X., GIOIA, J., JIANG, H., LIU, Y., PETROSINO, J. F., YERRAPRAGADA, S., FOX, G. E., HAAKE, S. K. & WEINSTOCK, G. M. 2007. Genome sequence of *Fusobacterium nucleatum* subspecies *polymorphum*—a genetically tractable *Fusobacterium*. *PLoS One* **2**: e659.
- KAYA OGLU, G. & ØRSTAVIK, D. 2004. Virulence factors of *Enterococcus faecalis*: relationship to endodontic disease. *Critical Reviews in Oral Biology & Medicine* **15**: 308-320.
- KHALIFA, L., BROSH, Y., GELMAN, D., COPPENHAGEN-GLAZER, S., BEYTH, S., PORADOSU-COHEN, R., QUE, Y.-A., BEYTH, N. & HAZAN, R. 2015a. Targeting *Enterococcus faecalis* biofilms with phage therapy. *Applied and environmental microbiology* **81**: 2696-2705.
- KHALIFA, L., COPPENHAGEN-GLAZER, S., SHLEZINGER, M., KOTT-GUTKOWSKI, M., ADINI, O., BEYTH, N. & HAZAN, R. 2015b. Complete genome sequence of *Enterococcus bacteriophage* EFLK1. *Genome announcements* **3**: e01308-15.
- KHALIFA, L., SHLEZINGER, M., BEYTH, S., HOURI-HADDAD, Y., COPPENHAGEN-GLAZER, S., BEYTH, N. & HAZAN, R. 2016. Phage therapy against *Enterococcus faecalis* in dental root canals. *Journal of oral microbiology* **8**: 32157.
- KISTLER, J. O., BOOTH, V., BRADSHAW, D. J. & WADE, W. G. 2013. Bacterial community development in experimental gingivitis. *PloS one* **8**: e71227.
- KOCHETKOVA, V., MAMONTOV, A., MOSKOVITSEVA, R., ERASTOVA, E., TROFIMOV, E., POPOV, M. & DZHUBALIEVA, S. 1989. Phagotherapy of postoperative suppurative-inflammatory complications in patients with neoplasms. *Sovetskaia meditsina* 23-26.
- LI, X., DING, P., HAN, C., FAN, H., WANG, Y., MI, Z., FENG, F. & TONG, Y. 2014. Genome analysis of *Enterococcus faecalis* bacteriophage IME-EF3 harboring a putative metallo-beta-lactamase gene. *Virus genes* **49**: 145-151.
- LIU, P., LIU, Y., WANG, J., GUO, Y., ZHANG, Y. & XIAO, S. 2014. Detection of *Fusobacterium nucleatum* and fadA adhesin gene in patients with orthodontic gingivitis and non-orthodontic periodontal inflammation. *PLoS One* **9**: e85280.
- LOOZEN, G., OZCELIK, O., BOON, N., DE MOL, A., SCHOEN, C., QUIRYNEN, M. & TEUGHEL, W. 2014. Inter-bacterial correlations in subgingival biofilms: a large-scale survey. *Journal of clinical periodontology* **41**: 1-10.
- LUI, A., MCBRIDE, B., VOVIS, G. & SMITH, M. 1979. Site specific endonuclease from *Fusobacterium nucleatum*. *Nucleic acids research* **6**: 1-15.
- LUM, A. G., PRIDE, D. T., SALZMAN, J., LY, M., ROBLES-SIKISAKA, R., ABELES, S. R. & BOEHM, T. K. 2014. Human oral viruses are personal, persistent and gender-consistent. *The ISME journal* **8**: 1753.
- LY, M., ABELES, S. R., BOEHM, T. K., ROBLES-SIKISAKA, R., NAIDU, M., SANTIAGO-RODRIGUEZ, T. & PRIDE, D. T. 2014. Altered oral viral ecology in association with periodontal disease. *MBio* **5**: e01133-14.
- MARKOISHVILI, K., TSITLANADZE, G., KATSARAVA, R., GLENN, J. & SULAKVELIDZE, A. 2002. A novel sustained-release matrix based on biodegradable poly (ester amide) s and impregnated with bacteriophages and an antibiotic shows promise in management of infected venous stasis ulcers and other poorly healing wounds. *International journal of dermatology* **41**: 453-458.

- MARSH, P. D. & DEVINE, D. A. 2011. How is the development of dental biofilms influenced by the host? *Journal of Clinical Periodontology* **38**: 28-35.
- MCGUIRE, A. M., COCHRANE, K., GRIGGS, A. D., HAAS, B. J., ABEEL, T., ZENG, Q., NICE, J. B., MACDONALD, H., BIRREN, B. W. & BERGER, B. W. 2014. Evolution of invasion in a diverse set of *Fusobacterium* species. *MBio* **5**: e01864-14.
- MILIUTINA, L. N. & VOROTYNTSEVA, N. V. 1993. Current strategy and tactics of etiotropic therapy of acute intestinal infections in children. *Antibiot Khimioter* **38**: 46-53.
- MOORE, W. & MOORE, L. V. 1994. The bacteria of periodontal diseases. *Periodontology 2000* **5**: 66-77.
- NAIDU, M., ROBLES-SIKISAKA, R., ABELES, S. R., BOEHM, T. K. & PRIDE, D. T. 2014. Characterization of bacteriophage communities and CRISPR profiles from dental plaque. *BMC microbiology* **14**: 175.
- ORTIZ, P., BISSADA, N. F., PALOMO, L., HAN, Y. W., AL-ZAHRANI, M. S., PANNEERSELVAM, A. & ASKARI, A. 2009. Periodontal therapy reduces the severity of active rheumatoid arthritis in patients treated with or without tumor necrosis factor inhibitors. *Journal of periodontology* **80**: 535-540.
- PAULSEN, I. T., BANERJEE, L., MYERS, G., NELSON, K., SESHADRI, R., READ, T. D., FOUTS, D. E., EISEN, J. A., GILL, S. R. & HEIDELBERG, J. 2003. Role of mobile DNA in the evolution of vancomycin-resistant *Enterococcus faecalis*. *Science* **299**: 2071-2074.
- PEREPANOVA, T., DARBEEVA, O., KOTLIAROVA, G., KONDRATEVA, E., MAĪSKAIA, L., MALYSHEVA, V., BAĪGUZINA, F. & GRISHKOVA, N. 1995. The efficacy of bacteriophage preparations in treating inflammatory urologic diseases. *Urologiia i nefrologiia* 14-17.
- PRIDE, D. T., SALZMAN, J., HAYNES, M., ROHWER, F., DAVIS-LONG, C., WHITE, R. A., LOOMER, P., ARMITAGE, G. C. & RELMAN, D. A. 2012. Evidence of a robust resident bacteriophage population revealed through analysis of the human salivary virome. *The ISME journal* **6**: 915-926.
- RUBINSTEIN, M. R., WANG, X., LIU, W., HAO, Y., CAI, G. & HAN, Y. W. 2013. *Fusobacterium nucleatum* promotes colorectal carcinogenesis by modulating E-cadherin/ β -catenin signaling via its FadA adhesin. *Cell host & microbe* **14**: 195-206.
- SAKANDELIDZE, V. 1991. The combined use of specific phages and antibiotics in different infectious allergoses. *Vrachebnoe delo* 60-63.
- SANTIAGO-RODRIGUEZ, T. M., NAIDU, M., ABELES, S. R., BOEHM, T. K., LY, M. & PRIDE, D. T. 2015. Transcriptome analysis of bacteriophage communities in periodontal health and disease. *BMC genomics* **16**: 549.
- SEDGLEY, C., LENNAN, S. & CLEWELL, D. 2004. Prevalence, phenotype and genotype of oral enterococci. *Oral microbiology and immunology* **19**: 95-101.
- SEDGLEY, C., NAGEL, A., SHELBURNE, C., CLEWELL, D., APPELBE, O. & MOLANDER, A. 2005. Quantitative real-time PCR detection of oral *Enterococcus faecalis* in humans. *Archives of oral biology* **50**: 575-583.
- SEGATA, N., HAAKE, S. K., MANNON, P., LEMON, K. P., WALDRON, L., GEVERS, D., HUTTENHOWER, C. & IZARD, J. 2012. Composition of the adult digestive tract bacterial microbiome based on seven mouth surfaces, tonsils, throat and stool samples. *Genome biology* **13**: R42.
- SLOTS, J. 1982. Selective medium for isolation of *Actinobacillus actinomycetemcomitans*. *Journal of Clinical Microbiology* **15**: 606-609.

- SMITH, C. J. & OSBORN, A. M. 2009. Advantages and limitations of quantitative PCR (Q-PCR)-based approaches in microbial ecology. *FEMS microbiology ecology* **67**: 6-20.
- SOCRANSKY, S., HAFFAJEE, A., CUGINI, M., SMITH, C. & KENT, R. 1998. Microbial complexes in subgingival plaque. *Journal of clinical periodontology* **25**: 134-144.
- SON, J., JUN, S., KIM, E., PARK, J., PAIK, H., YOON, S., KANG, S. & CHOI, Y. J. 2010. Complete genome sequence of a newly isolated lytic bacteriophage, EFAP-1 of *Enterococcus faecalis*, and antibacterial activity of its endolysin EFAL-1. *Journal of applied microbiology* **108**: 1769-1779.
- TOLEDO-ARANA, A., VALLE, J., SOLANO, C., ARRIZUBIETA, M. A. J., CUCARELLA, C., LAMATA, M., AMORENA, B., LEIVA, J., PENADÉS, J. R. & LASA, I. 2001. The enterococcal surface protein, Esp, is involved in *Enterococcus faecalis* biofilm formation. *Applied and environmental microbiology* **67**: 4538-4545.
- VAN DEN BOGAARD, A., MERTENS, P., LONDON, N. & STOBBERINGH, E. 1997. High prevalence of colonization with vancomycin-and pristinamycin-resistant enterococci in healthy humans and pigs in The Netherlands: is the addition of antibiotics to animal feeds to blame? *Journal of Antimicrobial Chemotherapy* **40**: 454-456.
- VENTOLA, C. L. 2015. The antibiotic resistance crisis: part 1: causes and threats. *Pharmacy and Therapeutics* **40**: 277.
- VIANNA, M., CONRADS, G., GOMES, B. & HORZ, H. 2006. Identification and quantification of archaea involved in primary endodontic infections. *Journal of clinical microbiology* **44**: 1274-1282.
- XU, Y., SINGH, K. V., QIN, X., MURRAY, B. E. & WEINSTOCK, G. M. 2000. Analysis of a gene cluster of *Enterococcus faecalis* involved in polysaccharide biosynthesis. *Infection and immunity* **68**: 815-823.
- YANG, N. Y., ZHANG, Q., LI, J. L., YANG, S. H. & SHI, Q. 2014. Progression of periodontal inflammation in adolescents is associated with increased number of *Porphyromonas gingivalis*, *Prevotella intermedia*, *Tannerella forsythensis*, and *Fusobacterium nucleatum*. *International journal of paediatric dentistry* **24**: 226-233.

Appendices

Appendix 1

Patient Information Sheet

Version 2.3 02/02/2016

Isolation of Bacteriophage as potential sources of oral antimicrobials

You are being invited to take part in a research study. Before you decide it is important for you to understand why the research is being done and what it will involve. Please take time to read the following information sheet carefully and discuss it with others if you wish. Ask us if there is anything that is not clear or if you would like more information. Take time to decide whether or not you wish to take part. Thank you for reading this.

What is the purpose of the study?

This study is part of PhD project that aims to investigate the presence of the bacteria and viruses in samples taken from saliva and dental plaque. We think the knowledge gained might be used in the treatment of gum diseases in the future. Saliva and dental plaque samples will be collected from patients attending for routine dental treatment.

Why have I been chosen?

You have been chosen because you are being treated for a gum condition. If you agree to take part, you will be one of several similar patients participating in this study.

Do I have to take part?

No, it is up to you to decide whether or not to take part. If you do decide to take part you will be given the opportunity to consider this information and ask any questions you may have when you return for treatment. You will then be asked to sign the consent form if you agree to take part in the study. If you decide to take part you are still free to withdraw at any time without giving a reason and any unused samples will also be destroyed.

What will happen if I agree to take part in the study?

You will receive your treatment as normal but instead of discarding the dental plaque removed during treatment, we will collect some in tubes. You will also be asked to donate saliva into a sterile tube prior to your treatment being started. We may ask you for another sample at your next appointment, because we are also investigating the bacteria and viruses in samples at different time points.

What are the possible disadvantages and risks of taking part?

The procedures of sampling plaque and saliva may take up to an additional 10 minutes but are they not associated with any further discomfort. It is unlikely that the study samples would highlight any infection; however, in the event that an issue is identified during the course of the study, we would arrange for you to have the appropriate treatment under the guidance of the consultant in charge of the dental hospital.

What are the possible benefits of taking part?

There are no direct benefits to you of taking part. It is hoped that the information we get from this study may help other people with gum disease in the future.

(Version 2.3, 02/02/2016, STH19056)

Patient Information Sheet

Version 2.3 02/02/2016

Isolation of Bacteriophage as potential sources of oral antimicrobials

You are being invited to take part in a research study. Before you decide it is important for you to understand why the research is being done and what it will involve. Please take time to read the following information sheet carefully and discuss it with others if you wish. Ask us if there is anything that is not clear or if you would like more information. Take time to decide whether or not you wish to take part. Thank you for reading this.

What is the purpose of the study?

This study is part of PhD project that aims to investigate the presence of the bacteria and viruses in samples taken from saliva and dental plaque. We think the knowledge gained might be used in the treatment of gum diseases in the future. Saliva and dental plaque samples will be collected from patients attending for routine dental treatment.

Why have I been chosen?

You have been chosen because you are being treated for a gum condition. If you agree to take part, you will be one of several similar patients participating in this study.

Do I have to take part?

No, it is up to you to decide whether or not to take part. If you do decide to take part you will be given the opportunity to consider this information and ask any questions you may have when you return for treatment. You will then be asked to sign the consent form if you agree to take part in the study. If you decide to take part you are still free to withdraw at any time without giving a reason and any unused samples will also be destroyed.

What will happen if I agree to take part in the study?

You will receive your treatment as normal but instead of discarding the dental plaque removed during treatment, we will collect some in tubes. You will also be asked to donate saliva into a sterile tube prior to your treatment being started. We may ask you for another sample at your next appointment, because we are also investigating the bacteria and viruses in samples at different time points.

What are the possible disadvantages and risks of taking part?

The procedures of sampling plaque and saliva may take up to an additional 10 minutes but are they not associated with any further discomfort. It is unlikely that the study samples would highlight any infection; however, in the event that an issue is identified during the course of the study, we would arrange for you to have the appropriate treatment under the guidance of the consultant in charge of the dental hospital.

What are the possible benefits of taking part?

There are no direct benefits to you of taking part. It is hoped that the information we get from this study may help other people with gum disease in the future.

(Version 2.3, 02/02/2016, 5TH19056)

Patient Consent Form (Version 2.3 02/02/2016)

Centre Number:

Study Number:

Patient Identification Number for this trial:

CONSENT FORM

Title of Project: **Isolation of bacteriophage as potential source of oral antimicrobials**

Principle investigator: Professor A Rawlinson

Chief investigator: Mohammed Al-Zubidi

Please initial all boxes

1. I confirm that I have read and understand the information sheet dated 02/02/2016 version 2.3 for the above study. I have had the opportunity to consider the information, ask questions and have had these answered satisfactorily.
2. I understand that my participation is voluntary and that I am free to withdraw at any time without giving any reason, without my medical care or legal rights being affected.
3. I understand that relevant sections of my medical notes and data collected during the study, may be looked at by individuals from regulatory authorities or from the NHS Trust, where it is relevant to my taking part in this research. I give permission for these individuals to have access to my records.
4. Further samples may be taken during dental treatment as patients are being recruited at different time stage of treatment.
5. I agree to take part in the above study.

Name of Participant

Date

Signature

Name of Person
giving consent.

Date

Signature

(Version 2.3, 02/02/2016, STH19056)

Apendix 2



Finance and Commercial

To Mohammed Al-Zubidi
Your ref STH19056
Date Issued 11.12.15

Certificate of Insurances (non clinical trial)

Trial Number NCT 15/19
Department Clinical Dentistry
Principal Investigator Prof. Andrew Rawlinson
Title of Trial
Investigation of bacteriophage as potential source of oral antimicrobials
Name of Investigators As stated
Commencement Date 01/02/2016

The University has in place insurance against liabilities for which it may be legally liable and this cover includes any such liabilities arising out of the above research project/study

Joanne Rollitt
Insurance Section



Health Research Authority

Yorkshire & The Humber - Sheffield Research Ethics Committee

Jarrow Business Centre

Viking Business Park

Rolling Mill Road

Jarrow

Tyne and Wear

NE32 3DT

Telephone: 0191 4283564

12 January 2016

Dr Mohammed Al-Zubidi
PhD student
School of Clinical Dentistry / University of Sheffield
School of Clinical Dentistry
Claremont Crescent
Sheffield
S10 2TA

Dear Dr Al-Zubidi

Study title:	Investigation of bacteriophage as potential source of oral antimicrobials
REC reference:	16/YH/0033
Protocol number:	STH19056
IRAS project ID:	186132

Thank you for your application for ethical review, which was received on 07 January 2016. I can confirm that the application is valid and will be reviewed by the Proportionate Review Sub-Committee in correspondence. To enable the Proportionate Review Sub Committee to provide you with a final opinion within 10 working days your application documentation will be sent by email to Committee members.

One of the REC members is appointed as the lead reviewer for each application reviewed by the Sub-Committee.

Please note that the lead reviewer may wish to contact you by phone or email between Friday 15 and Friday 22 January 2016 to clarify any points that might be raised by members and assist the Sub-Committee in reaching a decision. **Please note you will only have 24 hours to respond to any request for additional information.**

If you will not be available between these dates, you are welcome to nominate another key investigator or a representative of the study sponsor who would be able to respond to the lead reviewer's queries on your behalf. If this is your preferred option, please identify this person to us and ensure we have their contact details.

You are not required to attend a meeting of the Proportionate Review Sub-Committee.

Please do not send any further documentation or revised documentation prior to the review unless requested.

The documents to be reviewed are as follows:

Document	Version	Date
Other [C.V GS supervisor]		
Other [C.V ID supervisor]		
Participant consent form [Consent form]	2.1	01 October 2015
Participant information sheet (PIS) [PIS]	2.1	01 October 2015
REC Application Form [REC_Form_07012016]		07 January 2016
Referee's report or other scientific critique report [scientific review]		
Research protocol or project proposal [Research protocol]	2.1	30 October 2015
Summary CV for Chief Investigator (CI) [C.V CI]		
Summary CV for supervisor (student research) [C.V AD]		

No changes may be made to the application before the meeting. If you envisage that changes might be required, you are advised to withdraw the application and re-submit it.

Notification of the Sub-Committee's decision

We aim to notify the outcome of the Sub-Committee review to you in writing within 10 working days from the date of receipt of a valid application.

If the Sub-Committee is unable to give an opinion because the application raises material ethical issues requiring further discussion at a full meeting of a Research Ethics Committee, your application will be referred for review to the next available meeting. We will contact you to explain the arrangements for further review and check they are convenient for you. You will be notified of the final decision within 60 days of the date on which we originally received your application. If the first available meeting date offered to you is not suitable, you may request review by another REC. In this case the 60 day clock would be stopped and restarted from the closing date for applications submitted to that REC.

R&D approval

All researchers and local research collaborators who intend to participate in this study at sites in the National Health Service (NHS) or Health and Social Care (HSC) in Northern Ireland should apply to the R&D office for the relevant care organisation. A copy of the Site-Specific Information (SSI) Form should be included with the application for R&D approval. You should advise researchers and local collaborators accordingly.

The R&D approval process may take place at the same time as the ethical review. Final R&D approval will not be confirmed until after a favourable ethical opinion has been given by this Committee.

For guidance on applying for R&D approval, please contact the NHS R&D office at the lead site in the first instance. Further guidance resources for planning, setting up and conducting research in the NHS are listed at <http://www.rdforum.nhs.uk>. There is no requirement for separate Site-Specific Assessment as part of the ethical review of this research.

Communication with other bodies

All correspondence from the REC about the application will be copied to the research sponsor and to the R&D office for Sheffield Teaching Hospitals NHS Foundation Trust. It will be your responsibility to ensure that other investigators, research collaborators and NHS

care organisation(s) involved in the study are kept informed of the progress of the review, as necessary.

HRA Training

We are pleased to welcome researchers and R&D staff at our training days – see details at <http://www.hra.nhs.uk/hra-training/>

16/YH/0033

Please quote this number on all correspondence

Yours sincerely



Miss Kathryn Murray
REC Manager

Email: nrescommittee.yorkandhumber-sheffield@nhs.net

Copy to: *Mrs Sam Walmsley, Sheffield Teaching Hospitals NHS Foundation Trust*
Professor Simon Heller, Sheffield Teaching Hospitals NHS Foundation Trust

07 March 2016

Dr Mohammed Al-Zubidi
 PhD Student
 School of Clinical Dentistry
 University of Sheffield
 Claremont Crescent
 Sheffield S10 2TA

Dear Dr Al-Zubidi,

**Project Authorisation
 NHS Permission for Research to Commence**

STH ref:	19056	
NIHR CSP ref:	N/A	
REC ref:	16/YH/0033	
MHRA ref:	N/A	EudraCT No: N/A
Clinical Trial reg no:	N/A	
Study title:	Investigation of bacteriophage as potential source of oral antimicrobials	
Chief Investigator:	Dr Mohammed Al-Zubidi, University of Sheffield	
Principal Investigator:	Prof. Andrew Rawlinson, University of Sheffield	
Sponsor:	Sheffield Teaching Hospitals NHS Foundation Trust	
Funder:	Ministry of Higher Education & Scientific Research of Iraq (PhD)	
NIHR TARGET FPFV RECRUITMENT DATE	16 May 2016	

MANDATORY REPORTING OF RECRUITMENT

The Research Department is obliged to report study set up and recruitment performance for the Trust to NIHR and to report research activity for all studies to Trust Board. In order to meet these reporting requirements please be advised that it is now a **mandatory** condition of STH project authorisation that recruitment to **all** research studies* at STH is reported into EDGE (the Accrual Collation and Reporting Database). It is essential that recruitment is entered into EDGE **real-time** to enable directorates to accurately monitor performance. Please see item 2 of the 'Conditions of R&D Authorisation' for further details.

Please be informed that failure to report recruitment to EDGE may result in loss or delay in funding to the Trust and to the Directorate.

*Information regarding EDGE eligibility for reporting is detailed in the 'Conditions of R&D Authorisation'

The Research Department has received the required documentation as listed below:

1.	Sponsorship Agreement Clinical Trial Agreement Material Transfer Agreement Funding Award Letter	D. Patel signed REC Form 15 Dec 2015 on behalf of Sponsor N/A N/A: samples analysed at University of Sheffield Not available (PhD study)
2.	Monitoring Arrangements	N/A
3.	STH registration document	REC Form signed by Sponsor (15 Dec 2015) and CI (07 Jan 2016)
4.	Evidence of Favourable Scientific Review	STH ISR: 01 Dec 2015
5.	Protocol – final version	V2.1, 30 Oct 2015
6.	Participant Information Sheet	V2.3, 02 Feb 2016
7.	Consent Form	V2.3, 02 Feb 2016
8.	Letter of indemnity / insurance arrangements	NHS indemnity University of Sheffield Insurance, certificate issued 11 Dec 2015
9.	ARSAC certificate / IRMER assessment	N/A
10.	Ethical review - Letter of approval from NHS REC (Yorkshire & The Humber Sheffield REC)	22 Jan 2016 (PO) 27 Jan 2016 (FO with conditions) 04 Feb 2016 (conditions met)
11.	Site Specific Assessment	PI declaration received 22 Feb 2016 (all queries resolved 07 Mar 2016)
12.	Clinical Trial Authorisation from MHRA	N/A
13.	Evidence of hosting approvals - STH Principal Investigator - Clinical Director - General Manager - Research Finance - Data Protection Officer	RMS Sign Off: A. Rawlinson, 22 Feb 2016 A. Loescher, 24 Feb 2016 D. Marriott, 03 Mar 2016 L. Fraser, 07 Mar 2016 P. Wilson, 25 Feb 2016
14.	Honorary Contract/Letter of Access	N/A
15.	Associated documents	-

This project has been reviewed by the Research Department. NHS permission for the above research to commence has been granted on the basis described in the application form, protocol and supporting documentation on the understanding that the study is conducted in accordance with the Research Governance Framework, GCP and Sheffield Teaching Hospitals policies and procedures (see attached appendix).

Yours sincerely

PP
[Handwritten signature]

Professor S Heller
Director of R&D, Sheffield Teaching Hospitals NHS Foundation Trust
Telephone +44 (0) 114 2265934
Fax +44 (0) 114 2265937

cc: Kathryn Hurrell-Gillingham, Andrew Rawlinson, Graham Stafford, Charles William Ian Douglas (by e-mail)

Sheffield Teaching Hospitals NHS Foundation Trust

Conditions of R&D Authorisation

Please note the following requirements that must be adhered to by the investigator when embarking on a research project at Sheffield Teaching Hospitals NHS Foundation Trust (STH). The investigator must update the Research Department of the following:

1. Safety reporting

Investigators should ensure that they elicit information regarding adverse events from participants at each study visit. If a Serious Adverse Event (SAE) is discovered the investigator must alert the Sponsor immediately (within 24 hours) and must comply with sponsor requests for further information to ensure that events are reported to ethics and regulatory bodies within the timelines laid down in the Medicines for Human Use (Clinical Trials) Regulations 2004. Investigators should refer to the STH Research Department SOPs available by request or on the Department website <http://www.sheffieldclinicalresearch.org> for further guidance.

2. Recruitment reporting in EDGE

It is now a *mandatory* requirement of STH NHS Permission that recruitment to research studies at STH is reported using the EDGE and essential that recruitment is entered into EDGE *real-time*.

EDGE Exempt Studies

Not all studies are required to use the EDGE Accrual Collation and Reporting Database. Your CRO Research Coordinator will confirm during the set-up phase of your study whether you are required to record recruitment into EDGE.

Studies conducted in a STH Clinical Research Facility (CRF)* - These studies will be under the management of the CRF where accrual will be captured in the CRF Manager database and are therefore EDGE exempt.

*Recruitment for CRF Link studies (where the CRF provides the research environment for the PI and their team) will require reporting into EDGE as data for these studies are not captured in CRF Manager.

Definition of Recruited Participant: Eligible participant recruited onto the trial.

Note: Screen failures do not count as a recruited participant.

Once you have been issued with a login for EDGE, please refer to the training materials at this link to use the system: <http://www.sheffieldclinicalresearch.org/for-researchers/conducting-research/step-4/>

For further information regarding the use of EDGE or training provision please contact your local STH EDGE Administrators Gaurika Kapoor (gaurika.kapoor@sth.nhs.uk) and Zoe Whiteley (zoe.whiteley@sth.nhs.uk).



Health Research Authority
Yorkshire & The Humber - Sheffield Research Ethics Committee

Room 001
Jarrow Business Centre
Rolling Mill Road
Jarrow
Tyne & Wear
NE32 3DT

Tel: 0207 104 8282

27 January 2017

Dr Mohammed Al-Zubidi
PhD student
School of Clinical Dentistry / University of Sheffield
Claremont Crescent
Sheffield
S10 2TA

Dear Dr Al-Zubidi

Study Title:	Investigation of bacteriophage as potential source of oral antimicrobials
REC reference:	16/YH/0033
Protocol number:	STH19056
IRAS project ID:	186132

Thank you for sending the progress report for the above study dated 27 January 2017. The report will be reviewed by the Chair of the Research Ethics Committee, and I will let you know if any further information is requested.

The favourable ethical opinion for the study continues to apply for the duration of the research as agreed by the REC.

Where research involves the use of human tissue in England, Wales or Northern Ireland, legal authority to hold the tissue under the terms of the ethical approval remains in place for the duration of the approved project.

Yours sincerely



Kerry Dunbar
REC Assistant

E-mail: nrescommittee.yorkandhumber-sheffield@nhs.net

Copy to: *Mrs Sam Walmsley
Dr Nana Theodorou, Sheffield Teaching Hospitals NHS Trust*

IRAS 186132 Confirmation of Amendment Categorisation as Category A

Dear Mohammed

IRAS Project ID:	186132
Short Study Title:	Investigation of bacteriophage as source of oral antimicrobials
Date complete amendment submission received:	30/01/2017
Amendment No./ Sponsor Ref:	NSA01_Extension
Amendment Date:	30/01/2017
Amendment Type:	Non-substantial

Thank you for submitting the above referenced amendment. In line with the [UK Process for Handling UK Study Amendments](#) I can confirm that this amendment has been categorised as:

- Category A - An amendment that has implications for, or affects, ALL participating NHS organisations

You should now provide this email, together with the amended documentation, to the [research management support offices](#) and local research teams at your participating NHS organisations in England.

If you have participating NHS organisations in Northern Ireland, Scotland and/or Wales, you should communicate directly with the relevant research teams to prepare them for implementing the amendment, as per the instructions below. You do not need to provide this email or your amended documentation to their research management support offices, as we will pass these to the relevant national coordinating functions who will do this on your behalf.

Apendix 3

25th September 2014

Andrew Rawlinson
Head of Academic Unit of Restorative Dentistry
School of Clinical Dentistry/ University of Sheffield
Claremont Crescent
Sheffield
S10 2TA

Dear Andrew,

Minor Amendment**Letter of Continued NHS Permission**

STH ref:	STH17158		
NIHR CSP ref:	N/A		
REC ref:	13/YH/0114		
MHRA ref:	N/A	EudraCT no.:	N/A
Study title:	Enzyme Biomarkers in Periodontal Disease		
Chief Investigator:	A Rawlinson		
Principal Investigator:	A Rawlinson		
Sponsor:	Sheffield Teaching Hospitals NHS Foundation Trust		
Funder:	PhD/ Directorate		
Amendment Ref:	Minor Amendment 4 - change to consent form		

Thank you for submitting the following documents:

Document	Version/date
Consent form	Version 3, 19 Sep 14
Amendment 4 approval letter from REC	24 Aug 14

These have been reviewed by the Research Department who have no objection to the amendment and can confirm continued NHS permission for the study at STH.

Yours sincerely



R

Professor S Heller
Director of R&D, Sheffield Teaching Hospitals NHS Foundation Trust
Telephone +44 (0) 114 22 65934
Fax +44 (0) 114 22 65937



proud to make a difference

Chair: Tony Pedder OBE Chief Executive: Sir Andrew Cash OBE



Apendix 4

Ministry of Higher Education &
Scientific Research
Al Mustansiriya University
College of Dentistry
Dean Office

جمهورية العراق



وزارة التعليم العالي والبحث العلمي
الجامعة المستنصرية
كلية طب الاسنان
مكتب العميد

Ref.: 3670
Date: 30/12/2015

To whom it may concern

We confirm that the ethical approval for the collection of plaque samples and endodontic abscess for the study " Investigation of bacteriophage as potential sources for oral antimicrobial " has been accepted from patients attending our dental clinics.



Sincerely,
Assistant Professor
Dr. Hikmet A. Sh. Al Gharrawi
Dean

College of Dentistry / Al Mustansiriya University
Iraq - Baghdad
E-mail : Halgharrawi@yahoo.com

30/12/2015

Tel.: 5372237
5372238

E - mail : must_coll_ofdentistry@yahoo.com

هاتف / ٥٣٧٢٢٣٧
٥٣٧٢٢٣٨

Appendix 5

Re: IRAS176793 / STH18841 - Acknowledgement of Amendment (Amendment No./Ref. NSA
14Feb2017 & Category C)

Sent on behalf of Prof Simon Heller, Director of R&D, Sheffield Teaching Hospitals NHS FT

Dear Nicolas,

An in vitro study of the biomechanical performance of restored teeth (Using my extracted teeth for research)

Non-substantial Amendment 14Feb2017

- *Addition to the existing study team to work on biofilm formation and removal as part of the development of optimised laboratory oral model [Mohammed Al Zubidi (PhD Student) / Graham Stafford (Supervisor)]*
- *Addition to the existing study team to work on the restoration of the teeth [Keyvan Moharamzadeh (Supervisor) / Sandra Elkhatib (DClinDent Student)]*

This amendment has been received & acknowledged by the Research Department.

If you wish to discuss further, please do not hesitate to contact me.

Kind regards,

Sam

Sam Walmsley, Research Coordinator

Research Department

Sheffield Teaching Hospitals NHS Foundation Trust

D49, D Floor

Royal Hallamshire Hospital

Glossop Road

Sheffield S10 2JF

Direct line: [+44 \(0\)114 226 5932](tel:+441142265932)

Fax: [+44 \(0\)114 226 5937](tel:+441142265937)

Email: samantha.walmsley@sth.nhs.uk

Website: www.sheffieldclinicalresearch.org

Note: Working days are Mon, Tues, Weds and Fri.

----- Forwarded message -----

From: <hra.amendments@nhs.net>

To: <k.hurrell-gillingham@sheffield.ac.uk>

Cc: <n.martin@sheffield.ac.uk>, <Samantha.Walmsley@sth.nhs.uk>

Bcc:

Date: Thu, 23 Feb 2017 15:20:30 +0000

Subject: IRAS 176793. Confirmation of Amendment Categorisation as Category C

Dear Kathryn,

IRAS Project ID:	176793
Short Study Title:	Using My Extracted Teeth For Research
Date complete amendment submission received:	14/02/2017
Amendment No./ Sponsor Ref:	Amendment dated 14/02
Amendment Date:	14/02/2017
Amendment Type:	Non-substantial

Thank you for submitting the above referenced amendment. In line with the [UK Process for Handling UK Study Amendments](#) I can confirm that this amendment has been categorised as:

Category C - An amendment that has no implications that require management or oversight by the participating NHS organisations

As such, the sponsor may implement this amendment as soon as any relevant regulatory approvals are in place (for participating organisations in England, please see 'Confirmation of Assessment Arrangements' below).

As Chief Investigator/Sponsor, it remains your responsibility to ensure that the research management offices and local research teams (if applicable) at each of your participating organisations are informed of this amendment.

Note: you may only implement changes described in the amendment notice or letter.

Participating NHS Organisations in England – Confirmation of Assessment Arrangements

Further to the details above, I can confirm that no HRA assessment of this amendment is needed.

- If this study has HRA Approval, this amendment may be implemented at participating NHS organisations in England once the conditions detailed in the categorisation section above have been met
- If this study is a pre-HRA Approval study, this amendment may be implemented at participating NHS organisations in England that have NHS Permission, once the conditions detailed in the categorisation section above have been met. For participating NHS organisations in England that do not have NHS Permission, these sites should be covered by HRA Approval before the amendment is implemented at them, please see below;
- If this study is awaiting HRA Approval, I have passed your amendment to my colleague in the assessment team and you should receive separate notification that the study has received HRA Approval, incorporating approval for this amendment.

Please do not hesitate to contact me if you require further information.

Kind regards

Laura Greenfield

Laura Greenfield | Amendments Coordinator
Health Research Authority

HRA, The Old Chapel, Royal Standard Place, Nottingham, NG1 6FS
E: hra.amendments@nhs.net

T: 020 7104 8096
www.hra.nhs.uk